VOLUME 42, NUMBER 2, JUNE 2019

HADRONIC JOURNAL

HADRONIC JOURNAL Volume 42, Number 2, June 2019

Founded in 1978 by Prof. R. M. Santilli at Harvard University. Some of the past Editors include Professors S. L. Adler, A. 0. Barut, L. C. Biedenharn, N. N. Bogoliubov, M. Froissart, J.Lohmus, S. Okubo, Nobel Laureate Ilya Prigogine, M. L. Tomber, J. P.Vigier, J. Wess, Nobel Laureate Chen Ning Yang.

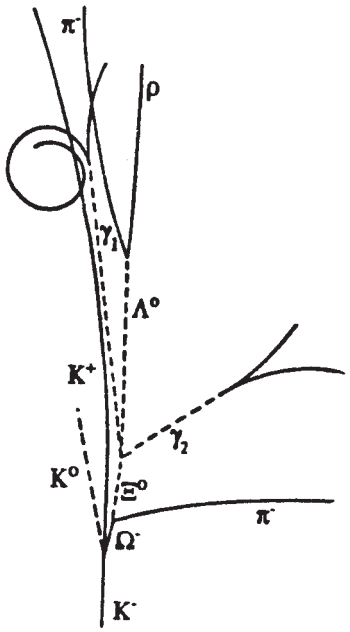

EDITORIAL BOARD

A.O.ANIMALU
A. K. ARINGAZIN
A. A. BHALEKAR
S. J. DHOBLE
J. DUNNING-DAVIES
T. L. GILL
L. P. HORWITZ
S. L. KALLA
S. I. KRUGLOV
M. NISHIOKA
R. F. O'CONNELL
Z. OZIEWICZ
E. RECAMI
M. SALEEM
B. G. SIDHARTH
S. SILVESTROV
H. M. SRIVASTAVA
E. TRELL
R.I. TSONCHEV
QI-REN ZHANG
C.A.WOLF
YI-ZHONG ZHUO

Founder and
Editor In Chief
R. M. SANTILLI

H/P HADRONIC PRESS, INC.

HADRONIC JOURNAL

VOLUME 42, NUMBER 2, JUNE 2019

Phase Shift Analysis in Nuclear Astrophysics and Three-Body Model for Some Nuclei

Part II. Phase Shift Analysis, 97-302

DOI 10.29083/HJ.42.02.2019

Dubovichenko Sergey Borisovich

Fesenkov Astrophysical Institute – Observatory 23, Kamenskoe plato, 050020, Almaty, Republica of Kazakhstan

Copyright © 2019 by Hadronic Press, Inc., Palm Harbor, FL 34684, USA

Dubovichenko S.B.

Phase Shift Analysis in Nuclear Astrophysics and Three-Body Model for Some Nuclei

Reviewers

Academician of the European Academy of Natural Sciences, corresponding member of the Russian Academy of Natural Sciences, Doctor of phys. and math. sciences RK, professor **Burtebayev N. T.** (INP, Almaty, RK)

Doctor of phys. and math. sciences RK and RF, professor **Burkova N. A.** (al-Farabi KazNU, Almaty, RK)

Scientific Editor of English edition

PhD **Albert V. Dzhazairov-Kakhramanov** (APFI, Almaty, RK)

Translated into English

Julia S. Dubovichenko (APFI, Almaty, RK)

I. Methods of Solution of the Schrödinger Equation
HADRONIC JOURNAL
VOLUME 42, NUMBER 1, MARCH 2019, 3-95

II. Phase Shift Analysis
HADRONIC JOURNAL
VOLUME 42, NUMBER 2, JUNE 2019, 97-302

III. The Three-Body Model
HADRONIC JOURNAL
VOLUME 42, NUMBER 3, OCTOBER 2019, 303-381

CONTENTS

INTRODUCTION..... 100
II. PHASE SHIFT ANALYSIS..... 103
Introduction..... 104
2.1 Phase shift analysis of the elastic $^4He^4He$ scattering..... 105
2.1.1 Overview of the experiment on the $^4He^4He$ elastic scattering.....105
2.1.2 The phase shift analysis methods of the $^4He^4He$ elastic scattering.....107
2.1.3 Verification of the computer program..... 109
2.1.4 The program for the $^4He^4He$ and $^4He^{12}C$ phase shift analysis..... 112
2.2 Phase shift analysis of the $^4He^{12}C$ elastic scattering..... 126
2.2.1 Differential cross sections..... 126
2.2.2 Phase shift analysis 127
2.3 Phase shift analysis of the elastic $N^{12}C$, $p^{14}C$ and $N^{16}O$ scattering 142
2.3.1 Differential cross sections..... 142
2.3.2 Control of the computer program..... 145
2.3.3 Phase shift analysis of the $p^{12}C$ scattering 149
2.3.4 The phase shift analysis of the $n^{12}C$ elastic scattering 154
2.3.5 Phase shift analysis of the $p^{14}C$ elastic scattering 163
2.3.6 Phase shifts and potentials of the $n^{16}O$ scattering 171
2.3.7 Phase shift analysis of the $p^{16}O$ scattering 178
2.3.8 Program for $N^{12}C$, $p^{14}C$ and $N^{16}O$ phase shift analysis.....200
2.4 Phase shift analysis of the elastic p^6Li scattering..... 212
2.4.1 The differential cross sections 212
2.4.2 Phase shift analysis 213
2.4.3 Program for the phase shift analysis 219
2.5 Phase shift analysis and computer programs for scattering of particles with the 1/2+1/2 spin..... 231

2.5.1 The system with the spin-orbital interaction 231
2.5.2 System with the spin-orbital and the singlet-triplet mixing..... 248
2.5.3 Phase shift analysis of the $p^{13}C$ elastic scattering
taking into account the spin-orbit 271
2.5.4. Phase shift analysis of the $n^{3}He$ elastic scattering 276
Conclusion 286
References 287
Author Information 301

Introduction

In many problems of the nuclear physics at low energies and nuclear astrophysics the knowledge of the scattering elastic phase shifts, which can be determined from the differential cross sections of scattering of the various nuclear particles is required [1]. Such phase shifts are used, in particular, for construction of the intercluster interaction potentials, for example, in the potential cluster model (PCM) of easy light nuclei [2]. The procedure of the phase shift analysis consists in the decomposition of the total scattering amplitude in a row by the partial waves or amplitudes and the analysis of the parameters appearing at the same time, which are called the scattering phase shifts. Such phase shifts allow one to obtain the data about the nature of strong interactions, the structure of resonance states and the general structure of an atomic nucleus [1].

The two-body processes with the formation of resonances in the nuclear physics at low energies also can be investigated by the means of the phase shift analysis. To solve this problem it is necessary to consider in details the energy behavior of the resonance partial scattering amplitude [1,3]. As a result, the phase shift analysis plays a large role in the search of nuclear resonances of the scattering processes and determination of their quantum numbers. The research of the scattering processes by the means of the phase shift analysis allows one to clarify many important aspects of the interactions of nuclear particles, because this analysis is based only on the most general conservation laws and is closely connected with experimental data [1,3].

The problem of determination or extraction of the nuclear phase shifts from the cross sections of elastic scattering in the mathematical plan is reduced to a multiple parameter variation problem. In other words, when the experimental scattering cross sections of nuclear particles and mathematical expressions obtained in the quantum mechanics, which describe these cross sections depending on some δ_L parameters - nuclear scattering phase shifts are known, there is a multiple parameter variation problem of finding of these parameters on the set interval of values taking into account the generalized Levinson's theorem [4]. In different nuclear systems depending on the energy of the colliding particles, the number of

elastic scattering phase shifts can change from 1–3 to 10–20 [5].

This book is directly based on the results about two tens scientific articles published generally for the last five-seven years in Russia, Europe, USA and the CIS countries and consists of three chapters. The first of them is devoted to the description of the general mathematical methods of calculation of some nuclear characteristics. The general criteria and methods of creation of the intercluster potentials in a continuous and discrete spectrum, which are used further for the consideration of some nuclei in the three-body model described in the third chapter, are defined.

The second chapter contains methods and results of the phase shift analysis of the elastic scattering of the nuclear particles ^{4}He^{4}He, n^{3}He, p^{6}Li, p^{12}C, n^{12}C, p^{13}C, p^{14}C, n^{16}O, p^{16}O and ^{4}He^{12}C at low and astrophysical energies. These results are used for the construction in the PCM of pair intercluster interaction potentials of the continuous spectrum. Here the various experimental measurements, methods of calculations of differential cross sections, computer programs and results of the phase shift analysis of elastic scattering of the particles stated above will be considered. For the first system ^{4}He^{4}He only the main expressions for the phase shift analysis, the computer program and versions of the control account are given at 25–29 MeV. For other systems, except the last, the area of energies approximately to 1–2.5 MeV is considered. In an elastic ^{4}He^{12}C scattering the phase shift analysis is made in the range of 1.5–6.5 MeV. The areas of the phase shift analysis given here are caused by the existence of the experimental data on the differential cross sections for the angular distributions or excitation functions.

The results obtained in the three-body single-channel models of some light nuclear nuclei, namely, ^{7}Li, ^{9}Be and ^{11}B are given in chapter three. They allow one to check the adequacy of the construction pair intercluster potentials on the basis of the elastic scattering phase shifts and characteristics of the bound states of light atomic nuclei. These results allow one to find out the applicability of the obtained potentials in the three-body problems. The potentials checked thus are used further for the calculations of some main characteristics of thermonuclear processes of the preliminary nucleosynthesis of the Universe and some solar cycles [2].

Let us note that the second and, especially, the third chapters of this book almost completely coincide with the results given in the

corresponding chapters of other book of the author: "Preliminary nucleosynthesis of the Universe" of Germany, Saarbrucken: Lambert Academy Publ. GmbH&Co. KG. 2014. 668 pages [2]. This material is selected to the separate book "Phase shift analysis...", primarily in order to reduce book [2] and allows if future the possibility of its enlargement and addition by new material on thermonuclear reactions at the next reedition. At the same time, the present book can also be extended at the inclusion in its new results by the phase shift analysis or three-body model.

II. Phase Shift Analysis

In many problems of nuclear physics of low energies and nuclear astrophysics the knowledge of elastic scattering phase shifts, which can be determined, for example, from differential cross sections of elastic scattering of various nuclear particles is required [1]. The procedure of the phase shift analysis consists in decomposition of the total scattering amplitude in a term on partial waves or amplitudes and analyses the parameters appearing at the same time called the phase shifts. Such phase shifts allow one to obtain the data on the nature of strong interactions, the structure of resonance states and the general structure of an atomic nucleus [1]. The phase shifts are used, in particular, for the creation of intercluster interaction potentials in the three-body potential cluster model considered further or by the consideration of some astrophysical problems [2].

Introduction

We will remind that the problem of determination or extraction of the nuclear phase shifts from the cross sections of elastic scattering in the mathematical plan is reduced to a multiple parameter variation problem. In other words, when the experimental scattering cross sections of nuclear particles and mathematical expressions, obtained in the quantum mechanics, which describe these cross sections depending on certain parameters δ_L – the nuclear phase shifts, the polyvalent variation problem of finding these parameters on the given interval of values takes place. This interval usually is in area of values of the phase shifts 0° and 180°, if takes into account the conclusions of the generalized Levinson's theorem [4].

Since there is no the general methods for the solving the multi-parameter variational problem to find a global minimum, we can expect to find mostly only some local minima at each energy and, on the basis of physical considerations, choose those that can be the solutions of the original problem. One of the criteria of such selection is the requirement of smooth behavior of each partial nuclear phase shift as functions of energy in the non-resonance area and transition of its value through 90° at resonance energy [1], and also finding of a phase shift in the given area of the angles.

In the different nuclear systems depending on energy of the colliding particles, the number of elastic scattering phase shifts can change from 1–3 to 10–20 [5]. For example, in the ^{4}He^{4}He scattering we used up to 20 partial waves, and, for example, in the p^{12}C system at low energies as it will be shown further, only one partial ^2S phase shift will be used. In this chapter the various experimental measurements, methods of calculations of differential cross sections, including the computer programs, and results for the phase shift analysis of the elastic ^{4}He^{4}He, n^{3}He, p^{6}Li, p^{12}C, n^{12}C, p^{13}C, p^{14}C, n^{16}O, p^{16}O and ^{4}He^{12}C scattering will be considered.

For the first system given above only the control account at energy of 22 and 30 MeV, which is used for the verification of the computer program is considered. In more detail this system is considered in [2]. For other processes of scattering the area up to 1–2.5 MeV is analyzed, except the last system – in the ^{4}He^{12}C scattering the phase shift analysis is made in the range of 1.5–6.5 MeV.

2.1 Phase shift analysis of the elastic ^{4}He^{4}He scattering

In the beginning we will consider the results of measurements of the elastic scattering differential cross sections and results of the phase shift analysis obtained from these cross sections for the ^{4}He^{4}He systems at different energies. The basic data of these studies relate to energies up to 120 MeV, but not in all of this area was carried out the serial phase shift analysis of experimentally measured differential cross sections of the elastic scattering [83].

2.1.1 Overview of the experiment on the ^{4}He^{4}He elastic scattering

We will provide the short review of the experimental data and results of the phase shift analysis of the ^{4}He^{4}He elastic scattering, executed in different works:

1. The measurement of the elastic scattering differential cross sections and the phase shift analysis in the energy range of 0.6–3.0 MeV (l.s.) are executed in work [84], where the cross sections and phase shifts are specified in the tables that is very convenient for their use and at any time allows to repeat all results by the finding of the phase shifts.

2. The energy range of 3.0–5.0 MeV has been considered in work [85], but the phase shifts and cross sections of scattering are given only in the figures.

3. The energies of 3.8–11.9 MeV were analyzed in work [86], where the results of the phase shift analysis are given in the table, and the scattering differential cross sections are shown only in figures.

4. The very accurate measurements of the elastic scattering differential cross sections and the phase shift analysis are executed in works [87,88], where for the energy range of 13–22.9 MeV the experimental cross sections and scattering phase shifts are given in tables.

5. The area 12.9–21.6 MeV was also considered in work [89], but the cross sections and phase shifts are given in it only in figures.

6. The very good data for energies of 18.0–29.5 MeV are provided in work [90], where elastic scattering cross sections and results of the phase shift analysis are specified in detailed tables.

7. At the energies of 23.1–38.4 MeV the experimental measurements of cross sections are executed and the phase shift analysis in work is carried out [91], however only the scattering cross section is specified in tables.

8. The measurement of cross sections and the phase shift analysis in the range of 53–120 MeV have been executed in work [92], but only tabular phase shifts are given there, and the scattering cross sections are given in figures.

9. The experimental study of the elastic scattering cross sections for energies 36.8–47.3 MeV were carried out in [93], where in detailed tables results of measurements of differential cross sections are yielded, but the phase shift analysis of these data was not carried out. The theoretical researches of some energies from this area are available only in work [94], where search of parameters of the optical potential is executed, and then, in the settlement way, the phase shifts of the ^{4}He^{4}He elastic scattering have been obtained. The quality of the optical adjustment made in this area of energies leaves much to be desired, as can be seen directly from the figures in [94]. In addition, at the extraction of the phase shifts of the optical potential was calculated only their real part and an imaginary part of the phase shift considered small, located at 1°–2°, that does not seem justified for energy in the region of 40 MeV or higher.

10. The energy of 38.5, 49.9 and 51.1 MeV have been considered in works [95,96,97] respectively, where the differential cross sections were measured, but the phase shift analysis of these data was not carried out. Instead, in works [95,97] the parameters of the optical potentials, and in [97], on their basis are obtained, elastic scattering phase shifts were calculated.

From the provided review it is clear that the standard phase shift analysis of the experimental data, i.e. elastic scattering differential cross sections in the ^{4}He^{4}He system at energies of 36.85–51.1 MeV, still is not executed. The quality of adjustment of parameters of the optical potentials for the energy range of 23–47 MeV [94] can hardly be considered satisfactory, which is not surprising, as all these results have been obtained in the 60th years when the computer facilities and methods of numerical calculations only began to develop.

Therefore, it is interesting to carry out an accurate and most comprehensive analysis of the experimental phase shift of elastic scattering

differential cross sections in the energy range 37–51 MeV. The tabular representation of the experimental cross sections of the ^{4}He^{4}He elastic scattering in this area of energies, provided in works [93,95,96] allows one to carry out such analysis. However, here we will be limited only by the check of the operability of the computer program, and the results of such analysis are given in works [5,83] and the book [2].

2.1.2 The phase shift analysis methods of the ^{4}He^{4}He elastic scattering

We will consider a problem of the phase shift analysis and methods of determination of phase shifts from the experimental data, i.e. we will define the ways and approaches, which were used in our phase shift analysis. The elastic scattering differential cross section of the identical particles with spin 0 + 0 is defined by the scattering phase shifts of the identical particles as follows [6]:

$$\frac{d\sigma(\theta)}{d\Omega} = \left|f(\theta) + f(\pi - \theta)\right|^2, \qquad (2.1.1)$$

where the scattering amplitude is presented in the form of the sum of Coulomb and nuclear amplitudes

$$f(\theta) = f_c(\theta) + f_N(\theta) \qquad (2.1.2)$$

also it is expressed through the nuclear δ_l and Coulomb σ_l phase shifts [6]:

$$f_c(\theta) = -\left(\frac{\eta}{2k\sin^2(\theta/2)}\right)\exp\{i\eta\ln[\sin^{-2}(\theta/2)] + 2i\sigma_0\}, \qquad (2.1.3)$$

$$f_N(\theta) = \frac{1}{2ik}\sum_l (2l+1)\exp(2i\sigma_l)[S_l - 1]P_l(\cos\theta),$$

where k – wave number of the relative movement of the $k^2 = 2\mu E/\hbar^2$ particles, E – energy of the colliding particles in the center of mass, μ – the reduced mass, η – the Coulomb parameter, θ – the scattering angle,

$P_L(\cos\theta)$ – Legendre's polynoms.

Usually the nuclear phase shifts of the elastic scattering are presented in the form

$$\delta_L = \mathrm{Re}\delta_L + i\mathrm{Im}\delta_L,$$

then for a scattering matrix and parameter of inelasticity we will obtain

$$S_L(k) = \eta_L(k)\exp[2i\mathrm{Re}\delta_L(k)],$$

$$\eta_L(k) = \exp[-2\mathrm{Im}\delta_L(k)].$$

The summation in the expression (2.1.3) is carried out only by even-numbered L, as odd partial waves do not give a contribution to the total cross section, and carried out to some L, the values of which depends on the energy.

The Coulomb scattering amplitude (2.1.3), using the expression

$$D = \sin^{-2}(\theta/2) = 2/[1 - \cos(\theta)],$$

it is possible to write down in the form

$$f_c = -\eta D/2k\,[\cos(C) + i\sin(C)],$$

where

$$C = 2\sigma_0 + \eta\ln D.$$

The nuclear amplitude can be provided in the following form

$$f_N = \frac{1}{2k}\sum_L \hat{L}\left\{\begin{array}{l}[B\cos(2\sigma_L) + A\sin(2\sigma_L)] + \\ +i[B\sin(2\sigma_L) - A\cos(2\sigma_L)]\end{array}\right\}P_L(x), \qquad (2.1.4)$$

where

$x = \cos(\theta)$, $\hat{L} = 2L + 1$, $A = \eta_L \cos(2\delta_L) - 1$, $B = \eta_L \sin(2\delta_L)$

depend only on the nuclear phase shifts, parameter of inelasticity and the orbital moment.

The Coulomb scattering phase shifts are expressed through the gamma-function [6]

$$\sigma_L = \arg\{\Gamma(L+1+i\eta)\}$$

and satisfy the recurrent process

$$\sigma_L = \sigma_{L+1} - \mathrm{arctg}\left(\frac{\eta}{L+1}\right).$$

Where from at once it is possible to obtain the following expression for the Coulomb phase shifts

$$\alpha_L = \sigma_L - \sigma_0 = \sum_{n=1}^{L} \mathrm{arctg}\left(\frac{\eta}{n}\right), \qquad \alpha_0 = 0.$$

The value α_1 is used in the transformed expressions (2.1.3), if to take out the general multiplier $\exp(2i\sigma_0)$. Then $\sigma_l \to \alpha_l$ c $\alpha_0 = 0$, that relieves us from need to calculate the Coulomb phase shifts in an explicit form, and the Coulomb amplitude takes the following form

$$f_c(\theta) = -\left(\frac{\eta}{2k\sin^2(\theta/2)}\right)\exp\{i\eta \ln[\sin^{-2}(\theta/2)]\} \ . \qquad (2.1.5)$$

In the ^{4}He^{4}He problem with zero spin the set of phase shifts depending on the total moment J and spin S passes into δ_l. As $S = 0$, the total moment is equal to the orbital moment $J = L$.

2.1.3 Verification of the computer program

For carrying out of this phase shift analysis the computer program in the

Basic language for the compiler Turbo Basic of Borland International Inc firm has been written [98], using the mode of double accuracy, which then was transferred to Fortran-90 [2]. The program was tested according to the made earlier phase shift analysis from the various works at different energies [10]. Here we will provide only some of these tests.

For example, at energy of 6.47 MeV (l.s.) the following phase shifts are given in work [86]: $\delta_0 = 79.5° \pm 2°$, $\delta_2 = 80.8° \pm 2°$. In our phase shift analysis the values $\delta_0 = 80.43°$ and $\delta_2 = 80.73°$ is turn out for them at $\chi^2 = 0.18$. The error of determination of the cross sections from figures of work [86] was accepted equal to 10%, as explains so small value χ^2.

At energy of 13 MeV in work [88] $\delta_0 = 29° \pm 4°$, $\delta_2 = 103° \pm 8°$, $\delta_4 = 3° \pm 1.5°$ was obtained, and our analysis gives $\delta_0 = 28.37°$, $\delta_2 = 105.03°$, $\delta_4 = 2.62°$ at $\chi^2 = 3.43$.

$\delta_0 = 7° \pm 2°$, $\delta_2 = 104° \pm 4°$, $\delta_4 = 16.2° \pm 2°$ was found in the same work for 17.8 MeV, and in our calculations we come to values $\delta_0 = 7.25°$, $\delta_2 = 103.93°$, $\delta_4 = 17.0°$ at $\chi^2 = 0.46$.

In work [88] also the energy of 22.9 MeV for which the following phase shifts are obtained is considered: $\delta_0 = 169.7° \pm 2°$, $\delta_2 = 94.0° \pm 2°$, $\delta_4 = 59.2° \pm 2°$, $\delta_6 = 1.09°$. Our phase shift analysis of these data gives the value $\delta_0 = 169.30°$, $\delta_2 = 94.49°$, $\delta_4 = 59.55°$, $\delta_6 = 1.0°$ at $\chi^2 = 1.46$.

At the energies of 13, 17.8 and 22.9 MeV the differential cross sections, their errors, scattering phase shifts and the value χ^2 are specified in the tables [88], but it is possible to compare only scattering phase shifts. It is rather difficult to compare χ^2 because in works [86,88] is not considered the value of χ^2 determined above (1.7.1), but its derivative depending on some constants connected with an experimental technique.

We will give the version of the control account, which is executed for the ^{4}He^{4}He elastic scattering at energy of 29.5 MeV in more detail. In work [90], where experimental cross sections and results of the phase shift analysis are yielded (see tab. 2.1.1), for the average χ^2 value 0.68 has been obtained, but the methods of its calculation differ a little from the stated above, therefore the value 0.68 cannot also be compared directly to our results. As a result of our calculations with the phase shifts from work [90] for the average χ^2 on all points 1.086 was obtained. If to consider the weight multipliers from [90] it is possible to obtain the value 0.6, which is

quite coordinated with the results of this work.

Furthermore, we have carried out the detailed calculations with the minimization of χ^2 for our program provided further and the comparison of results with the experimental data [90]. For the average χ^2 it has been obtained 0.600 (instead of 1.086), i.e. the improvement of the quality of the description of the experiment is observed almost twice at very little change of values of phase shifts, which are shown in tab. 2.1.1.

Tab. 2.1.1. The comparison of results of the phase shift analysis from work [90] and our results at 25.5 MeV and 29.5 MeV.

δ_L, deg	29.5 MeV		25.5 MeV	
	Results [90]	Our results	Results [90]]	Our results
δ_0	150,88±0.17	150.76	160,36±1.01	160.49
δ_2	86.90±0.13	86.61	89.37±1.54	89.00
δ_4	121.19±0.17	121.00	88.64±1.77	88.60
δ_6	2.20±0.11	2.16	1.61±0.39	1.41
δ_8	0.11±0.08	0.09	0.36±0.19	0.18

In work [90] the data were obtained at energy of 25.5 MeV were found, for which the phase shifts are also shown in tab. 2.1.1. Our calculation with these phase shifts leads to the value of $\chi^2 = 2.127$. Carrying out an additional variation of the scattering phase shifts, we will obtain the noticeable improvement of the description of the available data with $\chi^2 = 0.886$. For the phase shifts the values given in the last column of tab. 2.1.1, which coincide with the results [90] in the limits given in this work, the errors of scattering phase shifts are obtained.

The small differences in scattering phase shifts can be caused by the various values of constants or mass of particles, which are used in such calculations. For example, it is possible to use the exact values of mass of particles or their entire quantities, and the constant $\hbar^2/m_0$ can be other than the value 41.4686 MeV fm^2 used here. Therefore, in general it is possible to consider that in all cases considered above, which can be controlled cases for our results, in the limits given in various works of errors of phase shifts coincide with the data obtained earlier, by different authors.

2.1.4 The program for the ^{4}He^{4}He and ^{4}He^{12}C phase shift analysis

We will give the listing of the computer program in the Fortran language intended for the ^{4}He^{4}He and ^{4}He^{12}C phase shift analysis. What analysis will be made depends on the value of the NYS and LH parameter. In the case of ^{4}He^{4}He they have to be equal to 1 and 2 respectively, for carrying out of the ^{4}He^{12}C phase shift analysis of their value are equal to 0 and 1. Besides, for the big energy, about 30–40 MeV, the NP parameter has to be equal

NP = 2*LMA+LH,

but not the LMA that allows to taking into account the complex part of the scattering phase shifts.

The designations of some initial parameters of the program are given below

Z1=2.0D-000; Z2=2.0D-000 – Charges of particles
AM1=4.0D-000; AM2=4.0D-000 – Mass of the alpha particles
LMI=0 – The initial orbital moment
LH=1 – The step on the moment
LMA=2 – The maximum orbital moment
EP=1.0D-010 – Accuracy of search of a minimum
NI=10 – The number of iterations
NT=22 – The number of the experimental points
EL=130D-000 – The laboratory energy of the elastic scattering of particles
A1=41.4686D-000 – Constant value $\hbar^2/m_0$
PM=AM1*AM2/(AM1+AM2) – The reduced mass of the particles
FH=0.010D-000 – The initial step of the search of a minimum
NYS=1 – Call word – If = 1 Then ^{4}He^{4}He, And If = 0 Then ^{4}He^{12}C – for the search of phase shifts for two different systems of particles

Now we will provide the text, i.e. listing of the computer program in the Fortran-90 language.

PROGRAM FAZ_AL_AL

```
! THE PROGRAM OF THE PHASE SHIFT ANALYSIS FOR AL-AL
! AND AL-12C
IMPLICIT REAL(8) (A - Z)
INTEGER L,I,NT,LMI,LMA,LH,NYS,NP,NTT,NV,NI,LMI1,LH1,NPP
DIMENSION ST(0:50),FR(0:50),FM(0:50),ET(0:50), XP(0:50),ETA(0:50)
COMMON /A/ PI,NT,TT(0:50),GG,SS,LMI,LMA,LH,NYS,NP
COMMON /B/ SE(0:50),DS(0:50),DE(0:50),NTT
COMMON /C/ LH1,LMI1,P1,NPP
! ************* INITIAL VALUES **************
PI=4.0D-000*DATAN(1.0D-000)
P1=PI
Z1=2.0D-000; Z2=2.0D-000
AM1=4.0D-000; AM2=4.0D-000
AM=AM1+AM2
A1=41.46860D-000
PM=AM1*AM2/(AM1+AM2)
B1=2.0D-000*PM/A1
LMI=0; LMI1=LMI; LH=2; LH1=LH
LMA=4; LMA1=LMA
NYS=1; ! IF =1 THEN 4HE4HE, IF = 0 THEN 4HE12C
EP=1.0D-010
NV=1
FH=0.010D-000
NI=10
!NP=2*LMA+LH
NP=LMA
NPP=NP
! ***************** CROSS SECTIONS ***************
SE(1)=1357.0D-000; SE(2)=1203.0D-000; SE(3)=1074.0D-000;
SE(4)=870.0D-000; SE(5)=759.0D-000
SE(6)=688.0D-000; SE(7)=467.0D-000; SE(8)=271.0D-000;
SE(9)=196.0D-000; SE(10)=130.0D-000
SE(11)=93.90D-000;SE(12)=57.0D-000; SE(13)=350D-000;
SE(14)=130D-000; SE(15)=280D-000
SE(16)=24.7; SE(17)=86.5; SE(18)=157; SE(19)=270
SE(20)=337.0D-000; SE(21)=408.0D-000; SE(22)=418.0D-000
```

```
DE(1)=39.0D-000; DE(2)=40.0D-000; DE(3)=24.0D-000;
DE(4)=20.0D-000; DE(5)=16.0D-000;
DE(6)=17.0D-000
DE(7)=12.0D-000; DE(8)=7.0D-000; DE(9)=4.10D-000;
DE(10)=3.60D-000; DE(11)=20D-000;
DE(12)=1.50D-000
DE(13)=1.1; DE(14)=1.0; DE(15)=0.4; DE(16)=0.7;
DE(17)=2.0; DE(18)=3.6
DE(19)=6.50D-000; DE(20)=7.40D-000; DE(21)=8.20D-000;
DE(22)=8.30D-000
TT(1)=22.0D-000;  TT(2)=24.0D-000;  TT(3)=26.0D-000;
TT(4)=28.0D-000; TT(5)=30.0D-000
TT(6)=32.0D-000;  TT(7)=35.0D-000;  TT(8)=40.0D-000;
TT(9)=42.0D-000
TT(10)=45.0D-000; TT(11)=46.0D-000; TT(12)=48.0D-000;
TT(13)=50.0D-000
TT(14)=52.0D-000; TT(15)=55.0D-000; TT(16)=60.0D-000;
TT(17)=65.0D-000
TT(18)=70.0D-000; TT(19)=75.0D-000; TT(20)=80.0D-000;
TT(21)=85.0D-000; TT(22)=90.0D-000
! *************** FOR AL-AL ON E=13 ***************
NT=22;  NTT=NT; EL=130D-000
FR(0)=29.0D-000;  FR(2)=103.0D-000;  FR(4)=3.0D-000
FM(0)= 0.0D-000;  FM(2)=  0.0D-000;  FM(4)=0.0D-000
OPEN (4,FILE='FAZ.DAT')
DO L=LMI,LMA,LH
READ(4,*) L,FR(L),FM(L)
ENDDO
CLOSE(4)
 ! ************** ENERGY IN LAB. SYSTEM **************
 DO L=LMI,LMA,LH
 FM(L)=FM(L)*PI/180.0D-000
 FR(L)=FR(L)*PI/180.0D-000
 ET(L)=DEXP(-2.0D-000*FM(L))
 ENDDO
 FH=FH*PI/180.0D-000
```

```
DO I=LMI,LMA,LH
XP(I)=FR(I)
XP(I+LMA+LH)=FM(I)
ENDDO
! ********** TRANSFORM TO C.M. ******************
EC=EL*PM/AM1
SK=EC*B1
SS=DSQRT(SK)
GG=3.44476D-002*Z1*Z2*PM/SS
! ******* DIFFERENTIAL CROSS SECTION ************
CALL VAR(ST,FH,NI,XP,EP,XI,NV)
PRINT*, "XI-KV=; NI=; EL=",XI,NI,EL
! ********** TOTAL CROSS SECTION *****************
SIGMAR=0.0D-000; SIGMAS=0.0D-000
DO L=LMI,LMA,LH
FR(L)=XP(L)
FM(L)=XP(L+LMA+LH)
A=FR(L)
ETA(L)=1
!ETA(L)=DEXP(-2.0D-000*FM(L))
SIGMAR=SIGMAR+(2*L+1)*(1-(ETA(L))**2)
SIGMAS=SIGMAS+(2*L+1)*(ETA(L))**2*(DSIN(A))**2
ENDDO
SIGMAR=10.0D-000*4.0D-000*PI*SIGMAR/SK
SIGMAS=10.0D-000*4.0D-000*PI*SIGMAS/SK
PRINT*, "SIGMR-TOT=",SIGMAR
PRINT*, "SIGMS-TOT=",SIGMAS
PRINT*, "   T        SE        ST        XI"
! ***************** RESULTS ***********************
DO I=1,NT
WRITE(*,2) TT(I),SE(I),ST(I),DS(I)
ENDDO
PRINT*
PRINT*, "   L    FR(L)     FM(L)"
DO L=LMI,LMA,LH
FM(L)=FM(L)*180.0D-000/PI
```

```
 FR(L)=FR(L)*180.0D-000/PI
 WRITE(*,1) L,FR(L),FM(L)
 ENDDO
OPEN (4,FILE='SEC-AL-AL.DAT')
WRITE(4,*) "          AL-AL LAB E=; XI=",EL,XI
WRITE(4,*) "     T          SE          ST          XI"
DO I=1,NT
WRITE(4,2) TT(I),SE(I),ST(I),DS(I)
ENDDO
WRITE(4,*)
WRITE(4,*) "  L    FR(L)     FM(L)"
DO L=LMI,LMA,LH
WRITE(4,1) L,FR(L),FM(L)
ENDDO
CLOSE(4)
OPEN (4,FILE='FAZ.DAT')
DO L=LMI,LMA,LH
WRITE(4,1) L,FR(L),FM(L)
ENDDO
CLOSE(4)
1 FORMAT(1X,I5,E15.6,2X,E15.6)
2 FORMAT(1X,4(E10.3,2X))
3 FORMAT(1X,E15.5,2X,I5)
 END

 SUBROUTINE VAR(ST,PHN,NI,XP,EP,AMIN,NV)
 IMPLICIT REAL(8) (A - Z)
 INTEGER I,NP,LMI,LH,NT,NV,NI,IIN,NN,IN
 DIMENSION XPN(0:50),XP(0:50),ST(0:50)
 COMMON /C/ LH,LMI,PI,NP
 COMMON /B/ SE(0:50),DS(0:50),DE(0:50),NT
 !SHARED LH,LMI,NT,PI,DS(),NP
! ************** SEARCH OF THE MINIMUM ****************
 DO I=LMI,NP,LH
 XPN(I)=XP(I)
 ENDDO
```

```
 NN=LMI
 PH=PHN
 CALL DET(XPN,ST,ALA)
 B=ALA
 IF (NV==0) GOTO 3012
 DO IIN=1,NI
 NN=-LH
 GOTO 1119
1159 XPN(NN)=XPN(NN)-PH*XP(NN)
1119 NN=NN+LH
 IF (NN>NP) GOTO 3012
 IN=0
2229 A=B
 XPN(NN)=XPN(NN)+PH*XP(NN)
 IF (XPN(NN)<0.0D-000) GOTO 1159
 IN=IN+1
 CALL DET(XPN,ST,ALA)
 B=ALA
IF (B<A) GOTO 2229
 C=A
 XPN(NN)=XPN(NN)-PH*XP(NN)
 IF (IN>1) GOTO 3339
 PH=-PH
 GOTO 5559
3339 IF (ABS((C-B)/(B))<EP) GOTO 4449
  PH=PH/2.0D-000
5559 B=C
 GOTO 2229
4449 PH=PHN
 B=C
 IF (NN<NP) GOTO 1119
 AMIN=B
 PH=PH/NI
 ENDDO
3012  AMIN=B
 DO I=LMI,NP,LH
```

```
XP(I)=XPN(I)
ENDDO
END

SUBROUTINE DET(XP,ST,XI)
IMPLICIT REAL(8) (A - Z)
INTEGER I,N
DIMENSION XP(0:50),ST(0:50)
COMMON /B/ SE(0:50),DS(0:50),DE(0:50),N
! ********** DETERMINANT **********
S=0.0D-000
CALL SEC(XP,ST)
DO I=1,N
S=S+((ST(I)-SE(I))/DE(I))**2
DS(I)=((ST(I)-SE(I))/DE(I))**2
ENDDO
XI=S/N
END

SUBROUTINE SEC(XP,S)
IMPLICIT REAL(8) (A - Z)
INTEGER I,NP,LH,LMI,LMA,NT,NYS,L
DIMENSION S0(0:50),P(0:50),FR(0:50),ET(0:50), S(0:50),XP(0:50)
COMMON /A/ PI,NT,TT(0:50),GG,SS,LMI,LMA,LH,NYS,NP
! ********** CALCULATION OF THE CROSS SECTIONS ********
DO I=LMI,LMA,LH
FR(I)=XP(I)
ET(I)=1.0D-000
! IF NP=LMA GOTO 1234
! ET(I)=EXP(-2*XP(I+LMA+LH))
ENDDO
RECUL1=0.0D-000; AIMCUL1=0.0D-000
CALL CULFAZ(GG,S0)
DO I=1,NT
T=TT(I)*PI/180.0D-000
X=DCOS(T)
```

```
A=2.0D-000/(1-X)
S00=2.0D-000*S0(0)
BB=-GG*A
ALO=GG*DLOG(A)+S00
RECUL=BB*DCOS(ALO)
AIMCUL=BB*DSIN(ALO)
IF (NYS==0) GOTO 555
X1=DCOS(T)
A1=2.0D-000/(1.0D-000+X1)
BB1=-GG*A1
ALO1=GG*DLOG(A1)+S00
RECUL1=BB1*COS(ALO1)
AIMCUL1=BB1*SIN(ALO1)
555 RENUC=0.0D-000; AIMNUC=0.0D-000
DO L=LMI,LMA,LH
AL=ET(L)*DCOS(2.0D-000*FR(L))-1.0D-000
BE=ET(L)*DSIN(2.0D-000*FR(L))
LL=2.0D-000*L+1.0D-000
SL=2.0D-000*S0(L)
CALL POLLEG(X,L,P)
RENUC=RENUC+LL*(BE*DCOS(SL)+AL*DSIN(SL))*P(L)
AIMNUC=AIMNUC+LL*(BE*DSIN(SL)-AL*DCOS(SL))*P(L)
ENDDO
IF (NYS==0) GOTO 556
AIMNUC=2.0D-000*AIMNUC
RENUC=2.0D-000*RENUC
556 RE=RECUL+RECUL1+RENUC
AIM=AIMCUL+AIMCUL1+AIMNUC
S(I)=10.0D-000*(RE**2+AIM**2)/4.0D-000/SS**2
ENDDO
END

SUBROUTINE POLLEG(X,L,P)
IMPLICIT REAL(8) (A - Z)
INTEGER I,L
DIMENSION P(0:50)
```

```
! ************** THE LEGENDRE POLINOMIALS *************
P(0)=1.0D-000
P(1)=X
DO I=2,L
A=I*1.0D-000
P(I)=(2.0D-000*A-1)*X/A*P(I-1)-(A-1.0D-000)/A*P(I-2)
ENDDO
END

SUBROUTINE CULFAZ(G,F)
! ************** THE COULOMB PHASE SHIFTS **************
IMPLICIT REAL(8) (A - Z)
INTEGER I
DIMENSION F(0:50)
C=0.577215665D-000
S=0.0D-000; N=50
A1=1.202056903D-000/3.0D-000
A2=1.0369277550D-000/5.0D-000
DO I=1,N
AA=I*1.0D-000
A=G/AA-DATAN(G/AA)-(G/AA)**3/3.0D-000+(G/AA)**5/5.0D-000
S=S+A
ENDDO
FAZ=-C*G+A1*G**3-A2*G**5+S
F(0)=FAZ
DO I=1,20
A=I*1.0D-000
F(I)=F(I-1)+DATAN(G/A)
ENDDO
END
```

Furthermore, the control account of search the ^{4}He^{4}He elastic scattering phase shifts for the energy of 13 MeV, at which in work [88] the phase shifts $\delta_0 = 29° \pm 4°$, $\delta_2 = 103° \pm 8°$, $\delta_4 = 3° \pm 1.5°$ have been obtained, is provided. These phase shifts are accepted as initial, and at their further variation with 10 iterations, both according to the previous program in the

Turbo Basic [10] language, and on the basis of the program given above, we find $\delta_0 = 28.37°$, $\delta_2 = 105.03°$, $\delta_4 = 2.62°$ at $\chi^2 = 3.43$, that is clear from the listing of work of the program given further in the Fortran-90 language

χ^2	NI
3.943880354539536	1
3.437578175376997	2
3.432394633290976	3
3.432107724455588	4
3.432044190539325	5
3.432020692528544	6
3.432007556422437	7
3.432005733725609	8
3.432004938728721	9
3.432004743298262	10

χ^2 = ; NI = ; EL = 3.43200 10 1300

θ	σ_e	σ_t	χ^2_i
.22000E+02	.13570E+04	.12796E+04	.39401E+01
.24000E+02	.12030E+04	.11346E+04	.29238E+01
.26000E+02	.10740E+04	.10008E+04	.93096E+01
.28000E+02	.87000E+03	.87464E+03	.53776E-01
.30000E+02	.75900E+03	.75523E+03	.55540E-01
.32000E+02	.68800E+03	.64266E+03	.71117E+01
.35000E+02	.46700E+03	.48793E+03	.30429E+01
.40000E+02	.27100E+03	.27340E+03	.11779E+00
.42000E+02	.19600E+03	.20443E+03	.42244E+01
.45000E+02	.13000E+03	.12007E+03	.76028E+01
.46000E+02	.93900E+02	.97112E+02	.21321E+01
.48000E+02	.57000E+02	.58891E+02	.15896E+01
.50000E+02	.32500E+02	.30767E+02	.24826E+01
.52000E+02	.12300E+02	.12398E+02	.95282E-02
.55000E+02	.22800E+01	.20301E+01	.39027E+00
.60000E+02	.24700E+02	.24774E+02	.11250E-01
.65000E+02	.86500E+02	.85514E+02	.24313E+00

.70000E+02	.15700E+03	.16800E+03	.93323E+01
.75000E+02	.27000E+03	.25509E+03	.52640E+01
.80000E+02	.33700E+03	.33073E+03	.71799E+00
.85000E+02	.40800E+03	.38184E+03	.10177E+02
.90000E+02	.41800E+03	.39987E+03	.47720E+01

L	δ_r	δ_m
0	.283717E+02	.000000E+00
2	.105030E+03	.000000E+00
4	.261561E+01	.000000E+00

Here in the listing of results the following designations are accepted: θ – the scattering angle, σ_e – experimental cross sections, σ_t – the calculated cross sections, χ^2_i – partial χ^2 for *i*-th of the angle, δ_r – real part of the phase shift, δ_m – imaginary part of the phase shift, χ^2 – average value on all points, EL – energy in the laboratory system.

In the first line, at the printing of phase shifts the orbital moment $L = 0$, in the second $L = 2$ and in the third $L = 4$ is specified. For the search of a minimum, as well as in work [10], the 10 iterations NI are used. Only in this case the accuracy of the EP was set equal to 10^{-10}, and in the previous version of score 10^{-5} [10]. The first χ^2 and NI columns of the given listing show the convergence of χ^2 from the number of iteration NI.

Furthermore, the control account is provided for the energy of 29.5 MeV, for which in [10] according to the program on Basic have been obtained the phase shifts $\delta_0 = 150.76$, $\delta_2 = 86.61$, $\delta_4 = 121.00$, $\delta_6 = 2.16$, $\delta_8 = 0.09$ with $\chi^2 = 0.602$, provided in tab. 2.1.1. With such phase shifts according to the program given above $\chi^2 = 0.600$ is turned out as it is clear from the listing shown below with number of iterations NI = 0

$\chi^2 =$; NI = 0; EL = 0.600328 0 29.50

θ	σ_e	σ_t	χ^2_i
.22040E+02	.15230E+04	.15134E+04	.64891E+00
.24050E+02	.11640E+04	.11664E+04	.55570E-01
.26050E+02	.88590E+03	.86843E+03	.38892E+01

.28050E+02	.61610E+03	.61957E+03	.23236E+00
.30060E+02	.42260E+03	.41922E+03	.35643E+00
.32060E+02	.27000E+03	.26762E+03	.34211E+00
.34060E+02	.16020E+03	.16006E+03	.24306E-02
.36070E+02	.91500E+02	.91163E+02	.44395E-01
.38070E+02	.55530E+02	.55230E+02	.16734E+00
.40070E+02	.44680E+02	.44765E+02	.12421E+00
.42080E+02	.52960E+02	.52530E+02	.76193E+00
.44080E+02	.71740E+02	.71346E+02	.28489E+00
.46080E+02	.95440E+02	.94808E+02	.57926E+00
.48080E+02	.11846E+03	.11754E+03	.12657E+01
.50090E+02	.13558E+03	.13552E+03	.72584E-02
.52090E+02	.14562E+03	.14590E+03	.26152E+00
.54090E+02	.14760E+03	.14758E+03	.53350E-03
.56090E+02	.13986E+03	.14072E+03	.14564E+01
.58100E+02	.12710E+03	.12655E+03	.43671E+00
.60100E+02	.10783E+03	.10745E+03	.23062E+00
.62100E+02	.86660E+02	.86114E+02	.46841E+00
.64100E+02	.66120E+02	.65522E+02	.75651E+00
.66100E+02	.48430E+02	.48481E+02	.10080E-01
.68110E+02	.37430E+02	.37301E+02	.17753E+00
.70110E+02	.33770E+02	.33732E+02	.43056E-01
.72110E+02	.38340E+02	.38461E+02	.13210E+00
.74110E+02	.50740E+02	.51308E+02	.10928E+01
.76110E+02	.70820E+02	.71187E+02	.24362E+00
.78110E+02	.95550E+02	.96239E+02	.60125E+00
.80110E+02	.12420E+03	.12403E+03	.27579E-01
.82110E+02	.15340E+03	.15182E+03	.22344E+01
.84110E+02	.17750E+03	.17683E+03	.42129E+00
.86110E+02	.19700E+03	.19657E+03	.17685E+00
.88110E+02	.20974E+03	.20905E+03	.51222E+00
.90110E+02	.21120E+03	.21302E+03	.29660E+01

L	δ_r	δ_m
0	.150760E+03	.000000E+00
2	.866100E+02	.000000E+00

4	.121000E+03	.000000E+00
6	.216000E+01	.000000E+00
8	.900000E-01	.000000E+00

The difference of the value χ^2 at 0.02 is connected with errors of rounding of phase shifts at record of their values in the file from the program on Turbo Basic and their further use in the program in the Fortran-90 language. Hereinafter the imaginary part of the phase shift δ_m is equal to zero for all values of the orbital moment in this paragraph.

Using these phase shifts as initial, at an additional variation according to the new program on Fortran-90 given above with 10 iterations and with a greatest possible accuracy of 10^{-15}, we obtain the result given further for phase shifts with the smallest χ^2 value

$\chi^2 =$; NI = ; EL = 0.571434 10 29.500

θ	σ_e	σ_t	χ^2_i
.22040E+02	.15230E+04	.15144E+04	.52763E+00
.24050E+02	.11640E+04	.11671E+04	.90939E-01
.26050E+02	.88590E+03	.86891E+03	.36792E+01
.28050E+02	.61610E+03	.61990E+03	.27763E+00
.30060E+02	.42260E+03	.41943E+03	.31337E+00
.32060E+02	.27000E+03	.26775E+03	.30469E+00
.34060E+02	.16020E+03	.16015E+03	.33034E-03
.36070E+02	.91500E+02	.91219E+02	.30734E-01
.38070E+02	.55530E+02	.55273E+02	.12333E+00
.40070E+02	.44680E+02	.44803E+02	.25848E+00
.42080E+02	.52960E+02	.52569E+02	.62951E+00
.44080E+02	.71740E+02	.71391E+02	.22342E+00
.46080E+02	.95440E+02	.94863E+02	.48325E+00
.48080E+02	.11846E+03	.11761E+03	.10869E+01
.50090E+02	.13558E+03	.13560E+03	.13302E-02
.52090E+02	.14562E+03	.14600E+03	.47518E+00
.54090E+02	.14760E+03	.14770E+03	.17885E-01
.56090E+02	.13986E+03	.14085E+03	.19094E+01
.58100E+02	.12710E+03	.12668E+03	.25354E+00

.60100E+02	.10783E+03	.10757E+03	.10341E+00
.62100E+02	.86660E+02	.86228E+02	.29377E+00
.64100E+02	.66120E+02	.65613E+02	.54400E+00
.66100E+02	.48430E+02	.48542E+02	.48101E-01
.68110E+02	.37430E+02	.37326E+02	.11519E+00
.70110E+02	.33770E+02	.33722E+02	.70632E-01
.72110E+02	.38340E+02	.38419E+02	.55430E-01
.74110E+02	.50740E+02	.51240E+02	.84900E+00
.76110E+02	.70820E+02	.71105E+02	.14712E+00
.78110E+02	.95550E+02	.96154E+02	.46141E+00
.80110E+02	.12420E+03	.12395E+03	.59440E-01
.82110E+02	.15340E+03	.15175E+03	.24240E+01
.84110E+02	.17750E+03	.17678E+03	.48540E+00
.86110E+02	.19700E+03	.19654E+03	.20525E+00
.88110E+02	.20974E+03	.20903E+03	.54586E+00
.90110E+02	.21120E+03	.21300E+03	.29054E+01

L	δ_r	δ_m
0	.150729E+03	.000000E+00
2	.865625E+02	.000000E+00
4	.120914E+03	.000000E+00
6	.211725E+01	.000000E+00
8	.662343E-01	.000000E+00

Apparently, here it is possible to reduce χ^2 to 0.571 that possible thanks to essential raised, in comparison with programs on Basic from work [10], the accuracy of search a minimum of such multiparameter variation problem.

2.2 Phase shift analysis of the $^4He^{12}C$ elastic scattering

Now we will consider the methods of the phase shift analysis for the nonidentical particles with spins 0 + 0 and results of the phase shift analysis for elastic scattering in the $^4He^{12}C$ system at astrophysical energies. For obtaining these results the same computer program, as for the $^4He^4He$ elastic scattering, but with other program parameters (see paragraph 2.1.4) was used [99].

2.2.1 Differential cross sections

In case of the elastic scattering of the nonidentical particles with zero spin the expression for cross section takes the simplest form [6]

$$\frac{d\sigma(\theta)}{d\Omega} = \left|f(\theta)\right|^2,$$

where the total scattering amplitude $f(\theta)$ is presented in the form of sum of the Coulomb $f_c(\theta)$ and nuclear $f_N(\theta)$ amplitudes

$$f(\theta) = f_c(\theta) + f_N(\theta),$$

which are expressed through the nuclear $\delta_L \rightarrow \delta_L + i\Delta_L$ and Coulomb σ_L scattering phase shifts, and the form of amplitudes is given in the beginning of this chapter (see paragraph 2.1.2).

For the cross section of the elastic scattering at $f_c = 0$ the expression is known

$$\sigma_s = \frac{\pi}{k^2}\sum_L\left[(2L+1)\left(\left|1-S_L\right|^2\right)\right] = \frac{4\pi}{k^2}\sum_L(2L+1)\eta_L^2\sin^2\delta_L . \qquad (2.2.1)$$

The summation in this expression, unlike from the $^4He^4He$ scattering, is carried out by all possible L.

2.2.2 Phase shift analysis

We will give the results of the phase shift analysis obtained for the $^4He^{12}C$ elastic scattering in the energy range from 1.5 MeV to 6.5 MeV. Earlier the phase shift analysis of the differential cross sections at the energies of 2.5–5.0 MeV has been carried out in work [100]. The potential description of such scattering phase shifts on the basis of potentials with the forbidden states has been executed by us in work [101]. Here, using the experimental data on the excitation functions at seven angles from [100], we have repeated the phase shift analysis [100] in the energy range of 2.5–4.5 MeV. These results can be considered as the control test for our new computer program for Fortran-90 and the calculation methods used by us. We will notice that the measurement of excitation functions at such small amount of points on the scattering angles of is not enough for the reproducing the shape of angular distributions of $^4He^{12}C$ elastic scattering even at low energies with a good accuracy. Therefore, it is possible that the phase shift analysis does not allow one to obtain completely unambiguous values of the phase shifts, especially for the S waves in spite of the fact that as the initial phase shifts the known results of the phase shift analysis have been used [100].

The results of our analysis are given further in Fig.2.2.1 – Fig.2.2.5 by points. In Fig.2.2.1 together with the S phase shift the values of an average χ^2, which are obtained for the various scattering energies, are shown. As can be seen from these figures, the S phase shift differs from the data of work [100], shown by the solid curve, and phase shifts in all others partial waves will quite be coordinated by results [100]. However, as, the data on excitation functions undertook from figures of work [100], the possible error in the present phase shift analysis depending on the accuracy of data on cross sections can make about 2°–3° that in general allows to explain a divergence in results of these two phase shift analyses for the S elastic scattering phase shifts.

Furthermore, in work [102], the very accurate phase shift analysis of the experimental data at 49 energies in the range from 1.5 to 6.5 MeV has been made. Using these data, we have carried out the phase shift analysis at 1.466, 1.973, 2.073, 2.870, 3.371, 4.851, 5.799 and 6.458 MeV.

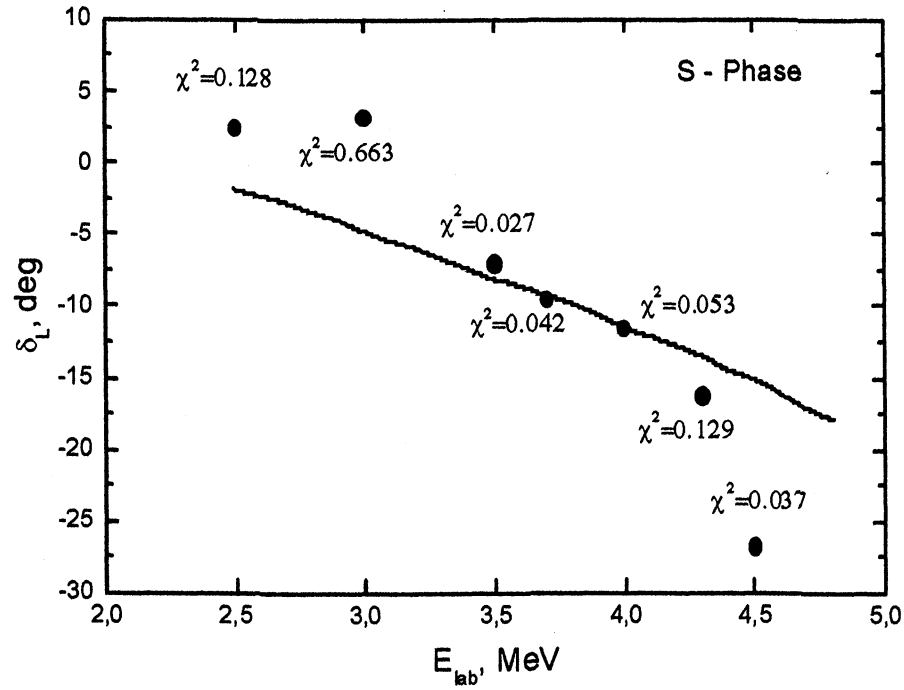

Fig.2.2.1. *S* phase shift of the $^4He^{12}C$ elastic scattering. A curve – data from [100]. Points – our results obtained on the basis of data [100].

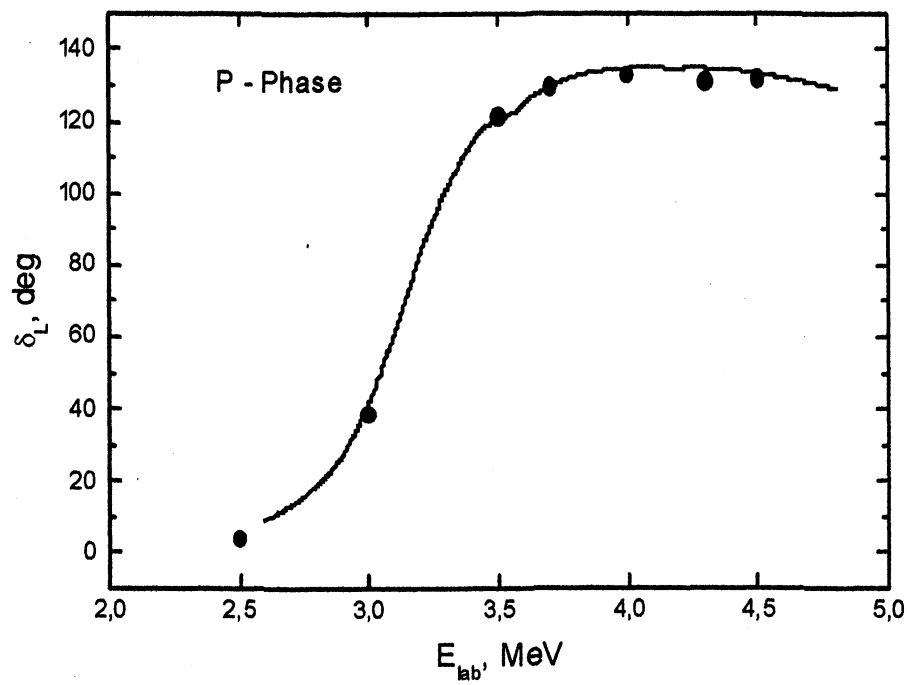

Fig. 2.2.2. *P* phase shift of the $^4He^{12}C$ elastic scattering. Designations, as in Fig. 2.2.1.

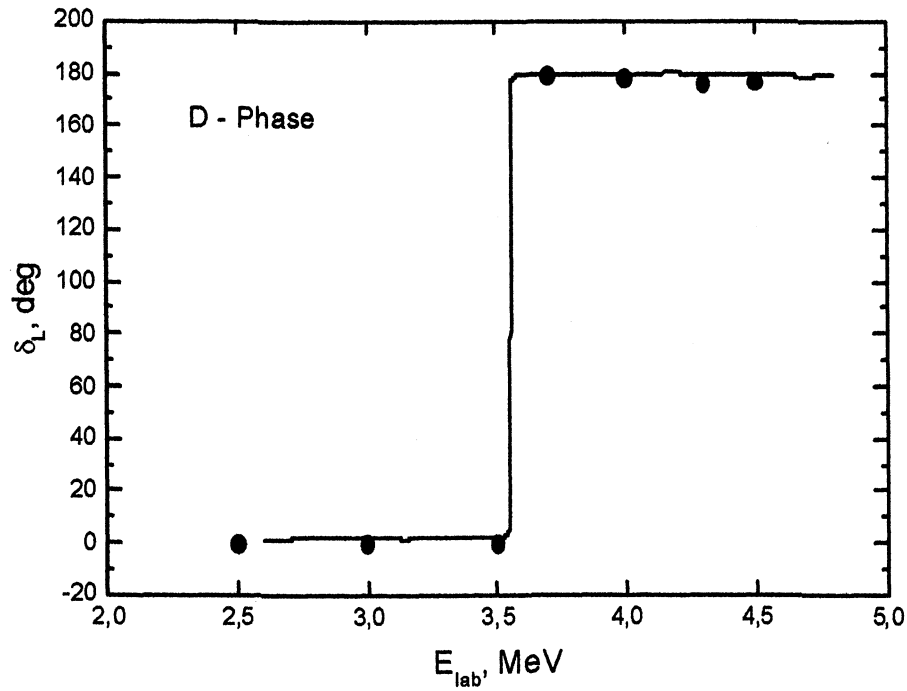

2.2.3. *D* phase shift of the $^4He^{12}C$ elastic scattering. Designations, as in Fig. 2.2.1.

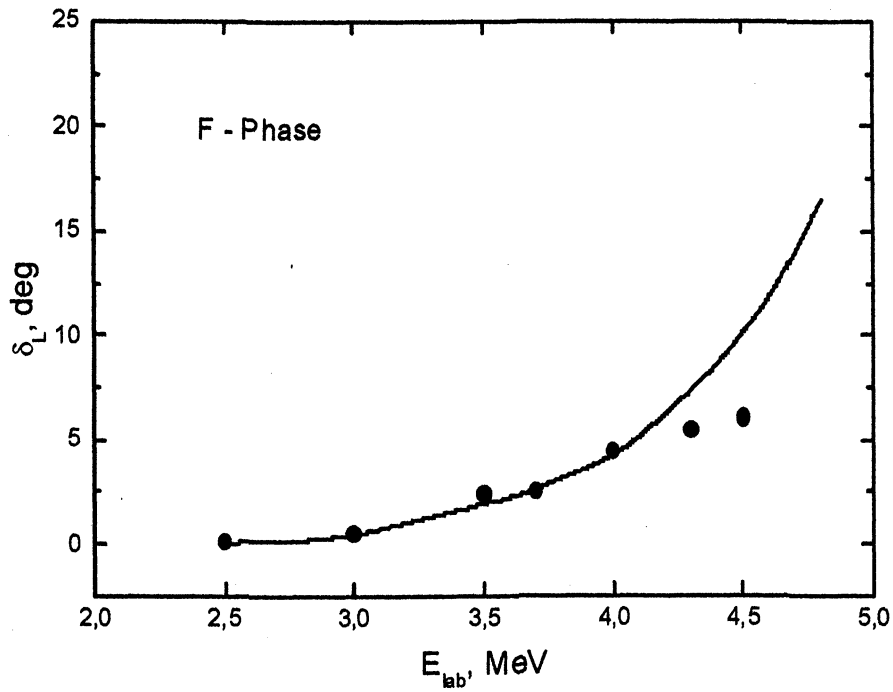

Fig. 2.2.4. *F* phase shift of the $^4He^{12}C$ elastic scattering. Designations, as in Fig. 2.2.1.

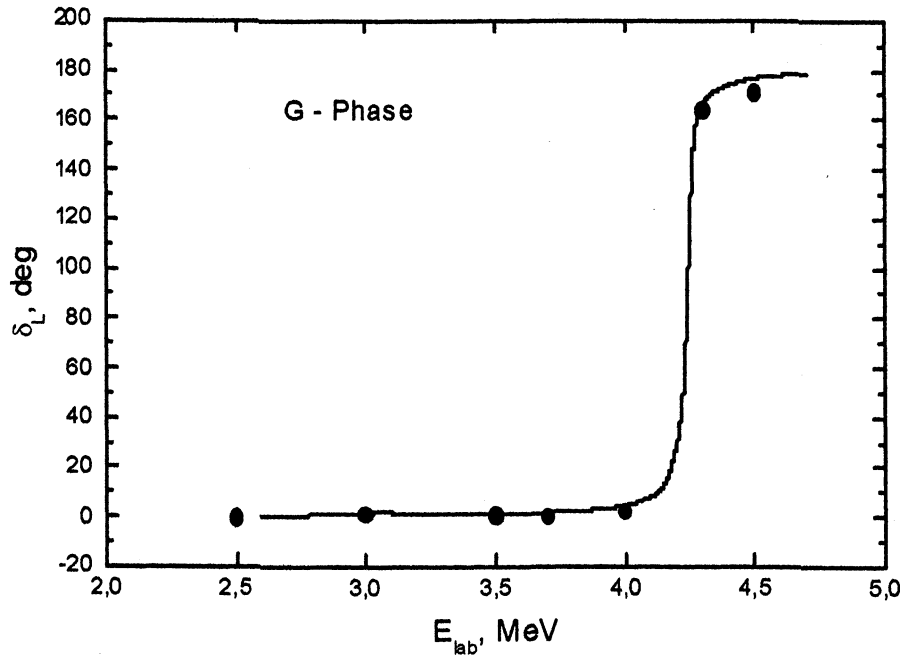

Fig. 2.2.5. *G* phase shift of the $^4He^{12}C$ elastic scattering. Designations, as in Fig.2.2.1.

The results obtained in our analysis are presented in tab.2.2.1 – tab.2.2.8 together with average χ^2 values in comparison with tabular data of work [102]. The spectrum of resonance levels and their widths observed in the $^4He^{12}C$ elastic scattering and given in the review is shown in tab. 2.2.9 [103].

Tab.2.2.1. The results of the phase shift analysis of the $^4He^{12}C$ elastic scattering and their comparison with data of work [102] at energy of 1.466 MeV.

E_{lab} = 1.466 MeV (χ^2 = 0.055)		
L	δ° (Our)	δ° [102]
0	-0.2	0.5±1.0
1	-0.4	-0.1±1.0
2	-1.1	-0.8±1.0

Tab.2.2.2. The results of the phase shift analysis of the $^4He^{12}C$ elastic scattering and their comparison with data of work [102] at energy of 1.973 MeV.

E_{lab} = 1.973 MeV (χ^2 = 0.077)		
L	δ° (Our)	δ° [102]
0	-2.6	-0.5±1.0
1	0.0	0.9±1.7
2	1.2	-0.1±1.3

Tab.2.2.3. The results of the phase shift analysis of the $^4He^{12}C$ elastic scattering and their comparison with data of work [102] at energy of 2.073 MeV.

E_{lab} = 2.073 MeV (χ^2 = 0.029)		
L	δ° (Our)	δ° [102]
0	-1.2	0±0.8
	-0.1	0.1±1.2
2	-1.1	-0.6±0.9

Tab.2.2.4. The results of the phase shift analysis of the $^4He^{12}C$ elastic scattering and their comparison with data of work [102] at energy of 2.870 MeV.

E_{lab} = 2.870 MeV (χ^2 = 0.038)		
L	δ° (Our)	δ° [102]
0	-3.1	-1±1.1
1	21.3	22.0±1
2	0.0	0.4±0.9
3	0.5	1.0±0.5

Tab.2.2.5. The results of the phase shift analysis of the $^4He^{12}C$ elastic scattering and their comparison with data of work [102] at energy of 3.371 MeV.

E_{lab} = 3.371 MeV (χ^2 = 0.1)		
L	δ° (Our)	δ° [102]
0	169.4	-
1	103.4	103.7±1.7
2	-1.7	0.0±0.7
3	0.2	0.8±0.6

Tab.2.2.6. The results of the phase shift analysis of the $^4He^{12}C$ elastic scattering and their comparison with data of work [102] at energy of 4.851 MeV.

E_{lab} = 4.851 MeV (χ^2 = 0.26)		
L	δ° (Our)	δ° [102]
0	164.2	164±1.1
1	128.4	129.5±0.9
2	177.1	178.8±0.9
3	15 5	16.4±0.8
4	176.9	177.2±0.8
5	-0.3	0.5±0.5

Tab.2.2.7. The results of the phase shift analysis of the $^4He^{12}C$ elastic scattering and their comparison with data of work [102] at energy of 5.799 MeV.

E_{lab} = 5.799 MeV (χ^2 = 0.37)		
L	Reδ° (Our)	Reδ°

Tab.2.2.8. The results of the phase shift analysis of the $^4He^{12}C$ elastic scattering and their comparison with data of work [102] at energy of 6.458 MeV.

E_{lab} = 6.458 MeV (χ^2 = 0.41)		
L	δ° (Our)	δ°

0	162	-
1	128.2	-
2	83.2	83±0.6
3	86.0	-
4	173.8	175.3±0.7
5	-1.0	0.2±0.4

0	151.2	153±5
1	11 .8	119.4±1
2	172	172±1.9
3	120.8	122.0±4
4	176.4	179.1±1.2
5	0.8	2±0.8
6	0.1	0.4±0.4

From these tables it is clear that the $^4He^{12}C$ scattering energy of 3.371 MeV falls on the level of 3.324 MeV with a width of 480±20 keV specified in tab. 2.2.9 and the review [103]. Though in tables of work [102] the phase shift for S waves is not given (dashes in tab. 2.2.5) at this energy, our phase shift analysis on the basis of only the real phase shifts of scattering allows to define all scattering phase shifts.

Tab. 2.2.9. A spectrum of levels of ^{16}O in the $^4He^{12}C$ elastic scattering with the T=0 isospin [103]. Here J^π – the total moment and parity, E_{lab} – the energy of the projectile particle in the laboratory system, Γ_{cm} – level width in system of the center of masses. In the table levels with a width less than 1 keV are italicized, and the state shown in bold, which are discussed in the text.

E_{lab}, MeV	J^π	Γ_{cm}, keV
3.324	**1^-**	**480±20**
3.5770±0.5	*2^+*	*0.625±0.1*
4.259	4^+	27±3
5.245±8	*4^+*	*0.28±0.05*
5.47	0^+	2500
5.809±18	**2^+**	**73±5**
5.92±20	3^-	800±100
6.518±10	0^+	1.5±0.5
7.043±4	1^-	99±7

The energy of 5.799 MeV falls on the level of 5.809±18 MeV with a width of 73(3) keV [103] (see tab. 2.2.9) and in tables of work [102] the values of scattering phase shifts for some partial waves are not given (dashes in tab. 2.2.7). In the phase shift analysis, which is carried out here it

is quite possible to describe these differential elastic scattering cross sections with average value of $\chi^2 = 0.37$ and find all partial phase shifts as it is shown in tab. 2.2.7. The non-resonance energy at 2.870, 4.851 and 6.458 MeV (see tab. 2.2.4, 2.2.6, 2.2.8) are described by phase shifts, which in the limits given in [102] errors and taking into account possible 10% errors of our extraction of experimental data from figures [102] coincide with results of work [102]. The last three energy of 1.466, 1.973 and 2.073 MeV (see tab. 2.2.1, 2.2.2, 2.2.3) are compatible to zero values of nuclear phase shifts, i.e. have ±1° values, and correspond to purely Coulomb, i.e. the Rutherford scattering.

In Figs. 2.2.6–2.2.13 are shown the quality of the description of the experimental differential cross sections of the $^4He^{12}C$ elastic scattering [102] with given in tab.2.2.8–2.2.1 scattering phase shifts at all considered energies. In the process of our phase shift analysis it was necessary to transfer the differential cross sections and angles given in work [102] in laboratory system to system of the center of masses, which is most convenient for calculations. The small differences in the scattering phase shifts can be caused, besides, by various values of constants or mass of particles which are used in such analysis. For example, it is possible to use the exact values of mass of particles [75] or their entire quantities, and the constant $\hbar^2/m_0$ can differ from 41.4686 MeV fm^2. Besides, the accuracy of definition of scattering phase shifts, in the carried out phase shift analysis, on the basis of data [102] is estimated by us at the level of 1°–2°.

The comparison of results of the last phase shift analysis [104], the obtained on the basis of experimental data of work [102] (points) and phase shift analysis of work [100] (squares) is given in Figs. 2.2.14 – 2.2.18. As seen from the given results in tab.2.2.1–tab.2.2.8 and Fig.2.2.14–Fig.2.2.18, the obtained phase shifts coincide practically with conclusions of work [102], but differ a little from data [100], especially in the *S* scattering wave. In general, it is clear as the analysis [100] was made in the early sixties of the XX century when the computer facilities in modern understanding of this word still practically did not exist, and the program and computing means only began to develop. At the same time, work [102] has been performed in the late eighties of the last century at quite developed computer and program systems and means.

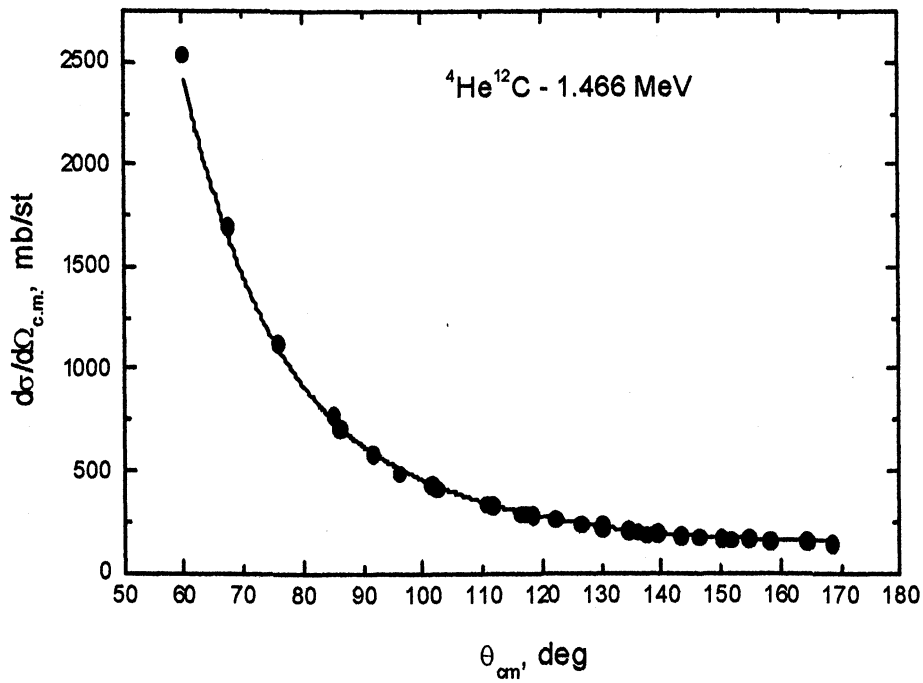

Fig. 2.2.6. Cross sections of the $^4He^{12}C$ elastic scattering at 1.466 MeV. Points – experimental data of work [102], a curve – results of our phase shift analysis.

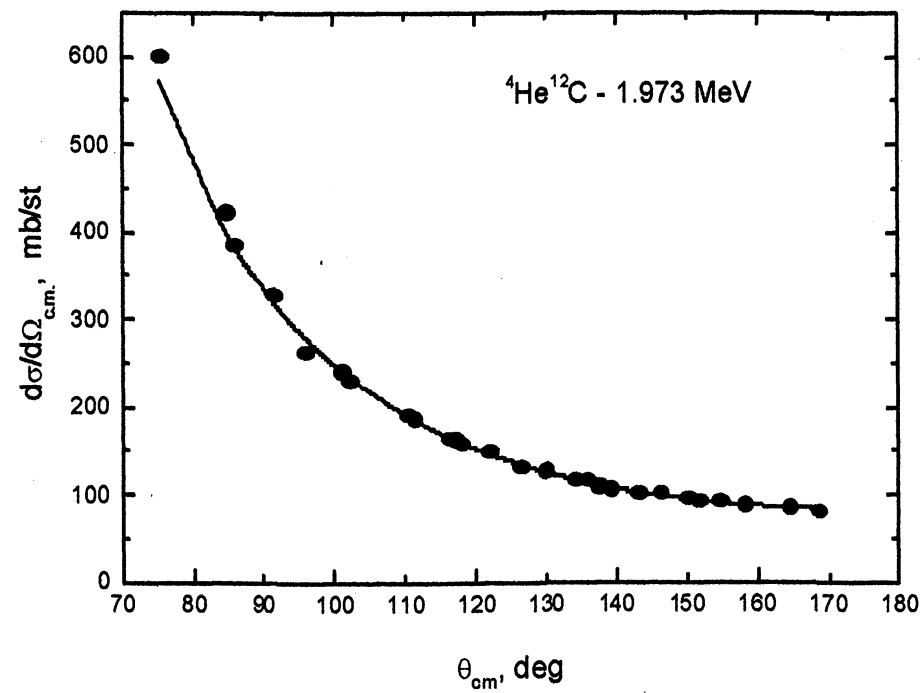

Fig. 2.2.7. The same as in Fig. 2.2.6, but at energy of 1.973 MeV.

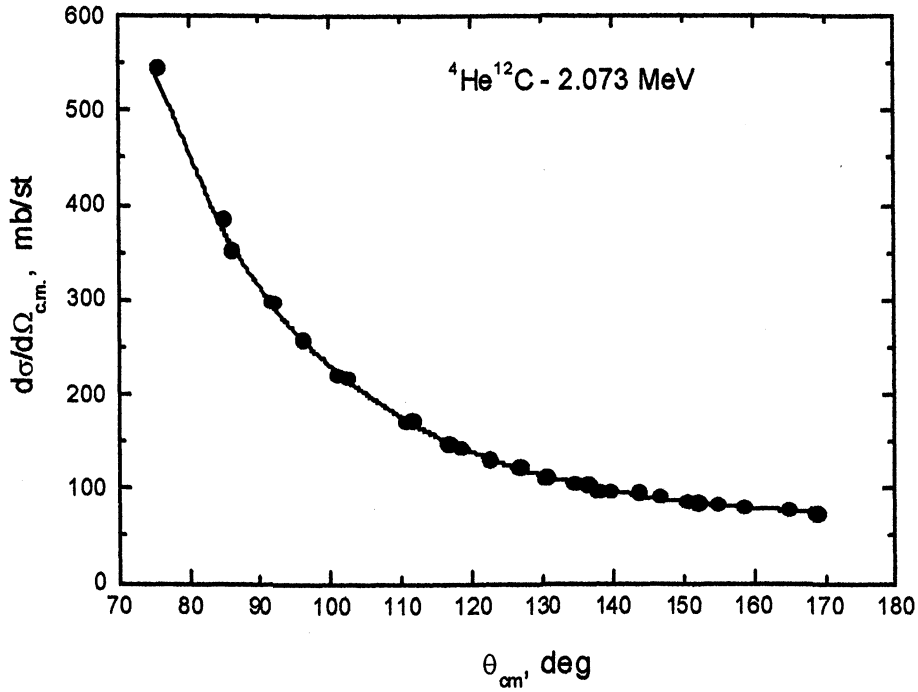

Fig. 2.2.8. The same as in Fig. 2.2.6, but at energy of 2.073 MeV.

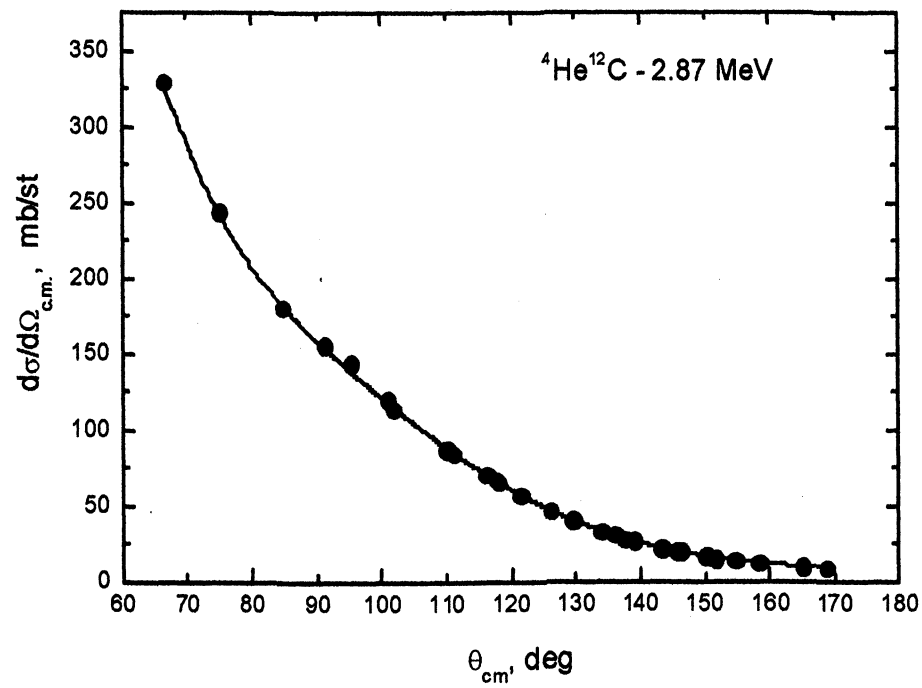

Fig. 2.2.9. The same as in Fig. 2.2.6, but at energy of 2.87 MeV.

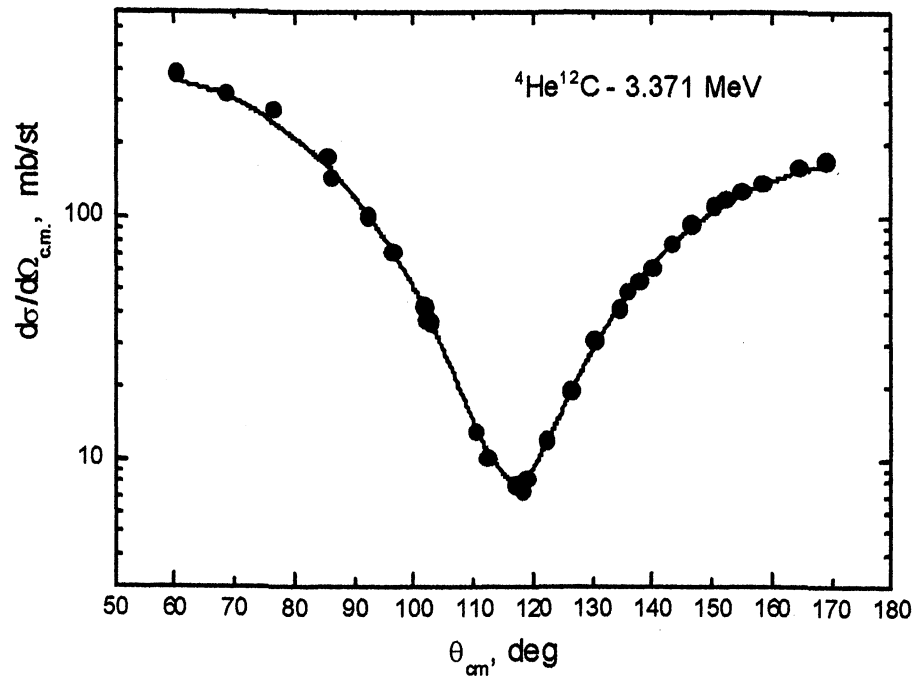

Fig. 2.2.10. The same as in Fig. 2.2.6, but at energy of 3.371 MeV.

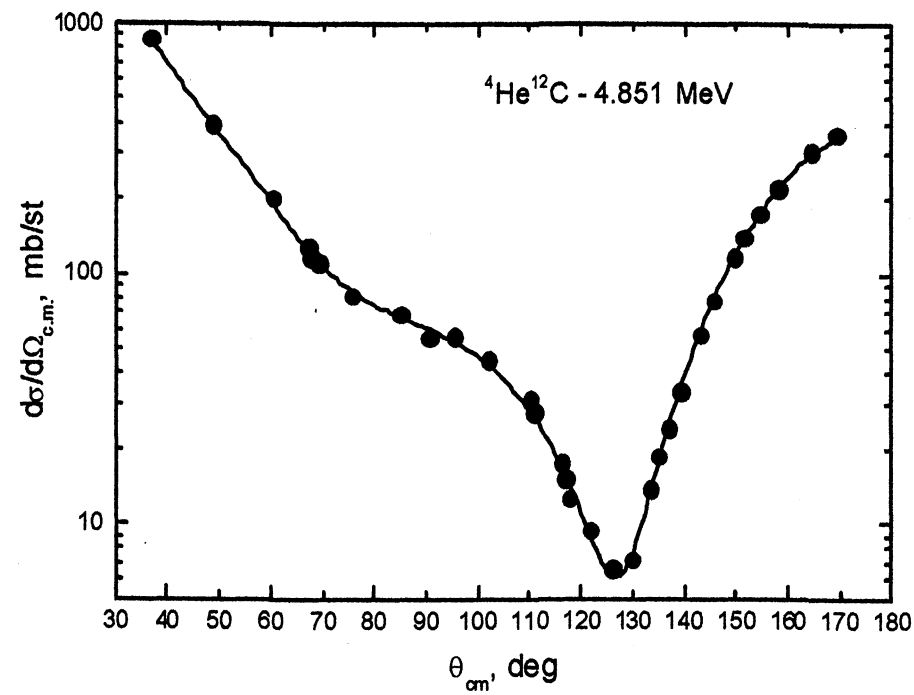

Fig. 2.2.11. The same as in Fig. 2.2.6, but at energy of 4.851 MeV.

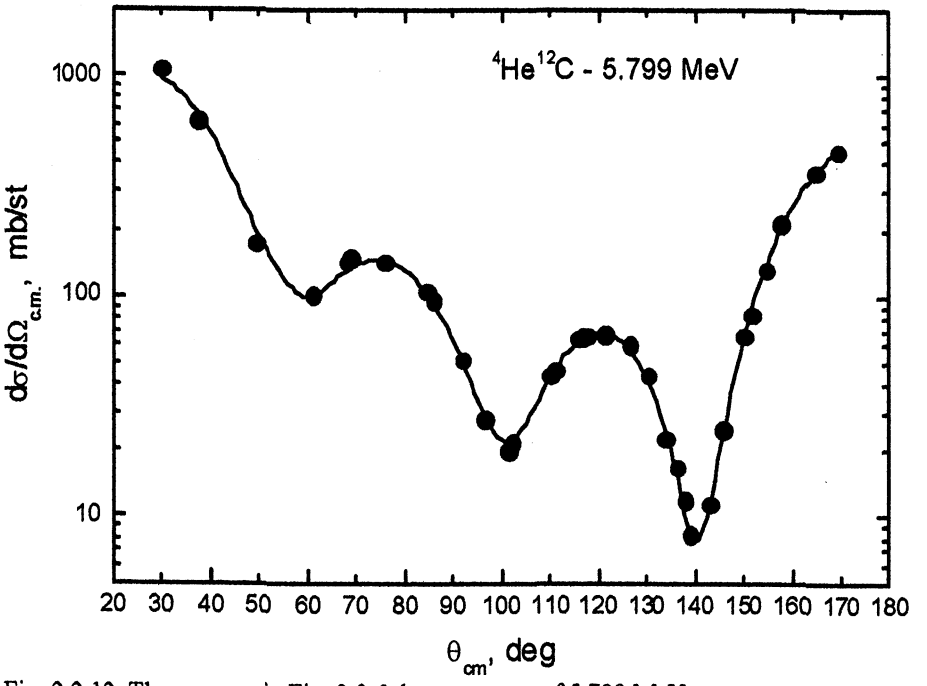

Fig. 2.2.12. The same as in Fig. 2.2.6, but at energy of 5.799 MeV.

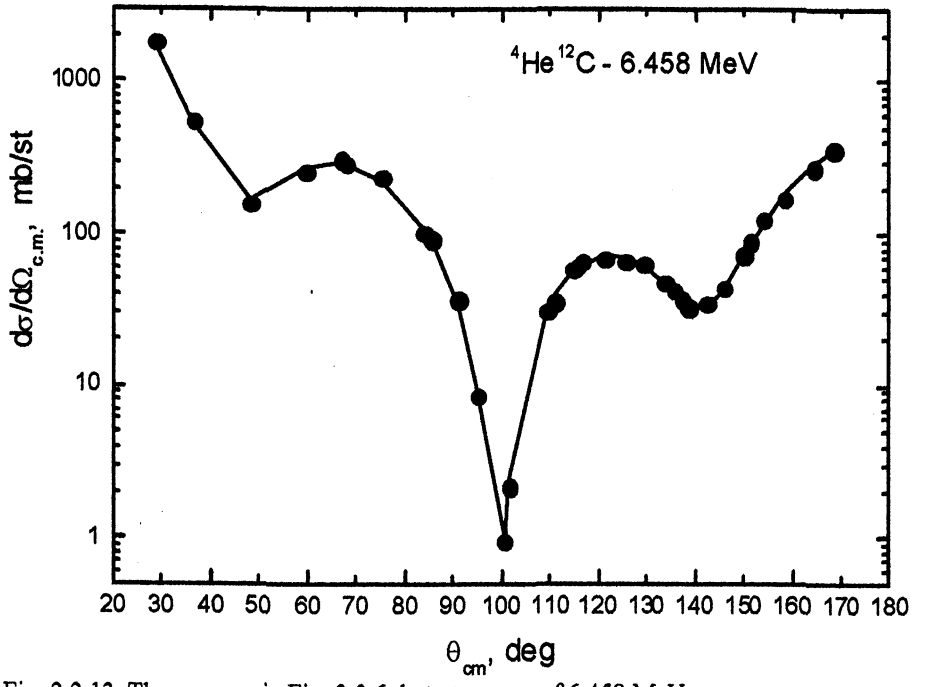

Fig. 2.2.13. The same as in Fig. 2.2.6, but at energy of 6.458 MeV.

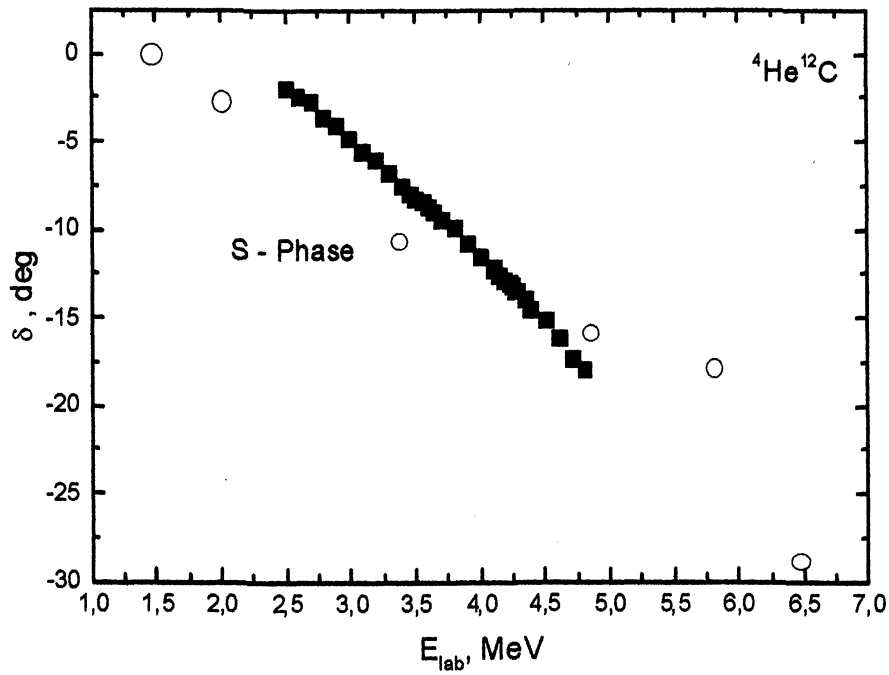

Fig. 2.2.14. The *S* phase shift of the ^{4}He^{12}C elastic scattering. Squares – data from work [100]. Circles – our results [104] obtained on the basis of data [102].

Thus, as a result of the phase shift analysis made here it is possible to draw the following conclusions:

1. The energy of 3.371 MeV falls on the level of 3.324 MeV with quite big width of 0.48 MeV and in the *P* wave the smooth resonance is well looked through.

2. According to works [100,102] in the *D* wave the resonance, which corresponds to the level at 3.577 MeV with very small width of 0.625 keV is observed. At this energy in Fig.2.2.16 the transition of the phase shift through 90°, provided also in tab.2.2.5 and 2.2.6, is observed. In addition, in results of analysis [102] another one resonance is appeared at 5.799 MeV, because at this energy in the *D* wave there is level of 5.809 MeV with relatively large width of 73 keV. For this energy the value of the phase shift (see tab.2.2.7) almost equals 90°. As a result the *D* phase shift given in Fig.2.2.16 passes through 90° twice, i.e. corresponds to two resonances, which are present at this partial wave.

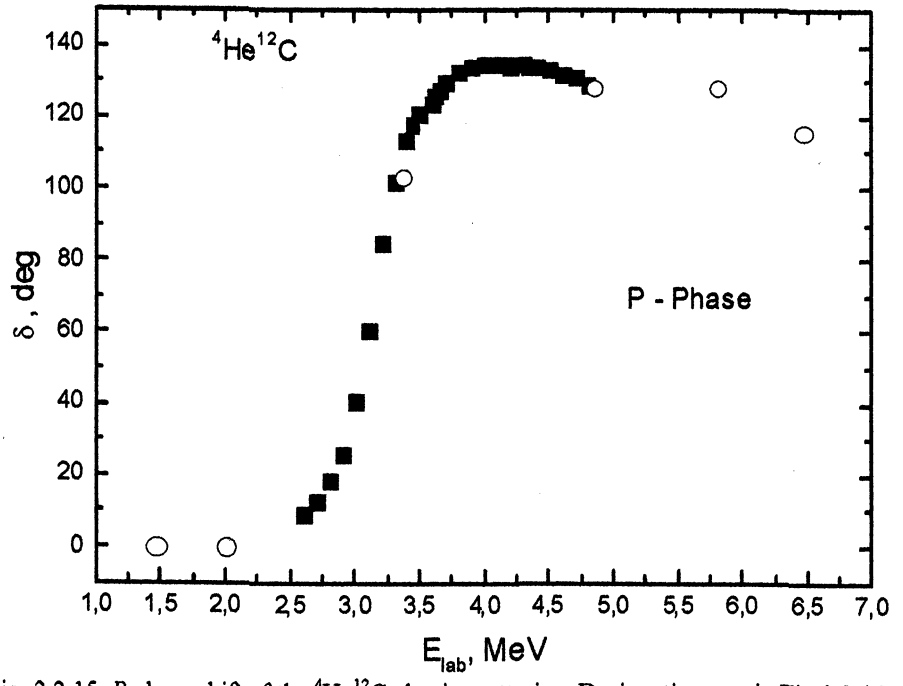

Fig. 2.2.15. *P* phase shift of the $^4He^{12}C$ elastic scattering. Designations, as in Fig.2.2.14.

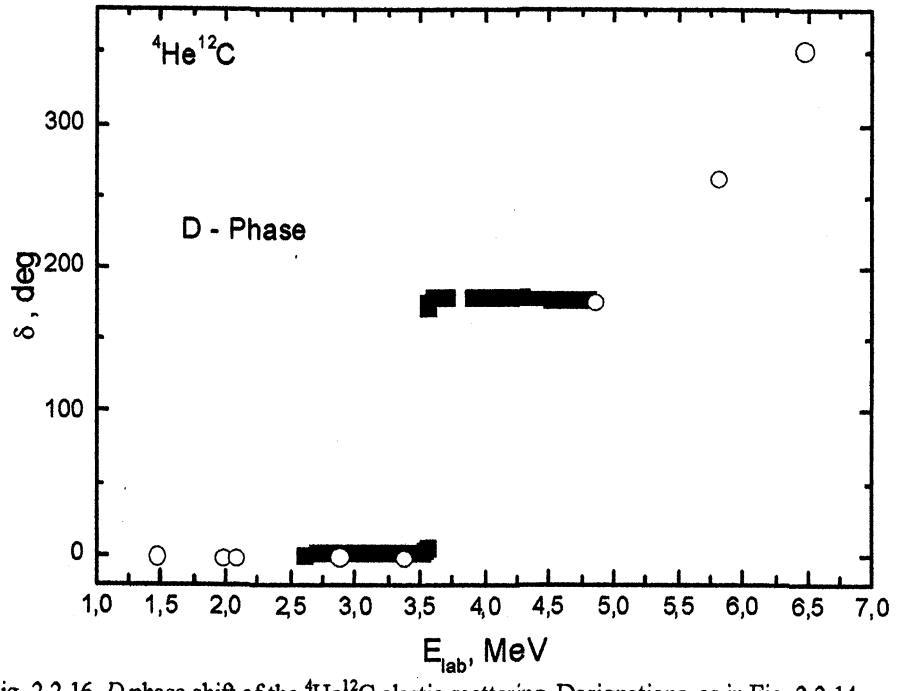

Fig. 2.2.16. *D* phase shift of the $^4He^{12}C$ elastic scattering. Designations, as in Fig. 2.2.14.

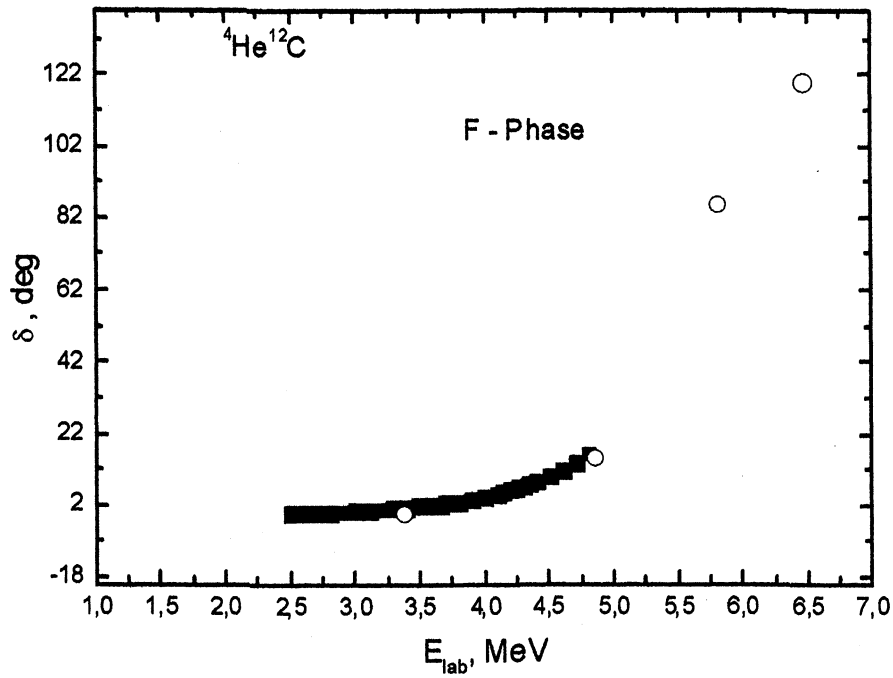

Fig. 2.2.17. *F* phase shift of the ^{4}He^{12}C elastic scattering. Designations, as in Fig. 2.2.14.

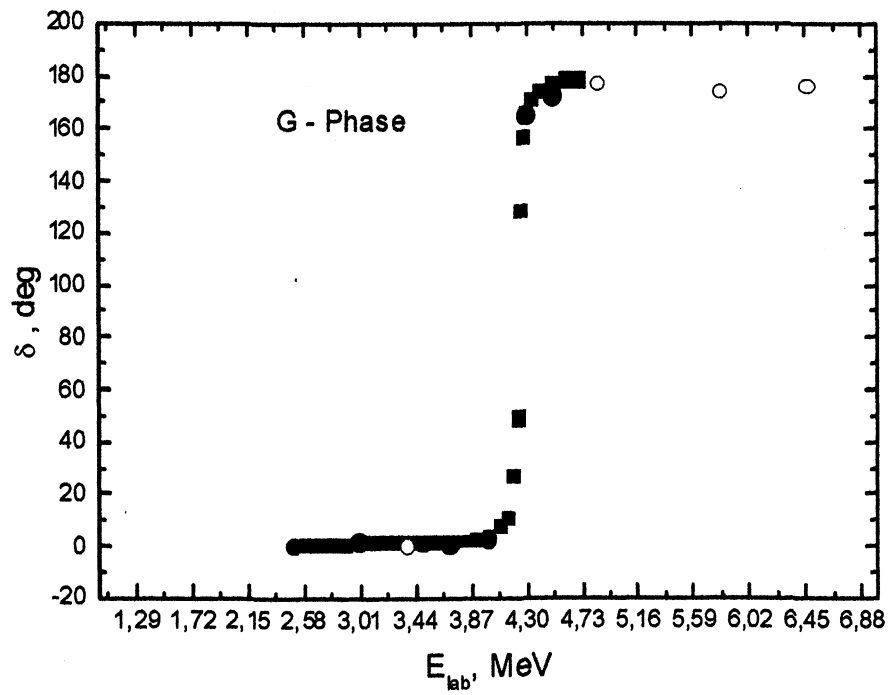

Fig. 2.2.18. *G* phase shift of the ^{4}He^{12}C elastic scattering. Designations, as in Fig. 2.2.14.

3. At the energy of 4.259 MeV with a width of 27 keV in the G wave there is the resonance level and in the results of works [100] and [102] there is visible disturbance of the phase shift, shown in Fig. 2.2.18.

4. The energy of 5.799 MeV is about a resonance at 5.47 MeV with very large width of 5 MeV and the moment 0^+, and S phase shift is experiencing some rising.

5. There is a resonance with a width of 0.8 MeV and $J^\pi = 3^-$ for the F wave at the energy of 5.92 MeV and the F phase shift shown in Fig. 2.2.17, at this energy has the value of about 90° (see also results given in tab. 2.2.7 and 2.2.8 for the F elastic scattering phase shifts).

6. At three energies in the range of 1.47-2.07 MeV it is observed the pure Rutherford scattering and all nuclear phase shifts are almost equal to zero.

Furthermore, elastic scattering phase shifts obtained here [105], are used for the creation of intercluster potentials and calculations of an astrophysical S-factor of the radiative $^{12}C(^4He,\gamma)^{16}O$ capture reaction [2,28, 106,122,123]. This process, along with a threefold helium cycle, is present at a chain of thermonuclear reactions at a hot stage of development of stars when the temperature in a star reaches hundreds of millions of Kelvin degrees [107]. At so high temperature the interacting particles have the sufficient energy for the essential increase in probability of passing through a Coulomb barrier. In that case they get to the area of strong interaction that leads to the increase the contribution of such reaction, i.e. its energy efficiency in total energy balance of star.

2.3 Phase shift analysis of the elastic $N^{12}C$, $p^{14}C$ and $N^{16}O$ scattering

In this paragraph the methods of the phase shift analysis for the particles with spins 0 + 1/2 and results of the phase shift analysis for the $p^{12}C$ systems will be considered. Apparently, the latest experimental data obtained at low, astrophysical energies are given in works of the Institute of Nuclear Physics (INP) of the Republic of Kazakhstan (RK) – they also will be used further in our phase shift analysis.

2.3.1 Differential cross sections

At the consideration of the elastic scattering in system of particles with spins 0 and 1/2 we will consider the spin-orbital splitting of the phase shifts, which takes place in the nuclear N^4He, $^3H^4He$, $N^{12}C$ systems, etc. In this case the elastic scattering of nuclear particles is completely described by two independent spin amplitudes (A and B), and the cross section is presented in the following form [6]:

$$\frac{d\sigma(\theta)}{d\Omega} = |A(\theta)|^2 + |B(\theta)|^2, \qquad (2.3.1)$$

where

$$A(\theta) = f_c(\theta) + \frac{1}{2ik}\sum_{L=0}^{\infty}\{(L+1)S_L^+ + LS_L^- - (2L+1)\}\exp(2i\sigma_L)P_L(\cos\theta)\ ,$$

$$B(\theta) = \frac{1}{2ik}\sum_{L=0}^{\infty}(S_L^+ - S_L^-)\exp(2i\sigma_L)P_L^1(\cos\theta)\,. \qquad (2.3.2)$$

Here $S_L^{\pm} = \eta_L^{\pm}\exp(2i\delta_L^{\pm})$ – a scattering matrix, $\eta^{\pm}_L$ – inelasticity parameters, and the signs "±" correspond to the total moment of the system $J = L \pm 1/2$.

The Coulomb amplitude of f_c can be presented in the form

$$f_c(\theta) = -\left(\frac{\eta}{2k\sin^2(\theta/2)}\right)\exp\{i\eta\ln[\sin^{-2}(\theta/2)] + 2i\sigma_0\}\ , \qquad (2.3.3)$$

where $P_n^m(x)$ – the associated Legendre polynomials, η – the Coulomb parameter, μ – the reduced mass of particles, k – wave number of the relative movement of particles in the input channel.

The associated Legendre polynomials or function $P_n^m(x)$ are presented in a form

$$P_n^m(x) = (1 - x^2)^{m/2}\frac{d^m P_n(x)}{dx^m},$$

and for $m = 1$ they can be found by the recurrent formulas of the form

$$P_{L+1}^1(x) = \frac{(2L+1)x}{L}P_L^1(x) - \frac{L+1}{L}P_{L-1}^1(x)$$

with the initial values

$$P_0^1(x) = 0\ , \quad P_1^1(x) = (1-x^2)^{1/2}\ , \quad P_2^1(x) = 3xP_1^1(x).$$

The values $P_n^2(x)$, which will meet to us further, are calculated on other recurrent formulas

$$P_{L+1}^2(x) = \frac{(2L+1)x}{L-1}P_L^2(x) - \frac{L+2}{L-1}P_{L-1}^2(x)$$

with the initial values

$$P_0^2(x) = P_1^2(x) = 0\ , \quad P_2^2 = 3(1-x^2)\ , \quad P_3^2(x) = 5xP_2^2(x).$$

Through the reduced amplitudes A and B it is possible to express the vector polarization in the elastic scattering of such particles [6]

$$P(\theta)=\frac{2\,\mathrm{Im}(AB^{*})}{|A|^{2}+|B|^{2}}.$$

Writing in the expression for the amplitude $B(\Theta)$, we obtain

$$\mathrm{Re}B=\frac{1}{2k}\sum_{L=0}^{\infty}[a\cdot\sin(2\sigma_{L})+b\cdot\cos(2\sigma_{L})]P_{L}^{1}(x),$$

$$\mathrm{Im}B=\frac{1}{2k}\sum_{L=0}^{\infty}[b\cdot\sin(2\sigma_{L})-a\cdot\cos(2\sigma_{L})]P_{L}^{1}(x),$$

where

$$a=\eta_{L}^{+}\cos(2\delta_{L}^{+})-\eta_{L}^{-}\cos(2\delta_{L}^{-}),$$

$$b=\eta_{L}^{+}\sin(2\delta_{L}^{+})-\eta_{L}^{-}\sin(2\delta_{L}^{-}).$$

Using similar method, for amplitude of $A(\Theta)$ it is possible to find the following recording format [108]

$$\mathrm{Re}A=\mathrm{Re}f_{c}+\frac{1}{2k}\sum_{L=0}^{\infty}[c\cdot\sin(2\sigma_{L})+d\cdot\cos(2\sigma_{L})]P_{L}(x),$$

$$\mathrm{Im}A=\mathrm{Im}f_{c}+\frac{1}{2k}\sum_{L=0}^{\infty}[d\cdot\sin(2\sigma_{L})-c\cdot\cos(2\sigma_{L})]P_{L}(x),$$

where

$$c=(L+1)\eta_{L}^{+}\cos(2\delta_{L}^{+})+L\eta_{L}^{-}\cos(2\delta_{L}^{-})-(2L+1),$$

$$d=(L+1)\eta_{L}^{+}\sin(2\delta_{L}^{+})+L\eta_{L}^{-}\sin(2\delta_{L}^{-}).$$

For the total cross section of the elastic scattering it is possible to obtain [6]

$$\sigma_s = \frac{\pi}{k^2}\sum_{\mathrm{L}}\left[(L+1)\left|1-S_{\mathrm{L}}^{+}\right|^2 + L\left|1-S_{\mathrm{L}}^{-}\right|^2\right]$$

or

$$\sigma_s = \frac{4\pi}{k^2}\sum_{\mathrm{L}}\left\{(L+1)[\eta_{\mathrm{L}}^{+}\sin\delta_{\mathrm{L}}^{+}]^2 + L[\eta_{\mathrm{L}}^{-}\sin\delta_{\mathrm{L}}^{-}]^2\right\}.$$

All these expressions were used further for the carrying out of the phase shift analysis of the $N^{12}C$ and $N^{16}O$ elastic scattering at energy up to 1.0–2.5 MeV [109].

2.3.2 Control of the computer program

The text of our computer program for calculation of the total and differential cross sections of the elastic scattering of particles with half-integer spin, which was used for the carrying out of the corresponding phase shift analysis is completely described further and tested on the elastic scattering in the p^4He system. Here only one version of the control account on this program for the p^4He scattering is given, in comparison with data from work [110], where the phase shift analysis for energy of 9.89 MeV is made, positive D phase shifts and an average on all points value $\chi^2 = 0.60$ were obtained.

In the analysis [110] 22 points of cross sections from work [111] are used at energy of 9.954 MeV (in [110] it is not specified which 22 points have been taken from the 24th, provided in work [111]) and several points on polarization from works [110,112]. In the latter case, apparently, 10 points at 8 angles are used 46.5°, 55.9°, 56.2°, 73.5°, 89.7°, 99.8°, 114.3°, 128.3° and three relatives the energies 9.89, 9.84, 9.82 MeV.

The phase shifts from work [110] are given in tab. 2.3.1, and average χ^2_σ only for the differential cross sections according to our program taking into account 24 points from [111] (energy is, still, equal to 9.954 MeV) and these phase shifts turns out equal to 0.586. The results of these calculations are shown in tab.2.3.2. For the 10 experimental data by the polarization from works [110,112] at the energies of 9.82–9.89 MeV at eight scattering

angles with the phase shifts from [110], it is possible to obtain the value $\chi^2_p = 0.589$ (energy is, still, equal to 9.954 MeV). These results are given in tab. 2.3.3.

Tab. 2.3.1. The phase shifts of the p^4He elastic scattering from work [110].

E, MeV	S_0, deg.	$P_{3/2}$, deg.	$P_{1/2}$, deg.	$D_{5/2}$, deg.	$D_{3/2}$, deg.
9.954	119,3 $^{+2.0}_{-1.8}$	112,4 $^{+3.5}_{-5.2}$	65,7 $^{+2.7}_{-3.2}$	5,3 $^{+1.6}_{-5}$	3,7 $^{+1.6}_{-2.8}$

Tab.2.3.2. The differential cross sections of the p^4He elastic scattering. Here $\theta°$ – the scattering angle in degrees, σ_e – experimental and σ_t – calculation cross sections.

$\theta°$	σ_e, mb/st	σ_t, mb/st	χ^2_i	$\theta°$	σ_e, mb/st	σ_t, mb/st	χ^2_i
25.10	371.00	366.85	0.31	109.90	21.00	20.70	0.51
30.89	339.00	331.54	1.21	120.60	23.00	259	0.79
35.07	305.00	308.40	0.31	122.80	24.50	24.19	0.40
49.03	232.00	230.61	0.09	130.13	31.90	31.91	0.00
54.70	205.00	199.10	2.07	130.90	33.20	32.90	0.21
60.00	176.00	170.56	39	134.87	37.80	38.44	0.71
70.10	124.00	120.59	1.89	140.80	47.30	47.69	0.17
80.00	82.00	79.77	1.85	145.00	54.00	54.62	0.33
90.00	49.20	48.82	0.15	149.40	61.60	61.88	0.05
94.07	39.10	39.44	0.19	154.90	70.60	70.54	0.00
1017	26.20	26.39	0.13	160.00	78.40	77.71	0.19
106.90	22.00	215	0.12	164.40	83.00	82.94	0.00

If to average the value χ^2 by all known points (24 + 10 = 34), i.e. use more general expression for χ^2

$$\chi^2 = \frac{1}{(N_\sigma + N_p)}\left\{\sum_{i=1}^{N}\left[\frac{\sigma_i^t - \sigma_i^e}{\Delta\sigma_i^e}\right] + \sum_{i=1}^{N}\left[\frac{P_i^t - P_i^e}{\Delta P_i^e}\right]\right\} = \frac{1}{(N_\sigma + N_p)}\left\{\chi_\sigma^2 + \chi_p^2\right\},$$

that turns out the value $\chi^2 = 0.5875 \approx 0.59$ in a good agreement with the results of work [110]. Here N_σ and N_P – number of data on cross sections (24 points) and on polarization (10 points), σ^e, P^e, σ^t, P^t – experimental and theoretical values of cross sections and polarization, $\Delta\sigma$ and ΔP – their errors.

Tab. 2.3.3. Polarization in the p^4He elastic scattering. Here $\theta°$ – the scattering angle in degrees, P_e – experimental polarization, ΔP_e – experimental errors for the polarization and P_t – calculation polarization.

$\theta°$	P_e, %	ΔP_e	P_t, %	χ^2_i
46.50	-330	10	-33.11	0.15
55.90	-41.30	20	-450	0.30
56.20	-44.40	0.90	-42.81	3.11
73.50	-62.60	3.00	-62.84	0.01
73.50	-64.80	1.90	-62.84	1.06
89.70	-76.10	3.60	-76.33	0.01
89.70	-75.50	40	-76.33	0.12
99.80	-59.30	50	-58.55	0.09
114.30	48.20	3.20	51.03	0.78
128.30	99.40	3.30	97.66	0.28

$S_0 = 119.01°$, $P_{3/2} = 1125°$, $P_{1/2} = 65.39°$, $D_{5/2} = 5.24°$, $D_{3/2} = 3.63°$,

If to execute the additional χ^2 minimization according to our program, then for χ^2_σ according to the cross sections we will obtain 0.576, for the $\chi^2_p = 0.561$ polarization and an average of $\chi^2 = 0.572 \approx 0.57$ at the following values of phase shifts

$S_0 = 119.01°$, $P_{3/2} = 1125°$, $P_{1/2} = 65.39°$, $D_{5/2} = 5.24°$, $D_{3/2} = 3.63°$,

which are completely in the error band given in work [110] and are shown in tab.2.3.1.

Thus, the program presented further allows to obtain the results, which

are well coinciding with earlier made analysis. Further it was tested according to the phase shift analysis, which is carried out in other works at low energies, but already directly for the elastic scattering in the $p^{12}C$ system.

Earlier the phase shift analysis of excitation functions for the $p^{12}C$ elastic scattering, measured in [113], at the energies in the range of 400–1300 keV (l.s.) and angles 106°–169°, has been carried out in work [114], where it is obtained that, for example, at $E_{lab} = 900$ keV the S phase shift has to lie in the area 153°–154°. With the same experimental data we have obtained the value 152.7°. To obtain this result the scattering cross section from the excitation functions of work [113] at the energies of 866–900 keV were used. The results of our calculations of σ_t in the comparison with experimental data of σ_e are given in tab.2.3.4. In the last column of the table the partial χ^2_i values on each point at 10% errors are given in the experimental cross sections, and for an average of all experimental points of χ^2 the 0.11 value has been obtained.

Tab. 2.3.4. The comparison of the theoretical and experimental cross sections of the $p^{12}C$ elastic scattering at energy of 900 keV.

θ°	σ_e, mb/st	σ_t, mb/st	χ^2_i
106	341	341.5	1.90E-04
127	280	281	5.76E-03
148	241	251.2	1.80E-01
169	250	237.5	50E-01

At the energy of 751 keV (l.s.) for the S phase shifts the values in the range of 155°–157° have been found in work [114]. The results obtained by us for this energy are given in tab.2.3.5.

Tab. 2.3.5. The comparison of the theoretical and experimental cross sections of the $p^{12}C$ elastic scattering at energy of 750 keV.

θ°	σ_e, mb/st	σ_t, mb/st	χ^2_i
106	428	428.3	3.44E-05

127	334	342.8	6.91E-02
148	282	299.1	3.66E-01
169	307	279.9	7.82E-01

The data on cross sections from the excitation functions in the range of energies of 749–754 keV were used and for the S phase shifts it is found 156.8° at average $\chi^2 = 0.30$. Thus, according to our program, at two energies of the $p^{12}C$ elastic scattering the phase shifts coinciding with the results of the analysis made on the basis of excitation functions in work [114] were obtained.

2.3.3 Phase shift analysis of the $p^{12}C$ scattering

The control calculations given above are well coordinated with the earlier results, therefore, according to our program, the phase shift analysis [115] of new experimental data on differential cross sections of the $p^{12}C$ scattering in the range of energies of 230–1200 keV (l.s.) has been made [116], measured in INP RK. The results of this analysis are given in tab. 2.3.6 and presented by points in Fig. 2.3.1 in comparison with data of work [114] which are shown by the dashed line.

Tab. 2.3.6. The results of the phase shift analysis of the $p^{12}C$ elastic scattering at low energies taking into account only the S phase shift.

E_{cm}, keV	$S_{1/2}$, deg.	χ^2
213	2.0	1.35
317	5	0.31
371	7.2	0.51
409	36.2	0.98
422	58.2	3.69
434	107.8	0.78
478	153.3	56
689	156.3	2.79
900	153.6	55
1110	149.9	1.77

In Figs.2.3.2a,b,c the experimental differential cross sections in the range of resonance at 457 keV (l.s.) are presented by points, the results of calculation of these cross sections on the basis of Rutherford's formula (the dotted curve), and also the cross sections obtained from our phase shift analysis (the solid line), which considers only the S phase shift and the analysis at the accounting of the S and P scattering phase shifts (the dotted curve). From the figures it is clear that in the range of a resonance it is not possible to describe well the cross section only on the basis of one S phase shift. The P wave presented in Fig.2.3.3, the accounting of which considerably improves the description of the experimental data begins to play a noticeable role. At the resonance energy of 457 keV (l.s.) for which the cross sections are shown in Fig.2.3.2b, the account of the P waves reduce the value χ^2 from 3.69 to 0.79.

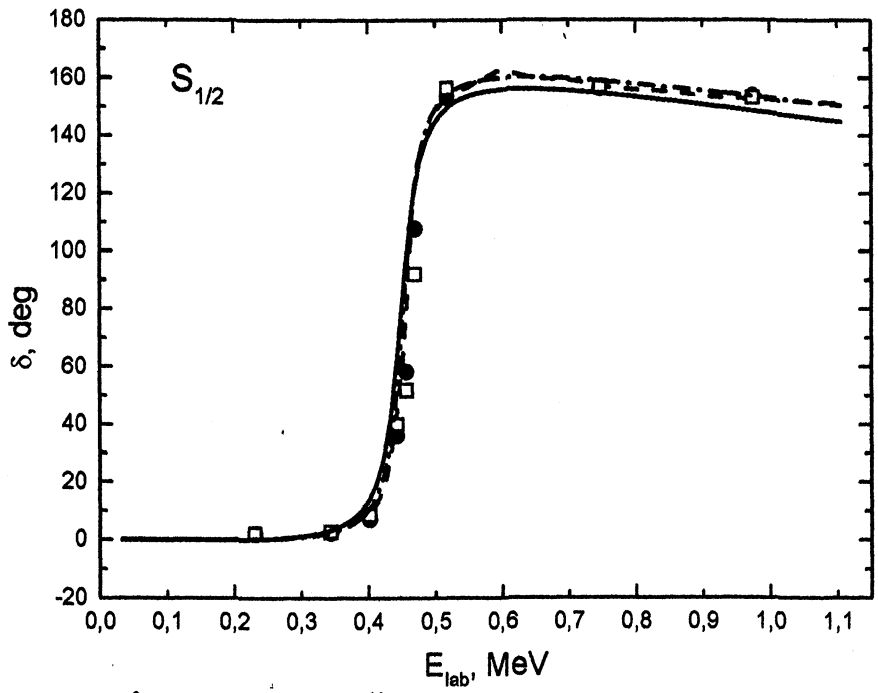

Fig.2.3.1. The ^2S phase shift of the $p^{12}C$ scattering at low energies. Points – results of the phase shift analysis for the S phase shifts taking into account in the phase shift analysis only S waves, open squares – results of the phase shift analysis for the S phase shifts taking into account S and P waves, a shaped curve – results [114].

In Fig.2.3.3 it is clear that at low energies the $P_{1/2}$ phase shift goes higher, than $P_{3/2}$, but at energy about 1.2 MeV they are crossed and further

$P_{3/2}$ goes higher in the negative range of the angles [117,118]. The value of the S phase shift taking into account the P wave practically is not changed and its shape is shown in Fig.2.3.1 by open squares. The accounting of the D wave in the phase shift analysis leads to its value about one degree in the range of the S resonance and practically does not influence to the behavior of calculated differential cross sections.

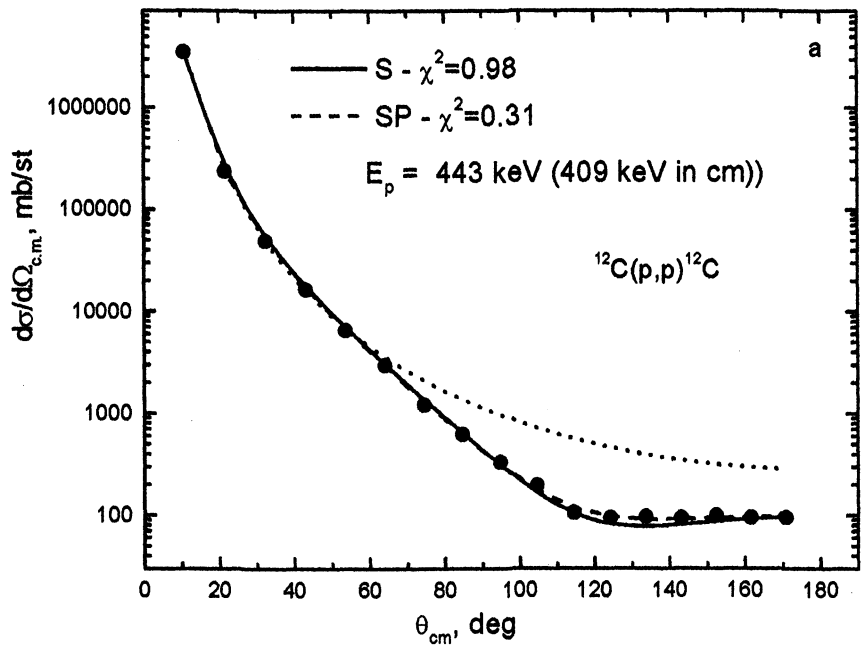

Fig.2.3.2a. The differential cross sections of the $p^{12}C$ elastic scattering. The solid curve is obtained on the basis of the phase shift analysis taking into account only the S wave, the dotted line – the Rutherford scattering, the dashed line – results of the phase shift analysis taking into account the S and P waves, points – an experiment [116].

The total cross section of elastic scattering is presented by points in Fig.2.3.4. They are calculated on the basis of taken from the experimental differential cross sections [116] of the S scattering phase shifts. The total cross sections obtained from the phase shift analysis of work [114] are represented by circles. In Fig. 2.3.4 in the energy range of 200–300 keV (l.s.) some plateau is observed. At the moment, it is not clear; it is caused by experimental inaccuracy, unforeseen errors of the phase shift analysis or really exists at these energies. For the clarification of this question new measurements of angular distributions of the elastic $p^{12}C$ scattering in the energy range from 100–150 to 300–400 keV with a step on energy about 50

keV or excitation functions are required at different angles [109].

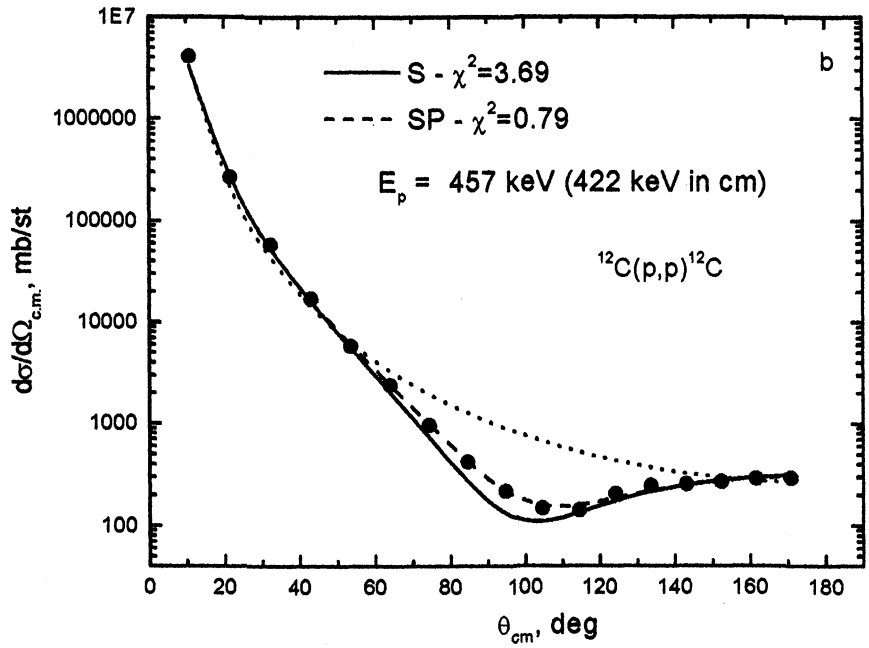

Fig. 2.3.2b. The differential cross sections of the $p^{12}C$ scattering. Signatures, as in Fig.2.3.2a.

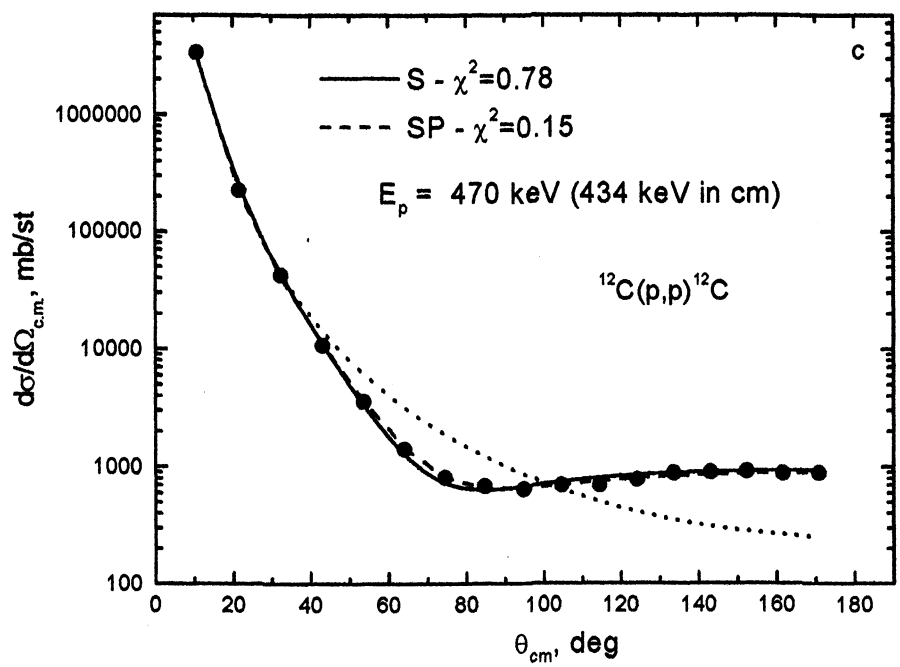

Fig. 2.3.2c. The differential cross sections of the $p^{12}C$ scattering. Signatures, as in Fig.2.3.2a.

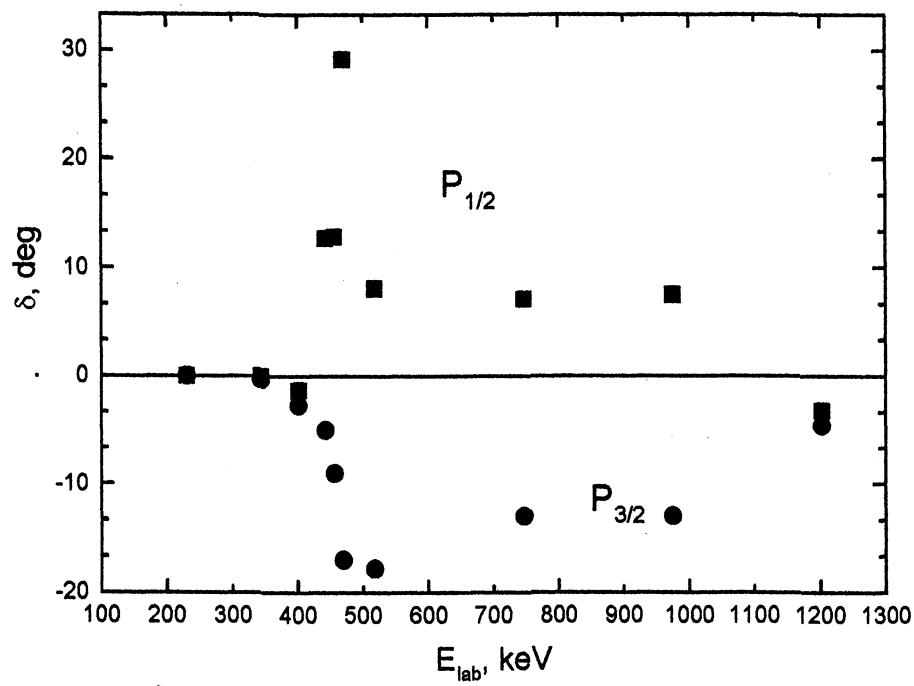

Fig.2.3.3. The ^2P phase shifts of the $p^{12}C$ scattering at low energies. Points – $P_{3/2}$ and squares – $P_{1/2}$ phase shifts, obtained as a result of the phase shift analysis taking into account the S and P waves.

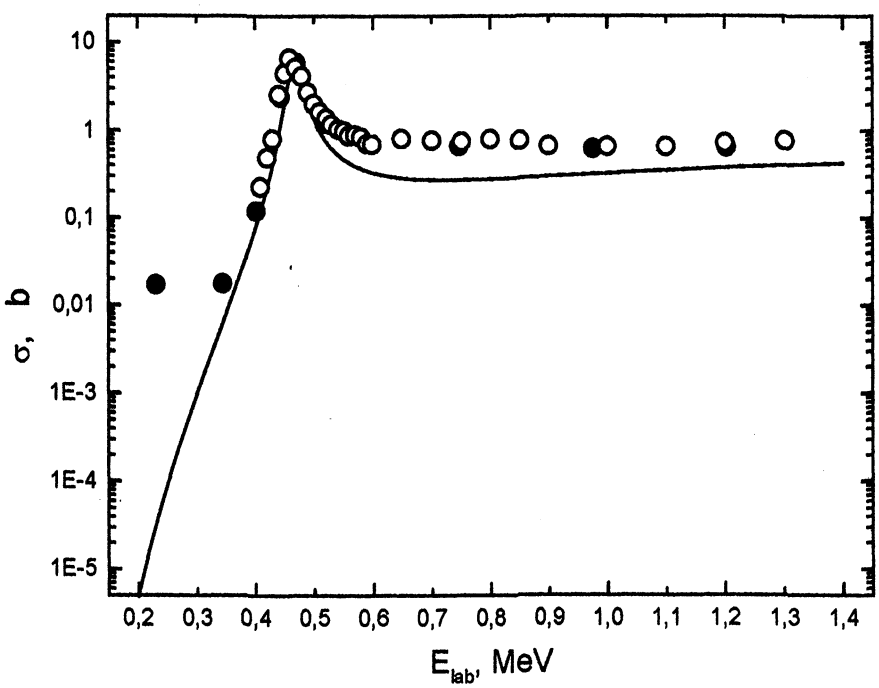

Fig.2.3.4. The total cross sections for the $p^{12}C$ elastic scattering. Points – total cross sections found from the phase shift scattering of works [116], circles – also for works [113,114].

In conclusion of this paragraph we will notice that in this case slightly another value $\hbar^2/m_0 = 41.80159$ MeV·fm^2 was used, than usually, which has been obtained with slightly other values of fundamental constants $\hbar^2$ and m_0 where the last designates the atomic unit of mass. However, as it will be clear further, this distinction practically does not affect the obtained results for the scattering phase shifts.

2.3.4 The phase shift analysis of the $n^{12}C$ elastic scattering

In this paragraph we will continue consideration of the phase shift analysis of the elastic scattering on light nuclei and on the basis of measurements [119] we will make the phase shift analysis of the $n^{12}C$ scattering. We did not manage to find the results of earlier carried out phase shift analysis for the $n^{12}C$ system even at low energies though they have to differ considerably from the similar analysis of the $p^{12}C$ scattering [115]. The reason for these differences is a significant distinction between the structure of the spectra of levels of ^{13}C and ^{13}N nuclei at energies up to 1.5–2 MeV above the thresholds of $n^{12}C$ and $p^{12}C$ cluster channels [120].

In particular, in the $p^{12}C$ elastic scattering there is the superthreshold resonance level of ^{13}N at energy of 0.42 MeV with $J^{\pi} = 1/2^+$, which leads to the $^2S_{1/2}$ resonance of phase shift, as has been shown in our work [115] in comparison with earlier results of the phase shift analysis [113,114]. In case of the $n^{12}C$ scattering there are no resonances in the spectra of ^{13}C up to energy of 1.9 MeV. For this reason it is interesting to find out a shape of the phase shifts of the $n^{12}C$ elastic scattering taken from the experimental data at low and, first of all, astrophysical energies.

Especially, as the reaction of the radiative capture in the $n^{12}C$ channel, apparently, at any energy is included into the chain of thermonuclear reactions of the preliminary nucleosynthesis [121]

$$\ldots {}^7\mathrm{Li}(n,\gamma)^8\mathrm{Li}(^4\mathrm{He},n)^{11}\mathrm{B}(n,\gamma)^{12}\mathrm{B}(\beta^-)^{12}\mathrm{C}(n,\gamma)^{13}\mathrm{C} \ldots,$$

which has led, finally, to the initial formation of the Sun, stars and all our Universe [122,123].

Extracted from the experimental differential cross sections of the elastic scattering phase shift allow to construct the interaction potentials of two

particles in the continuous spectrum, and perform the calculations of certain characteristics of their interaction in the scattering processes and reactions. For example, it can be the astrophysical S-factors or total cross sections of the reactions [124], including, the neutron radiative capture on ^{12}C in astrophysical energy range, which usually is considered in our previous works [23,28,122].

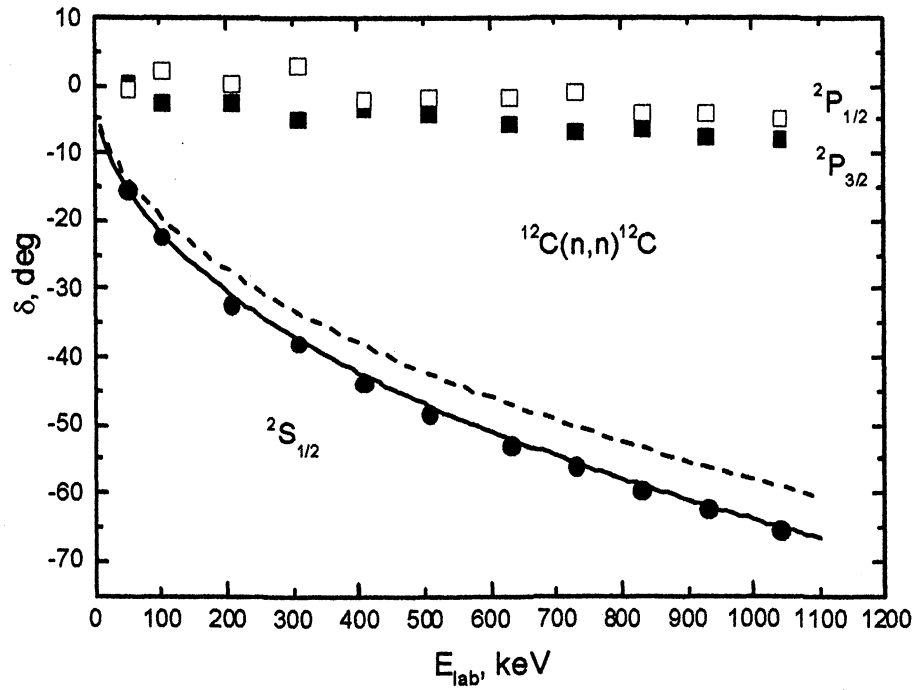

Fig. 2.3.5. Results of the phase shift analysis of the $n^{12}C$ elastic scattering for variant with negative values of the ^2S phase shifts. Points – results of the phase shift analysis for the $^2S_{1/2}$ phase shift, open squares – results of the phase shift analysis for the $^2P_{1/2}$ phase shift, black squares – results of the phase shift analysis for the $^2P_{3/2}$ phase shift. Curves – results of calculation with different potentials, which are explained in the text.

Therefore, on the basis of the methods described above the phase shift analysis of the known experimental data on differential cross sections of $n^{12}C$ elastic scattering in the energy range of 50-1040 keV (l.s.) has been made [119]. The results of our phase shift analysis for the S and P scattering phase shifts are presented in Fig. 2.3.5 and given in tab. 2.3.7. At the carrying out of the analysis the χ^2 value was calculated at 10% experimental errors of differential cross sections [119]. χ^2 value for each considered energy is given in the last column of tab.2.3.7.

Tab. 2.3.7. The results of the phase shift analysis of the $n^{12}C$ elastic scattering at low energies for the negative values of the ^2S phase shifts.

E_n, keV	$^2S_{1/2}$, deg	$^2P_{3/2}$, deg	$^2P_{1/2}$, deg	χ^2
50	-15.5	0.6	-0.3	0.023
100	-22	-2	3	0.016
157	-28.3	-1.0	-1.0	0.007
207	-32	-4	0.5	0.014
257	-35.6	-5	-0.4	0.009
307	-37.8	-4.6	3.3	0.033
357	-41.3	-2.7	-1.3	0.007
407	-43.7	-3.0	-1.8	0.027
457	-45.3	-5.1	5	0.029
507	-48.3	-3.9	-1.6	0.019
530	-49.1	-3.6	-3.4	0.020
630	-52.8	-5.4	-1.6	0.015
730	-56.0	-6.6	-0.6	0.031
830	-59.5	-6.2	-3.7	0.044
930	-61	-7.3	-3.7	0.042
1040	-65.4	-7.7	-4.6	0.096

From Fig. 2.3.5 it is clear that all ^2P phase shifts have the values in modulus no more than 10°, but their influence reduces the χ^2 value approximately an order of magnitude. The value of ^2S phase shift gradually decreases and, as will be seen below, it is well described by a Gaussian potential across the low energy range, which was included in the analysis.

In Fig.2.3.6 points present the differential cross sections for some considered energies from work [119] and the cross sections obtained from our phase shift analysis (the solid line), which considers S and P phase shifts given in tab.2.3.7. The accounting of the obtained small values of ^2P phase shifts has allowed one to improve considerably the quality of the description of differential cross sections even at the lowest energies in the range of 50–100 keV.

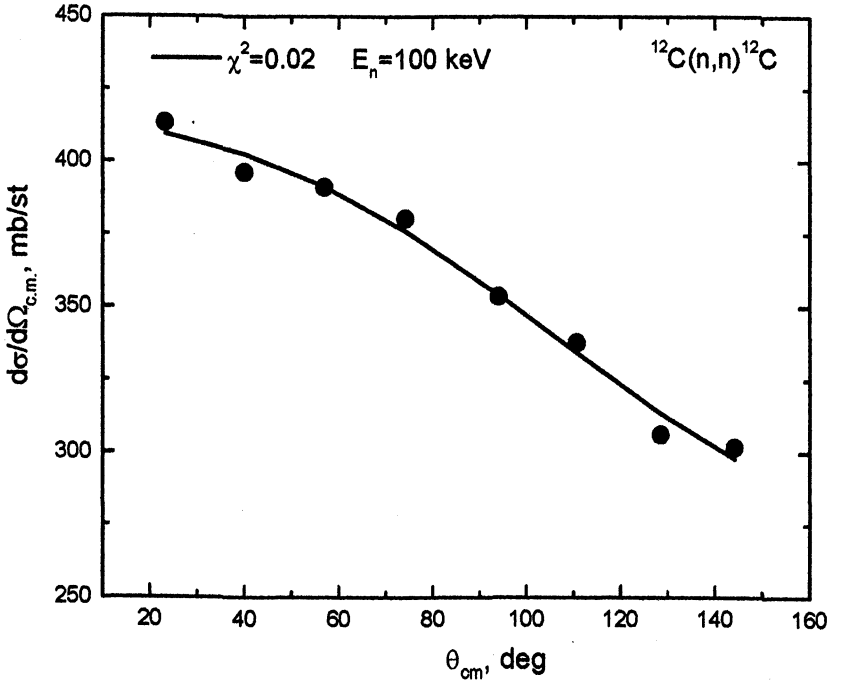

Fig.2.3.6a. The differential cross sections of the $n^{12}C$ elastic scattering. Solid curve – results of calculation of the cross sections with the found phase shifts, points – experimental differential cross sections of scattering [119].

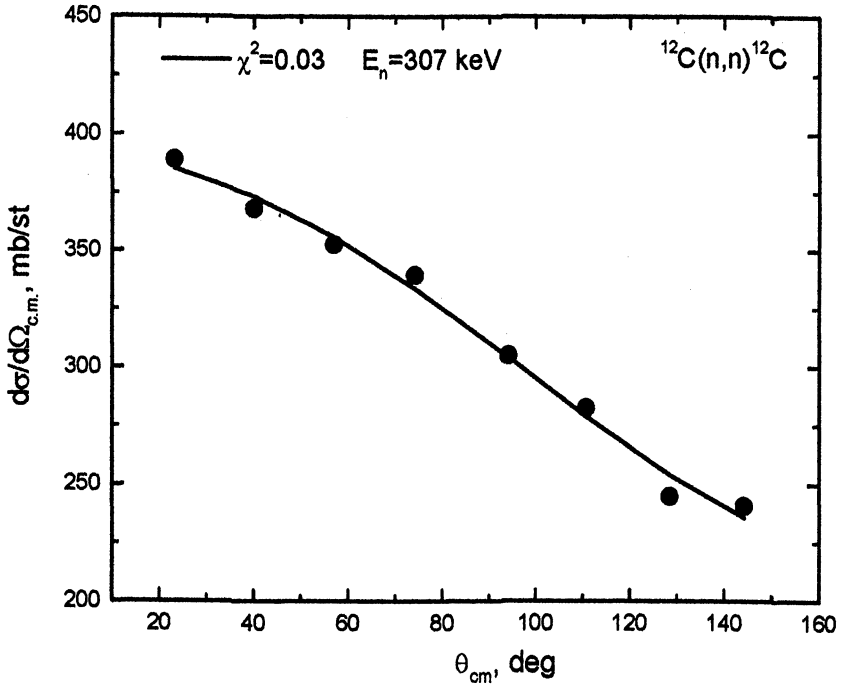

Fig.2.3.6b. The same that in Fig.2.3.6a.

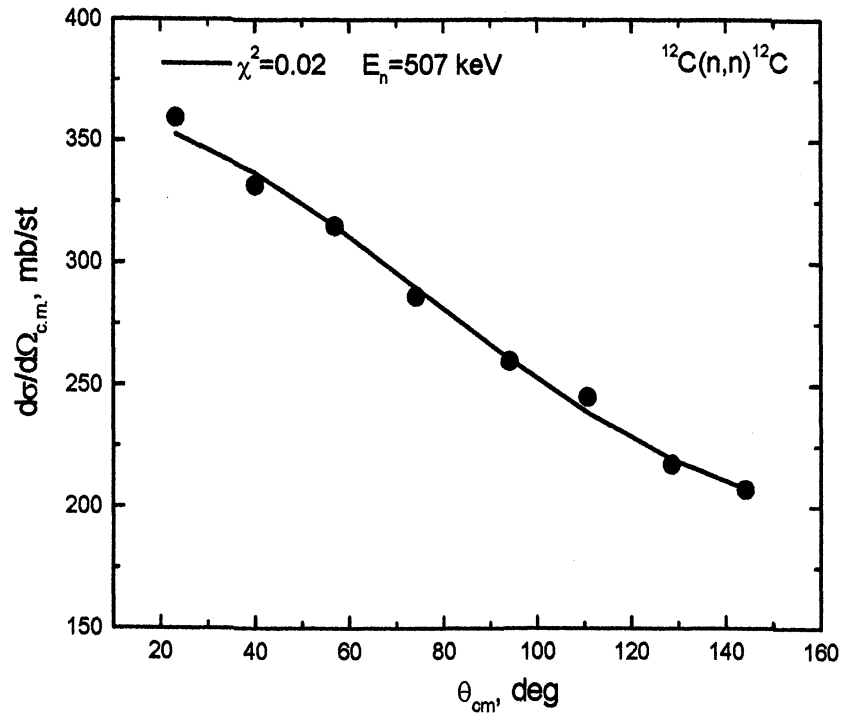

Fig.2.3.6c. The same that in Fig.2.3.6a.

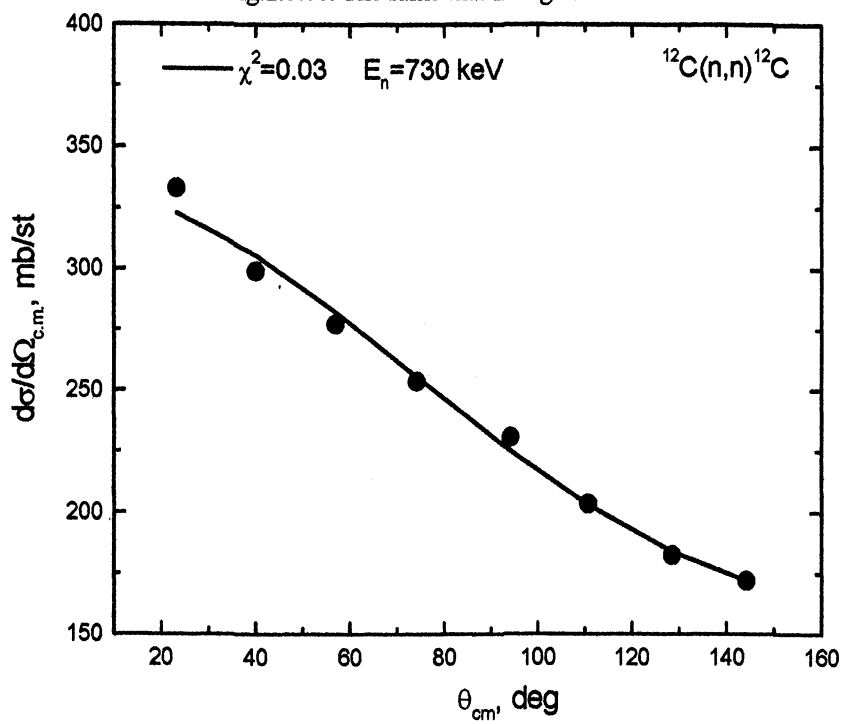

Fig.2.3.6d. The same that in Fig.2.3.6a.

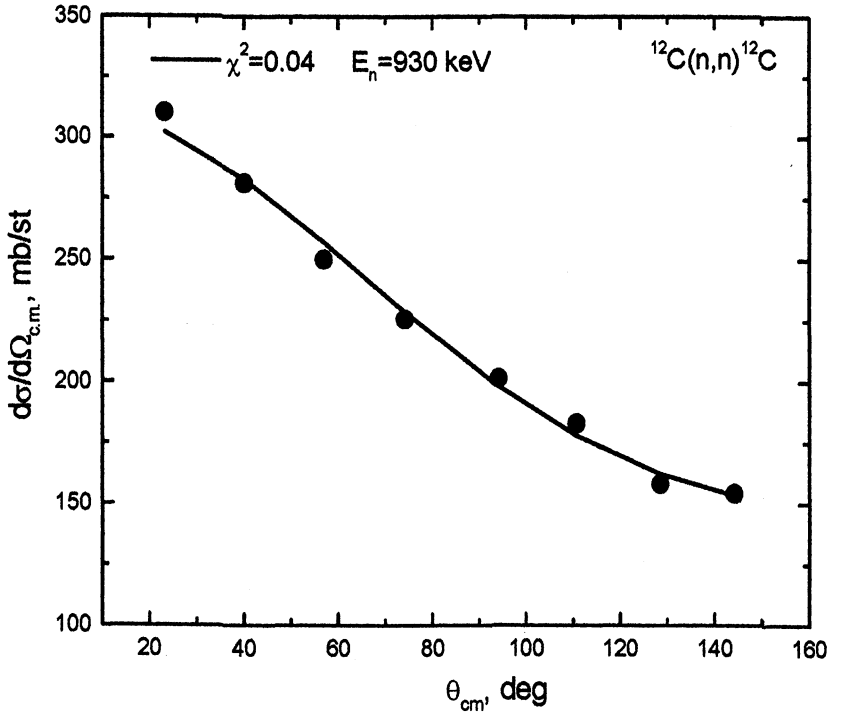

Fig.2.3.6e. The same that in Fig.2.3.6a.

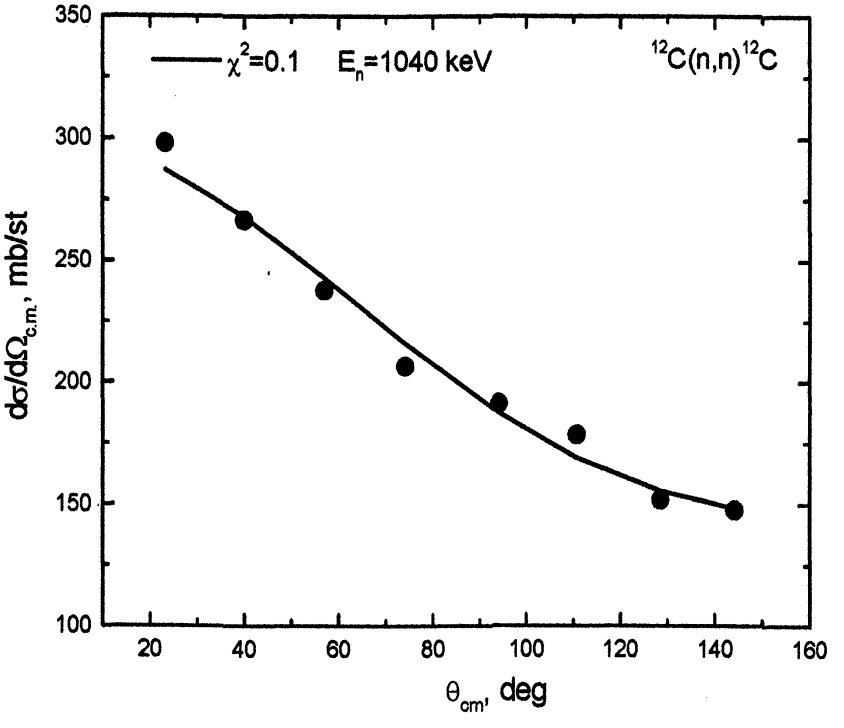

Fig.2.3.6f. The same that in Fig.2.3.6a.

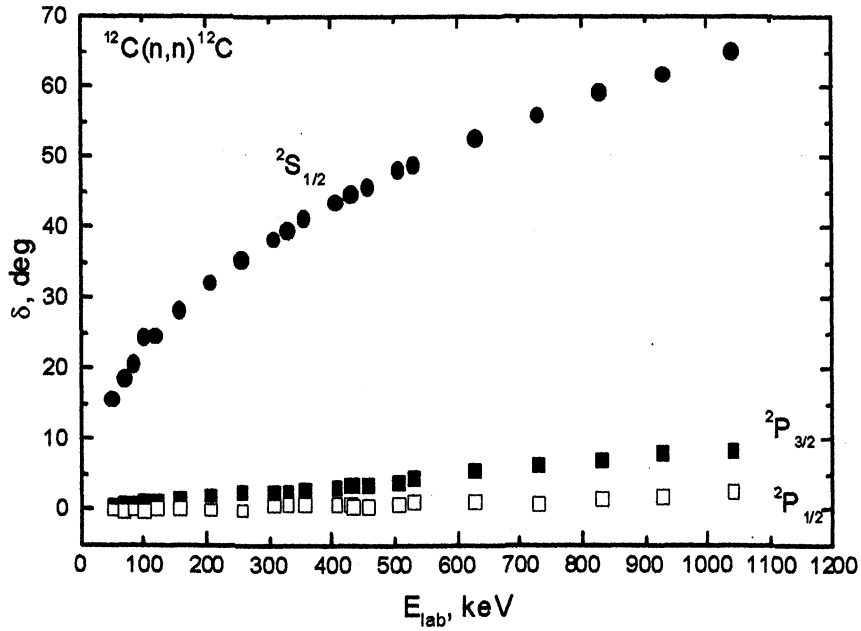

Fig.2.3.7. Results of the phase shift analysis of the $n^{12}C$ elastic scattering for variant with positive values of the ^2S phase shifts. Points – results of the phase shift analysis for the $^2S_{1/2}$ phase shift, open squares – results of the phase shift analysis for the $^2P_{1/2}$ phase shift, black squares – results of the phase shift analysis for the $^2P_{3/2}$ phase shift.

One more variant for a set of phase shifts in which the ^2S phase shift has positive values, also as well as the values of both ^2P phase shifts is given in Fig.2.3.7 and in tab.2.3.8. The χ^2 values for this variant of phase shifts practically do not differ from the first set of tab. 2.3.7, but the ^2S phase shift has the form close to resonance though in spectra of ^{13}C resonances are not observed [120]. Therefore the second set of phase shifts, apparently, does not correspond to the real situation and is given only for demonstration of the available ambiguity of phase shift sets here.

For an exception of the available ambiguity it is required to use the certain physical principles, for example, information on structure of spectra of levels of nucleus, in this case, ^{13}C [120]. Such information allows one to choose finally the real sets of phase shifts of elastic scattering, the variants of which can be obtained in the similar analysis. Besides, it is possible to use the potential description of the process of scattering, which as it will be shown further, allows one to estimate a difference of scattering phase shifts for neutrons and protons on one nucleus in one potential, i.e. at change only of a Coulomb part of interaction.

Tab. 2.3.8. Results of the phase shift analysis of the $n^{12}C$ elastic scattering at low energies for the positive ^2S values of the phase shifts.

E_{lab}, keV	$^2S_{1/2}$, deg	$^2P_{3/2}$, deg	$^2P_{1/2}$, deg	χ^2
50	15.7	0.6	0.06	0.036
100	24.5	1.1	0.0	0.029
157	28.3	1.5	0.1	0.007
207	33	1	0.0	0.014
257	35.6	2.7	0.0	0.009
307	38.4	2.7	0.1	0.05
357	41.3	2.9	1.0	0.007
407	43.6	3.4	1.0	0.028
457	45.8	3.8	0.7	0.037
507	48.3	4.2	1.0	0.019
530	50.0	4.7	1.2	0.021
630	52.8	5.6	1.1	0.015
730	56.1	6.5	0.8	0.031
830	59.3	7.1	1.6	0.045
930	61.9	8.1	1.9	0.044
1040	65.2	8.6	5	0.098

For example, in Fig.2.3.5 the ^2S phase shift of the potential with the point-like Coulomb member having a simple Gaussian form (1.6.2) is shown by the dashed curve and its parameters

$$V_0 = -102.05 \text{ MeV}, \gamma = 0.195 \text{ fm}^{-2}. \quad (2.3.4)$$

It has been obtained earlier for the $p^{12}C$ scattering at the description of the astrophysical S-factor of the proton radiative capture on ^{12}C in our previous work [125]. Such potential described the resonance form of the ^2S phase shift of the $p^{12}C$ scattering correctly, shown in Fig.2.3.1, and led to the acceptable consent with the experimental data in the calculations of the astrophysical S-factor.

In Fig.2.3.5 the calculations of the ^2S phase shifts were carried out for the $p^{12}C$ potential (2.3.4) specified above with the switched off Coulomb interaction, i.e. for the $n^{12}C$ scattering. From Fig.2.3.5 it is clear that the ^2S phase shift of the $n^{12}C$ scattering process does not contain the resonance. It is in a complete agreement with the observed spectra of ^{13}C [120]. In addition, it is clear that the results of the calculation of the ^2S phase shift are quite acceptable transfer the results of the $n^{12}C$ phase shift analysis, especially at the lowest energies.

For more exact description of the obtained data by the scattering phase shifts it is required to change a little the potential depth at the same geometry and to give -97.0 MeV that approximately for 5% differs from the initial parameters. The results of calculation of the ^2S phase shift with such potential are given in Fig.2.3.5 by the solid curve, which precisely describes the position of points of the ^2S phase shift of the $n^{12}C$ elastic scattering taken from the experiment.

Such potential, as well as previous, still contains one bound forbidden state, the existence of which follows from the analysis of structure of the forbidden and allowed bound states in the $N^{12}C$ system, which is carried out in works [2,28,122,125]. Averaging a little the width of capacity of γ, we will obtain

$$V_0 = -99.0 \text{ MeV}, \gamma = 0.2 \text{ fm}^{-2}, \qquad (2.3.5)$$

and the phase shift of such variant of potential does not differ from that provided in Fig.2.3.5 by the solid curve.

Thus, as a result of the carried out phase shift analysis of experimental differential cross sections a set of phase shifts of the $n^{12}C$ elastic scattering at the energies up to 1.0 MeV is obtained, which is coordinated with the spectra of levels of ^{13}C [120] and the potential calculations of the scattering phase shifts executed on the basis of the $p^{12}C$ interaction potential offered earlier. The obtained set of scattering phase shifts allows one to describe the value and shape of the differential cross sections of angular distributions of the $n^{12}C$ elastic scattering at low energies, which can be of interest in some problems of nuclear astrophysics [28,122].

Once again we will emphasize that the results of the made phase shift analysis, i.e. elastic scattering phase shifts of the system of particles, in this

case the $n^{12}C$, allow one to parametrize as it has been made above, the intercluster partial interaction potentials of scattering processes in this system. Such potentials, in turn, can be used further for the performance of certain calculations in the field of various astrophysical applications, which are partially considered, for example, in our works [28,120].

For the calculations of characteristics of nuclei the mass of ^{12}C was accepted equal to 12.0 amu, and mass of neutron m_n = 1.00866491597 amu [75]. We will notice that at the carrying out of the phase shift analysis there is no basic value, to use integer or exact mass of particles, because errors of cross sections make usually 5–10%.

2.3.5 Phase shift analysis of the $p^{14}C$ elastic scattering

Furthermore we will consider the possibility of the carrying out of the phase shift analysis for elastic cross sections of the $p^{14}C$ scattering. The excitation functions of the $p^{14}C$ elastic scattering from work [126], measured at 90°, 125°, 141° and 165° in the energy range from 0.6 to 3 MeV (l.s.) are shown by points in Figs. 2.3.8a,b,c,d. These data are used by us further for the carrying out of the phase shift analysis and extraction of the resonance shape of the $^2S_{1/2}$ scattering phase shift at 1.5 MeV. The methods of such analysis have been stated above, and the results are shown in Fig. 2.3.9a,b,c,d by points. The solid curves in Fig.2.3.8 show the cross sections calculated as a result of such analysis scattering phase shifts.

In our analysis about 120 first points given in work [126] in the energy range stated above were used. In addition, it has been obtained that for the description of cross sections in the excitation functions, at least, at the energies up to 2–3 MeV, it is not required to consider the ^2P or ^2D scattering waves, i.e. their values can just be accepted equal to zero. The χ^2 value at all energies and angles as only one point in cross sections of excitation functions for each energy and angle is considered, usually at the level of 10^{-2}–10^{-10} and the accounting of the partial scattering phase shift does not lead to its reduction.

The resonance energy, i.e. the energy at which the phase shift reaches 90°, as seen in Fig. 2.3.9, obtained from the excitation function at the scattering angle of 90° is in an interval of 1535–1562 keV, for which the value of the phase shift is concluded within 87°–93° with the value of

phase shift of 90° for energy of 1554 keV. The resonance energy obtained from the excitation functions at 125° is in an interval of 1551–1575 keV, for which the value of the phase shift is concluded within 84°–93°. The resonance energy obtained from the excitation function at 141° is in an interval of 1534–1611 keV, for which the value of the phase shift is concluded within 84°–90° with the value 90° at 1534, 1564 and 1611 keV.

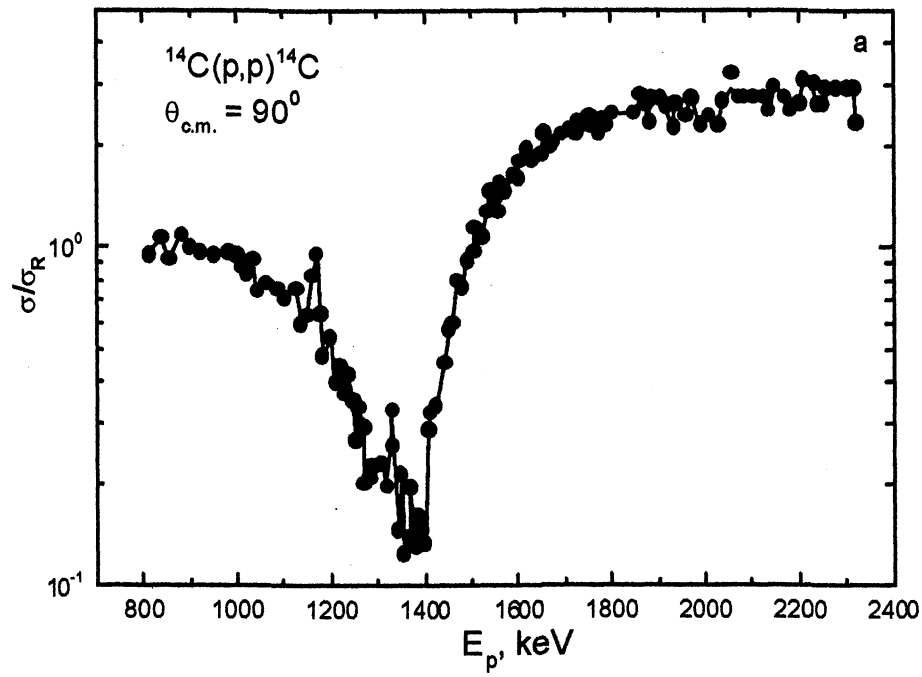

Fig.2.3.8a. The exitation functions in the $p^{14}C$ elastic scattering in the range of the $^2S_{1/2}$ resonance [126]. Solid curve – their approximation on the basis of the obtained phase shifts.

The resonance energy obtained from the excitation function at 165° is in an interval of 1544–1563 keV, for which the value of the phase shift is concluded within 87°–91°. At so marked scatter of values it is possible to say only that the resonance value of the phase shift in 90° is in limits of 1534–1611 keV, with an average value of energy 1572 keV in l.s., that in general will be coordinated with data [120] where the value of the resonance energy 1509 keV is specified in l.s.

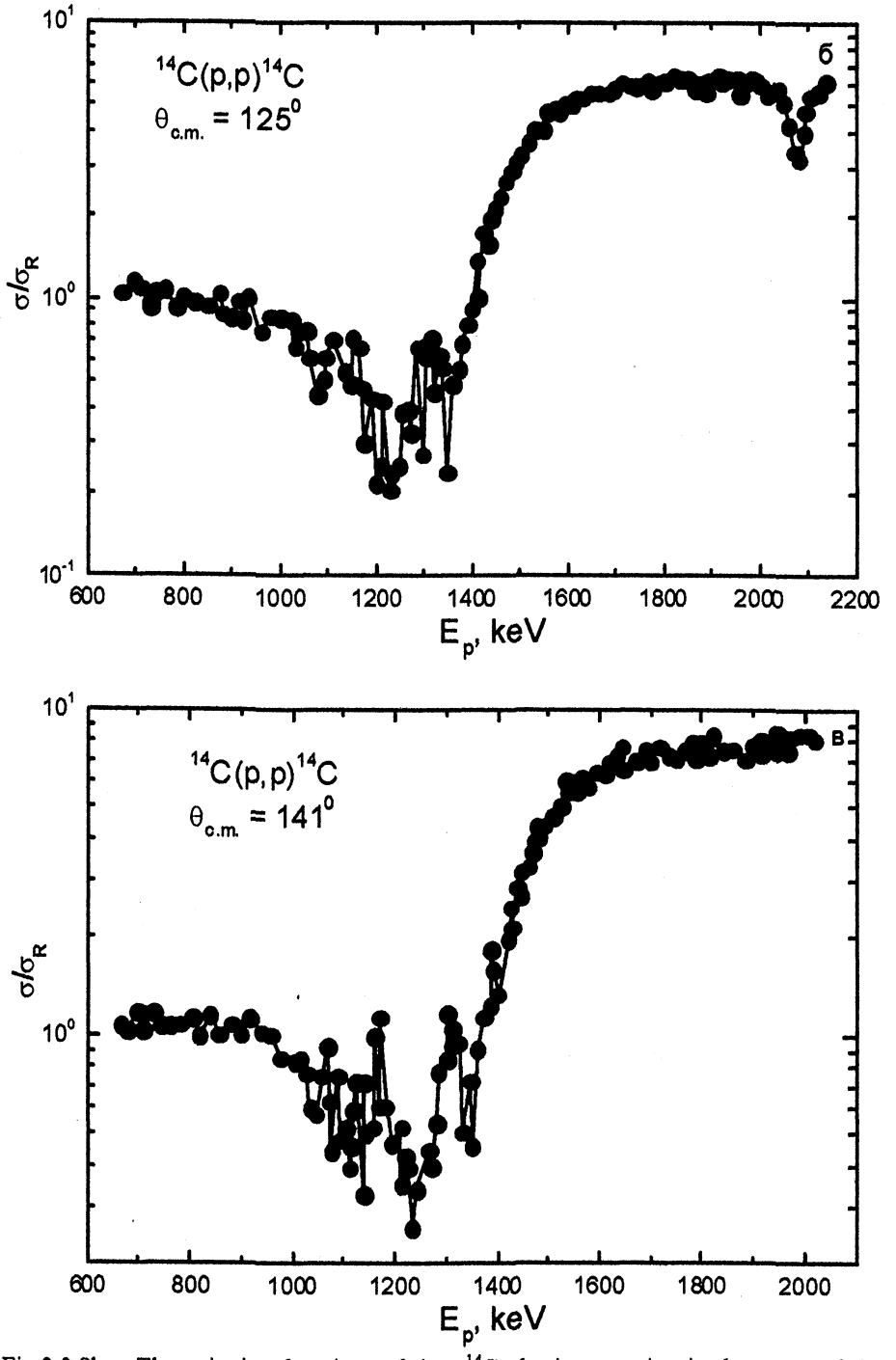

Fig.2.3.8b,c. The exitation functions of the $p^{14}C$ elastic scattering in the range of the $^2S_{1/2}$ resonance [126]. Solid curve – their approximation on the basis of the obtained phase shifts.

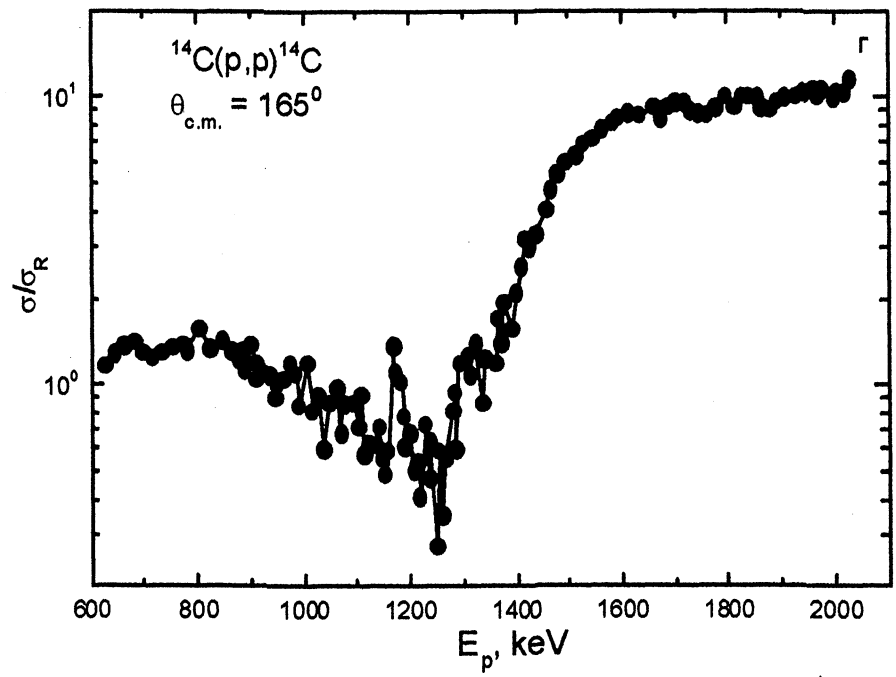

Fig. 2.3.8d. The exitation functions of the $p^{14}C$ elastic scattering in the range of the $^2S_{1/2}$ resonance [126]. Solid curve – their approximation on the basis of the obtained phase shifts.

It is necessary to notice that in work [126] the detailed analysis of the resonances, including, at 1.5 MeV was not carried out as it has been made earlier in works [127] on the basis of the proton capture reaction on ^{14}C. Here, as it was clear from results of the phase shift analysis, the resonance energy at 1.5 MeV is a little overestimated concerning the results [127]. However, as it is clear in Fig.2.3.8, errors of the experimental data by the scattering cross sections in excitation functions are too large to draw now the unambiguous conclusions about the energy of such resonance.

Apparently, the additional, more modern and more exact measurements of cross sections of the $p^{14}C$ elastic scattering, in order that on the basis of these data it was possible to draw more certain conclusions about the resonance energy in the $^2S_{1/2}$ phase shift at 1.5 MeV, are required. The difference between obtained here and in work [127] energies of this resonance in 63 keV, in general, does not play a basic role – as nevertheless it is clear where it is located.

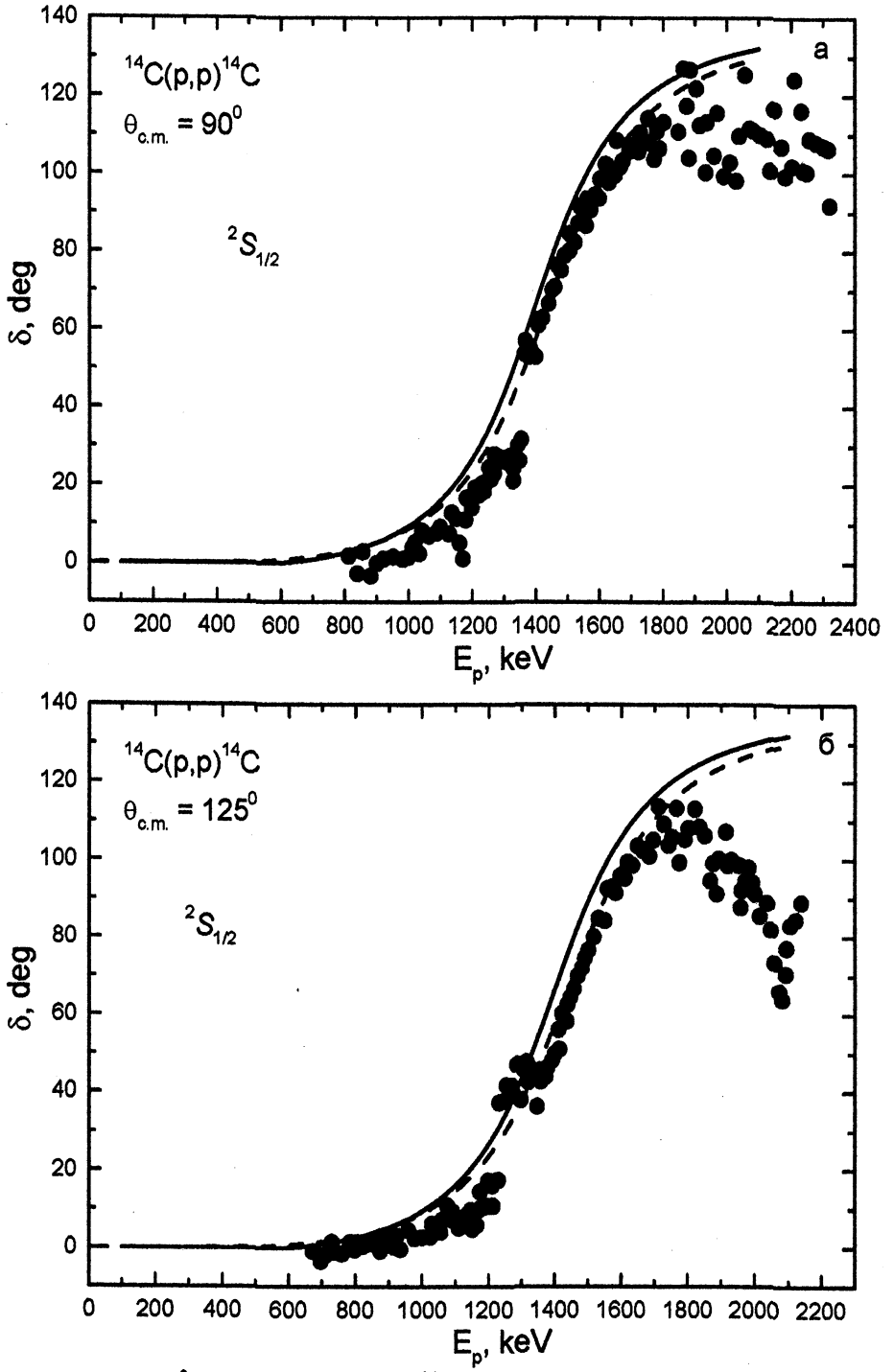

Fig.2.3.9a,b. The $^2S_{1/2}$ phase shift of the $p^{14}C$ elastic scattering at low energies obtained on the basis of the excitation functions shown in Fig. 2.3.8. Points – results of our phase shift analysis made on the basis of data [126], curves – calculation of the phase shift with the potentials given in the text.

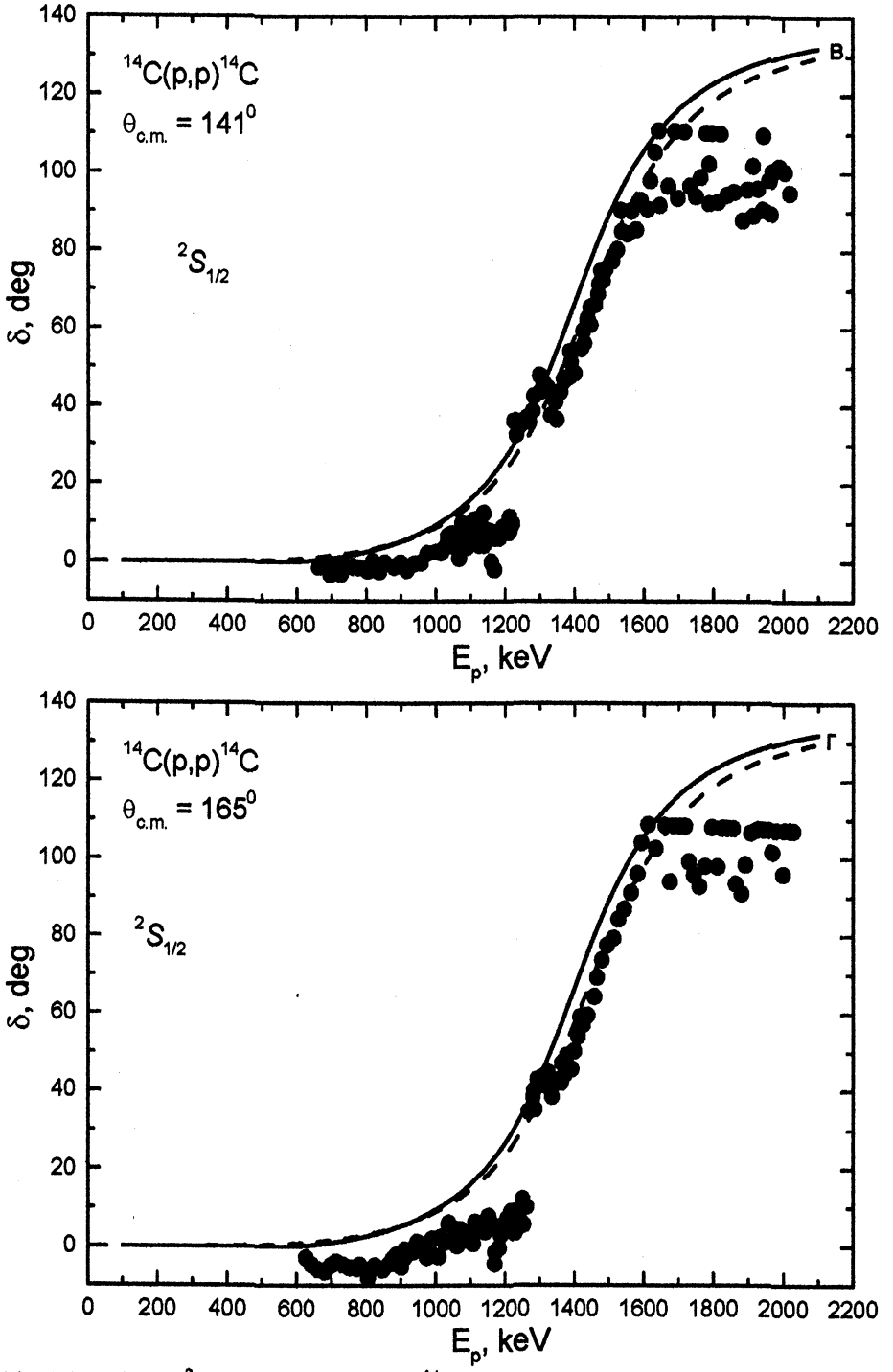

Fig. 2.3.9c,d. The $^2S_{1/2}$ phase shift of the $p^{14}C$ elastic scattering at low energies obtained on the basis of the excitation functions shown in Fig. 2.3.8. Points – results of our phase shift analysis made on the basis of data [126], curves – calculation of the phase shift with the potentials specified in the text.

Passing to the construction of the potentials of the $p^{14}C$ elastic scattering, in the beginning we will consider the classification of the orbital states according to Young tableaux. We will consider that the {4442} tableau corresponds to the ground bound state of ^{14}C [123,128,129]. The possible orbital Young tableaux in system $N = n_1 + n_2$ of particles can be defined as the direct external product of orbital tableaux of each subsystem that for the $p^{14}C$ system within a 1*p*-shell gives {1} × {4442} → {5442} + {4443} [123,128]. The first of the obtained tableaux is compatible to the orbital moment $L = 0$ and is forbidden as in a s-shell there cannot be five nucleons, and the second tableau is allowed and compatible to the orbital moment L, equal to one [123,128,129].

Thus, in the potential of the $^2S_{1/2}$ wave the forbidden bound state is contained, and the ^2P waves have only allowed BS. The ground state of ^{15}N in the $p^{14}C$ channel, which is at energy of -10.2074 MeV [120], belongs to the $^2P_{1/2}$ wave and does not contain the FS. (We will notice that the moment of ^{14}C is equal to $J^\pi = 0^+$, and the isospin T is equal to 1 as it is provided in work [120]).

However, we have not the complete tables of the multiplication of Young tableaux for the system with number of particles more than eight [130], which were used by us earlier for the similar calculations [123,128,129,131,132]. Therefore, the result obtained above should be considered only as the quality standard of the possible orbital symmetry for the BS, allowed or forbidden, in ^{15}N for the considered $p^{14}C$ channel.

For the description of the extracted in our analysis $^2S_{1/2}$ scattering phase shift a simple Gaussian potential of the form (1.6.2) with the bound FS and following parameters is used

$$V_0 = -5037.0 \text{ MeV}, \ \gamma = 12.0 \text{ fm}^{-2}, \qquad (2.3.6)$$

that lead to the scattering phase shifts with the resonance at 1500 keV in l.s. and the width of 530 keV in the c.m., what won't badly be coordinated with the available experimental data [120]. In this work in tab. 15.11 the value 1509(4) keV are given in l.s. with a total width of 404.9±6.3 keV in c.m. and with a proton width of 400.9±6.3 keV. The parameters of potential (2.3.6) were selected so that, in general, it is correct to reproduce the data of resonance from work [120] which were obtained earlier in works [127].

The phase shift of such potential is shown in Fig. 2.3.9a,b,c,d, by the solid curves and at the resonance energy of 1500 keV reaches the value of 90(1)°. The energy behavior of the scattering phase shift, in general, correctly describes the scattering phase shifts obtained in the phase shift analysis if to consider the shift of resonance energy approximately on 70 keV concerning the results [120,127]. The calculation curve of the phase shifts for this potential goes parallel to the points obtained in our phase shift analysis for all four scattering angles.

For more exact description of the data obtained in the phase shift analysis the potential is required

$$V_0 = -5035.5 \text{ MeV}, \ \gamma = 12.0 \text{ fm}^{-2}, \qquad (2.3.7)$$

It leads to the resonance energy of 1550 keV, its width of 575 keV, and the results of calculation of the $^2S_{1/2}$ phase shift are shown in all Figs.2.3.9 by the dashed curve. It is clear that this curve is shown the results of the phase shift analysis made here much better.

All potentials of the P scattering waves, as they do not contain the FS, can just be put equal to zero. Such potentials will lead to the scattering phase shifts, which are also equal to zero. In spectra of ^{15}N there are two resonance levels, which can be carried to the P waves in the p^{14}C channel. Namely, one of them lies approximately at 0.53 MeV and has the moment $J^{\pi} = 3/2^-$. However, their width in 0.2 keV and 8(3) keV are respectively so small (see tab. 15.11 in work [120]) that it is not possible to construct the corresponding potentials according to these data [133].

It should be again noted that on the known energy of resonance level in spectra of any nucleus [120] and its width the potential of the $^2S_{1/2}$ waves are under construction completely unambiguously, if the number of BS, forbidden or allowed states in this partial wave are given, which in this case is equal to one. In other words, it is impossible to find other combination of parameters V and γ, which would be capable to transfer the resonance energy of level and its width correctly. The depth of such potential of V unambiguously defines the location of the resonance, i.e. the resonance energy of the level, and its width γ sets the certain width of this resonance state [28,122,123,125,128,129,132,158], which have to correspond to the experimentally observed values [120]. In this case for the correct

reproduction of width of the resonance in case of 1509 keV, would have to reduce the potential width, increasing the γ parameter. Only in this case it would be possible to obtain more correct width of the resonance of about 400 keV.

2.3.6 Phase shifts and potentials of the $n^{16}O$ scattering

For carrying out of the calculations of radiative capture in the frame of modified PCM [2] it is required to know the potentials of the $n^{16}O$ elastic scattering in $^2S_{1/2}$, $^2P_{1/2}$, $^2P_{3/2}$, $^2D_{3/2}$ and $^2D_{5/2}$ waves, and also the interaction $^2D_{5/2}$ ground and first excited $^2S_{1/2}$ states of ^{17}O. For the transition to these BS there are the experimental data for total cross sections for radiative capture obtained in work [134].

For this system, as usual, the potentials of the scattering processes are under construction on the basis of elastic scattering phase shifts, which are higher than 1.1 MeV have been obtained in works [135,136]. For the energy range 0.2–0.7 MeV there are the results of the phase shift analysis [137], based on measurements of the differential cross sections of the $n^{16}O$ elastic scattering [138] in the range of the resonance at 0.433 MeV [103]. In work [137] also some preliminary results of the phase shift analysis are given in the range of the $^2D_{3/2}$ resonance at the energies of 750–1200 keV.

Later, new experimental data [139] on the excitation function at energies from 0.5 to 6.2 MeV, are listed in the database [140], and which, as far as we know, at energies in the range of the $^2D_{3/2}$ resonance of 1.0 MeV [103] in the phase shift analyses have not been considered. The data [139] are used by us further for carrying out of the phase shift analysis and the extraction of the shape of the phase shift in the $^2D_{3/2}$ wave of the $n^{16}O$ scattering. The used exitation functions at 40° in l.s. or 42.3° in c.m. [139] are shown in Fig.2.3.10 in the energy range from 0.75 to 1.25 MeV (l.s.) by open circles. In our analysis more than 500 points for cross sections at different energies from the excitation functions obtained in work [139] were used.

Let us notice that lower 0.7–0.8 MeV the ambiguity of the data [139] sharply increases, however, for the extraction of the $^2D_{3/2}$ scattering phase shift it is enough to consider the energy range shown in Fig.2.3.10, which has rather small ambiguity and such data can quite be used for the carrying

out of the phase shift analysis.

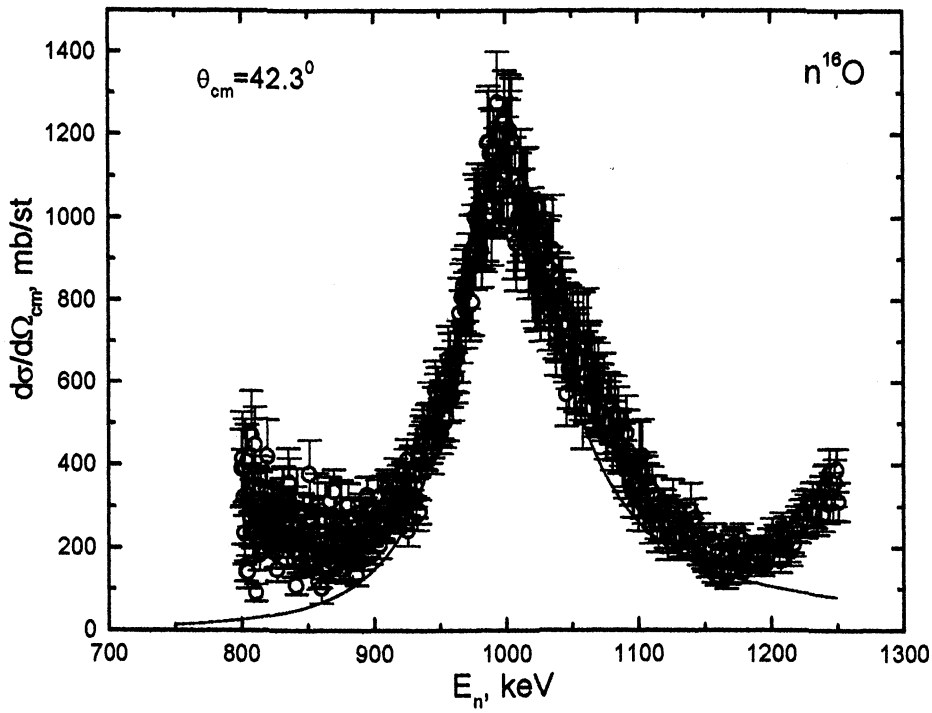

Fig.2.3.10. Exitation functions of the $n^{16}O$ elastic scattering in the range of the $^2D_{3/2}$ resonance at 1.0 MeV, shown by open circles [139]. Curve – calculation of the cross sections with the potential specified in the text.

The details of the search method of phase shifts used by us in the elastic scattering of the particles with spin 1/2 + 0 are given above and in work [141]. The main expressions for the cross sections used in the phase shift analysis are given in chapter 1, the beginning of this paragraph and works [6,141]. The results of the present analysis of the $n^{16}O$ elastic scattering in the energy range from 0.75 to 1.25 MeV are shown in Fig.2.3.11 by open circles. In Fig.2.3.11 the black squares show the results of the phase shift analysis from work [135], the obtained above 1.1 MeV, and the results of the analysis from [137] are given by triangles.

For description of the cross sections in excitation functions [139], at least, at the energies up to 1.2–1.25 MeV it is not required to consider the $^2S_{1/2}$ scattering phase shift as its presence does not change the χ^2 value, i.e. its values can be accepted equal to zero. The χ^2 values as only one point in cross sections for each energy is considered, has the average value $4.7 \cdot 10^{-3}$

with the maximum partial value $\chi^2_i = 0.6$ at energy of 999.5 keV.

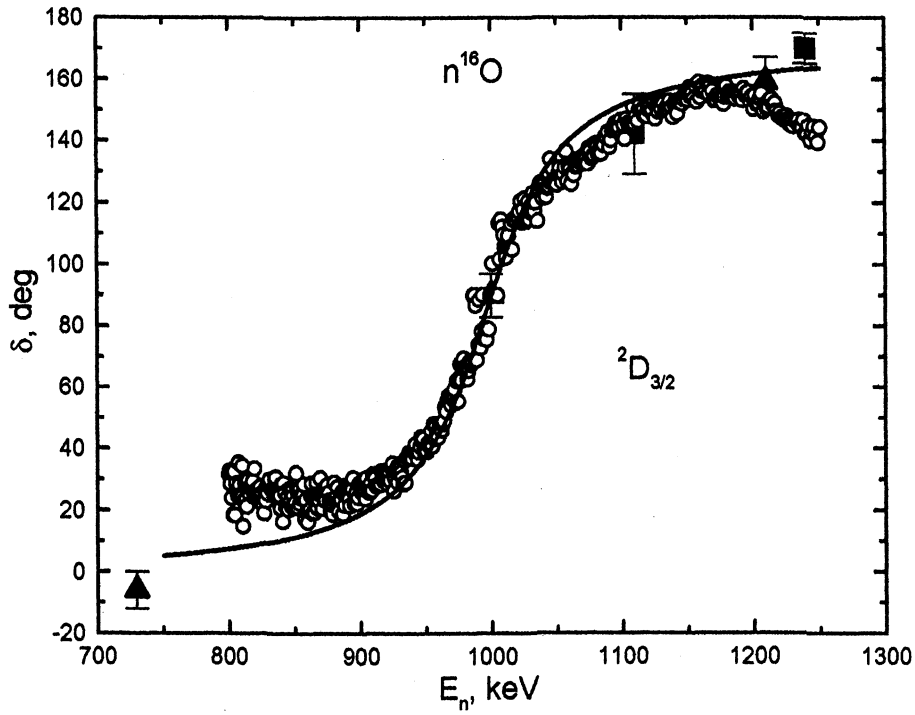

Fig.2.3.11. $^2D_{3/2}$ phase shift of the $n^{16}O$ elastic scattering at low energies. Open circles (○) – the results of our phase shift analysis made on the basis of data [139], black squares (■) – results of the phase shift analysis from work [135], triangles (▲) – results of the analysis from work [137], solid curve – calculation of the phase shift with the potential specified in the text.

For description of the $^2D_{3/2}$ scattering phase shift in Fig.2.3.11 obtained as a result of the phase shift analysis, it is possible to use a simple Gaussian potential (1.6.2) with the parameters

$$V_{D3/2} = -95.797 \text{ MeV}, \quad \gamma_{D3/2} = 0.17 \text{ fm}^{-2}, \qquad (2.3.8)$$

which has not got bound FS and leads to the resonance energy of 1000 keV at the phase shift of 90.0(1)° with a width of level of 88 keV in l.s. or 83 keV in c.m. At the same time, in tab.17.17 of work [103] for the value of width given the 96 keV in c.m or 102 keV in l.s. at energy of level 1000±2 keV in l.s.

The energy dependence of the $^2D_{3/2}$ scattering phase shift of the potential (2.3.8) is shown in Fig.2.3.11 by the solid curve. Such potential

well describes the behavior of the phase shift obtained by us in the range of the resonance and quite agrees with the previous extraction of the scattering phase shift, which were carried out in works [135,137]. The form of cross sections in the excitation functions calculated with a $^2D_{3/2}$ phase shift of potential (2.3.8) at zero values of other phase shifts, is shown in Fig.2.3.10 by the solid curve. From these results it is clear that the $^2D_{3/2}$ phase shift almost completely defines the behavior of such cross sections in the excitation function.

Furthermore, we will consider the total cross sections for the radiative capture taking into account the $E1$ transitions from the $^2P_{3/2}$ resonance in the $n^{16}O$ scattering at 433 keV to the $^2D_{5/2}$ ground and $^2S_{1/2}$ first excited state of ^{17}O. For the construction of the $^2P_{3/2}$ scattering potential, except the data about the location and width of such level from the review [103] (see tab. 17.17), we use the results of the phase shift analysis [137] shown by triangles in Fig.2.3.12.

As a result we find that for description of the resonance $^2P_{3/2}$ scattering phase shift at 433(2) keV (l.s.) with width of 45 keV in c.m. or 48 keV in l.s. [103] the potential without the forbidden or allowed BS with the following parameters is required

$$V_{P3/2} = -1583.545 \text{ MeV}, \quad \gamma_{P3/2} = 6.0 \text{ fm}^{-2}, \qquad (2.3.9)$$

which leads to the width of level of 44 keV in c.m. or 47 keV in l.s. at resonance of 433 keV (l.s.). The phase shift of such potential at resonance energy is equal to 90.0(0.2)°, and the complete dependence of the scattering phase shift from energy in the range of resonance is shown in Fig.2.3.12 by the solid curves.

Here, again, it is necessary to note that the well-known resonance energy level in the spectra of ^{17}O and its width the potential is constructed entirely clear. In other words, it is impossible to find other V_0 and γ parameters, which would be capable to describe correctly the resonance energy of level and its width, if the number of the BS, which, in this case, is equal to zero is given. The depth of such potential unambiguously defines the provision of a resonance, i.e. the resonance energy of level, and its width sets a certain width of this resonance state.

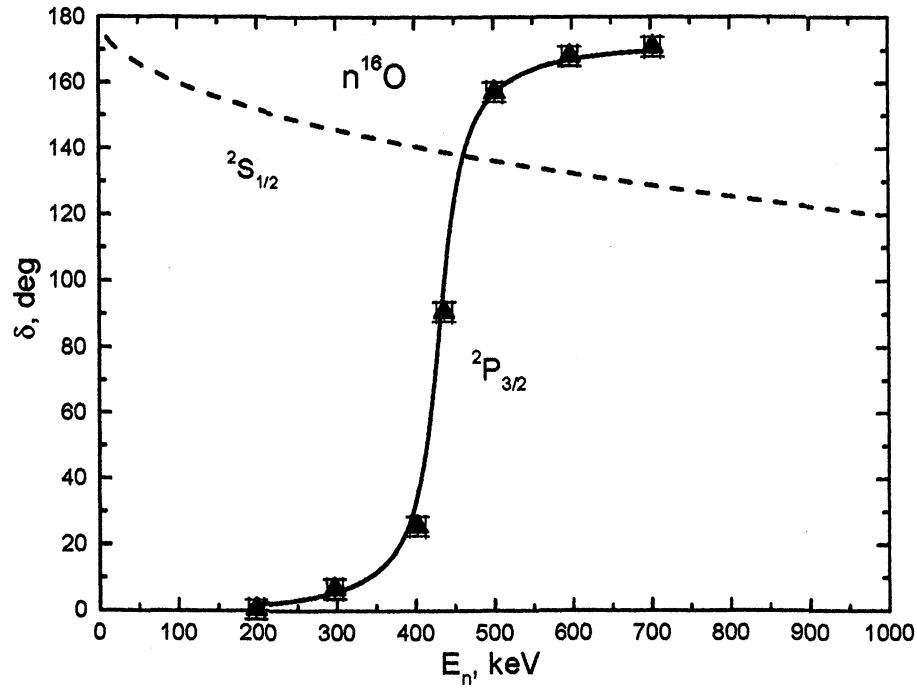

Fig.2.3.12. $^2S_{1/2}$ and $^2P_{3/2}$ phase shifts of the $n^{16}O$ elastic scattering at low energies. Triangles (▲) – results of the phase shift analysis from work [137]. Solid curve – calculation of the phase shift with a potential specified in the text.

In the spectra of ^{17}O lower than 1.0–1.3 MeV there are no resonance levels with $J^\pi = 1/2^-$ и $5/2^+$ moment [103], which could be compared to the $n^{16}O$ channel. Therefore, the $^2P_{1/2}$ and $^2D_{5/2}$ potentials of scattering waves have no bound FS or AS and can have the zero depth, i.e. zero scattering phase shifts. Such assumption was already used by us earlier and completely was repaid for some other systems of particles by the consideration of other processes of radiative capture [2].

Furthermore, for carrying out of calculations of the radiative capture in the frame of the modified PCM we will need the interaction potentials of $n^{16}O$ clusters in the BS. We will consider the electromagnetic transitions to the ground bound state from $J^\pi,T = 5/2^+,1/2$ at energy of -4.1436 MeV and first excited with $J^\pi = 1/2^+$ at -3.2729 MeV of ^{17}O in the $n^{16}O$ channel [103]. The width of such potentials was fixed on the basis of the correct description of the binding energy and charge radius of ^{17}O is equal to 2.710(15) fm [103], and then comparison of the calculated asymptotic constants of the $n^{16}O$ channel with other independent data, was carried out.

As a result, for the $^2D_{5/2}$ potential of the GS of ^{17}O in the n^{16}O channel without the FS the following parameters were found

$$V_{g.s} = -102.2656782 \text{ MeV}, \quad \gamma_{g.s} = 0.15 \text{ fm}^{-2}, \qquad (2.3.10)$$

which allow one to obtain the binding energy of -4.1436000 MeV with an accuracy of 10^{-7} MeV [141], the charge radius of 2.71 fm, mass radius of 2.73 fm, and the dimensionless asymptotic constant (1.6.3) on an interval of distances of 6–16 fm was equal to $C = 0.75(1)$. The phase shift of such potential with one bound AS decreases smoothly and at energy of 1.0 MeV accepts the value of 179.6°, i.e. actually has the zero value.

As the charge radius of neutron, as usual, the zero value was used, and its mass radius relied 0.8775(51) fm equal to the charge radius of proton specified in the base [75]. In work [142] for the AC of the GS the 0.9 fm$^{-1/2}$ is obtained, that after the recalculation with $\sqrt{2k}_0 = 0.933$ to dimensionless value gives 0.96. In work [65] for the GS the value of 0.77(8) is given in a dimensionless, that taking into account the errors will completely be coordinated with the value obtained above.

For the $^2S_{1/2}$ potential of the first excited state of ^{17}O in the n^{16}O channel with one bound forbidden state [2] the following parameters are found

$$V_{S1} = -81.746753 \text{ MeV}, \quad \gamma_{S1} = 0.15 \text{ fm}^{-2}, \qquad (2.3.11)$$

which lead to the binding energy of -3.2729000 MeV relatively to the threshold of the n^{16}O channel or 0.8707 MeV relatively to the GS of ^{17}O with an accuracy of 10^{-7} MeV [141], to the charge radius of 2.71 fm, mass radius of 2.80 fm and AC on an interval of distances of 6–17 fm equal to C = 3.09(1). The phase shift of such potential is shown in Fig.2.3.12 by the shaped curves – it smoothly falls down and at 1.0 MeV reaches the 119.6°. For this $^2S_{1/2}$ level in work [142] for the AC the value of 3.01 fm$^{-1/2}$ is obtained that after recalculation with $\sqrt{2k}_0 = 0.88$ gives 3.42. Apparently, in this case for the value of an asymptotic constant the acceptable consent between the different results turns out – difference between them makes approximately for 10%.

For the additional control of the calculation of energy of the bound

state the variation method [10,141], which for the ground state is already on a grid with dimension $N = 10$ at the independent variation of parameters for the potential (2.3.10) has allowed to obtain the energy of -4.1435998 MeV, was used. The parameters of the variation wave function are specified in tab. 2.3.9, and the value of the residuals does not exceed 10^{-8} [141]. The charge radius and asymptotic constant on the interval of 6–16 fm do not differ from the values, obtained above in the FDM. As for the real binding energy in such potential it is possible to accept the average value -4.1435999(1) MeV, the accuracy of the determination of the binding energy by two methods (FDM and VM) according to two various computer programs is at the level of ±0.1 eV in the full compliance with given in the FDM program the error of search of the binding energy of 10^{-7} MeV.

For the energy of the first excited, but bound state in the $n^{16}O$ channel, on the grid with the dimension $N = 10$ and an independent variation of parameters for potential (2.3.11) energy of -3.2728998 MeV is obtained. The parameters of variation wave function are specified in tab.2.3.10, and the value of the residuals does not exceed 10^{-10} [141].

Tab.2.3.9. The variation parameters and coefficients of the decomposition of the radial WF in the $n^{16}O$ system for the ground potential of $5/2^+$ state for potential (2.3.10). The WF normalization on an interval 0–30 fm is equal to N_0 = 9.999999999996603E-001.

i	α_i	C_i
1	2.970820484267648E-002	5.999898648526680E-002
2	1.355376641105716E-002	-5.268187781652860E-006
3	2.971441871730051E-002	-6.024647870785407E-002
4	6.553466412237838E-002	-3.087819670804185E-003
5	1.253831431831826E-001	-1.906462762571792E-002
6	2.156627509028788E-001	-6.585296562529887E-002
7	3.393826502547065E-001	-1.006636861923295E-001
8	5.166966410860497E-001	-4.627970949895152E-002
9	1.063579836670607	-1.116683372038532E-003

10	1.639614546923715	2.440471375269290E-004

Tab.2.3.10. The variation parameters and coefficients of the decomposition of the radial WF in the $n^{16}O$ system for the potential first excited of $1/2^+$ state for potential (2.3.11). The WF normalization on an interval of 0–30 fm is equal to N_0 = 9.999999975230215E-001.

i	α_i	C_i
1	1.268144327251019E-002	7.701423164869143E-003
2	4.193709029136675E-003	4.794229107401904E-005
3	2.881642596445175E-002	5.677769979981124E-002
4	6.245243687002310E-002	1.570309903921747E-001
5	1.259974114760052E-001	2.619817602771229E-001
6	2.163927688688810E-001	-4.833513946049395E-002
7	3.383830162751630E-001	-7.529455791580352E-001
8	5.187698913796229E-001	-4.062518687767323E-001
9	1.062316903143099	-5.106918680411997E-003
10	1.867671209905880	4.235490376362463E-004

The charge radius and the asymptotic constant on an interval of 6–20 fm do not differ from the values, obtained in the FDM calculations. For the real binding energy it is possible here to accept the average value -3.2728999(1) MeV, i.e. the energy determination accuracy by two methods according to two various computer programs is also at the level of ±0.1 eV = ±100 meV.

In all real calculations of characteristics of ^{17}O for the value of ^{16}O mass the value $m(^{16}O)$ = 15.994915 amu was used [143], and the mass of neutron was specified earlier.

2.3.7 Phase shift analysis of the $p^{16}O$ scattering

Apparently, one of the first measurements of the differential cross sections of the $p^{16}O$ elastic scattering with the carrying out of the phase shift analysis at the energies of 2.0–7.6 MeV have been made in work [144]. This analysis used the results of works [145] and [146] and some

unpublished results of [144] in two areas of energy 2.0–4.26 MeV and 4.25–7.6 MeV. The resonance at 2.66 MeV in laboratory system for the $^2P_{1/2}$ wave has been considered in details.

Subsequently, the polarization of the $p^{16}O$ elastic scattering in the range of 2.5–5.0 MeV have been measured in work [147] and new phase shift analysis is made at these energies which, however, obviously did not show resonance at 2.66 MeV [103]. Furthermore, in figures in work [148] and the table [149] (with the reference to [148]) the results of the detailed phase shift analysis of the $p^{16}O$ elastic scattering at energies of 1.5–3.0 and 2.5–3.0 MeV have been given respectively and [148] the presence of narrow resonance specified subsequently at the energy of 2.663(7) MeV with the width of 19(1) keV is confirmed. It corresponds to the first superthreshold state of ^{17}F at 3.104 MeV with $J^{\pi} = 1/2^-$ [103] and compare with $^2P_{1/2}$ wave in the $p^{16}O$ elastic scattering.

The processes of the $p^{16}O$ elastic scattering in the energy range of 1.0–3.5 MeV have been considered in many works (see, for example, their review in [103] and [150,151]). In particular, in works [152,153] is considered the range from 0.5–0.6 MeV to 2.0–2.5 MeV. In work [154] the measurements of the excitation functions at energies from 0.4 to 2.0 MeV are executed. However, in all these works [150-154] the phase shift analysis of the obtained experimental data was not made.

As a result, the phase shift analyses, which are available today have been carried out in the sixties and usually began with 2.0–2.5 MeV and further, at higher energies. There is only one point in scattering phase shifts at 1.5 MeV obtained in work [148], which has not been confirmed subsequently in other works. The study of an interval of energies from 2.0–2.5 MeV to 7–8 MeV and higher in the works given above is connected with the fact that the scattering phase shifts were under construction for further consideration of certain problems of nuclear physics – they did not occupy the area of astrophysical energies. Furthermore, we will consider the radiative capture in the field of astrophysical energies, approximately, to 2.0–2.5 MeV.

The results of the listed above works [150-154] and some other excitation functions and angular distributions are quite enough for the carrying out of the phase shift analysis up to 2.0–2.5 MeV and construction further of the $p^{16}O$ interaction potentials on the found scattering phase

shifts. Therefore, further we will carry out the phase shift analysis of the available experimental data from 0.4 to 2.5 MeV and we will obtain an exact type of the scattering phase shifts in this area of energies. Besides, we will recheck the results of some other phase shift analyses made in the 60th years of the last century.

2.3.7.1 Control of the phase shift analyses

In the beginning we will consider the results obtained in the phase shift analysis, which will be made on the basis of angular distributions of work [148] in the energy range of 1.5–3.0 MeV at 4 scattering energies in the range of angles 20°–160°. In other words, we will repeat the analysis made in [148] in the sixties of the last century.

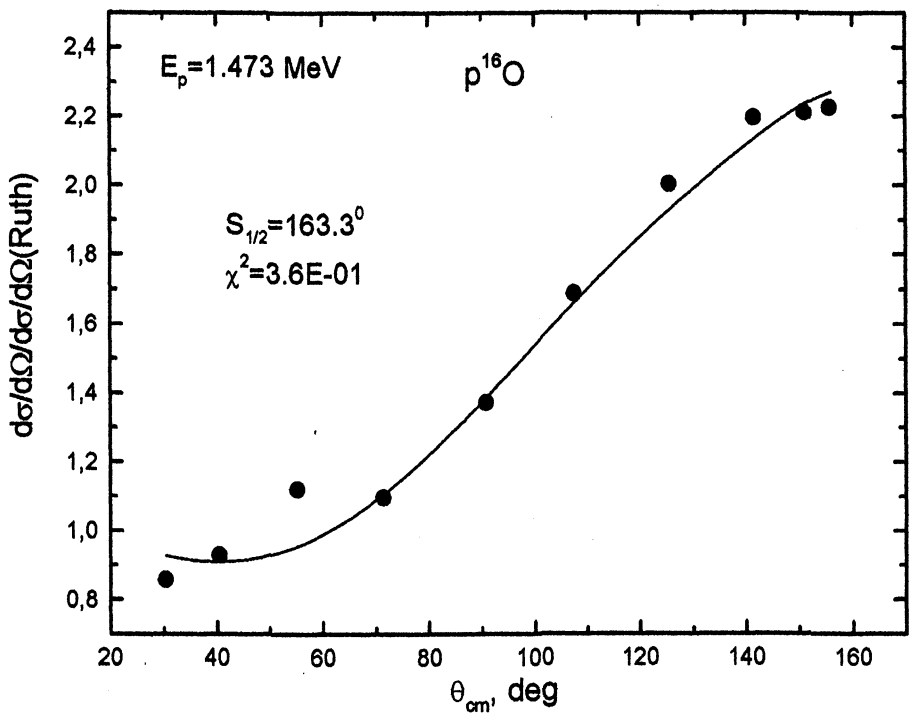

Fig.2.3.13a. The angular distributions of the p^{16}O elastic scattering measured in works [148] at the energy of protons of 1.473 MeV. Solid curve – calculation of these cross sections with the obtained scattering phase shifts.

The results of the description of cross sections with the phase shifts taken in our analysis are given by the solid curves in Fig. 2.3.13a,b,c,d, and

the phase shifts are shown by the open squares in Fig.2.3.13d in comparison with the data provided in works [144,147,149] and [148]. The χ^2 value obtained from 10% by the experimental errors is shown in Fig. 2.3.13a,b,c,d.

From the given results it is clear that only at energy of 2.978 MeV the phase shift from work [148] and obtained by us differs on 1.5–2°. For three other energies the coincidence is at the level of less than 1°, and for 2.48 MeV results completely coincide. As we will consider further the proton radiative capture on ^{16}O in the energy range to 2.5 MeV without taking into account the narrow resonance at 2.66 MeV [103], here there will not be considered in details the area of this resonance studied earlier in the phase shift analysis [144] and shown in Fig. 2.3.13d by open circles and also in the analysis of work [148].

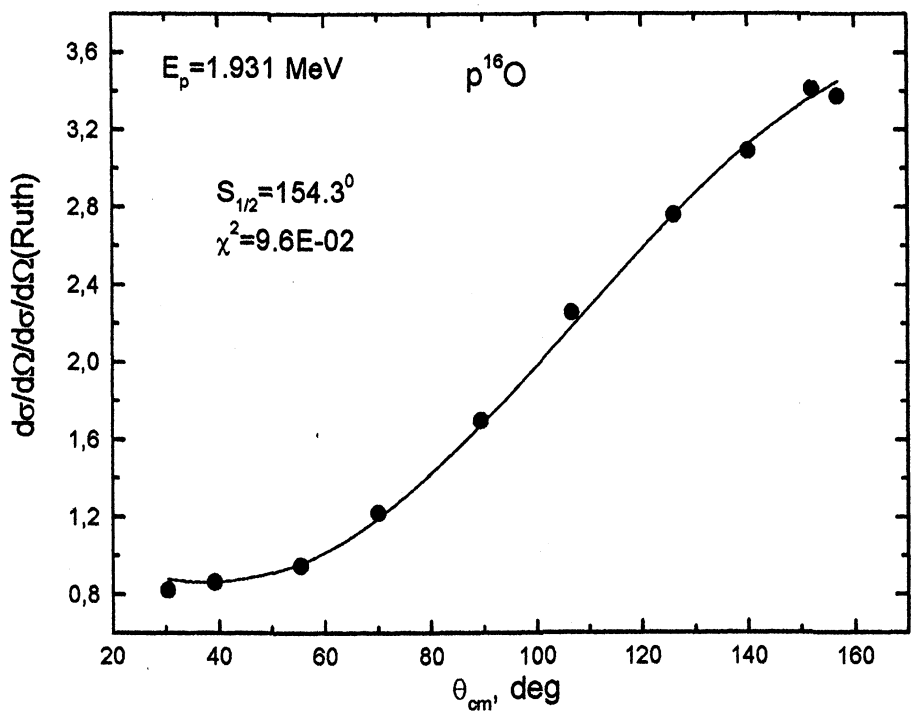

Fig.2.3.13b. The same as in Fig.2.3.13a, but at energy of protons of 1.931 MeV.

Let us give one more result for angular distributions from work [147] at energy of 2.5 MeV. In Fig.2.3.14 the differential cross sections measured in angular distributions were shown by points, and our results of calculation of these cross sections with the found phase shifts were shown by the solid

curve. The χ^2 value is equal to 0.67 with 10% experimental errors, it is obtained only at the accounting of one scattering phase shift shown in Fig 2.3.14 and equal to $S_{1/2} = 139.8°$ – this phase shift is shown in Fig. 2.3.13d by the open triangle. If we add to the analysis the $P_{1/2}$ scattering phase shift, then with 10 iterations [10] we will obtain $\chi^2 = 0.58$ and phase shifts: $S_{1/2} = 140.3°$and $P_{1/2} = 5.5°$. If we consider the $P_{3/2}$ phase shift, then with the same number of iterations we find $\chi^2 = 0.57$ and phase shifts: $S_{1/2} = 139.7°$, $P_{1/2} = -4.5°$ and $P_{3/2} = 4.6°$. From here it is clear that taking into account of P phase shifts at energy, which is adjacent to the narrow resonance region almost does not change the value of the S phase shift and significantly improves the χ^2 value.

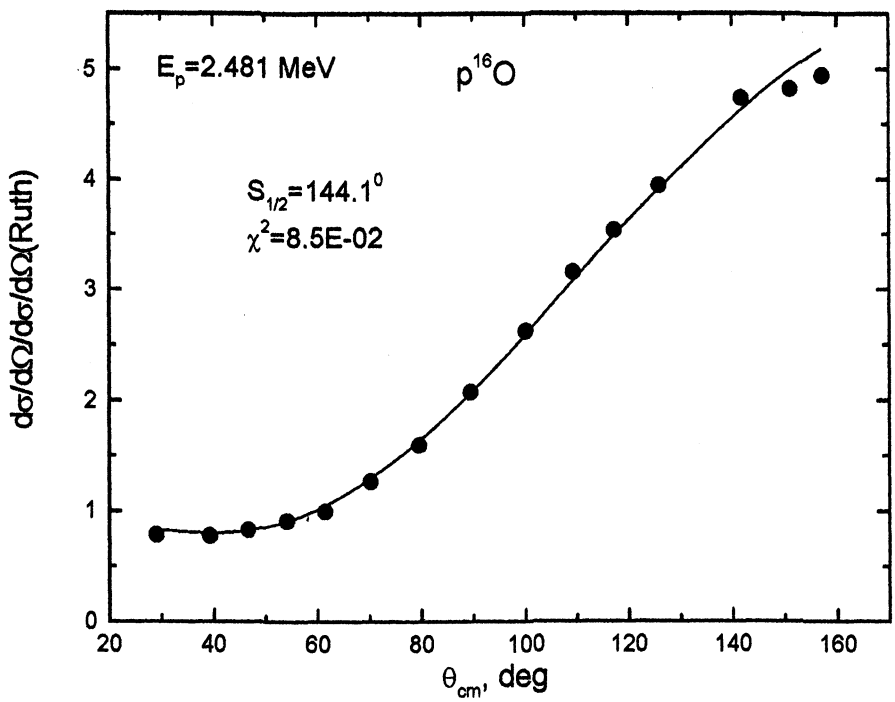

Fig. 2.3.13c. The same as in Fig.2.3.13a, but at energy of protons of 2.481 MeV.

In the work [147] the phase shift analysis has also been made and for this energy the following phase shifts are obtained: $S_{1/2} = 143.2°$, $P_{1/2} = 2.0°$, $P_{3/2} = 2.2°$, $D_{3/2} = 3.2°$ and $D_{5/2} = -1.6°$, and the χ^2 value isn't given in article. With such phase shifts the $\chi^2 = 0.62$ value with 10% the experimental errors were found in our calculations, and the results for the

cross sections of the elastic scattering are given in Fig.2.3.14 by the dashed curve, which practically merges with the solid.

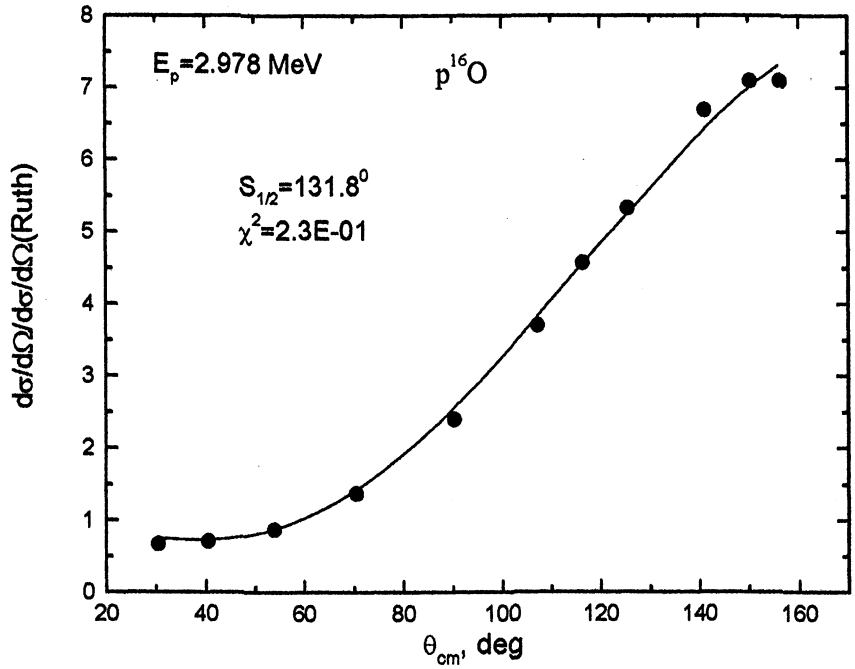

Fig.2.3.13d. The same as in Fig.2.3.13a, but at energy of protons of 2.978 MeV.

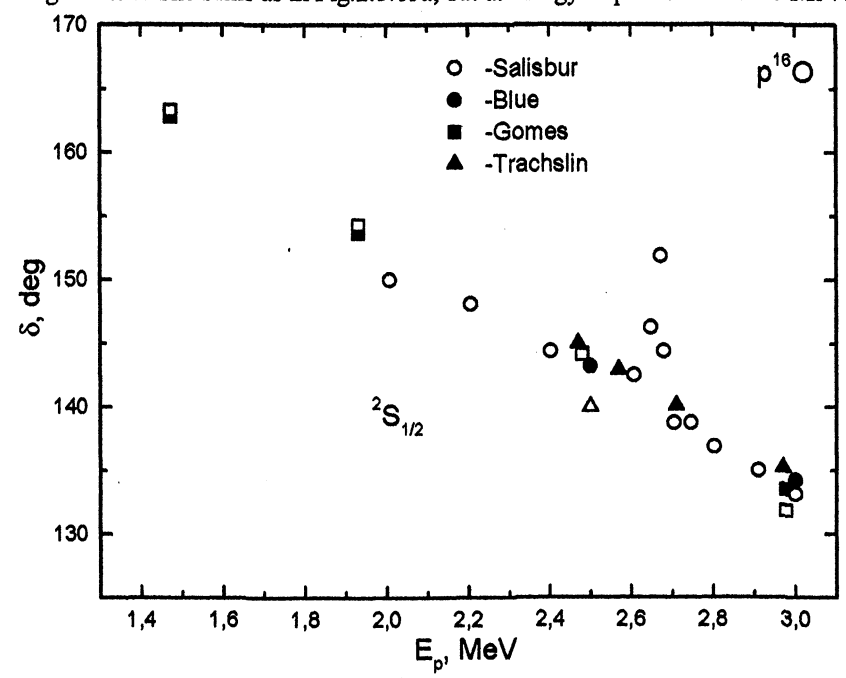

Fig.2.3.13d. The phase shifts of the p^{16}O elastic scattering obtained from the angular distributions of work [148] – open squares and [147] – open triangle. Other designations – results of works [144,147,148,149].

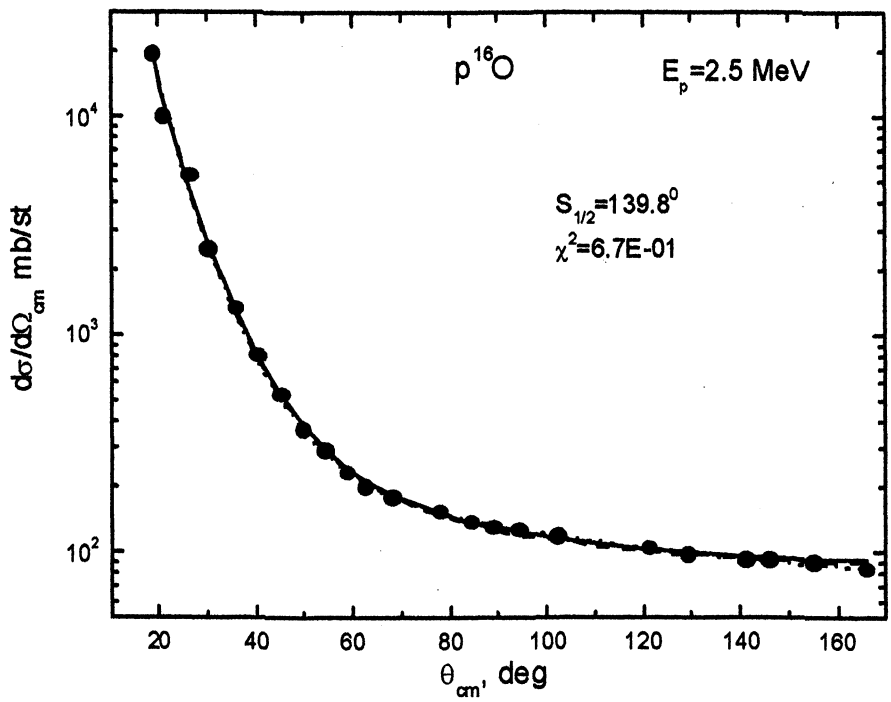

Fig.2.3.14. The angular distributions of the $p^{16}O$ elastic scattering measured in work [147]. Curves – calculation of cross sections on the basis of various phase shift analyses.

If we execute a variation of the phase shifts given in work [147] according to our program with 10 iterations, we will obtain $\chi^2 = 0.57$ with phase shifts: $S_{1/2}$ = 140.8°, $P_{1/2}$ = -2.8°, $P_{3/2}$ = 4.6°, $D_{3/2}$ = 3.1° and $D_{5/2}$= -2.3°. The scattering cross section with such phase shifts is shown in fig. 2.3.14 by the dot curves. From this figure it is clear that the accounting of the D phase shifts does not change the χ^2 value.

2.3.7.2 New phase shift analysis

As it was already told, in work [154] the measurements of exitation functions of the $p^{16}O$ elastic scattering at the energies from 0.4 to 2.0 MeV were carried out, however, as we know, the phase shift analysis for these data was not executed. The results of measurements of the excitation functions performed in this work at the scattering angle of 171.5° in c.m was shown in Fig.2.3.15a by points. the results of our phase shift analysis obtained on the basis of these data were shown in Fig.2.3.15b by the circles and in tab.2.3.11. The phase shift is shown in Fig.2.3.15b from 180°

because, as was shown earlier [2], in the S wave there has to be the forbidden bound state and at zero energy it is required to apply the generalized Levinson's theorem for the determination of the phase shift [4].

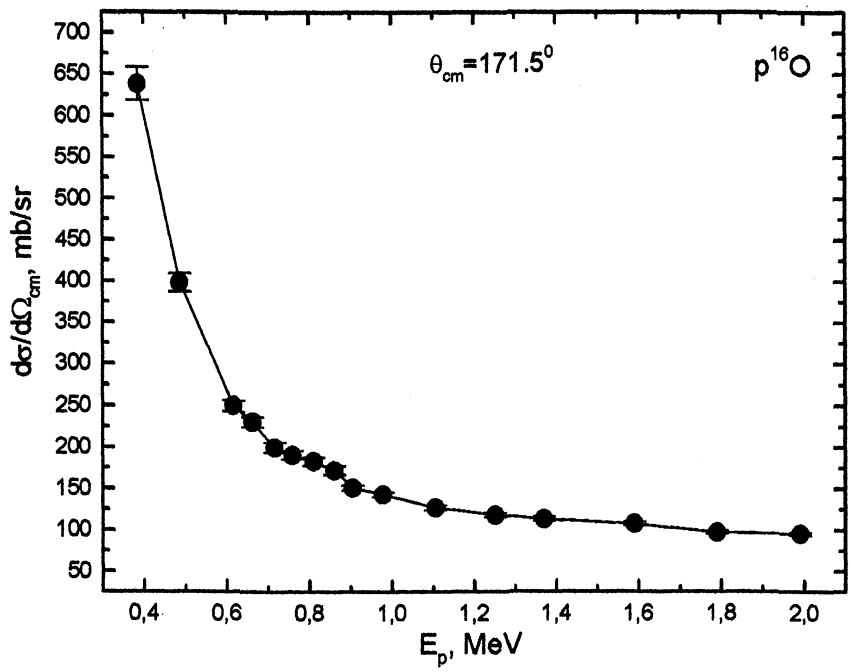

Fig.2.3.15a. The excitation functions of the $p^{16}O$ elastic scattering measured in work [154]. Solid curve – calculation of the cross sections with the obtained scattering phase shifts.

The values of the cross sections calculated with the obtained phase shifts are shown in Fig.2.3.15a by the solid curve. The χ^2 value with provided in [154] experimental errors cross sections in the excitation functions is given in Fig.2.3.15c by the solid curve. As can be seen from this figure, the χ^2 value at different energies does not exceed 10^{-5}. As a result one $S_{1/2}$ phase shift is found completely unambiguously. For all other results of the phase shift analyses made on excitation functions and provided further the χ^2 value is approximately at the same level.

For comparison in Fig.2.3.15b the results of phase shift analyses from works [144] are shown – point at 2 MeV and [148] – squares approximately at 1.5 and 2 MeV. From new results, shown in Fig.2.3.15b by circles, the $^2S_{1/2}$ scattering phase shift form at the lowest energies, which plays the main role by the consideration of the thermonuclear processes of radiative capture at astrophysical energies is well visible.

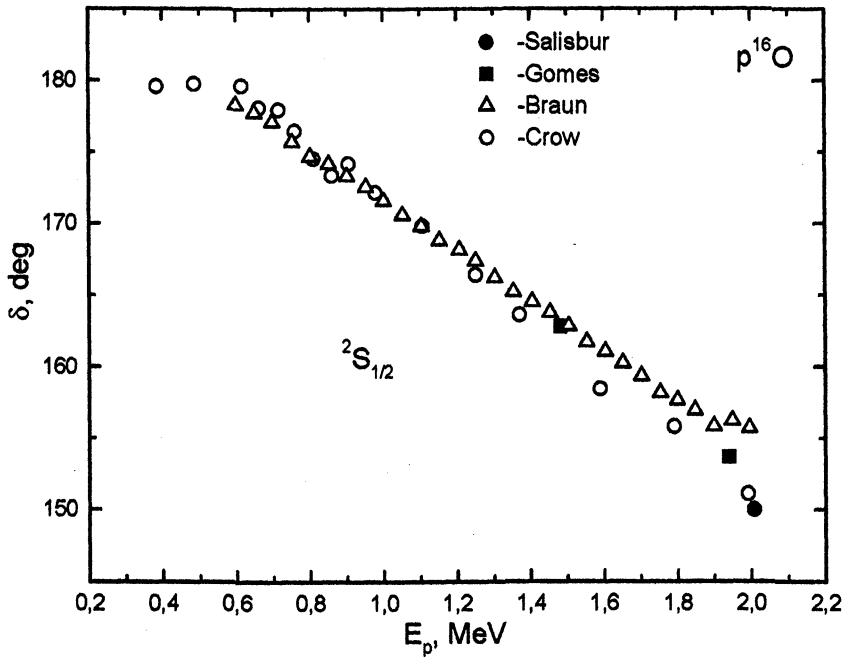

Fig.2.3.15b. The phase shifts of the $p^{16}O$ elastic scattering obtained by us from the excitation function of work [154] – open circles and [152] – open triangles. The comparison with results of phase shift analyses of works is given in [144,148].

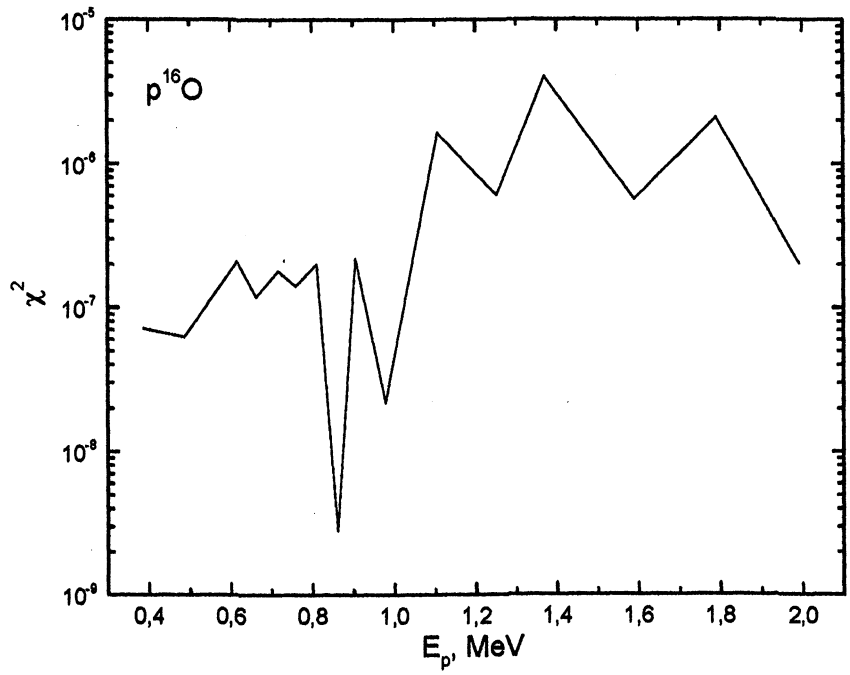

Fig.2.3.15c. The χ^2 value obtained with the scattering phase shifts shown in Fig.2.3.15b at the description of experimental excitation functions [154].

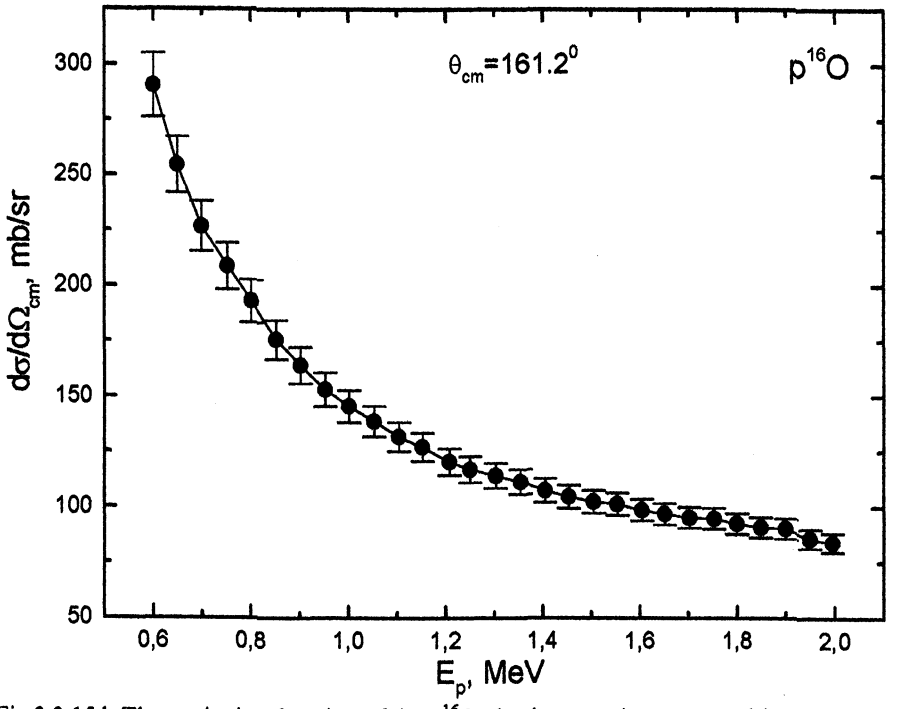

Fig.2.3.15d. The excitation function of the $p^{16}O$ elastic scattering measured in work [152]. Solid curve – calculation of the cross sections with the obtained scattering phase shifts.

Tab. 2.3.11. $^2S_{1/2}$ scattering phase shift obtained by us from data of work [154]

E_p, MeV	Phase shift, deg.
0.3855	179.59
0.4871	179.74
0.6162	179.65
0.6631	178.11
0.7162	177.96
0.759	176.46
0.8108	174.55
0.8612	173.37
0.9058	174.19
0.979	172.17
1.1063	169.82
1.2508	166.43

1.3704	163.61
1.5898	158.42
1.7903	155.78
1.9909	151.09

It is clear that at energy of 0.6 MeV and less this phase shift is almost equal to 180°. At energies higher than 1.5 MeV the good consent with the previous results of phase shift analyses is observed [144,148]. The difference of the true and former results on the scattering phase shifts obtained in the sixties of the last century does not exceed 1°–2°. Here it is possible to notice that the measurements of differential cross sections of work [154] have been performed in the mid-seventies and a little differ from data [144,148]. However, in other works the other value of constant $\hbar^2/m_0$ could be used that allows one to explain such distinction of the phase shifts. Let us remind that here the value $\hbar^2/m_0$ = 41.4686 MeV fm^2 was usually used.

Now we will consider the data on excitation functions from work [152] at energies of 0.6–2.0 MeV and scattering angle 160° in l.s. or 161.2° in c.m. The cross sections specified in [152] are given in l.s. and have been counted by us in c.m. – they are given by points in Fig.2.3.15d with 5% errors specified in [152]. For the recalculation of cross sections the following expression was used

$$\sigma_{cm} = \left| \frac{1+\gamma\cos(\theta_{cm})}{1+\gamma^2+2\gamma\cos(\theta_{cm})} \right|^{1.5} \sigma_{lab},$$

where $\gamma = m_1/m_2$, m – the masses of particles, meanwhile the m_1 particle is colliding. At this recalculation of cross sections the integer values of masses were used.

As it is seen from Fig.2.3.15b the scattering phase shift obtained on the basis of data [152] were shown by the triangles, the results of our phase shift analysis are quite acceptable coordinate with the previous extraction of phase shifts at the energies up to 2 MeV. The exception is made by two last points in the scattering phase shifts which, as well as the excitation functions [152] for these energies, differ a little from other results. In

Fig.2.3.15d by the solid curve the results of cross section calculation of the $p^{16}O$ elastic scattering with the phase shifts found in our analysis, which will be well coordinated with brought in [152] measurements are presented.

Furthermore, in work [155] good results for the differential cross sections at energy of 0.8–2.5 MeV and angle 170° in l.s. are obtained or 170.6° in c.m. with 4% of errors. However, the phase shift analysis of these data, as far as we know, still was not carried out. These results for the excitation functions are presented in Fig.2.3.16a by points, and the scattering phase shifts corresponding to them obtained in our analysis are shown in Fig. 2.3.16b by triangles. In Fig.2.3.16a the differential cross sections calculated with these scattering phase shifts are shown by the solid curve.

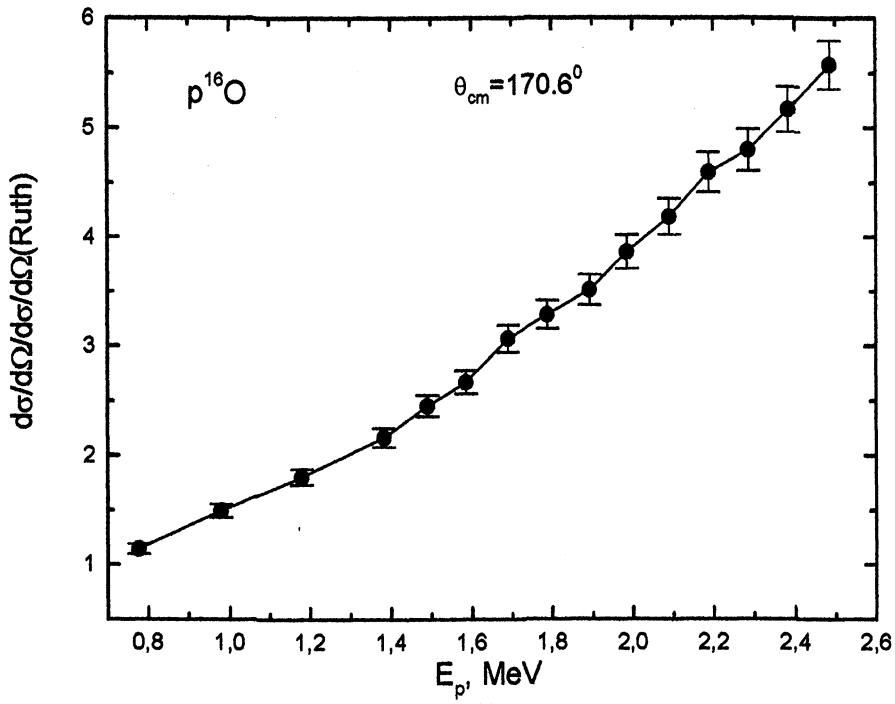

Fig.2.3.16a. The excitation functions of the $p^{16}O$ elastic scattering measured in [155]. Solid curve – the cross sections calculated with the obtained scattering phase shifts.

From Fig.2.3.16b it is clearly seen the coincidence of results for works [154] and [155], though the measurements of the excitation functions are executed at an interval of 10 years. The results of the phase shift analysis of the angular distributions taking into account only the $^2S_{1/2}$ phase shift given in work [155] at the energies from about 1.8 to 2.4 MeV have presented in

Fig. 2.3.16b by squares. The results of the description of these angular distributions are presented in Fig. 2.3.16b,c by the solid curves, and various points show the results of the experimental measurements with 4% errors from work [155].

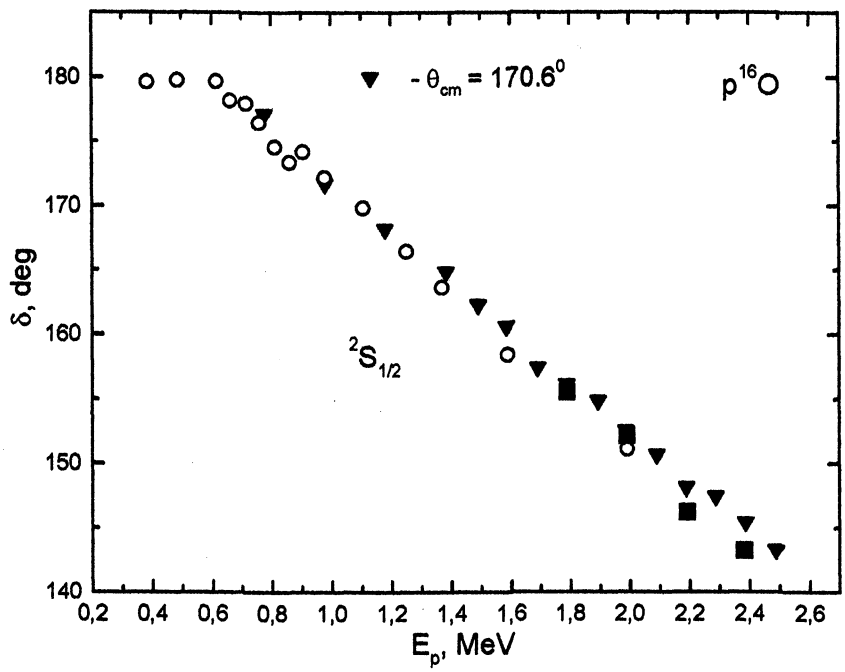

Fig.2.3.16b. Triangles – the phase shifts of the $p^{16}O$ elastic scattering obtained from the excitation functions of work [155]. The phase shifts with Fig.2.3.15b, obtained on the basis of data [154] were shown by circles. The squares have presented the results of the phase shift analysis of angular distributions from [155], shown in Fig. 2.3.16c,d.

In work [156] the excitation functions at angles 90° and 120° in l.s. or 93.6° and 123.1° in c.m have been measured in the energy range of protons from 0.5 to 3.5 MeV with 5% experimental errors. Here the results for the second angle at energy up to 2.5 MeV, which are given in Fig.2.3.17a by points have been used, and the consent of the experimental and calculated cross sections with the found phase shifts which are shown further in fig. 2.3.17b by black points is shown by the solid curve.

Also the comparison of the scattering phase shifts obtained in this work (triangles) on the basis of results [155] for angle 170.6° in c.m. is given in Fig. 2.3.17b and shown in Fig. 2.3.16b by the black triangles. In Fig.2.3.17b our results obtained on the basis of data of work [154] at 171.5° in c.m., which, apparently in Fig. 2.3.15b, are acceptable will be

coordinated with the results of the phase shift analyses of works [144,148] made earlier were shown by circles. The measurements [156] have been executed in the late nineties, and data of works [144,148] are published in the 60th years. However, the results on the phase shift analysis obtained on their basis in the energy range of 0.4–2.5 MeV, are quite acceptable will be coordinated among themselves that is clear from Fig.2.3.15b, Fig.2.3.16b and Fig.2.3.17b.

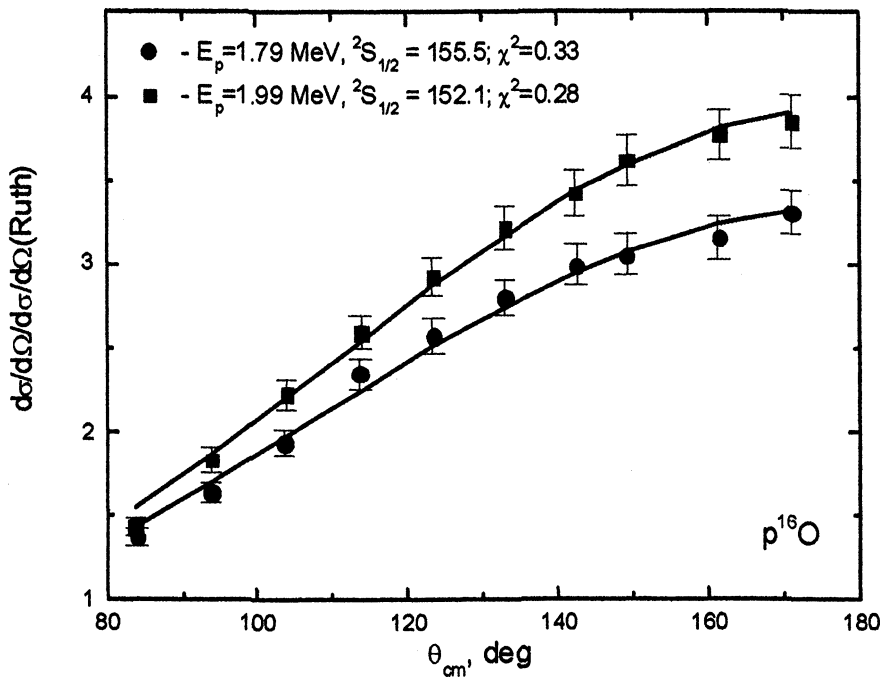

Fig.2.3.16c. The angular distributions of the $p^{16}O$ elastic scattering measured in [155]. Solid curves – the cross sections calculated with the scattering phase shifts obtained in our phase shift analysis.

Now let us consider newer experimental data with the excitation functions [153] and we will make their phase shift analysis. In work [153] the measurement of the excitation functions at energies from 0.6 to 2.5 MeV and the angles 140° and 178° in l.s. or 142.3° and 178.1° in c.m. is taken. In Fig.2.3.18a and Fig.2.3.18c the triangles and points show the results of these measurements, and the results of our phase shift analysis obtained on the basis of such excitation functions are given in Fig.2.3.18b and Fig.2.3.18d.

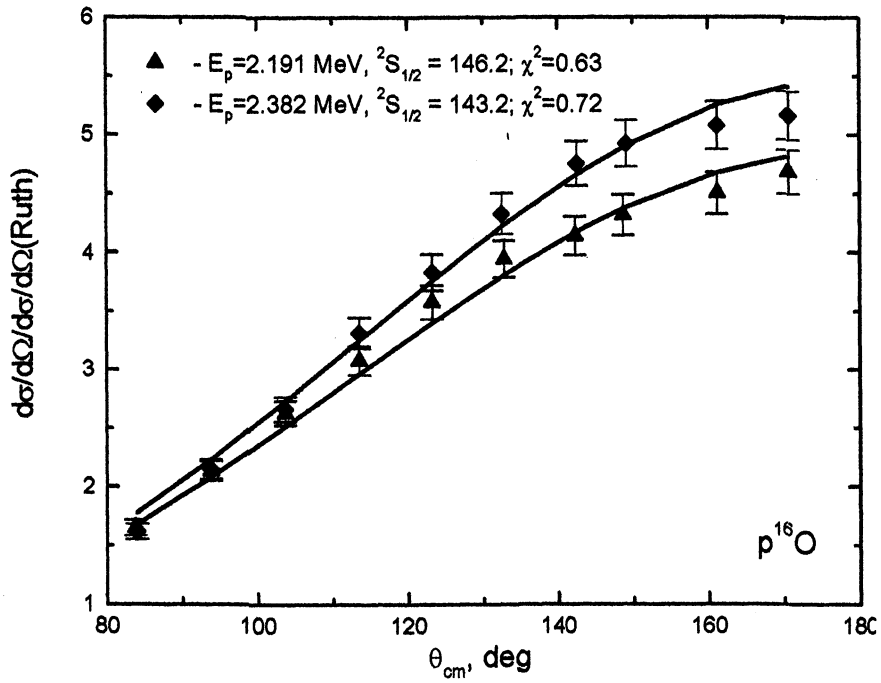

Fig.2.3.16d. The angular distributions of the $p^{16}O$ elastic scattering measured in [155]. Solid curves – the cross sections calculated with the obtained scattering phase shifts.

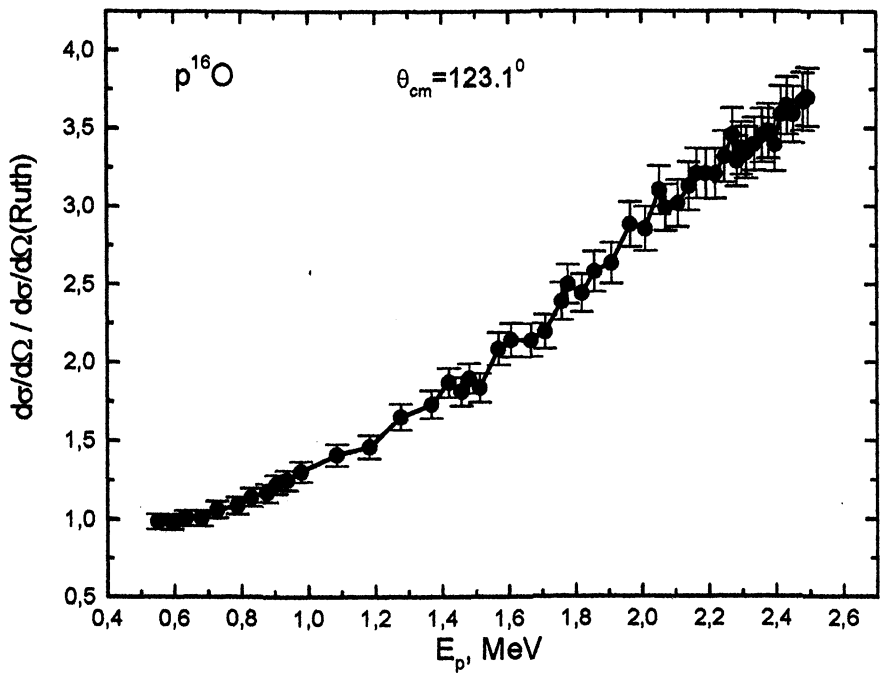

Fig.2.3.17a. The excitation functions of the $p^{16}O$ elastic scattering measured in [156]. Solid curve – the cross sections calculated with the obtained phase shifts.

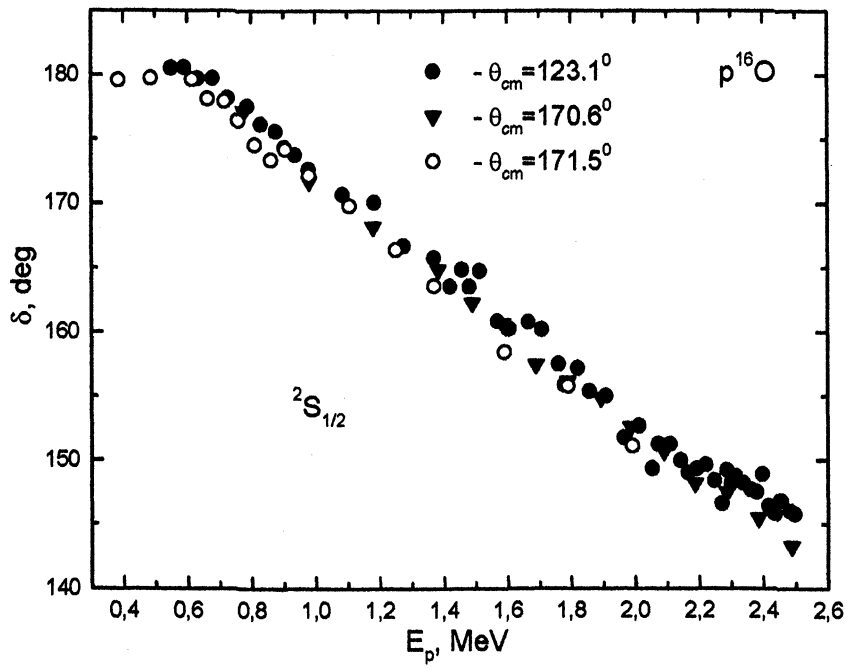

Fig.2.3.17b The phase shift of the $p^{16}O$ elastic scattering obtained by us from the excitation functions of work [156] – black points. The phase shifts were shown by circles in Fig. 2.3.15b obtained from the basis of data [154]. The results of the phase shift analysis of data [155] shown in Fig.2.3.16b have presented by the triangles.

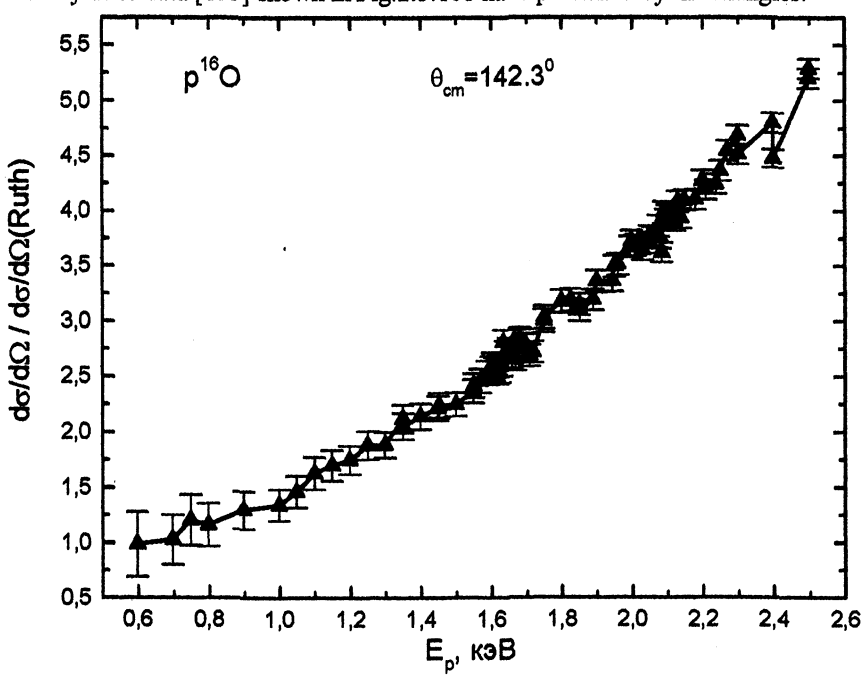

Fig. 2.3.18a. The excitation functions of the $p^{16}O$ elastic scattering measured in [153]. Solid curve – the cross sections calculated with the scattering phase shifts obtained in our phase shift analysis.

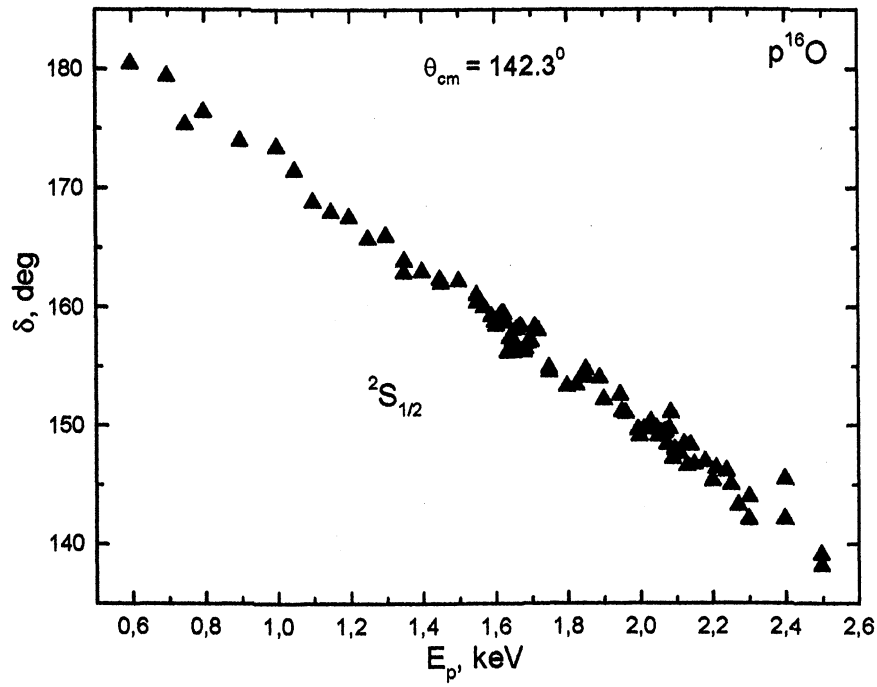

Fig. 2.3.18b. The phase shifts of the $p^{16}O$ elastic scattering obtained by us from the excitation functions of work [153].

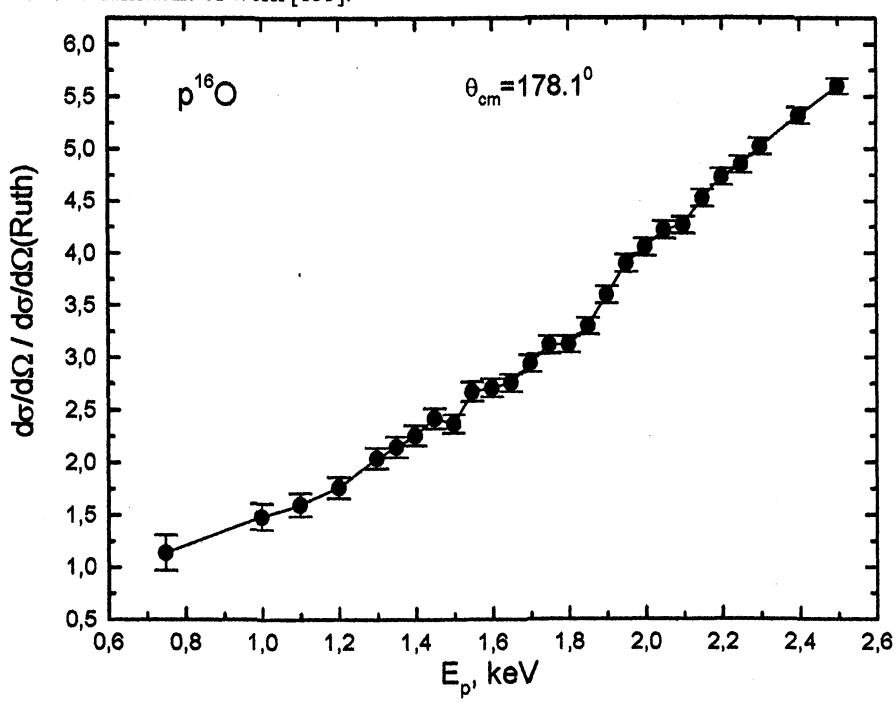

Fig.2.3.18c. The excitation functions of the $p^{16}O$ elastic scattering measured in [153]. Solid curve – the cross sections calculated with the obtained scattering phase shifts.

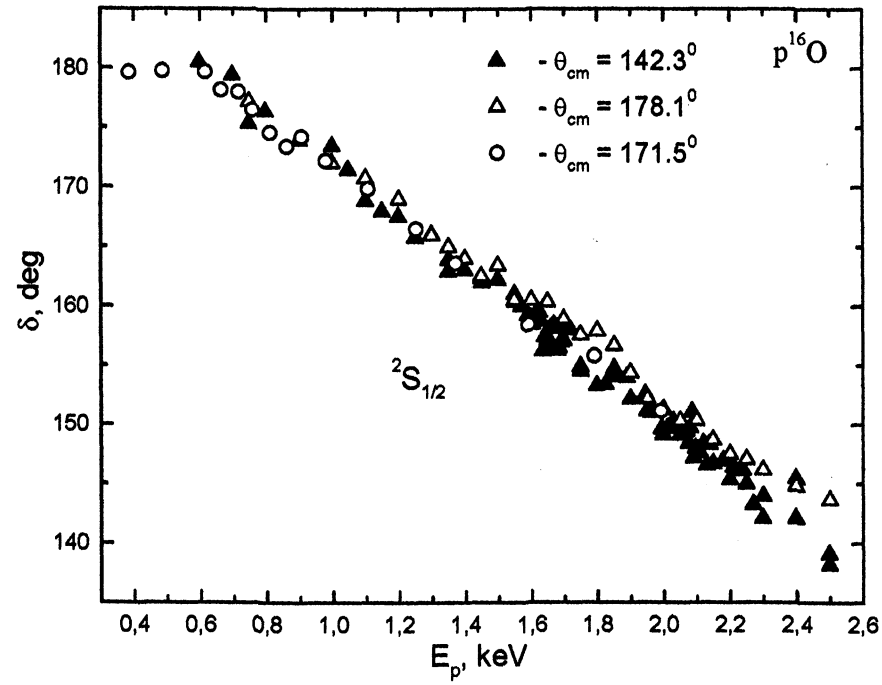

Fig.2.3.18g. The phase shifts of the $p^{16}O$ elastic scattering obtained by us from the excitation functions of work [153]. The comparison with the results of [154] – open circles for angle 171.5° (see ris.2.3.15b.).

The values of cross sections calculated with such phase shifts are given in Fig.2.3.18a and Fig.2.3.18c by the solid curves. From the obtained results the shape of the scattering phase shift form $^2S_{1/2}$ at the lowest energies is visible, which exceeds 180° on 1°–2° is visible.

Let us remind that as the phase shift analysis is made on one point in cross sections, i.e. at one value of cross section at the given energy, the $S_{1/2}$ phase shift is completely unambiguously. Therefore, the excess 180° in scattering phase shifts may indicate the real error in the determination of these phase shifts of the considered experimental data. The phase shifts for both scattering angles in comparison with the results obtained by us for data from work [154] were shown in Fig.2.3.18d. From this figure it is clear that the good consent in the scattering phase shifts between the results obtained in 1975 [154] and newer data [153] published in 2002 is observed. For the previous results obtained on the basis of data of work [154] and on the basis of [155] and [156] a little bigger divergence of phase shifts has been shown. However, results of our analysis of data higher than 2.2 MeV

[153] show a noticeable divergence in the scattering phase shifts obtained for these two angles, which reaches 4°–5° at energy of 2.5 MeV.

In conclusion, we will consider the results of the phase shift analysis of measurements of the differential cross sections in the excitation functions and angular distributions of the $p^{16}O$ elastic scattering given in work [157]. The points show the excitation functions in Fig.2.3.19a, and the solid curve shows the cross sections obtained by us with the found scattering phase shifts, and phase shifts are shown in fig.2.3.19b by the black triangles. In the same figure the comparison of our phase shifts obtained on the basis of various experimental data are given by points, circles and squares.

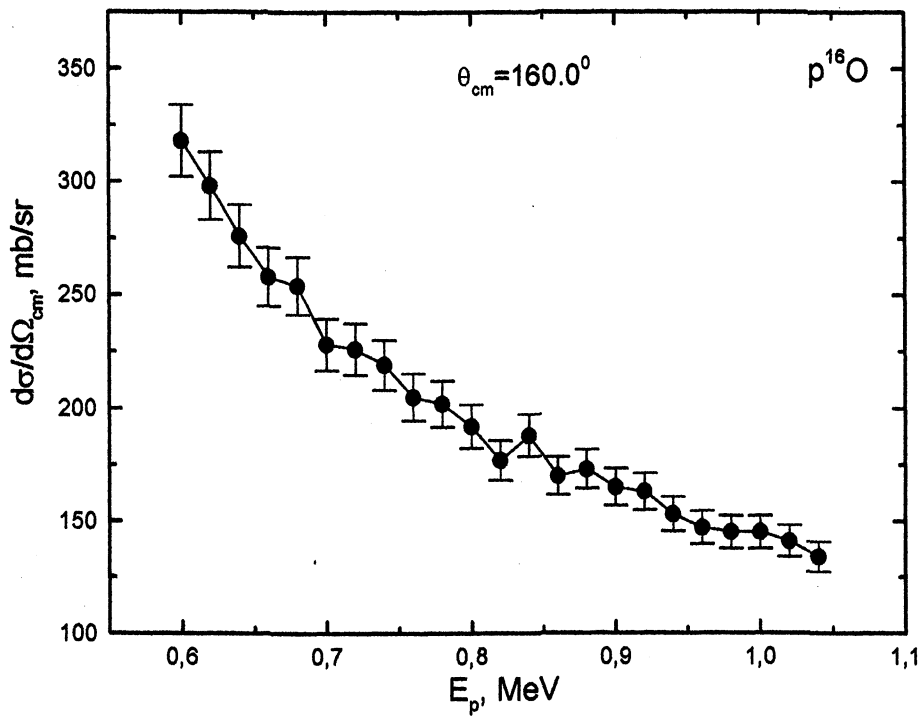

Fig.2.3.19a. The excitation functions of the $p^{16}O$ elastic scattering measured in work [157]. Curve – calculation of these cross sections with the obtained scattering phase shifts.

It is clear that the phase shifts lay lower than 0.8 MeV and obtained on the basis of data [157] are located slightly below than the results of our analysis of the data of work [154] submitted by the circles – difference makes about 2°–3°. Starting with 0.8 MeV and up to 1.0 MeV, the results for our data coincide with the phase shifts for data of work [154] with

accuracy of about 1°. Furthermore, the phase shifts obtained on the basis of measured in [157] angular distributions, are presented in Fig.2.3.19b by the open triangles, and quality of the description of cross sections and the χ^2 value at three energies in Fig.2.3.20. In Fig.2.3.20v the great χ^2 value almost equal to 1 is clear. Here higher, than a ^2S wave, components at the decomposition of the cross section in partial waves can already give a contribution.

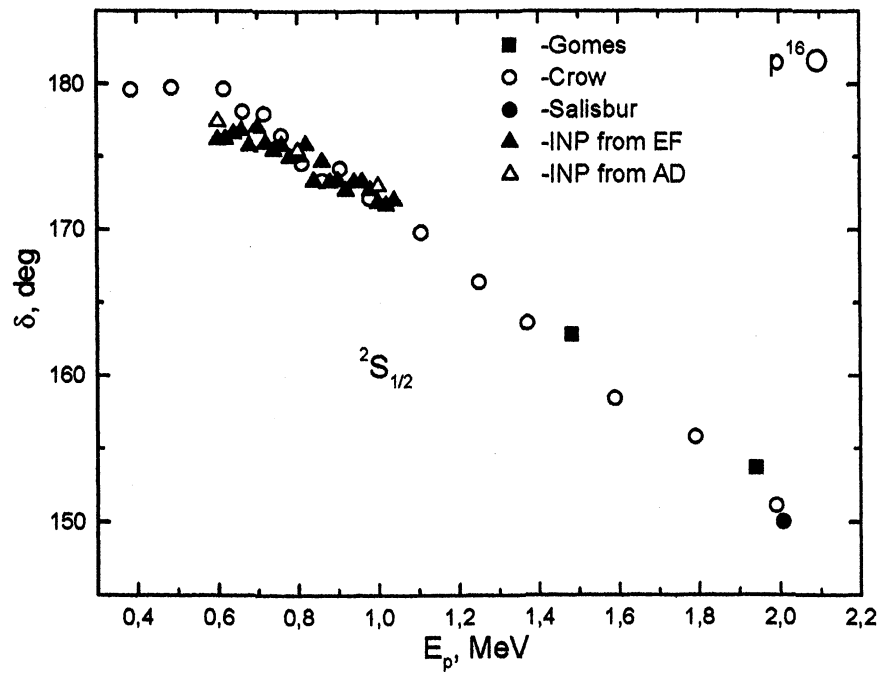

Fig.2.3.19b. The phase shifts of the $p^{16}O$ elastic scattering obtained by us from the differential cross sections of work [157] – triangles. Other designations – data from works [144,148,154].

The accounting of contribution of the ^2P waves with 20 iterations leads to the following values of the scattering phase shifts: $S = 172.4°$, $P_{1/2} = 2.4°$, $P_{3/2} = 2.4°$ at $\chi^2 = 0.68$. The accounting of contribution of the P and D waves with the same number of iterations leads to the scattering phase shifts: $S = 177.0°$, $P_{1/2} = -8.8°$, $P_{3/2} = 10.9°$, $D_{3/2} = 1.7°$, $D_{5/2} = 1.3°$ at $\chi^2 = 0.25$. The calculation results of cross sections with these phase shifts are shown in Fig.2.3.20c by the dashed curve. The improvement of the description of cross sections only in forward area of angles, i.e. approximately up to 70°–80° is observed. Such phase shifts will be quite

coordinated with obtained above (tab.2.3.11) on the basis of excitation functions, but at energy less than 0.8 MeV are located below the results of the phase shift analysis obtained on the basis of data of work [154].

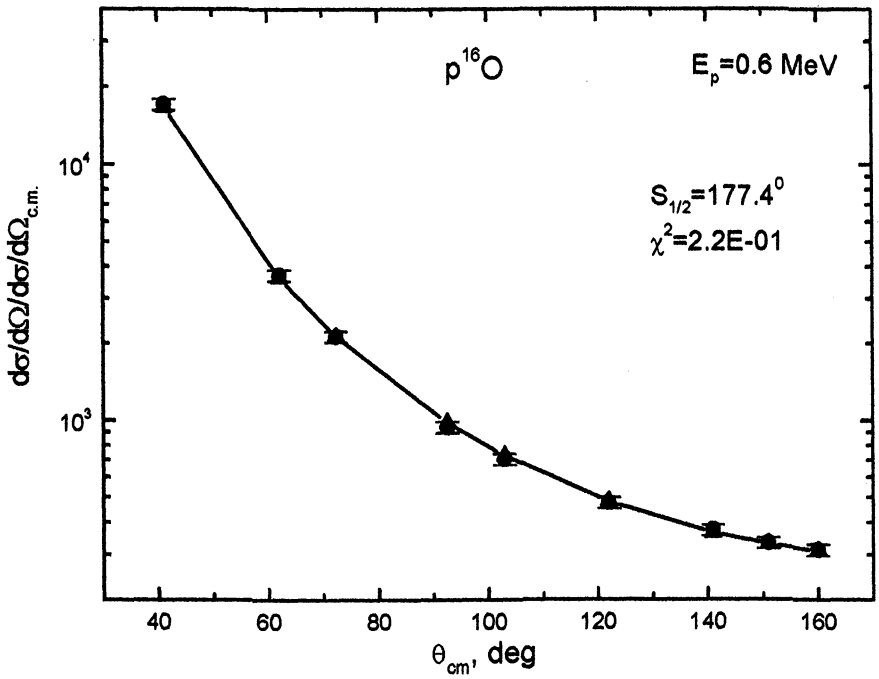

Fig.2.3.20a. The angular distributions of the $p^{16}O$ elastic scattering measured in work [157] at energy of protons of 0.6 MeV. Solid curve – calculation of cross sections with the obtained scattering phase shifts.

However, the accuracy of the phase shift analysis is estimated by us at the level of 2–3°, therefore the observed divergence in results is in limits of such errors. Thus, new results for phase shifts of the $p^{16}O$ elastic scattering at the description of data on the excitation functions from several works for the different scattering angles in the energy range of 0.4–2.5 MeV are obtained. Summary results of our phase shift analysis are given in Fig.2.3.21. Quite good consent of all obtained results among themselves and the made earlier phase shift analysis is visible at energy approximately up to 2.0 MeV.

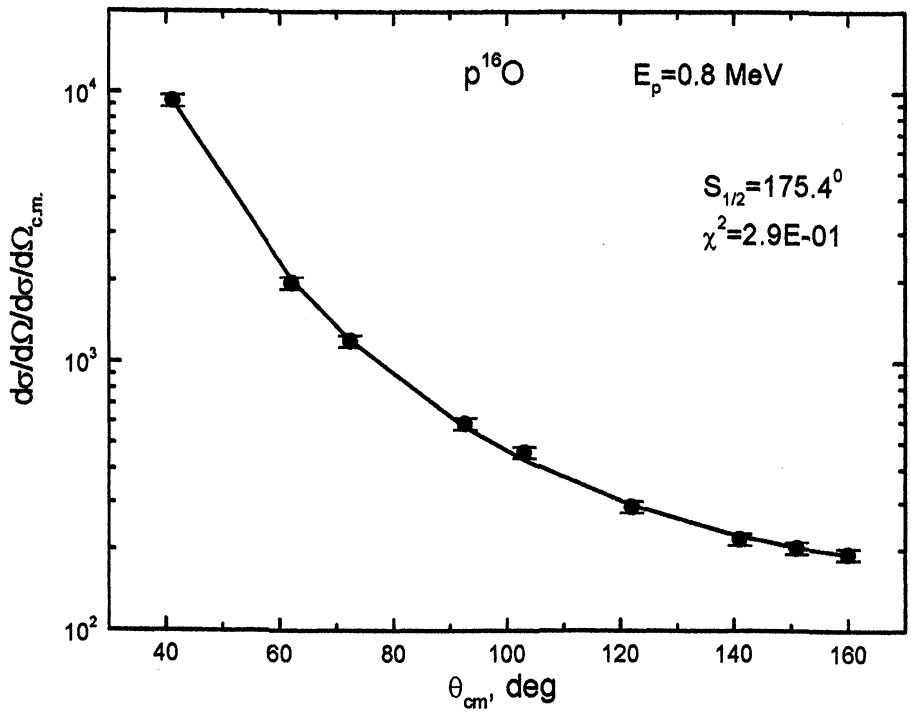

Fig. 2.3.20b. The same as in Fig.2.3.20a, but at energy of protons of 0.8 MeV.

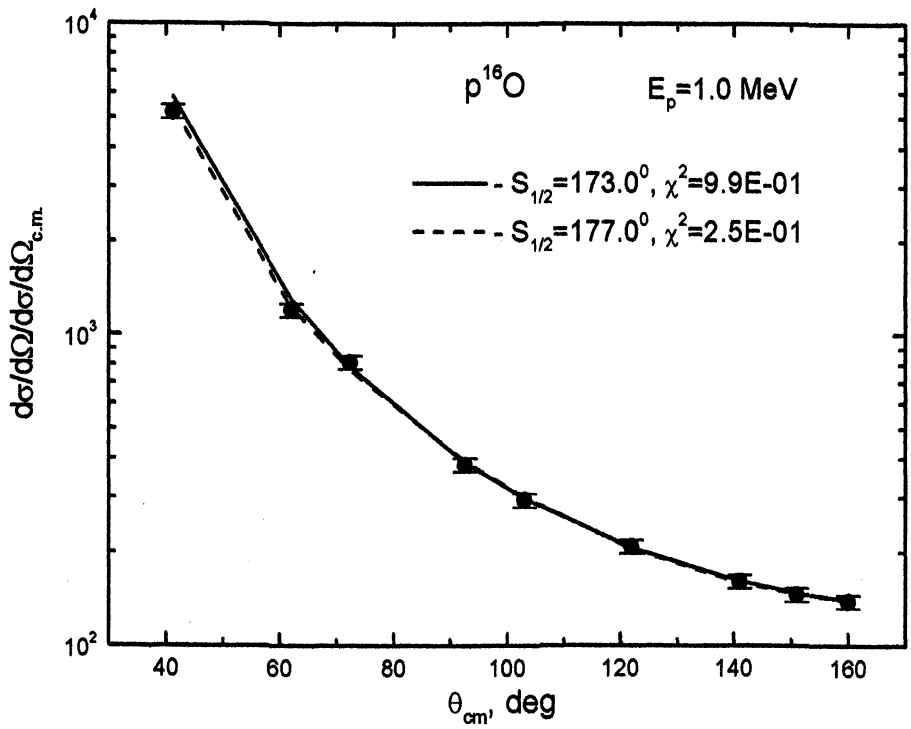

Fig.2.3.20c. The same as in Fig.2.3.20a, but at energy of protons of 1.0 MeV.

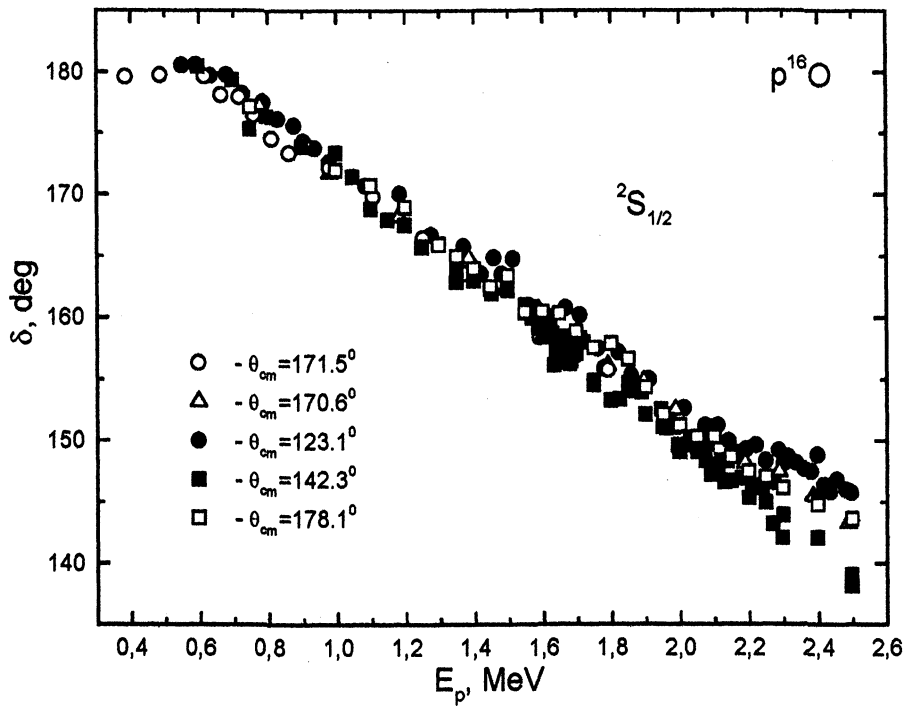

Fig. 2.3.21. All main phase shifts of the $p^{16}O$ scattering obtained in this work from the excitation functions at angles higher than 120°.

The results of the made phase shift analysis, i.e. phase shifts of the $p^{16}O$ elastic scattering, and the data of resonances of ^{17}F [103] will allow one to parametrize in the future the intercluster potentials of interaction for the scattering processes in the non-resonance $^2S_{1/2}$ wave. Such potentials, in turn, can be used further when performing the calculations in the various astrophysical problems like radiative capture of particles on light nuclei, and in this case, the determination of the astrophysical S-factor of the proton radiative capture on ^{16}O at ultralow energies.

2.3.8 Program for $N^{12}C$, $p^{14}C$ and $N^{16}O$ phase shift analysis

Let us provide the text of the computer program for carrying out of the phase shift analysis of the $p^{12}C$ elastic scattering in the Fortran-90 language. The program searching the elastic scattering phase shifts of two particles on the experimental differential cross sections, by the methods described in the previous paragraphs.

The description of the key parameters, variables, parameters of the

interaction potentials, units of the program and subprogrammes is further in the listing of the program and practically does not differ from the designations in the previous programs.

PROGRAM FAZ_ANAL_p12C

```
! * The program of the phase shift analysis of the p12C elastic scattering *
IMPLICIT REAL(8) (A-Z)
INTEGER          I,L,LMA,NI,NV,LMI,LH,LMII,LMAA,LHH,NTTT,
NTT,NPP,NT,NTP
CHARACTER(34) AA
CHARACTER(33) BB
CHARACTER(25) AC
CHARACTER(24) BC
CHARACTER(3) NOM
CHARACTER(6) EX,EX1
COMMON                                                    /A1/
SE(0:50),DS(0:50),DE(0:50),NT,POLE(0:50),POLED(0:50),DS1(0:50),NT
P,XIS,XIP,XI1
COMMON /A2/ NTTT,GG,SS,LMII,LMAA,LHH,NP
COMMON /A3/ POL(0:50),TT(0:100),REZ(0:50)
COMMON /A4/ LH,LMI,NTT,NPP
COMMON/A5/ PI
DIMENSION ST(0:50),FP(0:50),FM(0:50),XP(0:50)
! *************** The initial values ******************
PI=4.0D-000*DATAN(1.0D-000)
Z1=1.0D-000! the P charge
Z2=6.0D-000 ! the 12C charge
AM1=1.00727646577D-000;! The mass of P
AM2=12.0D-000; ! The mass of 12C
AM=AM1+AM2
A1=41.80159D-000
PM=AM1*AM2/AM
B1=2.0D-000*PM/A1
LMI=0; LH=1; LMA=0
! The minimum LMI and maximum LMA orbital! moment
EP=1.0D-05; LMII=LMI; LHH=LH; LMAA=LMA
```

```
! EP – accuracy of the search for a minimum of chi square
NV=1;! 1 – To carry out the minimization, 0 – without the minimization
FH=0.0123D-000! The initial step
NI=10! The number of iterations
NP=2*LMA; NPP=NP
! *************** The set of the energy in c.m. ****************
ECM=0.422D-000 ! An energy in c.m.
NT=17; NTT=NT; NTTT=NT! The number of points in the angles
NOM='422'
EX='-1.TXT'; EX1='-R.DAT'
AC='G:\BASICA\FAZ-ANAL\p12C\c'
BC='G:\BASICA\FAZ-ANAL\p12C\'
AA=AC//NOM//EX
BB=BC//NOM//EX1
OPEN (1,FILE=AA)
DO L=1,NT
READ(1,*) TT(L),SE(L),DE(L)
SE(L)=SE(L)*1000.0D-000
DE(L)=SE(L)*0.10D-000
ENDDO
CLOSE(1)
OPEN (1,FILE="G:\BASICA\FAZ-ANAL\p12C\FAZ.DAT")
DO L=LMI,LMA,LH
READ(1,*) FP(L),FM(L)
ENDDO
CLOSE(1)
! ******* The transfer of the initial phase shifts to the radians *
DO L=LMI,LMA,LH
FM(L)=FM(L)*PI/180.0D-000
FP(L)=FP(L)*PI/180.0D-000
ENDDO
FH=FH*PI/180.0D-000
DO I=LMI,LMA,LH
XP(I)=FP(I)
IF (I==LMA) GOTO 112
XP(I+LMA+LH)=FM(I+1)
```

```
112 ENDDO
! ********** Searching of the minimum of XI**2 **********
EL=ECM*AM1/PM
SK=ECM*B1
SS=DSQRT(SK)
GG=3.4495312D-002*Z1*Z2*PM/SS
CALL VAR(ST,FH,NI,XP,EP,XI,NV)
FM(0)=XP(0)
DO I=LMI,LMA,LH
FP(I)=XP(I)
IF (I==LMA) GOTO 111
FM(I+1)=XP(I+LMA+LH)
111 ENDDO
! ********** The printing of the results ************************
PRINT *,"  EL, ECM, SK, SS=",EL,ECM,SK,SS
PRINT *
PRINT *,"        T              SE              ST              XI "
DO I=1,NT
PRINT *,TT(I),SE(I),ST(I),DS(I)
ENDDO
PRINT *
PRINT *,"  XI=(XIS+XIP),XIS,XIP=",XI,XIS,XIP
PRINT *
PRINT *,"        L          FP          FM"
DO L=LMI,LMA,LH
FM(L)=FM(L)*180.0D-000/PI
FP(L)=FP(L)*180.0D-000/PI
PRINT *,L,FP(L),FM(L)
ENDDO
OPEN (1,FILE=BB)
WRITE(1,*) " EL,ECM=",EL,ECM
WRITE(1,*) "XI=(XIS+XIP),XIS,XIP=",XI,XIS,XIP
WRITE(1,*) "          T                    SE                    ST
XI"
DO I=1,NT
WRITE(1,*) TT(I),SE(I),ST(I),DS(I)
```

```
ENDDO
WRITE(1,*) "
WRITE(1,*) "        L          FP              FM"
DO I=LMI,LMA,LH
WRITE(1,*) I,FP(I),FM(I)
ENDDO
OPEN (1,FILE="G:\BASICA\FAZ-ANAL\p12C\FAZ.DAT")
DO I=LMI,LMA,LH
WRITE(1,*) FP(I),FM(I)
ENDDO
CLOSE(1)
END

SUBROUTINE VAR(ST,PHN,NI,XP,EP,AMIN,NV)
! The variation subprogramme for the minimization of a chi-square
IMPLICIT REAL(8) (A-Z)
INTEGER I,NI,NT,NV,NP,LMI,LH,NN,IN,NTT,NTP
COMMON                                                    /A1/
SE(0:50),DS(0:50),DE(0:50),NT,POLE(0:50),POLED(0:50),DS1(0:50),NT
P,XIS,XIP,XI1
COMMON /A3/ POL(0:50),TT(0:100),REZ(0:50)
COMMON /A4/ LH,LMI,NTT,NP
COMMON/A5/ PI
DIMENSION XPN(0:50),XP(0:50),ST(0:50)
DO I=LMI,NP,LH
XPN(I)=XP(I)
ENDDO
NN=LMI
PH=PHN
CALL DET(XPN,ST,ALA)
B=ALA
IF (NV==0) GOTO 3012
DO IIN=1,NI
NN=-LH
PRINT *,'FF=',ALA,IIN
1119  NN=NN+LH
```

```
IN=0
2229 A=B
XPN(NN)=XPN(NN)+PH*XP(NN)
IN=IN+1
CALL DET(XPN,ST,ALA)
B=ALA
IF (B<A) GOTO 2229
C=A
XPN(NN)=XPN(NN)-PH*XP(NN)
IF (IN>1) GOTO 3339
PH=-PH
GOTO 5559
3339 IF (ABS((C-B)/(B))<EP) GOTO 4449
PH=PH/2.0D-000
5559 B=C
GOTO 2229
4449 PH=PHN
B=C
IF (NN<NP) GOTO 1119
AMIN=B
PH=PHN
ENDDO
3012 AMIN=B
DO I=LMI,NP,LH
XP(I)=XPN(I)
ENDDO
END

SUBROUTINE DET(XP,ST,XI)
! ******* The subroutine for chi-square calculation **********
IMPLICIT REAL(8) (A-Z)
INTEGER I,NT,NTP
COMMON      /A1/      SE(0:50),DS(0:50),DE(0:50),NT,POLE(0:50),
POLED(0:50),DS1(0:50),NTP,XIS,XIP,XI1
COMMON /A3/ POL(0:50),TT(0:100),REZ(0:50)
DIMENSION XP(0:50),ST(0:50)
```

```
S=0.0D-000
CALL SEC(XP,ST)
S1=0.0D-000
DO I=1,NT
DS(I)=((ST(I)-SE(I))/DE(I))**2
S=S+DS(I)
ENDDO
XI=S/NT
END

SUBROUTINE SEC(XP,S)
! *** The subprogramme of the calculation of the scattering cross section *
IMPLICIT REAL(8) (A-Z)
INTEGER I,NT,LMI,LMA,LH,L
COMMON /A2/ NT,GG,SS,LMI,LMA,LH,NP
COMMON /A3/ POL(0:50),TT(0:100),REZ(0:50)
COMMON/A5/ PI
DIMENSION
S0(0:50),P(0:50),PP(0:50),FP(0:50),FM(0:50),XP(0:50),S(0:50)
DO I=LMI,LMA,LH
FP(I)=XP(I)
IF (I==LMA) GOTO 111
FM(I+1)=XP(I+LMA+LH)
111 ENDDO
FM(0)=FP(0)
CALL CULFAZ(GG,S0)
DO I=1,NT
T=TT(I)*PI/180.0D-000
X=DCOS(T)
A=2.0D-000/(1.0D-000-X)
S00=2.0D-000*S0(0)
BB=-GG*A
ALO=GG*DLOG(A)+S00
REC=BB*DCOS(ALO)
AMC=BB*DSIN(ALO)
REZ1=REC**2+AMC**2
```

```
REA=0.0D-000
AMA=0.0D-000
REB=0.0D-000
AMB=0.0D-000
DO L=LMI,LMA,LH
FPP=2.0D-000*FP(L)
FMP=2.0D-000*FM(L)
AA=DCOS(FPP)-DCOS(FMP)
BB=DSIN(FPP)-DSIN(FMP)
SL=2.0D-000*S0(L)
CALL FUNLEG(X,L,PP)
REB=REB+(BB*DCOS(SL)+AA*DSIN(SL))*PP(L)
AMB=AMB+(BB*DSIN(SL)-AA*DCOS(SL))*PP(L)
LL=2*L+1
JJ=L+1
AA=JJ*DCOS(FPP)+L*DCOS(FMP)-LL
BB=JJ*DSIN(FPP)+L*DSIN(FMP)
CALL POLLEG(X,L,P)
REA=REA+(BB*DCOS(SL)+AA*DSIN(SL))*P(L)
AMA=AMA+(BB*DSIN(SL)-AA*DCOS(SL))*P(L)
ENDDO
REA=REC+REA
AMA=AMC+AMA
RE=REA**2+AMA**2
AM=REB**2+AMB**2
S(I)=10.0D-000*(RE+AM)/4.0D-000/SS**2
REZ(I)=REZ1*10.0D-000/4.0D-000/SS**2
POL(I)=2.0D-000*(REB*AMA-REA*AMB)/(RE+AM)
ENDDO
END

SUBROUTINE POLLEG(X,L,P)
! ***** The subprogramme of calculation of the Legendre polinomials ***
IMPLICIT REAL(8) (A-Z)
INTEGER I,L
DIMENSION P(0:50)
```

```
P(0)=1.0D-000; P(1)=X
DO I=2,L
P(I)=(2*I-1)*X/I*P(I-1)-(I-1)/I*P(I-2)
ENDDO
END

SUBROUTINE FUNLEG(X,L,P)
! *** The subprogramme of calculation of the Legendre functions *******
IMPLICIT REAL(8) (A-Z)
INTEGER I,L
DIMENSION P(0:50)
P(0)=0.0D-000; P(1)=DSQRT(ABS(1.-X**2)); P(2)=3.0D-000*X*P(1)
IF (L>=3) THEN
DO I=2,L
P(I+1)=(2*I+1)*X/I*P(I)-(I+1)/I*P(I-1)
ENDDO
ENDIF
END

SUBROUTINE CULFAZ(G,F)
! *** The subprogramme of calculation of the Coulomb phase shifts ***
IMPLICIT REAL(8) (A-Z)
INTEGER I,N
DIMENSION F(0:50)
C=0.5772156650D-000; S=0.0D-000; N=50
A1=1.202056903D-000/3.0D-000; A2=1.036927755D-000/5.0D-000
DO I=1,N
A=G/I-DATAN(G/I)-(G/I)**3/3.0D-000+(G/I)**5/5.0D-000
S=S+A
ENDDO
FAZ=-C*G+A1*G**3-A2*G**5+S
F(0)=FAZ
DO I=1,20
F(I)=F(I-1)+DATAN(G/I)
ENDDO
END
```

The following control account on this program was carried out at resonance energy of 422 keV (c.m.) in the $p^{12}C$ elastic scattering taking into account the phase shift analysis in only one S wave.

EL, ECM, SK, SS = 4.574E-1 4.22E-1 1.87E-2 1.37E-1

θ	σ_e	σ_t	χ^2_i
10.83	409561	3256822.3428083	4.194371298676935
21.63	266969	227766.5412064077	2.156278956304461
32.39	58583.1	50674.784355610	1.8223143351212
43.07	17267.6	15925.09271621951	6.044624704055184E-1
53.66	5839.94	5640.62956376928	1.164778401875084E-1
64.14	2414.18	2060.5610732571380	2.145515754644307
74.5	965.24	740.3435278409627	5.428685268597148
84.71	422.29	265.4550687576415	13.793167214162040
94.79	217.01	120.1919175449456	19.9046247867550
104.7	147.11	103.6791667064438	8.715893867706498
114.5	140.23	133.5569838776437	2.264448667637590E-1
124.15	204.09	175.8612452117759	1.913110216888019
133.67	243.52	216.8648984979974	1.198095428652019
143.08	253.77	251.4932553653157	8.049114108914179E-3
152.39	267.64	278.2186995788807	1.562293138659170E-1
161.64	288.94	296.9745596276764	7.732302205565983E-2
170.84	292.72	308.0225110939944	2.732880319244108E-1

$\chi^2 = 3.69$

L	δ_p	δ_m
0	58.15	58.15

As a result we obtain the *S* value of 58.15° phase shift at rather great value of $\chi^2 = 3.69$. The value of the phase shifts and some other characteristics are shown in rounded, to the second sign after a comma, in the form. If to take into account the *P* wave in the analysis, then for the scattering phase shifts we will obtain the following control account:

EL, ECM, SK, SS = 4.57E-1 4.22E-1 1.87E-2 1.37E-1

θ	σ_e	σ_t	χ^2_i
10.83	4095610	3264781.541334357	4.115148756111661
21.63	266969	223190.0387772885	2.689114135211925
32.39	58583.1	49592.26685532391	2.355348513821907
43.07	17267.6	16111.41279780082	4.483243796400418E-1
53.66	5839.94	6059.579098437353	1.414498640631696E-1
64.14	2414.18	2415.589085838059	3.406713446204295E-5
74.5	965.24	982.7590318182862	3.294197102373393E-2
84.71	422.29	414.5062045985828	3.397513798561286E-2
94.79	217.01	205.28584114367	2.918797023030877E-1
104.71	147.11	149.1168415589131	1.860980323212324E-2
114.5	140.23	155.8558179281346	1.241662746301032
124.15	204.09	185.2840079884762	8.490808445689716E-1
133.67	243.52	219.3107960699812	9.883067178217969E-1
143.08	253.77	250.1596154521572	2.024073897229597E-2
152.39	267.64	274.7849530022851	7.126835104038670E-2
161.64	288.94	292.3439981186766	1.387916330759821E-2
170.84	292.72	302.7569167687375	1.175698198093965E-1

$\chi^2 = 7.90E\text{-}1$

L	δ_p	δ_m
0	52.13	52.13
1	-8.97	12.82

It is clear, that at the account in the phase shift analysis of the *S* and *P* scattering waves, the χ^2 value decreases from 3.69 till 0.79.

In listings the following designations are used: EL – energy of particles in laboratory system, ECM – energy of particles in system of the center of masses, SK – square of the wave number k^2, SS – the wave number k, L – the orbital moment, θ – the scattering angle, σ_e – the experimental cross sections, σ_t – the calculated cross sections, χ^2_i – partial χ^2 for i angle, δ_p – the phase shift with $J = L + 1/2$, δ_m – a phase shift at $J = L - 1/2$, χ^2 – average value on all points.

If to use the usual 41.4686 MeV·fm^2 value for the $\hbar^2/m_0$ constant value, then, as seen from the listing below, the χ^2 value changes approximately for 10%, and some phase shifts on 0.5° that practically does not affect to the

results even at the resonance energy:

$\chi^2 = 8.85E\text{-}1$

L	δ_p	δ_m
0	51.63	51.63
1	-9.40	12.87

From the given results it is clear that at 422 keV (c.m.) the *S* phase shift almost reaches the resonance value of 90°. At the energies in the range of the resonance as its width less than 32 keV [120], so sharp raising of the phase shift is observed that the energy change is approximately on 1 keV can lead to change of the phase shift to 40°–50°. Let us notice that the accuracy of determination of energy in the considered experiment makes about 1 keV, and the accuracy of determination of energy of resonance level has the value of 0.6 keV [120].

The scattering phase shifts found in result of the phase shift analysis are used further for the construction of the $p^{12}C$ intercluster potentials which, in turn, were applied for the calculations of the astrophysical *S*-factors of the proton radiative capture on ^{12}C [2,28,122,123,125]. This process is the first thermonuclear reaction of the CNO cycle, which is present at later stage of the development of the stable stars when there is a partial hydrogen burning. In the process of its burning out, the core of the star begins to collapse considerably, bringing in result to increase in the pressure and temperature in the star, and along with a proton-proton cycle the following chain of thermonuclear processes called, CNO or a carbon cycle [28,122] comes into effect. The CNO cycle is a set of the three linked with each other or, more precisely, partially blocked cycles. The first and the simplest CN from them – the cycle (the Bethe cycle or the carbon cycle) has been offered by Hans Bethe and, irrespective of him, by Carl Friedrich von Weizsäcker in 1939 [28,122,123].

2.4 Phase shift analysis of the elastic p^6Li scattering

Let us consider the processes of the p^6Li elastic scattering at astrophysical energies and we will make the phase shift analysis of the available experimental data. The results of such phase shift analysis will be required further for the creation of the intercluster interaction potentials at the calculation connected with the solution of astrophysical problems [158].

2.4.1 The differential cross sections

By the consideration of scattering processes in the system of particles with spins 1/2 and 1 without spin-orbital splitting of phase shifts, the elastic scattering cross section is presented in the simplest form [6]

$$\frac{d\sigma(\theta)}{d\Omega} = \frac{2}{6}\frac{d\sigma_d(\theta)}{d\Omega} + \frac{4}{6}\frac{d\sigma_q(\theta)}{d\Omega}, \qquad (2.4.1)$$

where the indexes d and q belong to the doublet (with spin 1/2) and quartet (with spin 3/2) state of the p^6Li system, and the cross sections themselves are expressed through the scattering amplitudes, which are registered like the expressions for the phase shift analysis in the $^4He^4He$ system

$$\frac{d\sigma_d(\theta)}{d\Omega} = |f_d(\theta)|^2, \qquad \frac{d\sigma_q(\theta)}{d\Omega} = |f_q(\theta)|^2,$$

where

$$f_{d,q}(\theta) = f_c(\theta) + f^N{}_{d,q}(\theta),$$

and

$$f_c(\theta) = -\left(\frac{\eta}{2k\sin^2(\theta/2)}\right)\exp\{i\eta\ln[\sin^{-2}(\theta/2)] + 2i\sigma_0\}\ , \qquad (2.4.2)$$

$$f_d^N(\theta) = \frac{1}{2ik}\sum_L (2L+1)\exp(2i\sigma_L)[S_L^d - 1]P_L(\cos\theta)\ ,$$

$$f_q^N(\theta) = \frac{1}{2ik}\sum_L (2L+1)\exp(2i\sigma_L)[S_L^q - 1]P_L(\cos\theta) \ ,$$

where $S_L^{d,q} = \eta_L^{d,q}\exp[2i\delta_L^{d,q}(k)]$ – a scattering matrix in a doublet (d) or a quartet (k) spin state [6].

The possibility of use the simple expressions for calculations of the elastic scattering cross sections is caused by the fact that in the range of low energies of the spin-orbital splitting of the phase shifts appears a little as in the elastic scattering there are no resonances with a certain total moment. It is confirmed by the results of the phase shift analysis made earlier in work [159], where was taken into account the spin-orbit splitting of the phase shifts, which did not exceed few degrees.

2.4.2 Phase shift analysis

Earlier the phase shift analysis of the differential cross sections and excitation functions for the p^6Li elastic scattering without the obvious account of the doublet ^2P wave has been executed in [159]. Our phase shift analysis is carried out at lower energies that are relevant for nuclear astrophysics, takes into account all of the lower partial waves, including the doublet ^2P wave and is based on the differential cross sections specified in works [160,161,162].

At the energy of 500 keV, on the basis of data [162], we find the ^2S and ^4S scattering phase shifts, which are given in tab. 2.4.1 at No.1. The obtained results of calculation of cross sections are quite coordinated with the experimental data at an average on all points of $\chi^2 = 0.15$. The error of the differential cross sections of these data was accepted equal to 10%. Account the doublet ^2P and quartet ^4P phase shifts has shown that their numerical values less than 0.1°.

The following five energies belong to new results of measurements of the differential cross sections executed in works [160,163] in the latest time. The first of them, 593.0 keV, gives the chance to find the $^{2,4}S$ phase shifts, which differ a little from phase shifts for the previous energy have the same χ^2 and are shown in tab.2.4.1 at No.2, and the phase shifts for the $^{2,4}P$ waves also tend to zero.

At the energy of 746.7 keV the $^{2,4}S$ phase shifts are found (tab. 2.4.1 No.3-1), which allow one to describe the cross sections with $\chi^2 = 0.24$ accuracy. Despite the smallness of the χ^2 value, an attempt to consider $^{2,4}P$ phase shifts has been made. In the beginning it was believed that the quartet ^4P phase shift is negligible that follows from the results [159], in which their account began only from 1.0–1.5 MeV. The results of our analysis taking into account only the ^2P phase shifts are presented in Fig.2.4.1a and in tab. 2.4.1 at №3-2. It is clear, that the account of the small doublet ^2P phase shift changes a little the ^2S wave value, increasing its value, and reduces $\chi^2 = 0.16$. The account of the quartet ^4P phase shift has given the negligible value for its numerical value, less than 0.1° that corresponds to the results [159].

Tab. 2.4.1. Results of the phase shift analysis of the p^6Li elastic scattering.

№	E_p, keV	^2S, deg.	^4S, deg.	^2P, deg.	^4P, deg.	χ^2
1	500	176.2	178.7	–	–	0.15
2	593.0	174.2	178.8	–	–	0.15
3-1	746.4	170.1	180.0	–	–	0.24
3-2	746.4	172.5	179.9	1.7	–	0.16
4-1	866.8	157.8	180.0	–	–	0.39
4-2	866.8	170.2	174.9	3.9	–	0.22
4-3	866.8	169.6	175.0	3.5	0.1	0.23
5-1	976.5	160.0	178.5	–	–	0.12
5-2	976.5	167.0	174.5	1.1	–	0.12
6-1	1136.3	144.9	180.0	–	–	0.58
6-2	1136.3	164.7	171.1	5.8	–	0.32
6-3	1136.3	166.4	169.9	5.5	0.1	0.32

The result of the search of phase shifts for energy of 866.8 keV taking into account only the $^{2,4}S$ waves is given in tab. 2.4.1 at No.4-1 at $\chi^2 = 0.39$. Apparently, the value of the ^2S phase shift sharply falls down in comparison with the previous energy. The account of the ^2P wave considerably increases its value (Fig. 2.4.1b and tab. 2.4.1 No.4-2) and

reduces the χ^2 value almost twice. The attempt to consider the quartet ^4P phase shift has resulted in the value about 0.1° (tab.2.4.1 No.4-3).

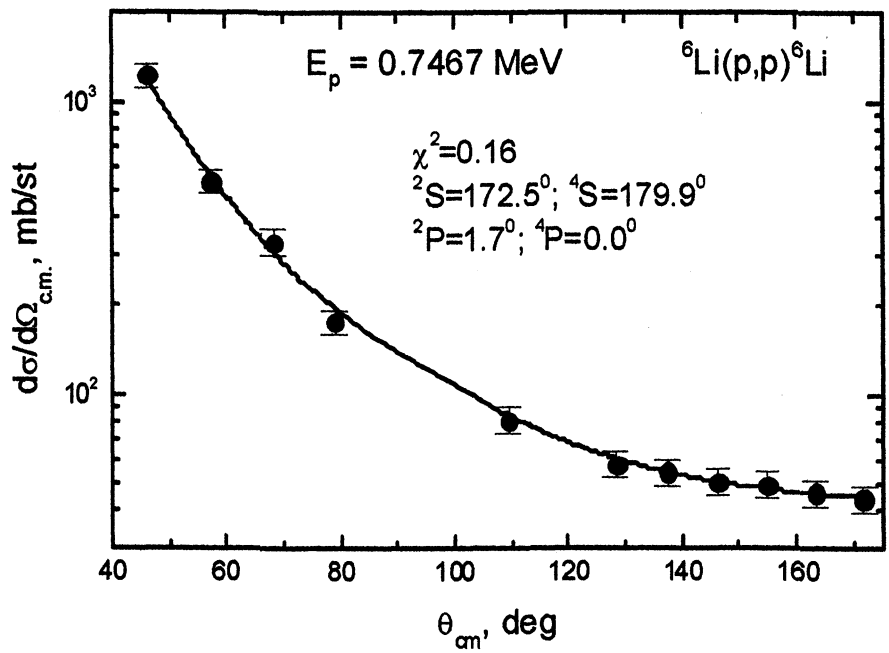

Fig. 2.4.1a. The cross sections of the p^{6}Li elastic scattering at 746.7 keV. Solid curve – calculation of the cross sections with the found phase shifts.

Any change of the ^4P wave in the large side, including, at other values of other phase shifts, led to the increase in χ^2. At this energy, as well as at all another considered energies from works [160,161], it is not possible to find any variant for a nonzero quartet phase shift at the tendency of the χ^2 value to minimum. For the following energy, 976.5 keV, excluding the $^{2,4}P$ waves the values of the ^2S and ^4S phase shifts are found, shown in tab.2.4.1 No.5-1. The subsequent account of the ^2P wave considerably increases the values of the ^2S phase shift, if to neglect the ^4P wave, as it is clear in Fig. 2.4.1c and tab. 2.4.1 No.5-2 at $\chi^2 = 0.12$. If to include in the analysis a quartet ^4P wave, then it aspires to zero at reduction of the χ^2 value. The last from the considered energies 1.1363 MeV from works [160,161], even at the account of only the $^{2,4}S$ waves, leads to rather small χ^2 equal to 0.58, as it is clear in tab.2.4.1 No.6-1. And in this case, the account of a ^2P wave leads to the noticeable increase in the value of a ^2S phase shift – the corresponding results of the calculation of cross sections are shown in

fig.2.4.1d and tab. 2.4.1 at No.6-2. The account of the quartet ^4P wave at this energy results in its value about 0.1°, as shown in tab. 2.4.1 No.6-3.

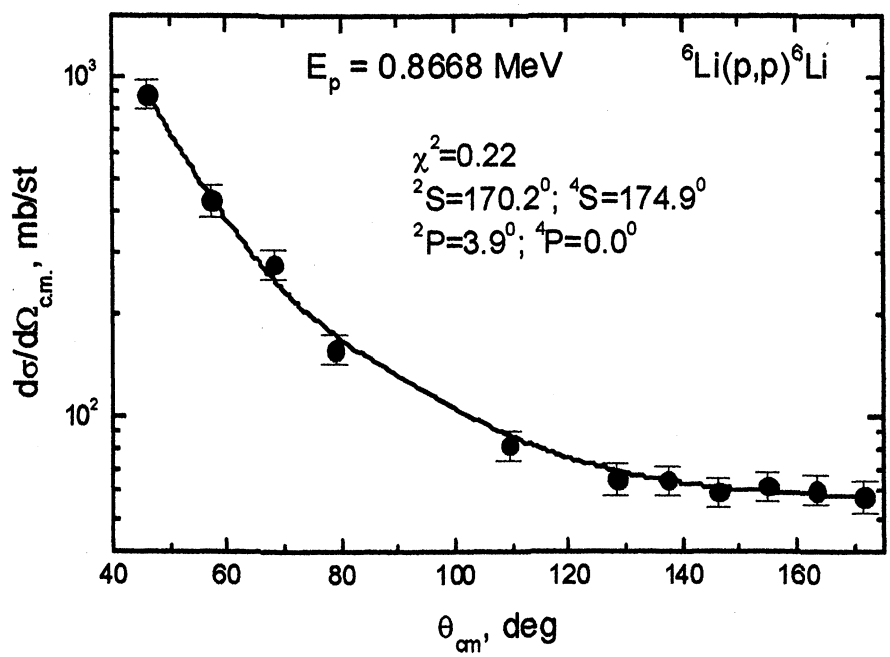

Fig. 2.4.1b. The cross sections of the p^{6}Li elastic scattering at 866.8 keV. Solid curve – calculation of the cross sections with the found phase shifts.

Thus, at the description of all experimental data from works [160,161] the accounting of the quartet ^4P waves in this energy range is not required, i.e. their value equals or less than 0.1°. It will be coordinated with the results [159], however, the doublet ^2P phase shift reaches the 5.5°–6° and its value cannot be neglected. The general form of the ^2S and ^4S scattering phase shifts is shown further in Fig.2.4.2a, and doublet ^2P phase shifts are given in Fig.2.4.2b. Despite the quite wide spacing of the results for the ^4S phase shifts, the doublet ^2S phase shift has a certain tendency to decrease, but there is it much more slowly, than follows from the results of the analysis [159]. If not to consider the doublet ^2P wave in our analysis, then for the ^2S phase shift the results are very close to the results of the phase shift analysis provided in work [159].

The errors of the elastic scattering phase shifts given in Fig.2.4.2 are defined by the ambiguity of the phase shift analysis, namely, at almost the same χ^2 value, which can differ by 5–10%, it is possible to obtain little

different values of the scattering phase shifts. This ambiguity for the $^{2,4}S$ and ^{2}P phase shifts is estimated at the level by 1°–1.5°.

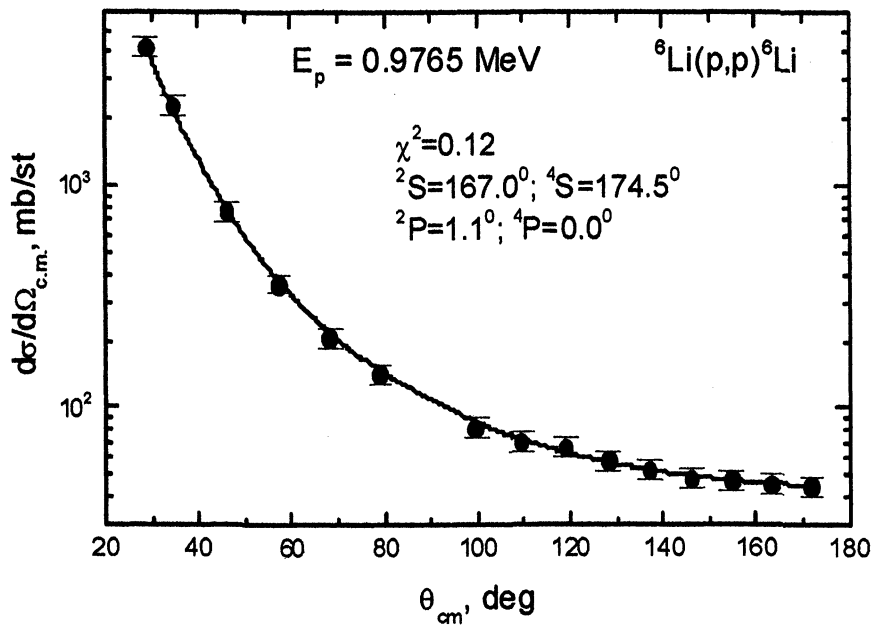

Fig. 2.4.1c. The cross sections of the p^6Li elastic scattering at 976.5 keV. Solid curve – calculation of cross sections with the found phase shifts.

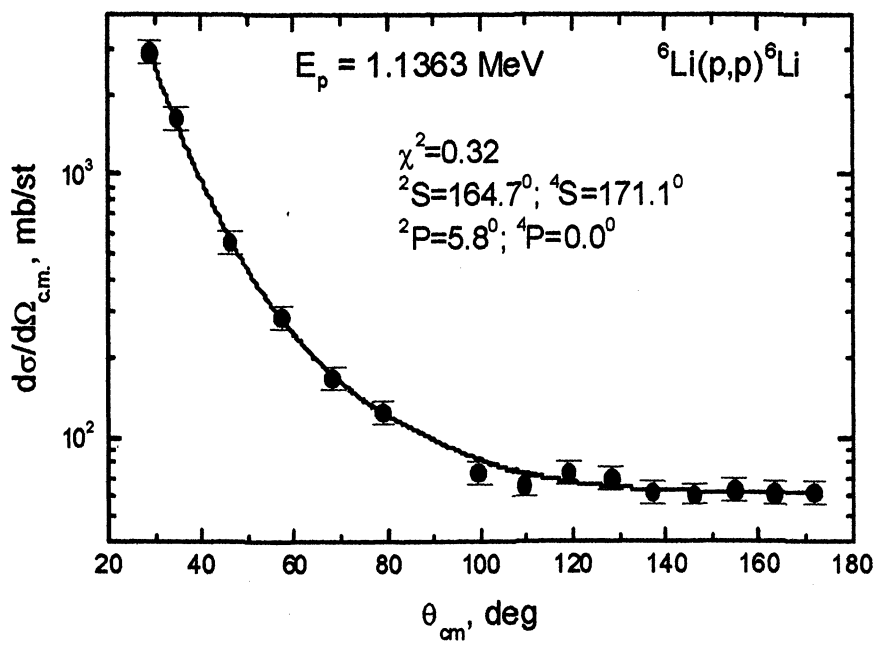

Fig. 2.4.1d. The cross sections of the p^6Li elastic scattering at 1136.3 keV. Solid curve – calculation of cross sections with the found phase shifts.

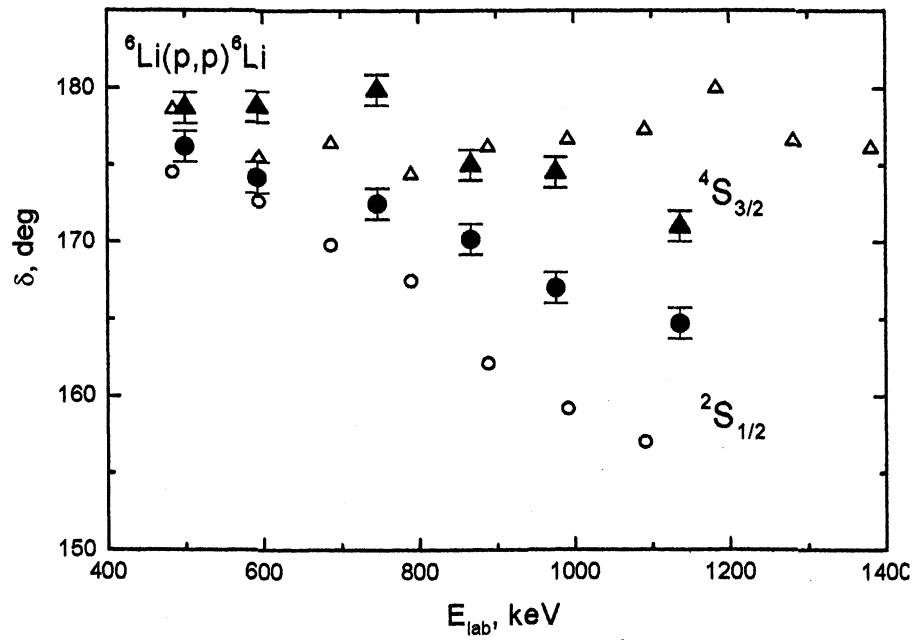

Fig.2.4.2a. The doublet and quartet S phase shifts of the p^{6}Li elastic scattering at low energies. The doublet and quartet S phase shifts in the presence of the ^2P wave, when the phase shift was accepted by ^4P equal to zero are given. The ^2S phase shift – points and ^4S – triangles, obtained according to works [160,161,162]. For the comparison by open triangles and circles have given the results of the phase shift analysis [159].

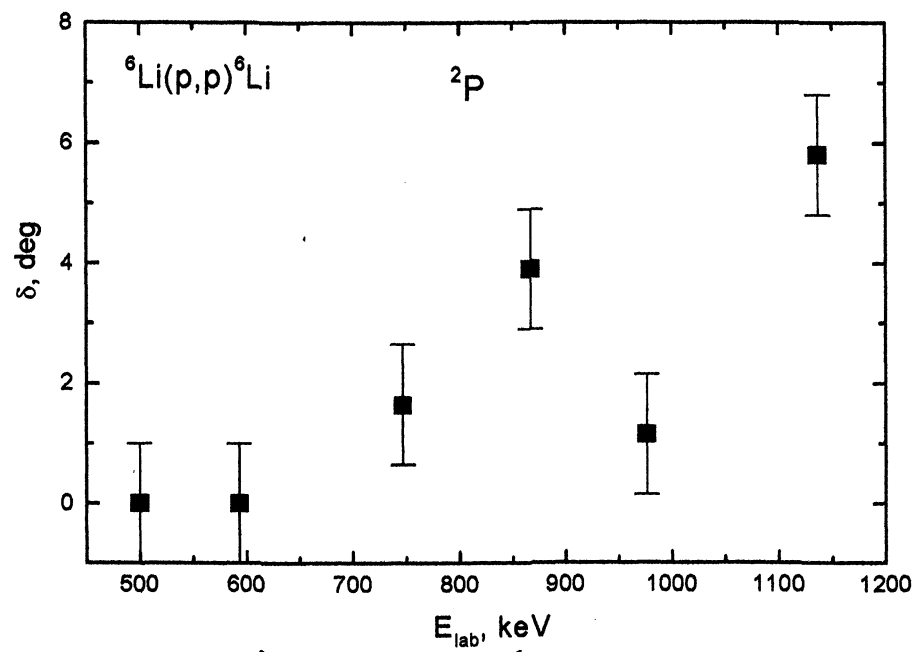

Fig.2.4.2b. The doublet ^2P phase shifts of the p^{6}Li elastic scattering at low energies. Squares – results of our phase shift analysis for the ^2P phase shift at $^4P = 0$.

2.4.3 Program for the phase shift analysis

Let us provide the listing of the computer program in the Fortran-90 language for carrying out of the p^6Li phase shift analysis at low energies without spin-orbital splitting of the phase shifts, which was used for the obtaining of the results described above. The designations of key parameters of the program coincide with the previous listings.

```
PROGRAM FAZ_ANAL_P6LI
! CALCULATE OF CROSS SECTION WITH COMPLEX
! PHASE SHIFTS FOR SYSTEM SPIN 1/2+1 WITHOUT LS
IMPLICIT REAL(8) (A-Z)
INTEGER
L,LL,TMA,T,LN,LV,NV,Z1,Z2,LN1,NT,NP,NPP,NI,NYS,NNN
REAL(8)
SECT(0:200),FK(0:200),FD(0:200),XP(0:200),FK1(0:200),FD1(0:200),S0
(0:200)
COMMON REAL(8) /A/
PI,ET(0:200),ES(0:200),ST(0:200),SSE(0:200),TE(0:200) /R/
LN1,NT,P1,NP,NPP,LV1,NNN,BB /T/
SECE(0:200),DS(0:200),DSEC(0:200),TMA /W/ GG,SS,LN,LV,NYS
CHARACTER(7) BB
CHARACTER(12) AA
CHARACTER(13) CC
! *************** INPUT PARAMETERS ***************
!AA='SEC11363.DAT'
!AA='SEC9765.DAT'
!AA='SEC8668.DAT'
AA='SEC7467.DAT'
!AA='SEC495.DAT'
!AA='SEC989.DAT'
!AA='SEC640.DAT'
!AA='SEC1585.DAT'
BB='FAZ.DAT'
!CC='SECT11363.DAT'
!CC='SECT9765.DAT'
```

```
!CC='SECT8668.DAT'
CC='SECT7467.DAT'
!CC='SECT495.DAT'
!CC='SECT989.DAT'
!CC='SECT640.DAT'
!CC='SECT1585.DAT'
!EL=1.1363D-000
!EL=0.9765D-000
!EL=0.8668D-000
!EL=0.7467D-000
EL=0.7464D-000
!EL=0.989D-000
!EL=1.585D-000
PI=4.0D-000*DATAN(1.0D-000)
P1=PI
NYS=0; ! =0 - P-6LI; =1 - 3HE-3HE
NNN=1;! THE NUMBER BY WHICH THE STEP AT EACH
ITERATION DECREASES
NV=1! =0 WITHOUT THE VARIATION = 1 WITH THE VARIATION
FH=0.0123D-000;! THE INITIAL STEP
NI=10;! THE NUMBER OF ITERATIONS
EPP=1.0D-010;! THE ACCURACY
LN=0; LN1=LN
LV=0
LV1=LV; NPP=2*LV
TMA=11
NT=TMA
AM1=1.0D-000; AM2=6.0D-000; Z1=1; Z2=3
A1=41.4686D-000
PM=AM1*AM2/(AM1+AM2)
B1=2.0D-000*PM/A1
NP=NPP+2
! ************** PHASE SHIFTS FOR P- 6LI ************
FD(0)=160.0D-000
FD(1)=5.D-000
FD(2)=1.D0-000
```

```
FK(0)=179.D-000
FK(1)=3.0D-000
FK(2)=1.1D-000
OPEN (1,FILE=BB)
DO I=LN,LV
READ(1,*) FD(I),FK(I)
ENDDO
CLOSE(1)
OPEN (1,FILE=AA)
DO L=1,NT
READ(1,*) TE(L),SECE(L)
!,DSEC(L)
PRINT *, TE(L),SECE(L),DSEC(L)
ENDDO
CLOSE(1)
DO L=LN,LV
FD(L)=FD(L)*PI/180.0D-000
FK(L)=FK(L)*PI/180.0D-000
ET(L)=1.0D-000
ES(L)=1.0D-000
ENDDO
FH=FH*PI/180.0D-000
!DO L=LN,LV
!XP(L)=FD(L)
!XP(L+LV+1)=FK(L)
!ENDDO
DO I=LN,LV
XP(2*I)=FD(I)
XP(2*I+1)=FK(I)
ENDDO
!  ********** TRANSFORM TO C.M. ******************
ECM=EL*PM/AM1
! ********  TOTAL CROSS SECTION  ******************
SK=ECM*B1
SS=DSQRT(SK)
GG=3.44476D-002*Z1*Z2*PM/SS
```

```
CALL CULFAZ(GG,S0)
DO I=1,NT
TT=TE(I)*PI/180.0D-000
S00=2.0D-000*S0(0)
X=DCOS(TT)
A=2.0D-000/(1.0D-000-X)
BBB=-GG*A
ALO=GG*DLOG(A)+S00
RECUL=BBB*DCOS(ALO)
AIMCUL=BBB*DSIN(ALO)
CUL=RECUL**2+AIMCUL**2
SCUL=CUL*10.0D-000/4.0D-000/SS**2
!SECE(I)=SECE(I)*SCUL
DSEC(I)=SECE(I)*0.1
!DSEC(I)=DSEC(I)*SCUL
ENDDO
SIGS=0.0D-000; SIGT=0.0D-000
DO LL=LN,LV
FK11=FK(LL)
FD11=FD(LL)
SIGS=SIGS+(2.0D-000*LL+1.0D-000)*DSIN(FK11)**2
SIGT=SIGT+(2.0D-000*LL+1.0D-000)*DSIN(FD11)**2
ENDDO
SIGS=10.0D-000*4.0D-000*PI*SIGS/SK
SIGT=10.0D-000*4.0D-000*PI*SIGT/SK
SIG=1.0D-000/4.0D-000*SIGS+3.0D-000/4.0D-000*SIGT
PRINT *,"                SIGMS-TOT=",SIG
! ********** DIFFERENTIAL CROSS SECTION **********
CALL VAR(SECT,FH,NI,XP,EPP,XI,NV)
PRINT *,'   T      SE       ST       XI'
DO T=1,TMA
WRITE(*,1) TE(T),SECE(T),SECT(T),DS(T)
ENDDO
1 FORMAT(1X,F8.3,3E15)
PRINT *,'  FD       FK'
DO L=LN,LV
```

```
!FD(L)=XP(L)*180.0D-000/PI
!FK(L)=XP(L+LV+1)*180.0D-000/PI
FD(L)=XP(2*L)*180.0D-000/PI
FK(L)=XP(2*L+1)*180.0D-000/PI
IF (FD(L)<+0.0D-000) THEN
FD1(L)=FD(L)+180.0D-000
ELSE
FD1(L)=FD(L)
ENDIF
IF (FK(L)<+0.0D-000) THEN
FK1(L)=FK(L)+180.0D-000
ELSE
FK1(L)=FK(L)
ENDIF
WRITE(*,3) FD1(L),FK1(L)
ENDDO
WRITE(*,5) XI
5 FORMAT(F15)
OPEN (1,FILE=CC)
WRITE(1,*)"     EL      ECM      XI"
WRITE(1,4) EL,ECM,XI
WRITE(1,*) "   T          SE          DS          ST          XI"
DO I=1,NT
WRITE(1,6)TE(I),SECE(I),DSEC(I),SECT(I),DS(I)
ENDDO
WRITE(1,*) "    FD         FK"
DO I=LN,LV
WRITE(1,3)FD1(I),FK1(I)
ENDDO
CLOSE(1)
OPEN (1,FILE=BB)
DO I=LN,LV
WRITE(1,3)FD(I),FK(I)
ENDDO
CLOSE(1)
6 FORMAT(1X,F8.3,4E15)
```

```
4 FORMAT(3F10.5)
2 FORMAT(4F10.5)
3 FORMAT(2F10.5)
END

SUBROUTINE VAR(ST,PHN,NI,XP,EP,AMIN,NV)
IMPLICIT REAL(8) (A-Z)
INTEGER I,LMI,NV,NI,NPP,NT,IIN,NN,NP,IN,KK,NNN
REAL(8) XPN(0:50),XP(0:50),ST(0:50),FD(0:50),FK(0:50)
COMMON REAL(8) /R/ LMI,NT,PI,NP,NPP,LV,NNN,BB
CHARACTER(7) BB
! ************************************************
!BB='FAZ.DAT'
DO I=LMI,NP
XPN(I)=XP(I)
ENDDO
CALL DET(XPN,ST,B)
IF (NV==0) GOTO 3013
! ----------------------------------------------------------------
KK=1
DO IIN=1,NI
PH=PHN/KK
NN=-1
1119  NN=NN+1
IN=0
2229 A=B
XPN(NN)=XPN(NN)+PH*XPN(NN)
IF (XPN(NN)>PI)GOTO 1118
IF (NN>NPP+2) THEN
IF (XPN(NN)<0.0D-000) GOTO 1118
ELSE
IN=IN+1
ENDIF
! ----------------------------------------------------------------
CALL DET(XPN,ST,B)
IF (B<A) GOTO 2229
```

```
1118 XPN(NN)=XPN(NN)-PH*XPN(NN)
IF (XPN(NN)>PI .AND. NN/=0 .AND. NN/=1)THEN
XPN(NN)=XPN(NN)-PI
ENDIF
PRINT *,'1=',B,NN,XPN(NN)*180.0/PI
IF (IN>1) THEN
IF (ABS(B-A)<EP .OR. ABS(PH*XPN(NN))<EP) GOTO 4449
PH=PH/2.0D-000
ELSE
PH=-PH/2.0D-000
ENDIF
GOTO 2229
! ---------------------------------------------------------------
4449 IF (NN+1<NP) THEN
PH=PHN
!/KK
GOTO 1119
ENDIF
PRINT *,'-------------------------------------------------------'
PRINT*, 'B=',B,IIN,PHN/KK/PI*180
PRINT *,'-------------------------------------------------------'
DO L=LMI,LV
FD(L)=XPN(2*L)*180.0D-000/PI
FK(L)=XPN(2*L+1)*180.0D-000/PI
ENDDO
OPEN (5,FILE=BB)
DO I=LMI,LV
WRITE(5,3)FD(I),FK(I)
ENDDO
CLOSE(5)
KK=NNN*KK
ENDDO
3013 AMIN=B
DO I=LMI,NP
XP(I)=XPN(I)
3 FORMAT(2F10.5)
```

```
ENDDO
END

SUBROUTINE DET(XP,ST,XI)
IMPLICIT REAL(8) (A-Z)
INTEGER I,NT
REAL(8) XP(0:50),ST(0:50)
COMMON REAL(8) /T/ SECE(0:200),DS(0:200),DSEC(0:200),NT
S=0.0D-000
CALL SEC(XP,ST)
DO I=1,NT
DS(I)=((ST(I)-SECE(I))/DSEC(I))**2
S=S+DS(I)
ENDDO
XI=S/NT
END

SUBROUTINE SEC(XP,ST)
IMPLICIT REAL(8) (A-Z)
INTEGER TT,L,TMA,LMA,LMI,NYS
REAL(8) S0(0:20),P(0:20),ST(0:200),FK(0:200),FD(0:200),XP(0:200)
COMMON REAL(8) /A/
PI,ET(0:200),ES(0:200),SKS(0:200),SDS(0:200),TE(0:200) /T/
SE(0:200),DS(0:200),DE(0:200),TMA /W/ GG,SS,LMI,LMA,NYS
RECUL1=0.0D-000; AIMCUL1=0.0D-000
DO L=LMI,LMA
!FD(L)=XP(L)
!FK(L)=XP(L+LMA+1)
FD(L)=XP(2*L)
FK(L)=XP(2*L+1)
ENDDO
CALL CULFAZ(GG,S0)
DO TT=1,TMA
T=TE(TT)*PI/180.0D-000
S00=2.0D-000*S0(0)
X=DCOS(T)
```

```
A=2.0D-000/(1.0D-000-X)
BB=-GG*A
ALO=GG*DLOG(A)+S00
RECUL=BB*DCOS(ALO)
AIMCUL=BB*DSIN(ALO)
IF (NYS==0) GOTO 555
X1=DCOS(T)
A1=2.0D-000/(1.0D-000+X1)
BB1=-GG*A1
ALO1=GG*DLOG(A1)+S00
RECUL1=BB1*DCOS(ALO1)
AIMCUL1=BB1*DSIN(ALO1)
555 RET=0.0D-000; AIT=0.0D-000; RES=0.0D-000; AIS=0.0D-000
DO L=LMI,LMA
AL=ET(L)*DCOS(2.0D-000*FK(L))-1.0D-000
BE=ET(L)*DSIN(2.0D-000*FK(L))
LL=2.0D-000*L+1.0D-000
SL=2.0D-000*S0(L)
CALL POLLEG(X,L,P)
RET=RET+LL*(BE*DCOS(SL)+AL*DSIN(SL))*P(L)
AIT=AIT+LL*(BE*DSIN(SL)-AL*DCOS(SL))*P(L)
AL=ES(L)*DCOS(2.0D-000*FD(L))-1.0D-000
BE=ES(L)*DSIN(2.0D-000*FD(L))
RES=RES+LL*(BE*DCOS(SL)+AL*DSIN(SL))*P(L)
AIS=AIS+LL*(BE*DSIN(SL)-AL*DCOS(SL))*P(L)
ENDDO
IF (NYS==0) GOTO 556
AIT=2.0D-000*AIT
RET=2.0D-000*RET
AIS=2.0D-000*AIS
RES=2.0D-000*RES
556 RETR=RECUL+RECUL1+RET
AITR=AIMCUL+AIMCUL1+AIT
RESI=RECUL+RECUL1+RES
AISI=AIMCUL+AIMCUL1+AIS
CUL=RECUL**2+AIMCUL**2
```

```
SCUL=CUL*10.0D-000/4.0D-000/SS**2
SKS(TT)=10.0D-000*(RETR**2+AITR**2)/4.0D-000/SS**2
SDS(TT)=10.0D-000*(RESI**2+AISI**2)/4.0D-000/SS**2
ST(TT)=(2.0D-000/6.0D-000*SDS(TT)+4.0D-000/6.0D-000*SKS(TT))
!/SCUL
ENDDO
END

SUBROUTINE POLLEG(X,L,P)
IMPLICIT REAL(8) (A-Z)
INTEGER L,I
REAL(8) P(0:20)
P(0)=1.0D-000; P(1)=X
DO I=2,L
P(I)=(2*I-1)*X/I*P(I-1)-(I-1)/I*P(I-2)
!P(I)=(2.0D-000*I-1.0D-000)*X/(1.0D-000*I)*P(I-1)-(1.0D-000*I-1.0D-
000)/(1.0D-000*I)*P(I-2)
ENDDO
END

SUBROUTINE CULFAZ(G,F)
IMPLICIT REAL(8) (A-Z)
INTEGER I,N,J
REAL(8) F(0:20)
C=0.577215665D-000; S=0.0D-000; N=1000
A1=1.2020569030D-000/3.0D-000; A2=1.0369277550D-000/5.0D-000
DO I=1,N
A=G/(1.0D-000*I)-DATAN(G/(1.0D-000*I))-(G/(1.0D-000*I))**3/3.0D-
000+(G/(1.0D-000*I))**5/5.0D-000
S=S+A
ENDDO
FAZ=-C*G+A1*G**3-A2*G**5+S; F(0)=FAZ
DO J=1,10
F(J)=F(J-1)+DATAN(G/(J*1.0D-000))
ENDDO
END
```

Now we will execute some control account on this program for search of the scattering phase shifts at energy of 746.4 keV in c.m. (in tab. 2.4.1 it is 3 variant) taking into account, S in the beginning, and then, S and P of the partial waves. The first of the control accounts, which is carried out only for a zero partial wave results to the following results:

θ	σ_e	σ_t	χ^2_i
46.150	.12221E+04	.12206E+04	.14291E-03
57.340	.53259E+03	.56204E+03	.30591E+00
68.300	.33140E+03	.31229E+03	.33259E+00
79.020	.17700E+03	.19794E+03	.13992E+01
109.450	.81443E+02	.83291E+02	.51460E-01
128.310	.57902E+02	.60517E+02	.20406E+00
137.350	.54128E+02	.54215E+02	.25420E-03
146.160	.50402E+02	.49847E+02	.12139E-01
154.800	.49110E+02	.46852E+02	.21136E+00
163.290	.46213E+02	.44907E+02	.79861E-01
171.680	.43990E+02	.43811E+02	.16535E-02

δ_d	δ_k
170.08	179.99

$\chi^2 = 0.236$

In this control account the phase shifts and χ^2 are obtained that coincide with the results, given above in tab.2.4.1 at number 3-1. In the listings given here the following designations are accepted: θ – the scattering angle, σ_e – experimental cross sections, σ_t – calculated cross sections, χ^2_i – partial χ^2 for i angle, δ_d – doublet phase shift, δ_k – quartet phase shift, χ^2 – average value on all experimental points.

At the account of two partial waves in the phase shift analysis we have

θ	σ_e	σ_t	χ^2_i
46.150	.12221E+04	.11875E+04	.80049E-01
57.340	.53259E+03	.54118E+03	.26020E-01
68.300	.33140E+03	.29882E+03	.96658E+00

79.020	.17700E+03	.18906E+03	.46396E+00
109.450	.81443E+02	.80736E+02	.75339E-02
128.310	.57902E+02	.59753E+02	.10226E+00
137.350	.54128E+02	.54042E+02	.25495E-03
146.160	.50402E+02	.50126E+02	.29924E-02
154.800	.49110E+02	.47469E+02	.11164E+00
163.290	.46213E+02	.45758E+02	.97024E-02
171.680	.43990E+02	.44800E+02	.33889E-01

δ_d	δ_k
172.49	179.93
1.67	0.00

$\chi^2 = 0.164$

In this version of the account the results coincide with the data given above in tab.2.4.1 at number 3-2 [163]. The phase shifts of the elastic scattering obtained in this paragraph were used further for the creation of intercluster potentials [163] and calculations of the astrophysical *S*-factor of the radiative proton capture on ^{6}Li [129,158,161].

2.5 Phase shift analysis and computer programs for scattering of particles with the 1/2+1/2 spin

Now let us consider the methods and computer programs on Fortran-90 for the phase shift analysis of processes of the elastic scattering of the nonidentical particles with the half-integer spin 1/2 + 1/2, for example, it can be elastic scattering of N^3He, N^3H or $p^{13}C$, etc.

2.5.1 The system with the spin-orbital interaction

The expressions used here for the differential cross sections, on the basis of which the program is written, are given in our work [10] together with the similar programs in the Turbo Basic language and for a triplet spin state have an appearance, which considers only the spin-orbital splitting of the scattering phase shifts

$$\frac{d\sigma_t(\theta)}{d\Omega} = \frac{1}{3}\left[|A|^2 + 2\left(|B|^2 + |C|^2 + |D|^2 + |E|^2\right)\right] . \qquad (2.5.1)$$

where

$$A = f_c(\theta) + \frac{1}{2ik}\sum_{L=0}\{(L+1)\alpha_L^+ + L\alpha_L^-\}\exp(2i\sigma_L)P_L(\cos\theta),$$

$$B = f_c(\theta) + \frac{1}{4ik}\sum_{L=0}\{(L+2)\alpha_L^+ + (2L+1)\alpha_L^0 + (L-1)\alpha_L^-\}\exp(2i\sigma_L)P_L(\cos\theta) ,$$

$$C = \frac{1}{2ik\sqrt{2}}\sum_{L=1}\{\alpha_L^+ - \alpha_L^-\}\exp(2i\sigma_L)P_L^1(\cos\theta), \qquad (2.5.2)$$

$$D = \frac{1}{2ik\sqrt{2}}\sum_{L=1}\frac{1}{L(L+1)}\{L(L+2)\alpha_L^+ - (2L+1)\alpha_L^0 - (L-1)(L+1)\alpha_L^-\}\cdot$$

$$\cdot\exp(2i\sigma_L)P_L^1(\cos\theta) ,$$

$$E=\frac{1}{4ik}\sum_{L=2}\frac{1}{L(L+1)}\{L\alpha_L^+-(2L+1)\alpha_L^0+(L+1)\alpha_L^-\}\cdot$$

$$\cdot\exp(2i\sigma_L)P_L^2(\cos\theta)$$

Here the α value for each state with the total moment of $J=L\pm1$ (α^+ and α^-) and $J=L$ (α^0) is determined.

For the scattering in the singlet spin state we have the expression for the differential cross section

$$\frac{d\sigma_s(\theta)}{d\Omega}=\left|f_s(\theta)\right|^2,$$

where

$$f_s(\theta)=f_c(\theta)+f_s^N(\theta),$$

$$f_c(\theta)=-\left(\frac{\eta}{2k\sin^2(\theta/2)}\right)\exp\{i\eta\ln[\sin^{-2}(\theta/2)]+2i\sigma_0\}\ ,$$

$$f_s^N(\theta)=\frac{1}{2ik}\sum_L(2L+1)\exp(2i\sigma_L)[S_L^s-1]P_L(\cos\theta)\ . \qquad (2.5.3)$$

Here the designations of the variables are the same, as for ^{4}He^{4}He scattering. The summarized cross section of the elastic scattering now is defined in the form

$$\frac{d\sigma(\theta)}{d\Omega}=\frac{1}{4}\frac{d\sigma_s(\theta)}{d\Omega}+\frac{3}{4}\frac{d\sigma_t(\theta)}{d\Omega}$$

Let us provide the listing of the computer program for the search of the scattering phase shifts in the system of nonidentical particles with half-integer spin, namely, p^{3}He. This program considers the spin-orbital splitting of the scattering phase shifts, but do not take into account the singlet-triplet mixing, which will be included in the next cross section.

```
PROGRAM FAZOVIY_ANALIZ_p3He_WITH_LS
IMPLICIT REAL(8) (A-Z)
INTEGER I,L,Z1,Z2,LMI,LH,LMA,LN,LV,NV,NI,NPP,NT,NTT,NP
DIMENSION ST(0:50),FT(0:50),XP(0:50)
COMMON /A/ LH,LMI,NT,PI,NP,NPP
COMMON /B/ SE(0:50),DS(0:50),DE(0:50),NTT
COMMON /C/ SS,GG,LN,LV,POL(0:50),TT(0:50)
COMMON /D/ FP(0:50),FPI(0:50),EP(0:50),F0(0:50),F0I(0:50),
E0(0:50),M(0:50),FMI(0:50),EM(0:50),FS(0:50),FSI(0:50), ES(0:50)
CHARACTER(9) BB
CHARACTER(7) AA
CHARACTER(15) CC
! ********* INPUT PARAMETERS **********************
AA='SEC.DAT'
BB='FAZLS.DAT'
PI=4.0D-000*DATAN(1.0D-000)
P1=PI
Z1=1! The p charge
Z2=2! The 3He charge
AM1=1.0D-000! The p weight
AM2=3.0D-000! The 3He mass
AM=AM1+AM2
A1=41.46860D-000
PM=AM1*AM2/(AM1+AM2)
B1=2.0D-000*PM/A1
LMI=0! The initial orbital moment
LH=1! A step by the moment
LMA=2! The maximum moment
LN=LMI
LV=LMA
EPP=1.0D-005
NV=1! If 1 then to vary the phase shifts if 0 – without variation
FH=0.01D-000
NI=5! The number of iterations
NPP=2*LMA
! ****** ECSPERIMENTAL CROSS SECTION 11.48 *******
```

```
NT=17! The number of the experimental points
NTT=NT
! ************ FOR P-3HE ON E=11.48 ******************
OPEN (1,FILE=AA)
DO L=1,NT
READ(1,*) TT(L),SE(L)
ENDDO
CLOSE(1)
OPEN (1,FILE=BB)
DO I=LN,LV
READ(1,*) FP(I),F0(I),FM(I),FS(I)
ENDDO
CLOSE(1)
! ******* TRANSFORM TO RADIANS ********************
DO L=LN,LV,LH
FM(L)=FM(L)*PI/180.0D-000
FP(L)=FP(L)*PI/180.0D-000
F0(L)=F0(L)*PI/180.0D-000
FMI(L)=FMI(L)*PI/180.0D-000
FPI(L)=FPI(L)*PI/180.0D-000
F0I(L)=F0I(L)*PI/180.0D-000
FT(L)=FT(L)*PI/180.0D-000
FS(L)=FS(L)*PI/180.0D-000
FSI(L)=FSI(L)*PI/180.0D-000
EP(L)=DEXP(-2.0D-000*FPI(L))
EM(L)=DEXP(-2.0D-000*FMI(L))
E0(L)=DEXP(-2.0D-000*F0I(L))
ES(L)=DEXP(-2.0D-000*FSI(L))
ENDDO
! ************************************************
FH=FH*PI/180.0D-000
NP=2*NPP+1
DO I=LMI,LMA,LH
XP(I)=FP(I)
ENDDO
DO I=LMI,LMA-1,LH
```

```
XP(I+LMA+1)=F0(I+1)
ENDDO
DO I=LMI,LMA-1,LH
XP(I+2*LMA+1)=FM(I+1)
ENDDO
DO I=LMI,LMA,LH
XP(I+3*LMA+1)=FS(I)
ENDDO
DO I=LMI,LMA,LH
XP(I+4*LMA+2)=FPI(I)
ENDDO
DO I=LMI,LMA-1,LH
XP(I+5*LMA+3)=F0I(I+1)
ENDDO
DO I=LMI,LMA-1,LH
XP(I+6*LMA+3)=FMI(I+1)
ENDDO
DO I=LMI,LMA,LH
XP(I+7*LMA+3)=FSI(I)
ENDDO
!  ********** TRANSFORM TO C.M. ********************
EL=11.48D-000
CC='SECTLS.DAT'
EC=EL*PM/AM1
SK=EC*B1
SS=DSQRT(SK)
GG=3.44476D-002*Z1*Z2*PM/SS
CALL VAR(ST,FH,NI,XP,EPP,XI,NV)
PRINT *,"                XI-KV=",XI
! ********* TOTAL CROSS SECTION ******************
DO I=LMI,LMA,LH
FP(I)=XP(I)
ENDDO
DO I=LMI,LMA-1,LH
F0(I+1)=XP(I+LMA+1)
ENDDO
```

```
DO I=LMI,LMA-1,LH
FM(I+1)=XP(I+2*LMA+1)
ENDDO
DO I=LMI,LMA,LH
FS(I)=XP(I+3*LMA+1)
ENDDO
F0(0)=FP(0); FM(0)=FP(0)
DO I=LMI,LMA,LH
FPI(I)=XP(I+4*LMA+2)
ENDDO
DO I=LMI,LMA-1,LH
F0I(I+1)=XP(I+5*LMA+3)
ENDDO
DO I=LMI,LMA-1,LH
FMI(I+1)=XP(I+6*LMA+3)
ENDDO
DO I=LMI,LMA,LH
FSI(I)=XP(I+7*LMA+3)
ENDDO
F0I(0)=FPI(0); FMI(0)=FPI(0)
DO L=LN,LV,LH
EP(L)=DEXP(-2.0D-000*FPI(L))
EM(L)=DEXP(-2.0D-000*FMI(L))
E0(L)=DEXP(-2.0D-000*F0I(L))
ES(L)=DEXP(-2.0D-000*FSI(L))
ENDDO
SRT=0.0D-000; SRS=0.0D-000;  SST=0.0D-000;  SSS=0.0D-000
DO L=LN,LV,LH
AP=FP(L)
AM=FM(L)
A0=F0(L)
ASS=FS(L)
L1=2*L+3
L2=2*L+1
L3=2*L-1
SRT=SRT+L1*(1.0D-000-EP(L)**2)+L2*(1.0D-000-
```

```
E0(L)**2)+L3*(1.0D-000-EM(L)**2)
SRS=SRS+L2*(1.0D-000-ES(L)**2)
SST=SST+L1*EP(L)**2*DSIN(AP)**2+L2*E0(L)**2*DSIN(A0)**2+L3
*EM(L)**2*DSIN(AM)**2
SSS=SSS+L2*ES(L)**2*DSIN(ASS)**2
ENDDO
SRT=10.0D-000*PI*SRT/SK/3.0D-000
SRS=10.0D-000*PI*SRS/SK
SIGR=1.0D-000/4.0D-000*SRS+3.0D-000/4.0D-000*SRT
SST=10.0D-000*4.0D-000*PI*SST/SK/3.0D-000
SSS=10.0D-000*4.0D-000*PI*SSS/SK
SIGS=1.0D-000/4.0D-000*SSS+3.0D-000/4.0D-000*SST
!PRINT *,"                SIGMS-TOT=",SIGS
PRINT *,"    T     SE        ST        XI"
DO I=1,NT
WRITE(*,2)TT(I),SE(I),ST(I),DS(I)
ENDDO
PRINT *,'   FP      F0      FM      FS'
DO L=LMI,LMA,LH
FM(L)=FM(L)*180.0D-000/PI
FP(L)=FP(L)*180.0D-000/PI
FMI(L)=FMI(L)*180.0D-000/PI
FPI(L)=FPI(L)*180.0D-000/PI
F0(L)=F0(L)*180.0D-000/PI
F0I(L)=F0I(L)*180.0D-000/PI
FS(L)=FS(L)*180.0D-000/PI
FSI(L)=FSI(L)*180.0D-000/PI
WRITE(*,2) FP(L),F0(L),FM(L),FS(L)
ENDDO
OPEN (1,FILE=CC)
WRITE(1,*)"      EL       ECM       XI"
WRITE(1,4) EL,EC,XI
WRITE(1,*) "   T          SE          ST          XI"
DO I=1,NT
WRITE(1,2) TT(I),SE(I),ST(I),DS(I)
ENDDO
```

```
WRITE(1,*) "   FP(L)   F0(L)   FM(L)   FS(L)"
DO L=LN,LV
WRITE(1,2) FP(L),F0(L),FM(L),FS(L)
ENDDO
CLOSE(1)
OPEN (1,FILE=BB)
DO L=LN,LV
WRITE(1,3) FP(L),F0(L),FM(L),FS(L)
ENDDO
CLOSE(1)
4 FORMAT(1x,3F10.3)
2 FORMAT(1x,4F10.3)
3 FORMAT(1x,4F14.7)
END

SUBROUTINE VAR(ST,PHN,NI,XP,EP,AMIN,NV)
IMPLICIT REAL(8) (A-Z)
INTEGER I,LMI,LH,NV,NI,NPP,NT,IIN,NN,NP
DIMENSION XPN(0:50),XP(0:50),ST(0:50)
COMMON /A/ LH,LMI,NT,PI,NP,NPP
! ************ THE SEARCH OF THE PHASE SHIFTS ********
DO I=LMI,NP,LH
XPN(I)=XP(I)
ENDDO
NN=LMI
PRINT *,NN,XPN(NN)*180.0D-000/PI
PH=PHN
CALL DET(XPN,ST,ALA)
B=ALA
IF (NV==0) GOTO 3013
PRINT *,ALA
DO IIN=1,NI
NN=-LH
PRINT *,ALA,IIN
GOTO 1119
1159 XPN(NN)=XPN(NN)-PH*XP(NN)
```

```
1119  NN=NN+LH
IN=0
2229 A=B
XPN(NN)=XPN(NN)+PH*XP(NN)
IF (NP==2*NPP+1) GOTO 7777
IF (NN<(NP/2)) GOTO 7777
IF (XPN(NN)<0) GOTO 1159
7777 IN=IN+1
CALL DET(XPN,ST,ALA)
B=ALA
GOTO 5678
5678 CONTINUE
IF (B<A) GOTO 2229
C=A
XPN(NN)=XPN(NN)-PH*XP(NN)
IF (IN>1) GOTO 3339
PH=-PH
GOTO 5559
3339 IF (ABS((C-B)/(B))<EP) GOTO 4449
PH=PH/2
5559 B=C
GOTO 2229
4449 PH=PHN
B=C
IF (NN<NP) GOTO 1119
AMIN=B
PH=PHN
ENDDO
3013 AMIN=B
DO I=LMI,NP,LH
XP(I)=XPN(I)
ENDDO
END
SUBROUTINE DET(XP,ST,XI)
! ****************** THE DETERMINANT ****************
IMPLICIT REAL(8) (A-Z)
```

```
INTEGER I,NT
DIMENSION XP(0:50),ST(0:50)
COMMON /B/ SE(0:50),DS(0:50),DE(0:50),NT
S=0.0D-000
CALL SEC(XP,ST)
DO I=1,NT
DS(I)=((ST(I)-SE(I)))**2/(0.025*SE(I))**2
S=S+DS(I)
ENDDO
XI=S/NT
END

SUBROUTINE SEC(XP,ST)
! ********** THE CROSS SECTION **********
IMPLICIT REAL(8) (A-Z)
INTEGER I,L,II,LH,LN,LV,NP,NPP,LMI,NT
COMMON                                                    /D/
FP(0:50),FPI(0:50),EP(0:50),F0(0:50),F0I(0:50),E0(0:50),FM(0:50),FMI(0
:50),EM(0:50),FS(0:50),FSI(0:50),ES(0:50)
COMMON /C/ SS,GG,LN,LV,POL(0:50),TT(0:50)
COMMON /A/ LH,LMI,NT,PI,NP,NPP
DIMENSION S0(0:50),P(0:50),P1(0:50),P2(0:50),ST(0:50),XP(0:50)
DO I=LN,LV,LH
FP(I)=XP(I)
ENDDO
DO I=LN,LV-1,LH
II=I+LV+1
F0(I+1)=XP(II)
ENDDO
DO I=LN,LV-1,LH
II=I+2*LV+1
FM(I+1)=XP(II)
ENDDO
DO I=LN,LV,LH
II=I+3*LV+1
FS(I)=XP(II)
```

```
ENDDO
F0(0)=FP(0); FM(0)=FP(0)
DO I=LN,LV,LH
II=I+4*LV+2
FPI(I)=XP(II)
ENDDO
DO I=LN,LV-1,LH
II=I+5*LV+3
F0I(I+1)=XP(II)
ENDDO
DO I=LN,LV-1,LH
II=I+6*LV+3
FMI(I+1)=XP(II)
ENDDO
DO I=LN,LV,LH
II=I+7*LV+3
FSI(I)=XP(II)
ENDDO
F0I(0)=FPI(0); FMI(0)=FPI(0)
DO L=LN,LV,LH
 EP(L)=DEXP(-2.0D-000*FPI(L))
EM(L)=DEXP(-2.0D-000*FMI(L))
E0(L)=DEXP(-2.0D-000*F0I(L))
ES(L)=DEXP(-2.0D-000*FSI(L))
ENDDO
CALL CULFAZ(GG,S0)
DO I=1,NT
T=TT(I)*PI/180.0D-000
X=DCOS(T)
CALL CULAMP(X,GG,S0,RECUL,AMCUL)
CALL POLLEG(X,LV,P)
CALL FUNLEG1(X,LV,P1)
CALL FUNLEG2(X,LV,P2)
RES=0.0D-000;    AMS=0.0D-000;  REA=0.0D-000;  AMA=0.0D-000;
REB=0.0D-000; AMB=0.0D-000
REC=0.0D-000;  AMC=0.0D-000;  RED=0.0D-000;  AMD=0.0D-000;
```

```
REE=0.0D-000; AME=0.0D-000
DO L=LN,LV,LH
FP1=2.0D-000*FP(L); FM1=2.0D-000*FM(L); F01=2.0D-000*F0(L)
SL=2.0D-000*S0(L); C=DCOS(SL); S=DSIN(SL); FS1=2.0D-000*FS(L)
AL1P=EP(L)*DCOS(FP1)-1.0D-000
AL2P=EP(L)*DSIN(FP1)
AL1M=EM(L)*DCOS(FM1)-1.0D-000
AL2M=EM(L)*DSIN(FM1)
AL10=E0(L)*DCOS(F01)-1.0D-000
AL20=E0(L)*DSIN(F01)
A1=(L+1)*AL1P+L*AL1M
A2=(L+1)*AL2P+L*AL2M
REA=REA+(A2*C+A1*S)*P(L)
AMA=AMA+(A2*S-A1*C)*P(L)
B1=(L+2)*AL1P+(2*L+1)*AL10+(L-1)*AL1M
B2=(L+2)*AL2P+(2*L+1)*AL20+(L-1)*AL2M
REB=REB+(B2*C+B1*S)*P(L)/2.0D-000
AMB=AMB+(B2*S-B1*C)*P(L)/2.0D-000
IF (L<1) GOTO 2111
C1=AL1P-AL1M
C2=AL2P-AL2M
CC1=1.0D-000/(DSQRT(2.0D-000))
REC=REC+(C2*C+C1*S)*P1(L)*CC1
AMC=AMC+(C2*S-C1*C)*P1(L)*CC1
DD1=1.0D-000/(DSQRT(2.0D-000)*L*(L+1))
D1=L*(L+2)*AL1P-(2*L+1)*AL10-(L**2-1)*AL1M
D2=L*(L+2)*AL2P-(2*L+1)*AL20-(L**2-1)*AL2M
RED=RED+(D2*C+D1*S)*P1(L)*DD1
AMD=AMD+(D2*S-D1*C)*P1(L)*DD1
2111 IF (L<2) GOTO 2222
EE1=1.0D-000/(2*L*(L+1))
E1=L*AL1P-(2*L+1)*AL10+(L+1)*AL1M
E2=L*AL2P-(2*L+1)*AL20+(L+1)*AL2M
REE=REE+(E2*C+E1*S)*P2(L)*EE1
AME=AME+(E2*S-E1*C)*P2(L)*EE1
2222 ENDDO
```

```
RES=0.0D-000;  AMS=0.0D-000
DO L=LN,LV,LH
SL=2.0D-000*S0(L)
C=DCOS(SL)
S=DSIN(SL)
FS1=2.0D-000*FS(L)
ALS=ES(L)*DCOS(FS1)-1.0D-000
BS=ES(L)*DSIN(FS1)
RES=RES+(2*L+1)*(BS*C+ALS*S)*P(L)
AMS=AMS+(2*L+1)*(BS*S-ALS*C)*P(L)
ENDDO
9191 CONTINUE
RES=RECUL+RES
AMS=AMCUL+AMS
SES=10.0D-000*(RES**2+AMS**2)/4.0D-000/SS**2
REA=RECUL+REA
AMA=AMCUL+AMA
REB=RECUL+REB
AMB=AMCUL+AMB
AA=REA**2+AMA**2
BB=REB**2+AMB**2
CC=REC**2+AMC**2
DD=RED**2+AMD**2
EE=REE**2+AME**2
SET=10.0D-000*(AA+2*(BB+CC+DD+EE))/4.0D-000/SS**2/3.0D-000
S=3.0D-000/4.0D-000*SET+1.0D-000/4.0D-000*SES
ST(I)=S
ENDDO
END

SUBROUTINE CULAMP(X,GG,S0,RECUL,AMCUL)
! ********* THE COULOMB AMPLITUDE ***********
IMPLICIT REAL(8) (A-Z)
DIMENSION S0(0:20)
A=2.0D-000/(1.0D-000-X)
S00=2.0D-000*S0(0)
```

```
BB=-GG*A
AL=GG*DLOG(A)+S00
RECUL=BB*DCOS(AL)
AMCUL=BB*DSIN(AL)
END

SUBROUTINE POLLEG(X,L,P)
! ****************** THE LEGENDRE'S POLYNOM **********
IMPLICIT REAL(8) (A-Z)
INTEGER I,L
DIMENSION P(0:20)
P(0)=1.0D-000
P(1)=X
DO I=2,L
P(I)=(2.0D-000*I-1.0D-000)*X/I*P(I-1)-(I-1.0D-000)/I*P(I-2)
ENDDO
END
SUBROUTINE FUNLEG1(X,L,P)
! ****************** THE LEGENDRE'S FUNCTION **********
IMPLICIT REAL(8) (A-Z)
INTEGER I,L
DIMENSION P(0:20)
P(0)=0.0D-000
P(1)=DSQRT(ABS(1.0D-000-X**2))
DO I=2,L
P(I)=(2.0D-000*I-1.0D-000)*X/(I-1.0D-000)*P(I-1)-I/(I-1.0D-000)*P(I-2)
ENDDO
END

SUBROUTINE FUNLEG2(X,L,P)
! ****************** THE LEGENDRE'S FUNCTION **********
IMPLICIT REAL(8) (A-Z)
INTEGER L
DIMENSION P(0:20)
P(0)=0.0D-000
P(1)=0.0D-000
```

```
P(2)=3.0D-000*ABS(1.0D-000-X**2)
DO I=3,L
P(I)=(2.0D-000*I-1.0D-000)*X/(I-2.0D-000)*P(I-1)-(I+1.0D-000)/(I-2.0D-
000)*P(I-2)
ENDDO
END

SUBROUTINE CULFAZ(G,F)
! ****************** THE COULOMB PHASE SHIFTS **********
IMPLICIT REAL(8) (A-Z)
INTEGER I,N
DIMENSION F(0:20)
C=0.577215665D-000
S=0.D-000
N=50
A1=1.202056903D-000/3.D-000
A2=1.036927755D-000/5.D-000
DO I=1,N
A=G/I-DATAN(G/I)-(G/I)**3/3.D-000+(G/I)**5/5.D-000
S=S+A
ENDDO
FAZ=-C*G+A1*G**3-A2*G**5+S
F(0)=FAZ
DO I=1,20
F(I)=F(I-1)+DATAN(G/I)
ENDDO
END
```

Now let us provide the results of the control account on this program for case of the p^3He elastic scattering at the energy of 11.48 MeV, where in works [164,165], taking into account the singlet-triplet mixing for χ^2 the value of 0.45 have been obtained. The differential cross sections, their errors and the scattering phase shifts obtained in the phase shift analysis, which we use for the control calculations, i.e. we consider the cross sections and χ^2 with obtained in [164,165] phase shifts are specified in these works in a tabular style.

Furthermore, in listing of the results the following designations are accepted: θ – the scattering angle, σ_e – experimental cross sections, σ_t – calculated cross sections, χ^2_i – partial χ^2 for i angle, χ^2 – average χ^2 value, δ_m –triplet phase shift with $J = L - 1$, δ_0 – phase shift at $J = L$, δ_p – phase shift at $J = L + 1$, δ_s – singlet scattering phase shift.

In the first line of listing the phase shifts correspond to the orbital moment $L = 0$, in the second $L = 1$ and in the third $L = 2$

$$\chi^2 = 7.375E\text{-}001$$

θ	σ_e	σ_t	χ^2_i
27.640	223.100	229.159	1.179
31.970	222.000	222.687	0.015
36.710	211.900	211.146	0 .020
82.530	54.270	53.522	0.302
90.000	36.760	36.249	0.309
96.030	25.700	25.467	0.133
103.800	16.780	16.162	2.165
110.550	13.210	12.598	3.444
116.570	13.210	13.120	0.075
125.270	20.260	19.962	0.341
133.480	32.210	32.333	0.023
140.790	45.950	46.975	0.794
147.210	58.820	61.388	3.052
153.900	75.460	76.517	0.313
162.140	92.720	93.062	0.022
165.670	97.700	98.823	0.212
166.590	101.100	100.157	0.139

δ_p	δ_0	δ_m	δ_s
-88.800	-88.800	-88.800	-84.600
66.700	49.400	44.300	21.400
2.500	2.500	2.500	-18.600

Because this program does not take into account the singlet-triplet

mixing, so the results for the χ^2 become slightly more than in works [164,165].

Now for the comparison we will give the results with the same phase shifts, when performing the control calculation on the Turbo Basic language in our previous work [10], where the value $\chi^2 = 0.74$ has been obtained:

θ	σ_e	σ_t
27.64	223.10	229.16
31.97	222.00	222.69
36.71	211.90	211.15
82.53	54.27	53.52
90.00	36.76	36.25
96.03	25.70	25.47
103.80	16.78	16.16
110.55	13.21	12.60
116.57	13.21	13.12
125.27	20.26	19.96
133.48	32.21	32.33
140.79	45.95	46.98
147.21	58.82	61.39
153.90	75.46	76.52
162.14	92.72	93.06
165.67	97.70	98.82
166.59	101.10	100.16

It is clear, that these results coincide to within rounding errors, i.e. do not depend on the language, in which the program is written. However, the transition to the Fortran-90 language has allowed to increase significantly the speed of work of all computer programs and a possibility of use of higher precision of the search of χ^2 minimum.

Now if to execute a full variation of the phase shifts according to our new computer program, with search of the minimum χ^2 value, then after, about, 3000 iterations we will obtain the following result for the differential scattering cross sections:

$$\chi^2 = 2.27\text{E-}001$$

θ	σ_e	σ_t	χ^2_i
27.640	223.100	224.854	0.099
31.970	222.000	221.150	0.023
36.710	211.900	211.107	0.022
82.530	54.270	53.832	0.104
90.000	36.760	36.715	0.002
96.030	25.700	26.026	0.257
103.800	16.780	16.737	0.011
110.550	13.210	13.072	0.175
116.570	13.210	13.423	0.415
125.270	20.260	19.928	0.430
133.480	32.210	31.955	0.100
140.790	45.950	46.330	0.109
147.210	58.820	60.563	1.405
153.900	75.460	75.569	0.003
162.140	92.720	92.038	0.087
165.670	97.700	97.785	0.001
166.590	101.100	99.116	0.616

δ_p	δ_0	δ_m	δ_s
-84.530	-84.530	-84.530	-93.630
56.144	46.185	42.904	44.694
3.404	3.584	4.982	-19.086

The obtained new scattering phase shifts differ a little from the previous results, and χ^2 has decreased more than three times.

2.5.2 System with the spin-orbital and the singlet-triplet mixing

Further let us consider the scattering of nonidentical particles with the half-integer spin, taking into account spin-orbital interactions, mixing of various orbital states at the expense of tensor forces and mixing of the singlet-triplet states. The scattering differential cross section has more difficult form, because scattering phase shifts are included in the formulas for the cross sections, both, and coupling parameters of states with the different spin and orbital moment, and the fullest expressions for such cross

sections are given in work [166]

$$\frac{d\sigma(\theta)}{d\Omega}=\frac{1}{2k^2}\{|A|^2+|B|^2+|C|^2+|D|^2+|E|^2+|F|^2+|G|^2+|H|^2\}. \qquad (2.5.4)$$

The scattering amplitudes of A, B, C, etc. are registered in the following form:

$$A=f_c^{'}+\frac{1}{4}\sum_{L=0}^{\infty}P_L(x)\Big\{-\sqrt{L(L-1)}U^{L-1}_{L,1;L-2,1}+(L+2)U^{L+1}_{L,1;L,1}+(2L+1)U^{L}_{L,1;L,1}+$$
$$+(L-1)U^{L-1}_{L,1;L,1}-\sqrt{(L+1)(L+2)}\,U^{L+1}_{L,1;L+2,1}\Big\},$$

$$B=f_c^{'}+\frac{1}{4}\sum_{L=0}^{\infty}P_L(x)\Big\{\sqrt{L(L-1)}U^{L-1}_{L,1;L-2,1}+(L+1)U^{L+1}_{L,1;L,1}+(2L+1)U^{L}_{L,0;L,0}+$$
$$+LU^{L-1}_{L,1;L,1}+\sqrt{(L+1)(L+2)}\,U^{L+1}_{L,1;L+2,1}\Big\},$$

$$C=\frac{1}{4}\sum_{L=0}^{\infty}P_L(x)\Big\{\sqrt{L(L-1)}U^{L-1}_{L,1;L-2,1}+(L+1)U^{L+1}_{L,1;L,1}-(2L+1)U^{L}_{L,0;L,0}+$$
$$+LU^{L-1}_{L,1;L,1}+\sqrt{(L+1)(L+2)}\,U^{L+1}_{L,1;L+2,1}\Big\}, \qquad (2.5.5)$$

$$D=-\frac{1}{4}i\sin\theta\sum_{L=1}^{\infty}P_L^{'}(x)/\sqrt{L(L+1)}\Big\{-\sqrt{(L+1)(L-1)}U^{L-1}_{L,1;L-2,1}+\sqrt{L(L+1)}U^{L+1}_{L,1;L,1}-$$
$$-\sqrt{L(L+1)}U^{L-1}_{L,1;L,1}+\sqrt{L(L+2)}\,U^{L+1}_{L,1;L+2,1}-(2L+1)U^{L}_{L,1;L,0}\Big\},$$

$$E=-\frac{1}{4}i\sin\theta\sum_{L=1}^{\infty}P_L^{'}(x)/\sqrt{L(L+1)}\Big\{-\sqrt{(L+1)(L-1)}U^{L-1}_{L,1;L-2,1}+\sqrt{L(L+1)}U^{L+1}_{L,1;L,1}-$$
$$-\sqrt{L(L+1)}U^{L-1}_{L,1;L,1}+\sqrt{L(L+2)}U^{L+1}_{L,1;L+2,1}+(2L+1)U^{L}_{L,1;L,0}\Big\},$$

$$F=-\frac{1}{4}i\sin^2\theta\sum_{L=2}^{\infty}P_L^{'}(x)/\sqrt{(L-1)L(L+1)(L+2)}\Big\{-\sqrt{(L+1)(L+2)}U^{L-1}_{L,1;L-2,1}+$$
$$+\sqrt{\frac{L(L-1)(L+2)}{L+1}}U^{L+1}_{L,1;L,1}-(2L+1)\sqrt{\frac{(L-1)(L+2)}{L(L+1)}}U^{L}_{L,1;L,1}+$$
$$+\sqrt{\frac{(L-1)(L+1)(L+2)}{L}}U^{L-1}_{L,1;L,1}-\sqrt{L(L-1)}\,U^{L+1}_{L,1;L+2,1}\Big\},$$

$$G=-\frac{1}{4}i\sin\theta\sum_{L=1}^{\infty}P_L'(x)/\sqrt{L(L+1)}\left\{\sqrt{(L-1)(L+1)}U^{L-1}_{L,1;L-2,1}+(L+2)\sqrt{\frac{L}{L+1}}U^{L+1}_{L,1;L,1}-\right.$$
$$\left.-\frac{(2L+1)}{\sqrt{L(L+1)}}U^{L}_{L,1;L,1}-(L-1)\sqrt{\frac{(L+1)}{L}}U^{L-1}_{L,1;L,1}-\sqrt{L(L+2)}U^{L+1}_{L,1;L+2,1}-(2L+1)U^{L}_{L,0;L,1}\right\},$$

$$H=-\frac{1}{4}i\sin\theta\sum_{L=1}^{\infty}P_L'(x)/\sqrt{L(L+1)}\left\{\sqrt{(L-1)(L+1)}U^{L-1}_{L,1;L-2,1}+(L+2)\sqrt{\frac{L}{L+1}}U^{L+1}_{L,1;L,1}-\right.$$
$$\left.-\frac{(2L+1)}{\sqrt{L(L+1)}}U^{L}_{L,1;L,1}-(L-1)\sqrt{\frac{(L+1)}{L}}U^{L-1}_{L,1;L,1}-\sqrt{L(L+2)}U^{L+1}_{L,1;L+2,1}+(2L+1)\,\mathrm{U}^{L}_{L,0;L,1}\right\}.$$

The scattering matrix is presented in the form

$$U^{J}_{L,S;L',S'}=U^{J}_{L',S';L,S}=\exp[i(\alpha_L+\alpha_{L'})](S^{J}_{L',S';L,S}-\delta_{L,L'}\delta_{S,S'})$$

and, for example, at $L=1$ and $J=1$ taking into account the $\varepsilon^{1}_{1,0}=\varepsilon^{J}_{S,S'}$ coupling of the singlet and triplet states are registered

$$S^{1}_{1,0;1,0}=\cos^2\varepsilon^{1}_{1,0}\exp(2i\delta^{1}_{0,1})+\sin^2\varepsilon_{1,1}\exp(2i\delta^{1}_{1,1}),$$

$$S^{1}_{1,1;1,1}=\sin^2\varepsilon^{1}_{1,0}\exp(2i\delta^{1}_{0,1})+\cos^2\varepsilon_{1,1}\exp(2i\delta^{1}_{1,1}),$$

$$S^{1}_{1,0;1,1}=S^{1}_{1,1;1,0}=\frac{1}{2}\sin(2\varepsilon^{1}_{1,0})\left(\exp(2i\delta^{1}_{0,1})-\exp(2i\delta^{1}_{1,1})\right),$$

where $\delta_{k,k'}$ – Kronecker symbol, $x=\cos(\theta)$, the values without the stroke designate an initial state, and with a stroke – the final at the same total J moment, the Coulomb α_L phase shifts are defined in the paragraph 1, and the nuclear $\delta^{J}_{S,L}$ phase shifts are considered complex to allow the inelastic channels.

The $\varepsilon_1=\varepsilon^{J}_{S,S'}$ coupling of the triplet (S and S' spins, and the total moment are equal to 1) S and the D states is defined by the following expressions for a scattering matrix

$$S^1_{0,0} = \cos^2\varepsilon_1 \exp(2i\delta^1_0) + \sin^2\varepsilon_1 \exp(2i\delta^1_2),$$

$$S^1_{2,2} = \sin^2\varepsilon_1 \exp(2i\delta^1_0) + \cos^2\varepsilon_1 \exp(2i\delta^1_2),$$

$$S^1_{0,2} = S^1_{2,0} = \frac{1}{2}\sin(2\varepsilon_1)\left[\exp(2i\delta^1_0) - \exp(2i\delta^1_2)\right].$$

The dashes at the Legendre polinomials designate the derivatives, and the scattering Coulomb amplitude is written in a form

$$f_c^{'}(\theta) = -\left(\frac{i\eta}{2\sin^2(\theta/2)}\right)\exp\left\{i\eta\ln[\sin^{-2}(\theta/2)]\right\} .$$

The derivatives of the polinomials are bound with the Legendre functions, about which it was told earlier, as follows

$$P_n^m(x) = (1-x^2)^{m/2}\frac{d^m P_n(x)}{dx^m} = (1-x^2)^{m/2}\frac{d^{m+n}(x^2-1)^n}{dx^{m+n}} = \sin^m\theta\frac{d^m P_n(\cos\theta)}{(d\cos\theta)^m}.$$

If to neglect by tensor interaction and singlet-triplet coupling in the expressions given above, then the scattering matrix will take a usual form of $\exp(2i\delta_{S,L})$ with a complex phase shift.

The following program in the Fortran-90 language is based on all these expressions and includes a singlet-triplet coupling of EPS [166], which is considered only for $L = 1$. In the program obviously are given the values of the experimental cross sections, their errors and the scattering phase shifts. The designations of variables, parameters and units, as in the previous program.

The operators

```
READ(1,*) TT(L),SE(L),DE(L)
```

and

READ(1,*) FP(I),F0(I),FM(I),FS(I),EPS(I)

at the beginning of the program is read from the file

AA='SEC.DAT'

BB='FAZTENZ.DAT'

the same data, which are obviously given in the program, i.e. the basic data can be used from the program or from these files.

```
PROGRAM FAZ_ANAL_P_3He_WIRH_LS_AND_TS
IMPLICIT REAL(8) (A-Z)
INTEGER
I,L,LH,LN,LV,LMA,LMI,NT,NP,NPP,Z1,Z2,LMI1,LH1,NT2,NT1,NI
DIMENSION ST(0:50),FP(0:50),F0(0:50),FM(0:50),FS(0:50),ES(0:50)
DIMENSION
XP(0:50),FPI(0:50),F0I(0:50),FMI(0:50),FSI(0:50),EPS(0:50),EP(0:50),E0
(0:50),EM(0:50)
COMMON /B/ SE(0:50),DS(0:50),DE(0:50),NT
COMMON /C/ LH,LMI,NT1,PI,NP,NPP
COMMON /A/ SS,GG,P1,LMI1,LMA,LH1,NT2,POL(0:50), TT(0:50)
CHARACTER(11) BB
CHARACTER(7) AA
CHARACTER(12) CC
! *************** INPUT PARAMETERS ****************
AA='SEC.DAT'
BB='FAZTENZ.DAT'
CC='SECTTENZ.DAT'
PI=4.0D-000*DATAN(1.0D-000)
P1=PI
Z1=1
Z2=2
AM1=1.0D-000
AM2=3.0D-000
AM=AM1+AM2
```

```
A1=41.4686D-000
PM=AM1*AM2/(AM1+AM2)
B1=2.0D-000*PM/A1
LMI=0
LH=1
LMA=2
LN=LMI
LMI1=LMI
LV=LMA
LH1=LH
EPP=1.0D-05
NV=1
FH=0.01D-000
NI=500
NPP=2*LMA
! **** ECSPERIMENTAL CROSS SECTION 11.48 *********
SE(1)=223.1D-000;          SE(2)=222.0D-000;          SE(3)=211.9D-000;
SE(4)=54.27D-000; SE(5)=36.76D-000
SE(6)=25.7D-000;           SE(7)=16.78D-000;          SE(8)=13.21D-000;
SE(9)=13.21D-000; SE(10)=20.26D-000
SE(11)=321D-000;           SE(12)=45.95D-000;         SE(13)=58.82D-000;
SE(14)=75.46D-000
SE(15)=92.72D-000; SE(16)=97.7D-000; SE(17)=101.1D-000
DE(1)=5.58D-000; DE(2)=5.55D-000; DE(3)=5.3D-000; DE(4)=1.36D-
000; DE(5)=0.92D-000
DE(6)=0.64D-000; DE(7)=0.42D-000; DE(8)=0.33D-000; DE(9)=0.33D-
000; DE(10)=0.51D-000
DE(11)=0.81D-000;          DE(12)=1.15D-000;          DE(13)=1.47D-000;
DE(14)=1.89D-000
DE(15)=32D-000; DE(16)=44D-000; DE(17)=53D-000
TT(1)=27.64D-000; TT(2)=31.97D-000; TT(3)=36.71D-000; TT(4)=853D-
000
TT(5)=90.0D-000;           TT(6)=96.03D-000;          TT(7)=103.8D-000;
TT(8)=110.55D-000
TT(9)=116.57D-000; TT(10)=125.27D-000; TT(11)=133.48D-000
TT(12)=140.79D-000; TT(13)=147.21D-000; TT(14)=153.9D-000
```

```
TT(15)=1614D-000; TT(16)=165.67D-000; TT(17)=166.59D-000
NT=17
NT1=NT
NT2=NT
! ********** DO P-3HE ON E=11.48 ******************
FP(0)=-88.8D-000;   FPI(0)=0.D-000
FP(1)=66.7D-000;    FPI(1)=0.D-000
FP(2)=5D-000;      FPI(2)=0.D-000
FP(3)=1.D-000;      FPI(3)=0.D-000
F0(0)=FP(0);        F0I(0)=0.D-000
F0(1)=49.4D-000;    F0I(1)=0.D-000
F0(2)=5D-000;      F0I(2)=0.D-000
F0(3)=1.D-000;      F0I(3)=0.D-000
FM(0)=FP(0);        FMI(0)=0.D-000
FM(1)=44.3D-000;   FMI(1)=0.D-000
FM(2)=5D-000;     FMI(2)=0.D-000
FM(3)=1.D-000;      FMI(3)=0.D-000
FS(0)=-84.6D-000;   FSI(0)=0.D-000
FS(1)=21.4D-000;    FSI(1)=0.D-000
FS(2)=-18.6D-000;   FSI(2)=0.D-000
FS(3)=1.D-000;      FSI(3)=0.D-000
EPS(1)=11.2D-000
EPS(3)=0.D-000
OPEN (1,FILE=AA)
DO L=1,NT
READ(1,*) TT(L),SE(L),DE(L)
ENDDO
CLOSE(1)
OPEN (1,FILE=BB)
DO I=LN,LV
READ(1,*) FP(I),F0(I),FM(I),FS(I),EPS(I)
ENDDO
CLOSE(1)
! ************ TRANSFORM TO RADIANS **************
DO L=LN,LV,LH
FM(L)=FM(L)*PI/180.0D-000
```

```
FP(L)=FP(L)*PI/180.0D-000
F0(L)=F0(L)*PI/180.0D-000
EPS(L)=EPS(L)*PI/180.0D-000
FMI(L)=FMI(L)*PI/180.0D-000
FPI(L)=FPI(L)*PI/180.0D-000
F0I(L)=F0I(L)*PI/180.0D-000
FS(L)=FS(L)*PI/180.0D-000
FSI(L)=FSI(L)*PI/180.0D-000
EP(L)=EXP(-2.0D-000*FPI(L))
EM(L)=EXP(-2.0D-000*FMI(L))
E0(L)=EXP(-2.0D-000*F0I(L))
ES(L)=EXP(-2.0D-000*FSI(L))
ENDDO
! ************************************************
FH=FH*PI/180.0D-000
NP=5*LMA+2
IF (NP>(5*LMA+2)) GOTO 9988
DO L=LN,LV,LH
FMI(L)=0
FPI(L)=0
F0I(L)=0
FSI(L)=0
ENDDO
9988 DO I=LMI,LMA,LH
XP(I)=FP(I)
ENDDO
DO I=LMI,LMA-1,LH
XP(I+LMA+1)=F0(I+1)
ENDDO
DO I=LMI,LMA-1,LH
XP(I+2*LMA+1)=FM(I+1)
ENDDO
DO I=LMI,LMA,LH
XP(I+3*LMA+1)=FS(I)
ENDDO
DO I=LMI,LMA,LH
```

```
XP(I+4*LMA+2)=EPS(I)
ENDDO
DO I=LMI,LMA,LH
XP(I+5*LMA+3)=FPI(I)
ENDDO
DO I=LMI,LMA-1,LH
XP(I+6*LMA+4)=F0I(I+1)
ENDDO
DO I=LMI,LMA-1,LH
XP(I+7*LMA+4)=FMI(I+1)
ENDDO
DO I=LMI,LMA,LH
XP(I+8*LMA+4)=FSI(I)
ENDDO
 ! ************ TRANSFOM TO C.M. ********************
EL=11.480D-000
EC=EL*PM/AM1
SK=EC*B1
SS=DSQRT(SK)
GG=3.44476D-002*Z1*Z2*PM/SS
CALL VAR(ST,FH,LMA,NI,XP,EPP,XI,NV)
PRINT *,"                XI-KV=",XI
 ! ************* TOTAL CROSS SECTION *************
DO I=LMI,LMA,LH
FP(I)=XP(I)
ENDDO
DO I=LMI,LMA-1,LH
F0(I+1)=XP(I+LMA+1)
ENDDO
DO I=LMI,LMA-1,LH
FM(I+1)=XP(I+2*LMA+1)
ENDDO
DO I=LMI,LMA,LH
FS(I)=XP(I+3*LMA+1)
ENDDO
DO I=LMI,LMA,LH
```

```
EPS(I)=XP(I+4*LMA+2)
ENDDO
F0(0)=FP(0); FM(0)=FP(0)
DO I=LMI,LMA,LH
FPI(I)=XP(I+5*LMA+3)
ENDDO
DO I=LMI,LMA-1,LH
F0I(I+1)=XP(I+6*LMA+4)
ENDDO
DO I=LMI,LMA-1,LH
FMI(I+1)=XP(I+7*LMA+4)
ENDDO
DO I=LMI,LMA,LH
FSI(I)=XP(I+8*LMA+4)
ENDDO
F0I(0)=FPI(0); FMI(0)=FPI(0)
DO L=LN,LV,LH
EP(L)=EXP(-2.0D-000*FPI(L))
EM(L)=EXP(-2.0D-000*FMI(L))
E0(L)=EXP(-2.0D-000*F0I(L))
ES(L)=EXP(-2.0D-000*FSI(L))
ENDDO
SRT=0.0D-000; SRS=0.0D-000;  SST=0.0D-000;  SSS=0.0D-000
DO L=LN,LV,LH
AP=FP(L)
AM=FM(L)
A0=F0(L)
ASS=FS(L)
L1=2*L+3
L2=2*L+1
L3=2*L-1
SRT=SRT+L1*(1.0D-000-EP(L)**2)+L2*(1.0D-000-
E0(L)**2)+L3*(1.0D-000-EM(L)**2)
SRS=SRS+L2*(1.0D-000-ES(L)**2)
SST=SST+L1*EP(L)**2*SIN(AP)**2+L2*E0(L)**2*SIN(A0)**2+L3*E
M(L)**2*SIN(AM)**2
```

```
SSS=SSS+L2*ES(L)**2*SIN(ASS)**2
ENDDO
SRT=10.0D-000*PI*SRT/SK/3.0D-000
SRS=10.0D-000*PI*SRS/SK
SIGR=1.0D-000/4.0D-000*SRS+3.0D-000/4.0D-000*SRT
SST=10*4*PI*SST/SK/3
SSS=10.0D-000*4*PI*SSS/SK
SIGS=1.0D-000/4.0D-000*SSS+3.0D-000/4.0D-000*SST
PRINT *,"                SIGMS-TOT=",SIGS
PRINT *,"    T      SE       ST       XI"
DO I=1,NT
WRITE(*,2) TT(I),SE(I),ST(I),DS(I)
ENDDO
PRINT *,"    FP       F0       FM       FS       EPS"
DO L=LMI,LMA,LH
FM(L)=FM(L)*180.0D-000/PI
FP(L)=FP(L)*180.0D-000/PI
FMI(L)=FMI(L)*180.0D-000/PI
FPI(L)=FPI(L)*180.0D-000/PI
F0(L)=F0(L)*180.0D-000/PI
F0I(L)=F0I(L)*180.0D-000/PI
FS(L)=FS(L)*180.0D-000/PI
FSI(L)=FSI(L)*180.0D-000/PI
EPS(L)=EPS(L)*180.0D-000/PI
WRITE(*,2) FP(L),F0(L),FM(L),FS(L),EPS(L)
ENDDO
 !READ *, A
 !IF (A==0) GOTO 1111
 !PRINT
 !PRINT *,"    T      POL "
 !DO I=1,NT
 !PRINT *,TT(I);POL(I)
 !ENDDO
OPEN (1,FILE=CC)
WRITE(1,*)"      EL       ECM       XI"
WRITE(1,4) EL,EC,XI
```

```
WRITE(1,*) "  T          SE          DE          ST          XI"
DO I=1,NT
WRITE(1,3) TT(I),SE(I),DE(I),ST(I),DS(I)
ENDDO
WRITE(1,*) "  FP(L)   F0(L)   FM(L)   FS(L)"
DO L=LN,LV
WRITE(1,2) FP(L),F0(L),FM(L),FS(L),EPS(L)
ENDDO
CLOSE(1)
OPEN (1,FILE=BB)
DO L=LN,LV
WRITE(1,3) FP(L),F0(L),FM(L),FS(L),EPS(L)
ENDDO
CLOSE(1)
!OPEN (1,FILE=AA)
!DO L=1,NT
!WRITE(1,3) TT(L),SE(L),DE(L)
!ENDDO
!CLOSE(1)
4 FORMAT(3F10.5)
2 FORMAT(5F10.5)
3 FORMAT(4F14.7)
END

SUBROUTINE VAR(ST,PHN,LMA,NI,XP,EP,AMIN,NV)
! ******* THE SEARCH OF PHASE SHIFTS ******************
IMPLICIT REAL(8) (A-Z)
INTEGER I,LH,NT,NP,NPP,NN,NI,LMA,LMI
DIMENSION XPN(0:50),XP(0:50),ST(0:50)
COMMON /C/ LH,LMI,NT,PI,NP,NPP
DO I=LMI,NP,LH
XPN(I)=XP(I)
ENDDO
NN=LMI
PH=PHN
CALL DET(XPN,ST,ALA)
```

```
B=ALA
IF (NV==0) GOTO 3013
DO IIN=1,NI
NN=-LH
PRINT *,ALA,IIN
GOTO 1119
1159 XPN(NN)=XPN(NN)-PH*XP(NN)
1119  NN=NN+LH
IN=0
2229 A=B
XPN(NN)=XPN(NN)+PH*XP(NN)
IF (NN<(5*LMA+3)) GOTO 7777
IF (XPN(NN)<0) GOTO 1159
7777 IN=IN+1
CALL DET(XPN,ST,ALA)
B=ALA
IF (B<A) GOTO 2229
C=A
XPN(NN)=XPN(NN)-PH*XP(NN)
IF (IN>1) GOTO 3339
PH=-PH
GOTO 5559
3339 IF (ABS((C-B)/ABS(B))<EP) GOTO 4449
PH=PH/2
5559 B=C
GOTO 2229
4449 PH=PHN
B=C
IF (NN<NP) GOTO 1119
AMIN=B
PH=PHN
ENDDO
3013 AMIN=B
DO I=LMI,NP,LH
XP(I)=XPN(I)
ENDDO
```

```
END

SUBROUTINE DET(XP,ST,XI)
! ********** THE DETERMINANT **********
IMPLICIT REAL(8) (A-Z)
INTEGER I,NT
DIMENSION XP(0:50),ST(0:50)
COMMON /B/ SE(0:50),DS(0:50),DE(0:50),NT
S=0.0D-000
CALL SEC(XP,ST)
DO I=1,NT
DS(I)=( (ST(I)-SE(I) )/DE(I) )**2
S=S+DS(I)
ENDDO
XI=S/NT
END

SUBROUTINE SEC(XP,ST)
! ********** THE CROSS SECTION **********
IMPLICIT REAL(8) (A-Z)
INTEGER I,II,L,LN,LV,LH,NT
COMMON /A/ SS,GG,PI,LN,LV,LH,NT,POL(0:50),TT(0:50)
DIMENSION
S0(0:50),P(0:50),P1(0:50),P2(0:50),XP(0:50),ST(0:50),F0(0:50),FP(0:50),
FM(0:50),FS(0:50),EPS(0:50)
DIMENSION
F0I(0:50),FPI(0:50),FMI(0:50),FSI(0:50),EP(0:50),EM(0:50),ES(0:50),E0(
0:50)
DO I=LN,LV,LH
FP(I)=XP(I)
ENDDO
DO I=LN,LV-1,LH
II=I+LV+1
F0(I+1)=XP(II)
ENDDO
DO I=LN,LV-1,LH
```

```
II=I+2*LV+1
FM(I+1)=XP(II)
ENDDO
DO I=LN,LV,LH
II=I+3*LV+1
FS(I)=XP(II)
ENDDO
DO I=LN,LV,LH
II=I+4*LV+2
EPS(I)=XP(II)
ENDDO
F0(0)=FP(0); FM(0)=FP(0)
DO I=LN,LV,LH
II=I+5*LV+3
FPI(I)=XP(II)
ENDDO
DO I=LN,LV-1,LH
II=I+6*LV+4
F0I(I+1)=XP(II)
ENDDO
DO I=LN,LV-1,LH
II=I+7*LV+4
FMI(I+1)=XP(II)
ENDDO
DO I=LN,LV,LH
II=I+8*LV+4
FSI(I)=XP(II)
ENDDO
F0I(0)=FPI(0); FMI(0)=FPI(0)
DO L=LN,LV,LH
EP(L)=DEXP(-2.0D-000*FPI(L))
EM(L)=DEXP(-2.0D-000*FMI(L))
E0(L)=DEXP(-2.0D-000*F0I(L))
ES(L)=DEXP(-2.0D-000*FSI(L))
ENDDO
CALL CULFAZ(GG,S0)
```

```
DO I=1,NT
T=TT(I)*PI/180.0D-000
X=DCOS(T)
CALL CULAMP(X,GG,S0,RECUL,AMCUL)
CALL POLLEG(X,LV,P)
CALL FUNLEG1(X,LV,P1)
CALL FUNLEG2(X,LV,P2)
REA=0.0D-000;  AMA=0.0D-000;  REB=0.0D-000;  AMB=0.0D-000;
REC=0.0D-000; AMC=0.0D-000; RED=0.0D-000; AMD=0.0D-000
REE=0.0D-000;  AME=0.0D-000;  RRG=0.0D-000;  AAG=0.0D-000;
REH=0.0D-000; AMH=0.0D-000; REF=0.0D-000; AMF=0.0D-000
DO L=LN,LV,LH
FP1=2.0D-000*FP(L)
FM1=2.0D-000*FM(L)
F01=2.0D-000*F0(L)
SL=2.0D-000*S0(L)
C=DCOS(SL)
S=DSIN(SL)
FS1=2.0D-000*FS(L)
SO=DSIN(EPS(L))**2
CO=DCOS(EPS(L))**2
AL1P=EP(L)*DCOS(FP1)-1.0D-000
AL2P=EP(L)*DSIN(FP1)
AL1M=EM(L)*DCOS(FM1)-1.0D-000
AL2M=EM(L)*DSIN(FM1)
AL10=SO*ES(L)*DCOS(FS1)+CO*E0(L)*DCOS(F01)-1.0D-000
AL20=SO*ES(L)*DSIN(FS1)+CO*E0(L)*DSIN(F01)
A1=(L+2.0D-000)*AL1P+(2.0D-000*L+1.0D-000)*AL10+(L-1.0D-
000)*AL1M
A2=(L+2.0D-000)*AL2P+(2.0D-000*L+1.0D-000)*AL20+(L-1.0D-
000)*AL2M
REA=REA+(A1*C-A2*S)*P(L)/2.0D-000
AMA=AMA+(A1*S+A2*C)*P(L)/2.0D-000
ALS=CO*ES(L)*DCOS(FS1)+SO*E0(L)*DCOS(F01)-1.0D-000
BS=CO*ES(L)*DSIN(FS1)+SO*E0(L)*DSIN(F01)
RES=(2.0D-000*L+1.0D-000)*(ALS*C-BS*S)
```

```
AMS=(2.0D-000*L+1.0D-000)*(ALS*S+BS*C)
B1=(L+1.0D-000)*AL1P+L*AL1M
B2=(L+1.0D-000)*AL2P+L*AL2M
REB=REB+(B1*C-B2*S+RES)*P(L)/2.0D-000
AMB=AMB+(B1*S+B2*C+AMS)*P(L)/2.0D-000
REC=REC+(B1*C-B2*S-RES)*P(L)/2.0D-000
AMC=AMC+(B1*S+B2*C-AMS)*P(L)/2.0D-000
IF (L<1) GOTO 1211
SI2=1.0D-000/2.0D-000*DSIN(2.0D-000*EPS(L))
AL1=SI2*(ES(L)*DCOS(FS1)-E0(L)*DCOS(F01))
AL2=SI2*(ES(L)*DSIN(FS1)-E0(L)*DSIN(F01))
RE1=(2.0D-000*L+1.0D-000)*(AL2*C+AL1*S)/DSQRT(L*(L+1.0D-
000))
AM1=(2.0D-000*L+1.0D-000)*(AL2*S-AL1*C)/DSQRT(L*(L+1.0D-
000))
C1=AL1P-AL1M
C2=AL2P-AL2M
RED=RED+(C2*C+C1*S-RE1)*P1(L)/2.0D-000
AMD=AMD+(C2*S-C1*C-AM1)*P1(L)/2.0D-000
REE=REE+(C2*C+C1*S+RE1)*P1(L)/2.0D-000
AME=AME+(C2*S-C1*C+AM1)*P1(L)/2.0D-000
D1=(L+2.0D-000)/(L+1.0D-000)*AL1P-(2.0D-000*L+1.0D-
000)/(L*(L+1.0D-000))*AL10-(L-1.0D-000)/L*AL1M
D2=(L+2.0D-000)/(L+1.0D-000)*AL2P-(2.0D-000*L+1.0D-
000)/(L*(L+1.0D-000))*AL20-(L-1.0D-000)/L*AL2M
RRG=RRG+(D2*C+D1*S-RE1)*P1(L)/2.0D-000
AAG=AAG+(D2*S-D1*C-AM1)*P1(L)/2.0D-000
REH=REH+(D2*C+D1*S+RE1)*P1(L)/2.0D-000
AMH=AMH+(D2*S-D1*C+AM1)*P1(L)/2.0D-000
1211 IF (L<2) GOTO 2122
F1=1.0D-000/(L+1.0D-000)*AL1P-(2.0D-000*L+1.0D-000)/(L*(L+1.0D-
000))*AL10+AL1M/L
F2=1.0D-000/(L+1.0D-000)*AL2P-(2.0D-000*L+1.0D-000)/(L*(L+1.0D-
000))*AL20+AL2M/L
REF=REF+(F2*C+F1*S)*P2(L)/2.0D-000
AMF=AMF+(F2*S-F1*C)*P2(L)/2.0D-000
```

```
2122 ENDDO
RET=0.0D-000; AMT=0.0D-000; RES=0.0D-000;  AMS=0.0D-000
DO L=LN,LV,LH
SL=2.0D-000*S0(L)
C=DCOS(SL)
S=DSIN(SL)
FS1=2.0D-000*FS(L)
ALS=ES(L)*DCOS(FS1)-1.0D-000
BS=ES(L)*DSIN(FS1)
RES=RES+(2.0D-000*L+1.0D-000)*(BS*C+ALS*S)*P(L)
AMS=AMS+(2.0D-000*L+1.0D-000)*(BS*S-ALS*C)*P(L)
ENDDO
RES=RECUL+RES
AMS=AMCUL+AMS
REA=RECUL+REA
AMA=AMCUL+AMA
REB=RECUL+REB
AMB=AMCUL+AMB
AA=REA**2+AMA**2
BB=REB**2+AMB**2
CC=REC**2+AMC**2
DD=RED**2+AMD**2
EE=REE**2+AME**2
FF=REF**2+AMF**2
HH=REH**2+AMH**2
GGG=RRG**2+AAG**2
SUM=AA+BB+CC+DD+EE+GGG+HH+FF
S=10.0D-000*SUM/2.0D-000/SS**2/4.0D-000
ST(I)=S
!    POL(I)    =    -    2*(REA*REE+AMA*AME+REB*REH
+AMB*AMH+REC*RRG+AMC*AAG+RED*REF+AMD*AMF)/SUM
ENDDO
END

SUBROUTINE CULAMP(X,GG,S0,RECUL,AMCUL)
! ********** THE COULOMB AMPLITUDE **********
```

```
IMPLICIT REAL(8) (A-Z)
DIMENSION S0(0:50)
A=2.0D-000/(1.0D-000-X)
S00=2.0D-000*S0(0)
BB=-GG*A
AL=GG*DLOG(A)+S00
RECUL=-BB*DSIN(AL)
AMCUL=BB*DCOS(AL)
END

SUBROUTINE POLLEG(X,L,P)
! ********** THE LEGENDRE'S POLYNOMS **********
IMPLICIT REAL(8) (A-Z)
INTEGER I,L
DIMENSION P(0:50)
P(0)=1.0D-000; P(1)=X
DO I=2,L
P(I)=(2.0D-000*I-1.0D-000)*X/I*P(I-1)-(I-1.0D-000)/I*P(I-2)
ENDDO
END

SUBROUTINE FUNLEG1(X,L,P)
! ********** THE LEGENDRE'S FUNCTION **********
IMPLICIT REAL(8) (A-Z)
INTEGER I,L
DIMENSION P(0:50)
P(0)=0.0D-000; P(1)=DSQRT(DABS(1.0D-000-X**2))
DO I=2,L
P(I)=(2.0D-000*I-1.0D-000)*X/(I-1.0D-000)*P(I-1)-I/(I-1.0D-000)*P(I-2)
ENDDO
END

SUBROUTINE FUNLEG2(X,L,P)
! ********** THE LEGENDRE'S FUNCTION **********
IMPLICIT REAL(8) (A-Z)
INTEGER I,L
```

```
DIMENSION P(0:50)
P(0)=0.0D-000; P(1)=0.0D-000; P(2)=3.0D-000*DABS(1.0D-000-X**2)
DO I=3,L
P(I)=(2.0D-000*I-1.0D-000)*X/(I-2.0D-000)*P(I-1)-(I+1.0D-000)/(I-2.0D-
000)*P(I-2)
ENDDO
END

SUBROUTINE CULFAZ(G,F)
! ********** THE COULOMB PHASE SHIFTS **********
IMPLICIT REAL(8) (A-Z)
INTEGER I,N
DIMENSION F(0:50)
C=0.577215665D-000; S=0.0D-000; N=50
A1=1.202056903D-000/3.0D-000; A2=1.036927755D-000/5.0D-000
DO I=1,N
A=G/I-DATAN(G/I)-(G/I)**3/3.0D-000+(G/I)**5/5.0D-000
S=S+A
ENDDO
FAZ=-C*G+A1*G**3-A2*G**5+S
F(0)=FAZ
DO I=1,20
F(I)=F(I-1)+DATAN(G/(I))
ENDDO
END
```

With the same phase shifts as in the previous case [164,165] and without mixing we obtain, according to this program, the same result, which is given by the first as the control account for the previous program with χ^2 = 7.375E-001

χ^2 = 7.375E-001

θ	σ_e	σ_t	χ^2_i
27.64000	223.10000	229.15944	1.17923
31.97000	222.00000	222.68747	.01534
36.71000	211.90000	211.14558	.02026

82.53000	54.27000	53.52241	.30217
90.00000	36.76000	36.24893	.30859
96.03000	25.70000	25.46703	.13250
103.80000	16.78000	16.16202	2.16494
110.55000	13.21000	12.59755	3.44437
116.57000	13.21000	13.11973	.07482
125.27000	20.26000	19.96234	.34064
133.48000	32.21000	32.33282	.02299
140.79000	45.95000	46.97500	.79443
147.21000	58.82000	61.38791	3.05158
153.90000	75.46000	76.51701	.31277
162.14000	92.72000	93.06232	.02177
165.67000	97.70000	98.82336	.21196
166.59000	101.10000	100.15680	.13898

δ_p	δ_0	δ_m	δ_s	ε
-88.800	-88.800	-88.800	-84.600	0.000
66.700	49.400	44.300	21.400	0.000
2.500	2.500	2.500	-18.600	0.000

The initiating of mixing in the P wave as it has been made in works [164,165], allows one to describe better cross sections of the elastic scattering at the same phase shifts [164,165]

$\chi^2 =$ 2.93E-001

θ	σ_e	σ_t	χ^2_i
27.640	223.100	228.038	0.783
31.970	222.000	221.732	0.002
36.710	211.900	210.383	0.082
82.530	54.270	54.215	0.002
90.000	36.760	36.966	0.050
96.030	25.700	26.151	0.497
103.800	16.780	16.739	0.010
110.550	13.210	13.031	0.295
116.570	13.210	13.394	0.310
125.270	20.260	19.972	0.400

133.480	32.210	32.075	0.028
140.790	45.950	46.482	0.214
147.210	58.820	60.704	1.642
153.900	75.460	75.656	0.011
162.140	92.720	92.029	0.089
165.670	97.700	97.733	0.000
166.590	101.100	99.054	0 .654

δ_p	δ_0	δ_m	δ_s	ε
-88.800	-88.800	-88.800	-84.600	0 .000
66.700	49.400	44.300	21.400	11.200
2.500	2.500	2.500	-18.600	0.000

The obtained average χ^2 value is slightly less than value of 0.45, provided in works [164,165]. The calculations [164,165] were carried out at the beginning of the middle 60th years of the last century on rather simple computers and, apparently, at rather not high precision that lead to such small distinction of the results for χ^2.

Besides, in the real calculations, perhaps, several other values of the constants were used, for example, $\hbar^2/m_0$ and the mass of particles, and rounding of [164,165] phase shifts given in articles to the second sign after a comma can also exert impact on the χ^2 value. Therefore, it is quite possible to consider that in the provided control accounts the acceptable χ^2 value consent with the results of works obtained in [164,165].

For the comparison we will give the results at the same scattering phase shifts and mixing parameter, which have been obtained in our previous work [10] for the similar programs in the Turbo Basic language at average $\chi^2 = 0.29$

θ	σ_e	σ_t	χ^2_i
27.64	223.10	228.04	0.78
31.97	222.00	221.73	0.00
36.71	211.90	210.38	0.08
82.53	54.27	54.22	0.00
90.00	36.76	36.97	0.05

96.03	25.70	26.15	0.49
103.80	16.78	16.74	0.01
110.55	13.21	13.03	0.29
116.57	13.21	13.39	0.31
125.27	20.26	19.97	0.32
133.48	32.21	32.07	0.03
140.79	45.95	46.48	0.21
147.21	58.82	60.70	1.64
153.90	75.46	75.66	0.01
162.14	92.72	92.03	0.09
165.67	97.70	97.73	0.00
166.59	101.10	99.05	0.66

Here, the results up to rounding error coincide with each other and do not depend on the programming language.

If to execute a detailed variation of the scattering phase shifts and the mixing parameter ε, then as a result we will obtain about 10000 iterations, that for the best description of the available experimental data requires almost zero mixing

$\chi^2 = 2.25E\text{-}001$

θ	σ_e	σ_t	χ^2_i
27.640	223.100	224.736	0.086
31.970	222.000	221.181	0.022
36.710	211.900	211.217	0.017
82.530	54.270	53.839	0.100
90.000	36.760	36.717	0.002
96.030	25.700	26.025	0.259
103.800	16.780	16.736	0.011
110.550	13.210	13.072	0.175
116.570	13.210	13.423	0.415
125.270	20.260	19.927	0.427
133.480	32.210	31.953	0.101
140.790	45.950	46.328	0.108
147.210	58.820	60.562	1.405
153.900	75.460	75.570	0.003

162.140	92.720	92.043	0.085
165.670	97.700	97.791	0.001
166.590	101.100	99.123	0.611

δ_p	δ_0	δ_m	δ_s	ε
-83.342	-83.342	-83.342	-97.861	0 .000
52.520	50.021	50.444	44.905	-0.00017
3.222	0.122	2.667	-19.114	0.000

Apparently, it is possible to consider that the mixing is not required for the best description of the available experimental data, though the point at 147°, as well as in case of the calculation in the previous program with $\chi^2 = 2.27E\text{-}001$, is described rather badly though χ^2 averages practically coincide. Let us notice that the change of mixing parameter ε to any direction leads to the noticeable raising of an average χ^2, considerably worsening the description of the used experimental data.

The results given in this paragraph directly belong to check of the operability of the computer programs written on the basis of the known methods of calculation of the differential cross sections, but not to obtaining new results on the phase shift analysis of the p^3He elastic scattering [10]. New results for the phase shift analysis in system of particles with the spin 1/2 + 1/2 are given, for example, in the following paragraph for the $p^{13}C$ system.

2.5.3 Phase shift analysis of the $p^{13}C$ elastic scattering taking into account the spin-orbit

Now let us consider the $p^{13}C$ system of the particles at low energies, to which there correspond the 1/2 + 1/2 spins. At the energies lower than 0.5–1 MeV the deviation of the measured differential cross section from the Rutherford value quite can be characterized only by one point at a certain value of scattering angle and the given energy. Such deviation, as it will be shown further, is quite unambiguously described by one triplet *S* scattering phase shift even in the resonance range of the $p^{13}C$ system.

On the basis of these representations in [167,168] the measurement of the differential cross sections, namely, the excitation functions for the $p^{13}C$

elastic scattering has been executed at the energies from 0.25 to 0.75 MeV. The measurements of the cross sections at each energy were taken only at one scattering angle, and for the different energies four values of the angles were used. These data we use further for the carrying out of the phase shift analysis of the $p^{13}C$ elastic scattering at low energies and definitions of the resonance form of the triplet ${}^3S_1$ phase shift at energy range of 0.55 MeV.

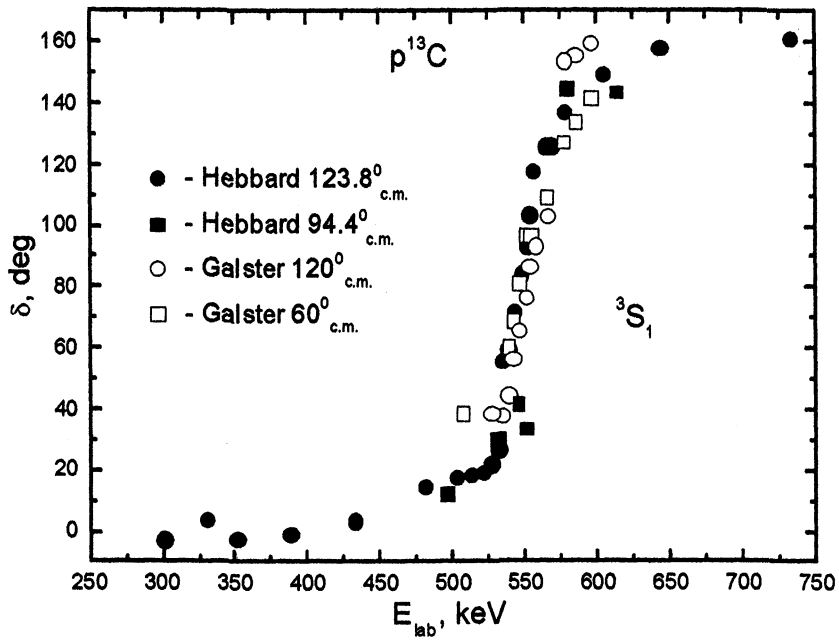

Fig.2.5.1. The triplet ${}^3S_1$ phase shift of the $p^{13}C$ scattering at low energies. Points and squares – the results of our phase shift analysis by data [167] at 94.4° and 123.8° in c.m., circles and open squares – the results of our phase shift analysis by data [168] at 60° and 120° in c.m.

On the basis of the computer programs checked in the previous paragraph with the spin-orbital mixing, the phase shift analysis of the experimental data on differential cross sections of the $p^{13}C$ elastic scattering (excitation functions) in the energy range of 300–750 keV l.s.) specified in works [167,168] has made. As a result of the phase shift analysis it has been shown that the singlet ${}^1S_0$ phase shift of the $p^{13}C$ elastic scattering in the considered energy range was closed to zero – its value did not exceed 2–3 degree. The form of the triplet ${}^3S_1$ phase shift is shown below in Fig. 2.5.1, and its values are given in tab. 2.5.1 and 2.5.2. This phase shift has obviously expressed resonance, which corresponds to the

level of ^{14}N in the cluster p^{13}C channel with $J^{\pi},T = 1^{-},1$ at energy of 0.55 MeV (l.s.) [120].

Furthermore, the results of the phase shift analysis of the experimental data from [167] in the energy range of 301–732 keV and 495–613 keV at two values of the angles, which are presented in Fig. 2.5.1 by black points and squares respectively are given in tab.2.5.1. Tab. 2.5.2 contains the results of the phase shift analysis of experimental data from work [168], which are presented in Fig.2.5.1 by circles (at the energies of 526-595 keV) and open squares (for the energy of 506-595 keV). According to work [167] the extracted elastic scattering phase shift passes through 90° at energy of 551 keV, and for data [168] it occur at 557 keV.

The width of the resonance is in the range of 20–25 keV that will quite be coordinated with the results of work [120], where the value 23(1) keV at the energy of the resonance of 551 keV is given. The resonance width taken from the experimental data for the triplet $^3S_1$ phase shifts has smaller, than in the p^{12}C scattering [115], value, and further its description will require very narrow potential that has to lead us to the width order parameter of β = 2–3 fm^{-2} [169].

Tab. 2.5.1. The results of the phase shift analysis of the p^{13}C elastic scattering at low energies on the experimental data of work [167]. In the analysis only one $^3S_1$ phase shift is considered, the others are considered equal or close to zero.

The $^3S_1$ phase shift is obtained by data [167] at 123.8° (c.m.). The black points in Fig.2.5.1.	
E_{lab}, keV	$^3S_1$, deg
301	-2.6
330	3.7
351	-2.1
388	-0.8
432	3.4
479.8	14.7
502	17.7

512	18.6
520.8	19.5
526	22.1
531.2	26.7
533.7	55.6
538	59.6
542.4	72.1
547.5	84.2
551.2	93.6
553.1	103.6
555.4	117.8
563.9	126.0
566	126.0
568.3	126.0
577.3	137.5
604	149.7
643.3	158.3
732.1	161.2
The $^3S_1$ phase shift is obtained by data [167] at 94.4° (c.m.). The black squares in Fig.2.5.1.	
E_{lab}, keV	$^3S_1$, deg
495	12.6
530	30.4
544.6	41.9
550	33.7
579	145.0
613	144.0

Tab.2.5.2. The results of the phase shift analysis of the $p^{13}C$ elastic scattering at low energies on the experimental data of work [168]. In the analysis only one $^3S_1$ phase shift is considered, the others are

considered equal or close to zero.

The $^3S_1$ phase shift is obtained by data [168] at 120° (c.m.). The circles in Fig.51.	
E_{lab}, keV	$^3S_1$, deg
526	38.7
534	38.0
538	44.4
541	56.5
545	66.0
549.9	76.7
553	87.0
557	93.5
565.1	103.0
576.8	154.0
584.4	155.8
595.3	159.6
The $^3S_1$ phase shift is obtained by data [168] at 60° (c.m.). The open squares in Fig.2.5.1.	
E_{lab}, keV	$^3S_1$, deg
506.4	38.5
537.8	60.7
541.1	69.2
545.4	81.2
549.5	97.0
553.1	97.0
564.7	109.3
576.3	127.6
584.3	134.2
594.9	141.7

However, rather exact extraction on the basis of the carried out phase shift analysis of the triplet S phase shift from the experimental data allows one to hope for the quite unambiguous creation of the potential $p^{13}C$ interactions. The resonance form of the phase shift with so small width of the resonance allows one to avoid, at the creation of potentials, continuous ambiguity, peculiar to optical model [6], because only quite certain width of the potential is capable to describe its resonance form correctly.

Furthermore, the obtained scattering phase shifts are used for the creation of the intercluster interaction potentials [169] and the calculations of the astrophysical S-factor of the proton radiative capture on ^{13}C [170] at astrophysical energies. This process is included into the CNO thermonuclear cycle, and it is its second reaction and gives, apparently, an essential contribution to the energy exit of the thermonuclear reactions [124,170,171] leading to burning of the Sun and stars of our Universe [28,122].

2.5.4. Phase shift analysis of the n^3He elastic scattering

On the basis of the methods described above the phase shift analysis of the known experimental data on the differential cross sections of the elastic n^3He scattering in the range of energies of 1–5 MeV (l.s.) has been carried out [172,173,174]. The results of the first version of the phase shift analysis for the elastic scattering phase shifts are presented in Fig. 2.5.2. At the carrying out of the analysis the χ^2 value was calculated with brought in [172-174] experimental errors of the differential cross sections.

From Fig.2.5.2 it is clear that the S phase shifts of the n^3He process of scattering do not contain the resonances in a full consent with the observed spectra of ^4He [175]. The resonance with $J^\pi,T = 0^-,0$ at 21.01 MeV in c.m. with a neutron width of $\Gamma_n = 0.2$ MeV, which for the $^3P_0$ phase shift is on 0.576 MeV in l.s. higher the threshold of the n^3He channel located at 20.578 MeV [175], is located below the available experimental data given in works [172-174].

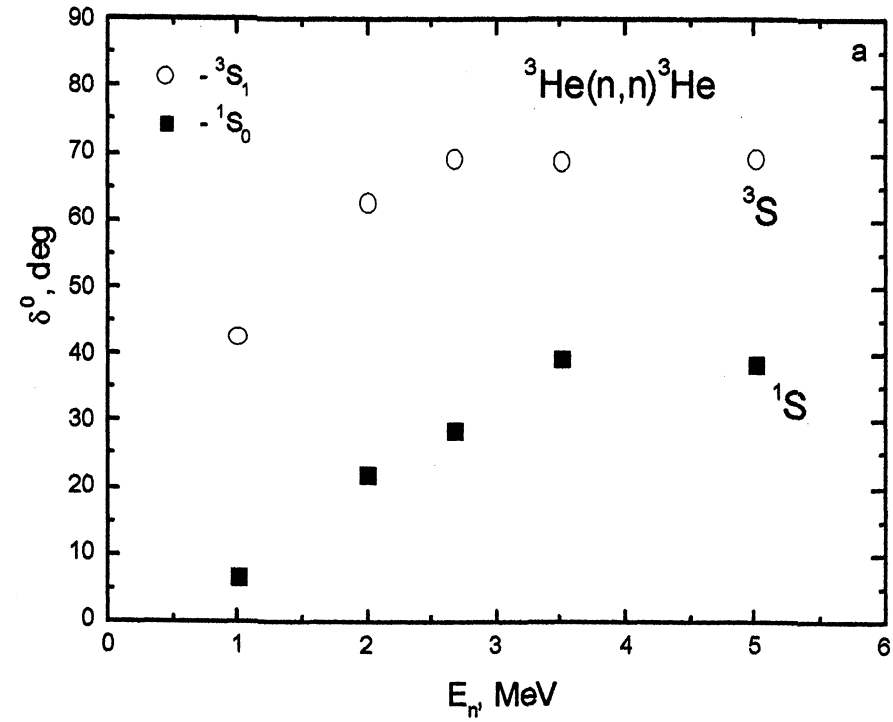

Fig.2.5.2a. Phase shifts of the n^{3}He elastic scattering at low energies.

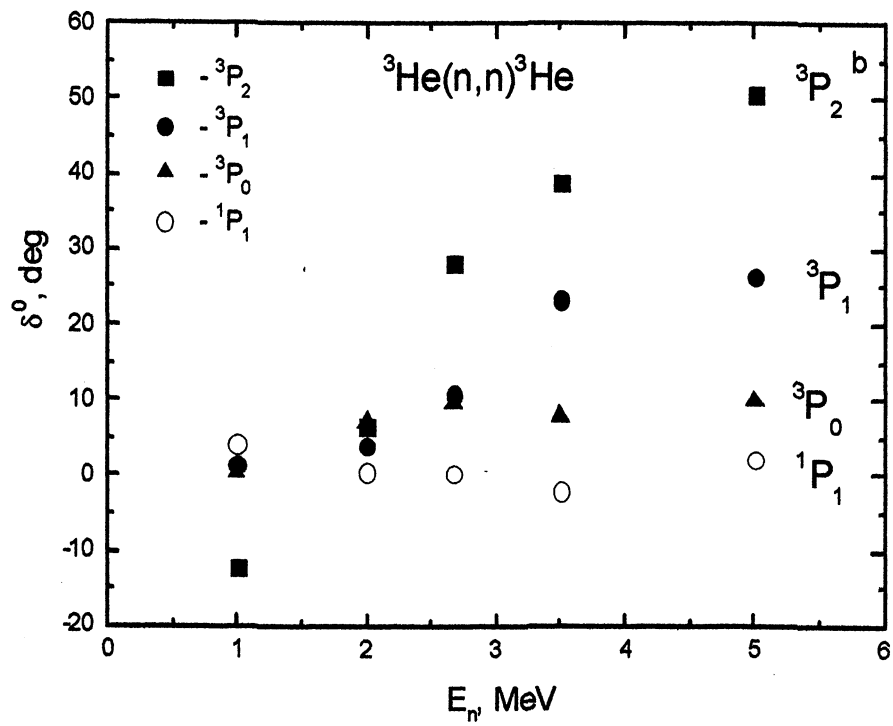

Fig. 2.5.2b. The phase shifts of the n^{3}He elastic scattering at low energies.

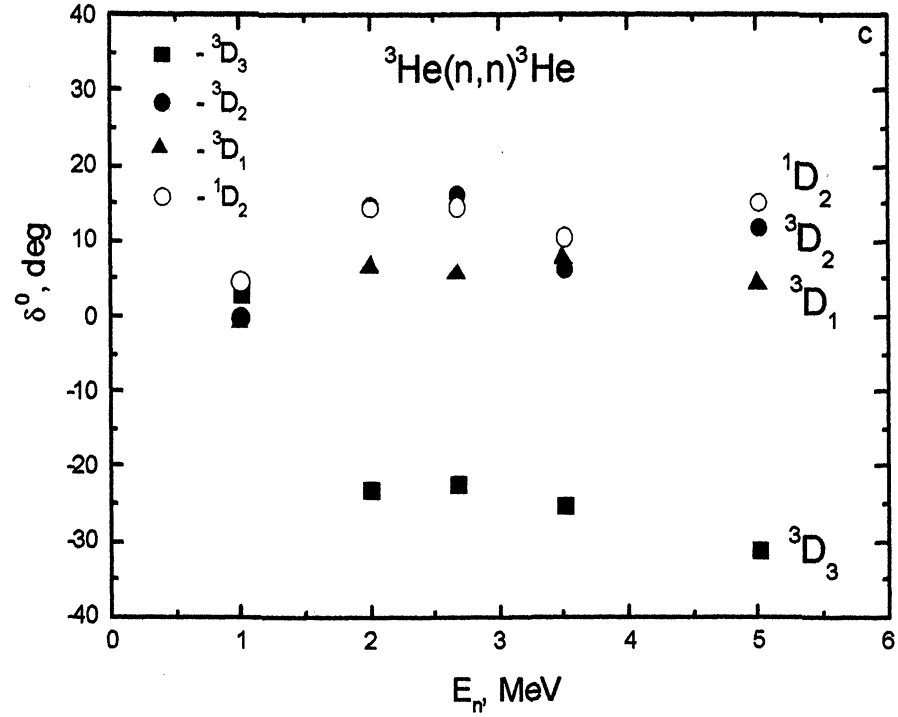

Fig. 2.5.2c. The phase shifts of the n^{3}He elastic scattering at low energies.

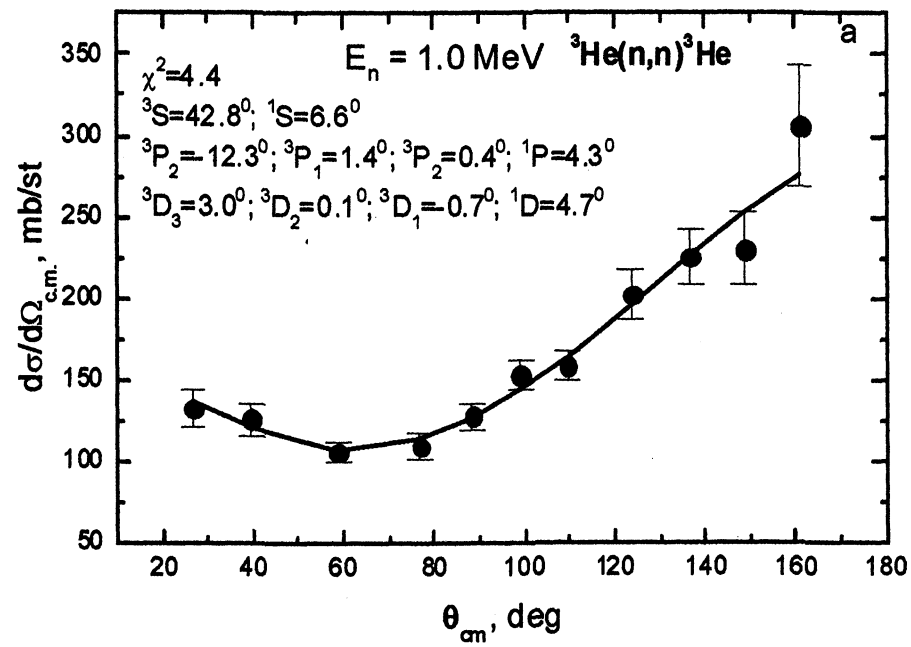

Fig.2.5.3a. The differential cross sections of the n^{3}He elastic scattering. The experimental data of work [172].

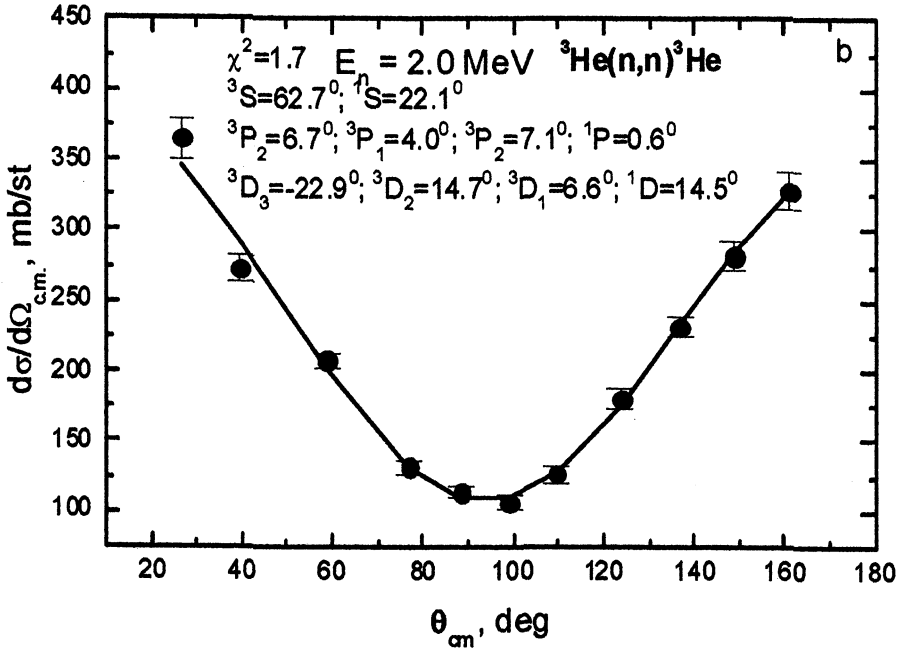

Fig.2.5.3b. The differential cross sections of the n^{3}He elastic scattering. The experimental data of work [172].

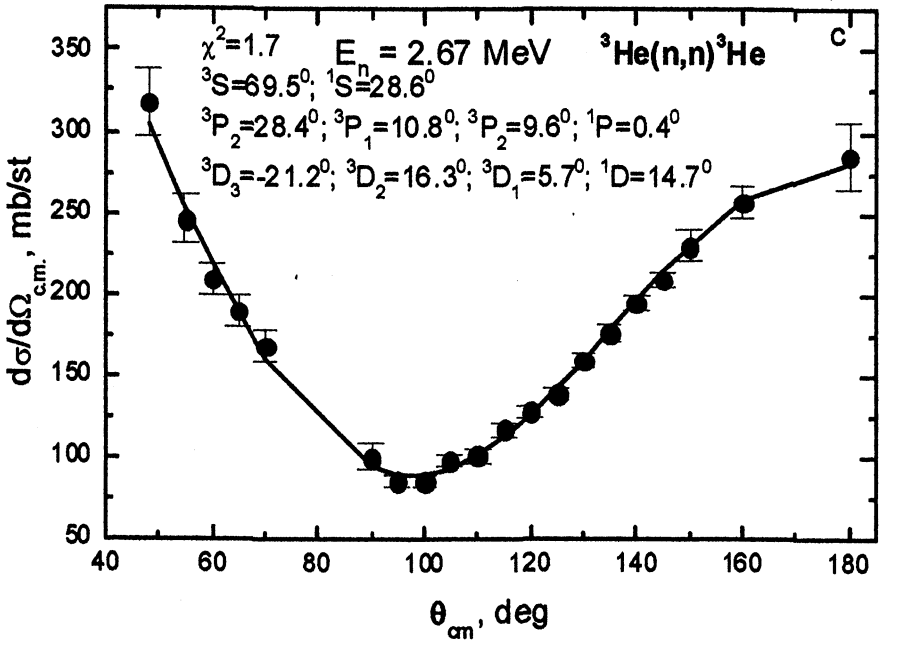

Fig.2.5.3b. The differential cross sections of the n^{3}He elastic scattering. The experimental data of work [173].

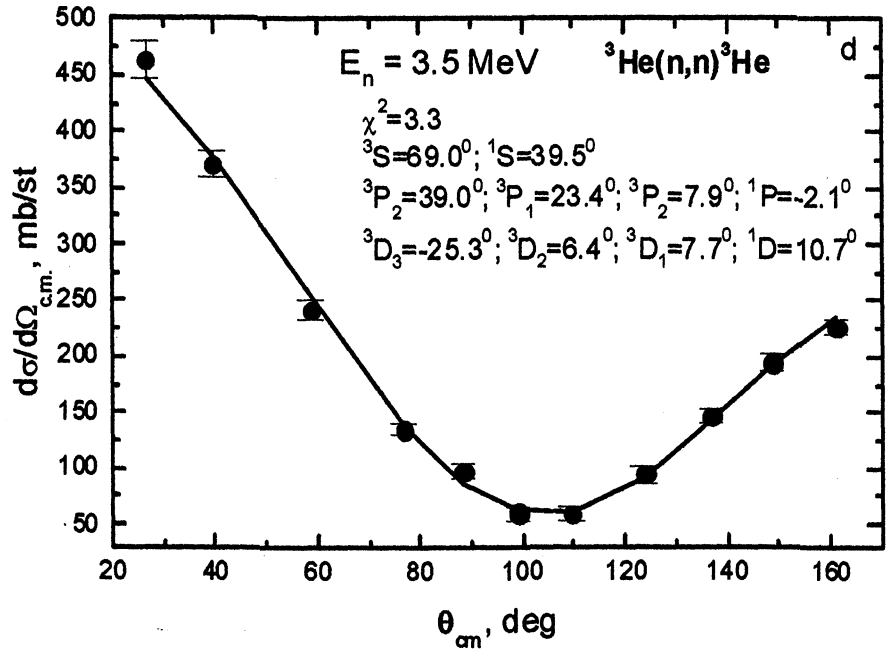

Fig.2.5.3d. The differential cross sections of the n^{3}He elastic scattering. The experimental data of work [172].

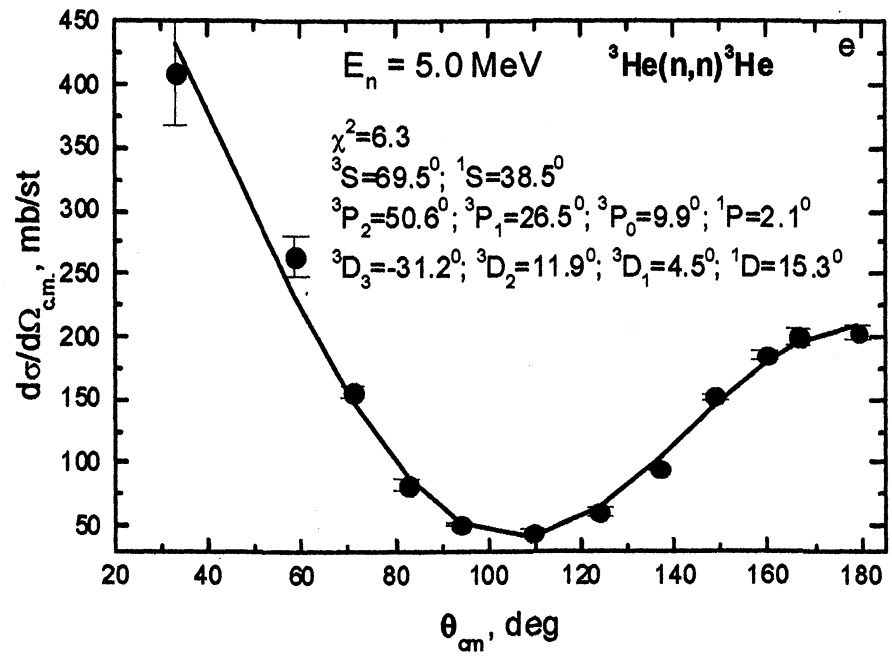

Fig.2.5.3e. The differential cross sections of the n^{3}He elastic scattering. The experimental data of work [174].

In Fig.2.5.3 the differential cross sections have presented by points for

the considered energies from works [172-174], and by the solid curves have shown the cross sections obtained from our phase shift analysis, i.e. calculated with the n^3He scattering phase shifts found here at energies up to 5.0 MeV.

The resonance with $J^\pi,T = 2^-,0$ at 21.84 MeV in c.m. with $\Gamma_n = 0.75$ MeV and $J^\pi,T = 2^-,1$ at 23:33 MeV in c.m. with $\Gamma_n = 2.37$ MeV, which lie in the scattering phase shifts at 1.68 MeV and 3.67 MeV in l.s. are obviously not shown in the $^3P_2$ phase shifts. Finally, two last resonances with 1^-1, and $1^-,0$ at 23.64 MeV with $\Gamma_n = 2.65$ MeV and 24.25 MeV in c.m. with $\Gamma_n = 2.87$ MeV [175] for the $^3P_1$ or $^1P_1$ scattering phase shifts, which have to be at the energies of 4.08 MeV and 4.90 MeV in l.s. are also not shown obviously in the phase shift analysis.

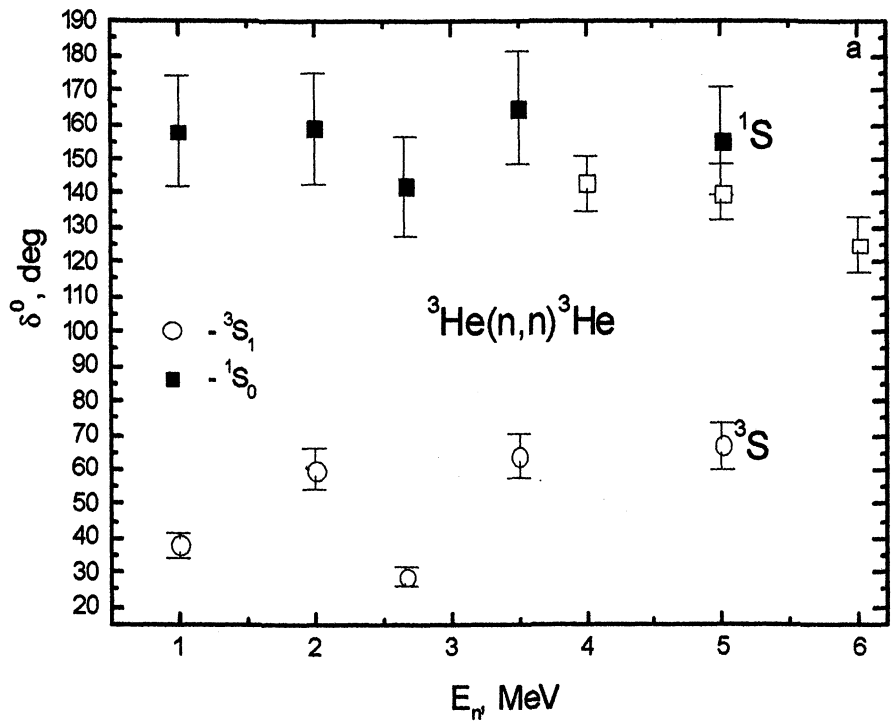

Fig.2.5.4a. The phase shifts of the n^3He elastic scattering at low energies. The points have shown the singlet phase shifts of the p^3H elastic scattering from work [176].

Lack of the obvious resonances in the specified scattering phase shifts for these partial waves can be explained with the fact that their resonance energy lie a little away from the energies considered in this analysis – at these energies the experimental data just are absent. Besides, some of these

resonances have too large width equal, in fact, to a half of resonance energy that also complicates the determination of their location on the available experimental data.

In this version of the phase shift analysis the singlet ^1S phase shift starts from zero, but according to Levinson [4] theorem in the presence of the bound states forbidden or allowed in this partial wave phase shift has to begin with $N\pi$, where N – number of such states. In this case there are two bound states – the ground and the first excited state at energy of 20.21 MeV relative to the ground state. In ^{4}He it lies below a threshold of the n^{3}He channel [175], i.e. in this channel it is bound at energy of -0.37 MeV.

So, the $^1S_0$ phase shift has to begin from 360 degrees – we will call such version of the analysis the second, and its results are presented in Fig. 2.5.4 (the $^1S_0$ phase shift is shown from 180° to place it together with the $^3S_1$ phase shift in one figure) with the differential cross sections shown in Fig.2.5.5. In Fig.2.5.5 the points are still represent the experimental data on the differential cross sections [172-174], and the curves are calculated with the found scattering phase shifts of scattering cross section.

Now the variant of the phase shift analysis taking into account only S and P scattering waves, which appear quite enough for the description of the available differential cross sections at the considered energies is under consideration. Comparing these results to the previous analysis it is possible to see that the accounting of the D wave affects a little the χ^2 value. The error of the obtained scattering phase shifts is estimated approximately at 10%, as shown in Fig.2.5.4a for the singlet ^1S phase shifts that approximately corresponds to an error of the differential cross sections [172-174] used in the analysis.

For the comparison, the open squares in Fig.2.5.4a show the singlet p^{3}H phase shifts of the elastic scattering obtained earlier in work [176]. From these results it is clear, that the singlet ^1S phase shift of the n^{3}He elastic scattering found in this analysis almost coincides with a similar phase shift for the p^{3}H scattering [176,177].

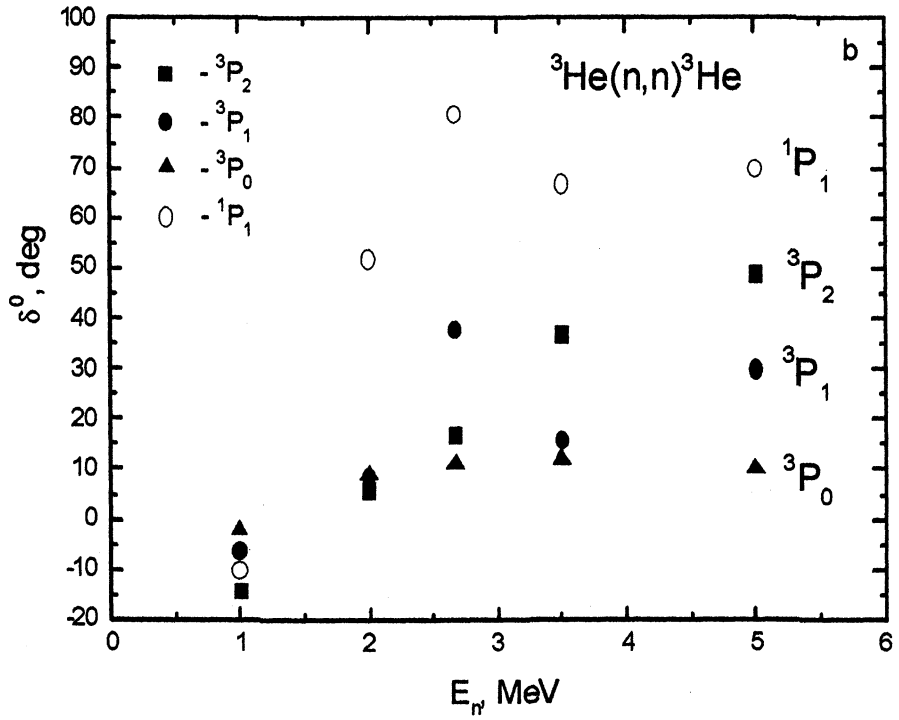

Fig.2.5.4b. The phase shifts of the n^3He elastic scattering at low energies. The singlet p^3H phase shifts of the elastic scattering from work [176] have shown by points.

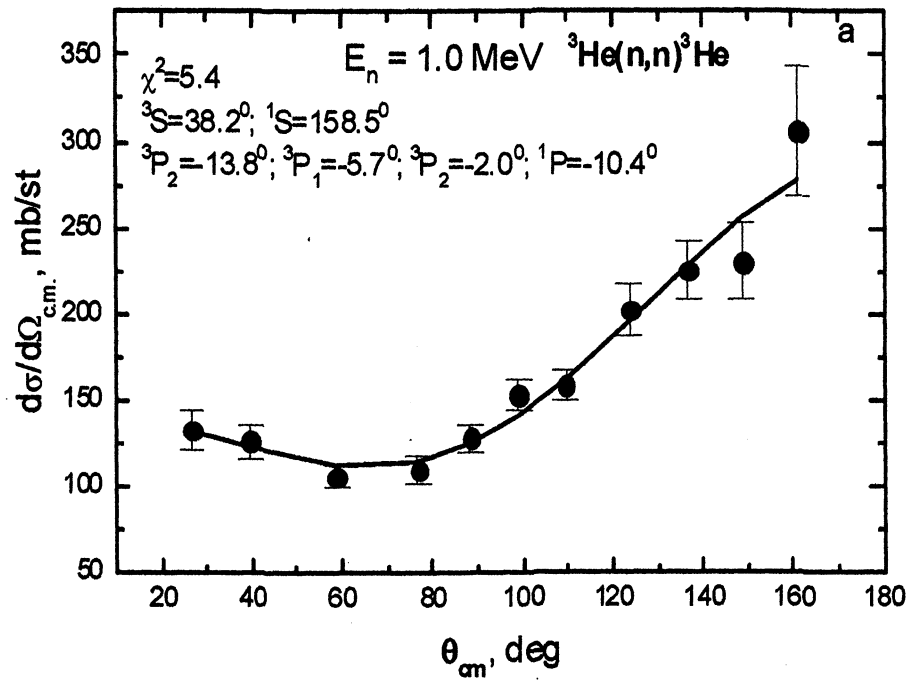

Fig.2.5.5a. The differential cross sections of the n^3He elastic scattering. The experimental data of work [172].

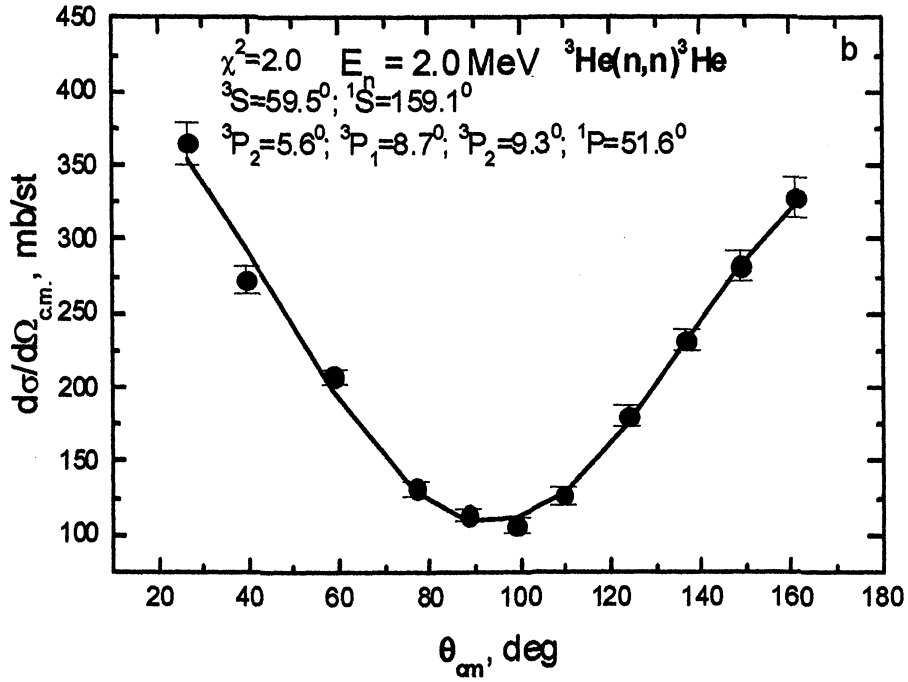

Fig.2.5.5b. The differential cross sections of the n^3He elastic scattering. The experimental data of work [172].

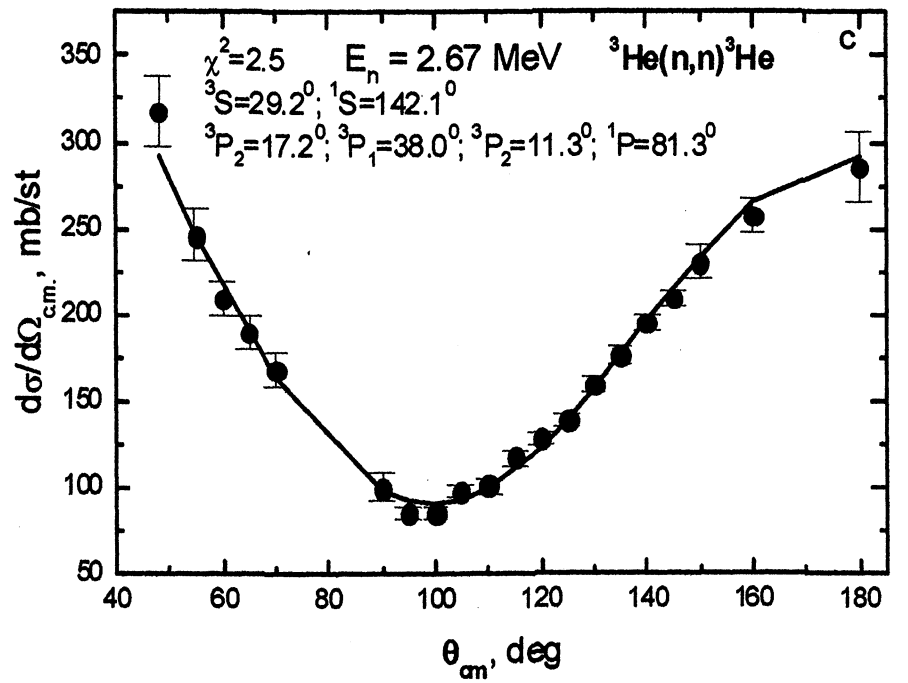

Fig.2.5.5c. The differential cross sections of the n^3He elastic scattering. The experimental data of work [173].

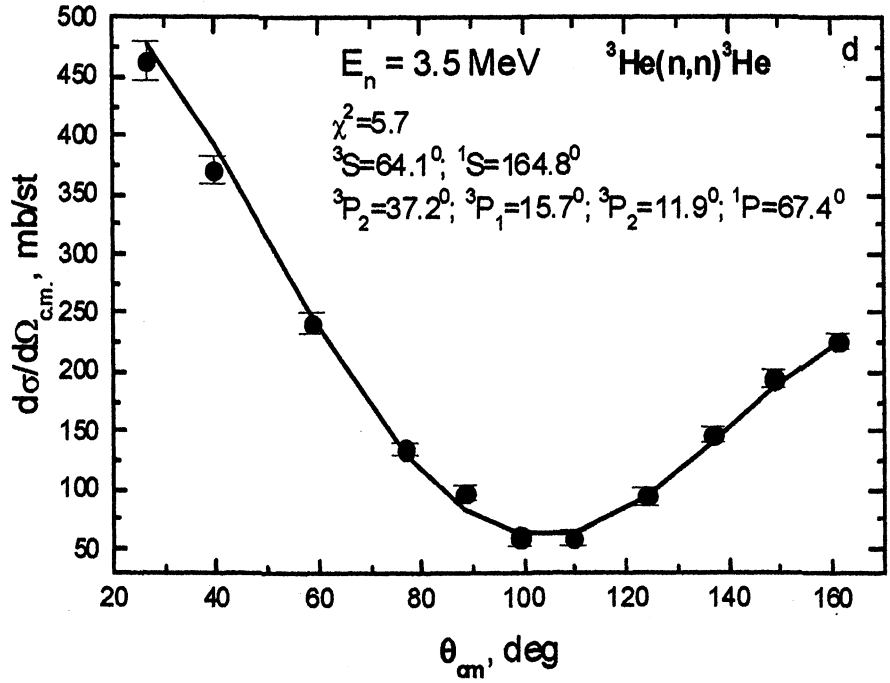

Fig.2.5.5d. The differential cross sections of the n^3He elastic scattering. The experimental data of work [172].

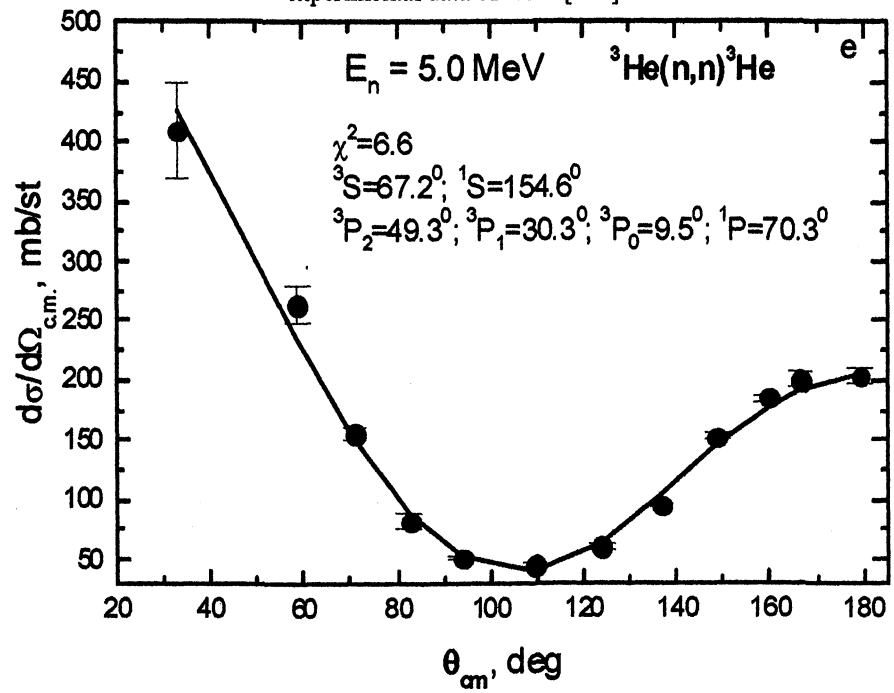

Fig.2.5.5e. The differential cross sections of the n^3He elastic scattering. The experimental data of work [174].

Conclusion

Thus, the used algorithms of the application of the numerical methods for finding of the specific solutions of the general multiparameter variation problem for the functionality of χ^2, which determines the accuracy of the description of the experimental data on the basis of the chosen theoretical representation, allows one to define quite unambiguously scattering phase shifts the of nuclear particles [10]. The used methods and algorithms have allowed to obtain new results for the phase shift analysis in the elastic n^3He, p^6Li, $p^{12}C$, $n^{12}C$, $p^{13}C$, $p^{14}C$, $n^{16}O$, $p^{16}O$, $^4He^4He$ and $^4He^{12}C$ scattering at any low energies, including, astrophysical.

Thus, the scattering phase shifts found in such a way, well describe the experimental cross sections of the elastic scattering, defining, that most, the provision of some low-lying resonance levels of the atomic nuclei considered in these channels. The scattering phase shifts obtained here are applied further for the creation of the intercluster potentials of interaction, which can be used for calculations of the total cross sections of the photonuclear processes and the astrophysical *S*-factors at ultralow or thermal energies [122,178].

REFERENCES

1. Nichitiu F. Phase shift shifts analysis in physics. Romania: Acad. Publ. 1980. 416p.

2. Dubovichenko S.B. Primordial nucleosynthesis of the Universe. Third edition of the book "Selected method for nuclear astrophysics", corrected and added. Germany, Saarbrucken: Lambert Academy Publ. GmbH&Co. KG. 2014. 668p.

3. Nichitiu F. Methods for determining resonances in phase shift shift analysis // Phys. Part. Nucl. 1981. V.12. №4. P.805-847.

4. Nemets O.F., Neudatchin V.G., Rudchik A.T., Smirnov Y.F., Tchuvil'sky Yu.M. Nucleon association in atomic nuclei and the nuclear reactions of the many nucleons transfers. Kiev: Naukova dumka 1988. 488p. (in Russian).

5. Dubovichenko S.B. Partial-wave analysis of elastic ^{4}He^{4}He scattering in the energy range 40-50 MeV // Phys. Atom. Nucl. 2008. V.71. P.65-74.

6. Hodgson, P.E. The Optical model of elastic scattering. Oxford: Clarendon Press 1963. 211p.

7. Marchuk G.I., Kolesov V.E. Application of numerical methods for the calculation of neutron cross-cross sections. M.:Atromizdat 1970. 304p.

8. Structure of atomic nuclei, Ed. Flugge S., Springer – Verlag, Berlin - Gottingen – Heidelberg, 1957.

9. Mott N., Massy H. The theory of atomic collisions, Oxford, Claren Press, 1965.

10. Dubovichenko S.B. Calculation method of the nuclear characteristics. Almaty: Complex 2006. 311p.; arXiv:1006.4947 [nucl-th]. (in Russian).

11. Brown G.E., Jackson A.D. The nucleon - nucleon interaction, North - Holland Pablishing Company, Amsterdam, 1976.

12. Bateman H., Erdeyn A. Math. library. Higher transcendental functions. V.2. M.: Nauka. 1968. 295p. (in Russian).

13. Lebedev N.N. Special functions and their applications. M.: Fiz.-Math. Lit. 1963. 358p. (in Russian).

14. Dubovichenko S.B. The program of calculation of actual nuclear scattering phase shift shifts // Bull. Kaz.GASA. Almaty. 2003. №9/10.

P.220-227.

15. Dubovichenko S.B. The program of calculation of complex nuclear scattering phase shift shifts // Abstracts. Computational and Informational Technologies in Science. Engineering and Education. Kaz.NU Almaty. Kazakhstan. 6 - 10 October. 2004; http://www.ict.nsc.ru/ws/show_abstract.dhtml?ru+110+7834+S.

16. Popov B.A., Tesler G. S. Computer calculation of functions. Kiev: Naukova dumka. 1984. 598p. (in Russian).

17. http://physics.ucsc.edu/~peter/242/numerov.pdf .

18. Dubovichenko S.B. Numerical methods for the solution of the Schrödinger equation // Bull. AGU Fiz.-math. Ser. Almaty. 2004. №9. P.82-87.

19. Filchakov P.F. Numerical and graphical methods of Applied Mathematics. Live: 1870. 792p.

20. Dymarskiy Ya.S. et al. Programmer handbook. L.: 1963. 628p.

21. Polozhiy G.N. Math workshop. M.: Fiz. – math. Literature. 1960. 512p.

22. Danilina N.I. Numerical methods. M.: High School. 1976. 368p.

23. Dubovichenko S.B. Properties of the light nuclei in potential cluster model. Almaty: KazSU. 332p. KazINTI. 1998. №8172 Ka98. (in Russian).

24. Zaguskii V.L. Guide on numerical methods of solution of equations. M.: Fiz.-Mat. Lit. 1960. 215p. (in Russian).

25. Melent'ev P.V. Approximate calculus. M.: Fiz.-Mat. Lit. 1962. 387p. (in Russian).

26. Demidovich B.P., Maron I.F. Foundation of calculus mathematics. M.: Nauka. 1966. 664p. (in Russian).

27. Korn G., Korn T. Mathematical Handbook. New-York: McGraw Hill Book Co. 1968. 832p.

28. Dubovichenko S.B. Thermonuclear processes of the Universe. Second edition, revised and updated. Series "Kazakhstan space research" V.7. Almaty: A-tri 2011. 402p.; arXiv:1012.0877 [nucl-th]. (in Russian).

29. Kukulin V.I., Neudachin V.G., Smirnov Yu.F., El Khovari R. The role of the Pauli principle in the formation of optical potentials // Bull. Acad. Sci. USSR Ser. Fiz. 1974. V.38. P.2123-2128.

30. Voevodin V.V., Kuznetsov Y.A. Reference mathematical library. Matrix and calculations. M .: Fiz.-Math. Lit. 1984. 318p. (in Russian).

31. Dubovichenko S.B., Chechin L.M. Variational methods for solution of the Schrödinger equation // Bull. ASU Fiz.-Math. Ser. 2003. №.2 (8). P.50-58.

32. Brown G.E., Jackson A.D. The nucleon-nucleon interaction. Amsterdam: North-Holland Publ. Co. New York: American Elsevier Publ. Co. 1976. 242p.

33. Dubovichenko S.B., Chechin L.M. Methods for solving of the generalized eigenvalue problem// Bull. Kaz.NPU. ser. phys.-math. Almaty. Kazakhstan. 2003. №1(7). P.110-115.

34. Dubovichenko S.B., Takibaev N.Zh., Chechin L.M Physical Processes in the Far and Near Space. Almaty: Daik-Press 2008. 228p.; arXiv:1012.1705 [nucl-th]. (in Russian).

35. Skornyakov L.A. Reference mathematical library. General algebra. Moscow: Nauka 1990. 591p. (in Russian).

36. Popov B.A., Tesler G. S. Computer calculation of functions. Kiev: Naukova Dumka 1984. 598p. (in Russian).

37. Demidovich B.P., Maron I.F. Foundation of calculus mathematics. Moscow: Nauka 1966. 664p. (in Russian).

38. Dubovichenko S.B., Chechin L.M. Modern methods of programming the actual physical problems // Book: Current problems and challenges of informatization in Kazakhstan. Almaty. Kazakhstan. 2004. P.358-390.

39. Janke - Emde - Losch. Tafeln hoherer funktionen, Stuttgard, 1960.

40. Luke Yu.L. Mathematical functions and their approximations. New York: Academic Press. 1975. 568p.

41. Melkanoff M. A fortran program for elastic scattering analysis with nuclear optical model // Univ. California Pres., Berkley, Los Angeles, 1961, 116p.

42. Lutz H.F., Karvelis M.D. Numerical calculation of coulomb wave functions for repulsive coulomb fields // Nucl. Phys., 1963, V.43, P.31-44.

43. Melkanoff M. Nuclear optical model calculations. // Meth. in Comput. Phys., Acad. press, N-Y, 1966, V.6, P.1-80.

44. Gody W.J., Hillstrom K.E. Chebyshev approximations for the coulomb phase shift shifts // Meth. Comput., 1970, V.111, P.671-677.

45. Smith W.R. Nuclear penetrability and phase shift shift subroutine // Usics Communs., 1969, V.1, P.106-112.

46. Froberg C.E. Numerical treatment of Coulomb wave functions // Rev. Mod. Phys., 1955, V.27, P.399-411.

47. Abramowitz M. Tables of Coulomb wave function, v.1, Washington, N.B.S., 1952, 141p.

48. Barnet A., et al. Coulomb wave function for all real η and ρ // Comput. Phys. Comm., 1974, V.8, P.377-395.

49. Danilov V. L. et al. Reference mathematical library. Mathematical analysis. Functions, limits and continued fractions. M.: Fiz.-Mat. Lit. 1961. 439p. (in Russian).

50. Kuznetsov D. S. Special functions. M.: Graduate School. 1965. 272p. (in Russian).

51. Dubovichenko S.B., Chechin L.M. Calculating methods of the Coulomb functions and scattering phase shift shifts // Bull. KazNPU. ser. phys.-math. Almaty. 2003. №1(7). P.115-122.

52. Handbook of mathematical functions. Edit. M. Abramowitz and I. Stegun. NBS., 1964.

53. Dubovichenko S.B., Zhusupov M.A. On calculation of the Coulomb wave functions // Interaction of radiative with matter. Alma-Ata. KazSU. 1980. P.99-104.

54. Dubovichenko S.B., Zhusupov M.A. The computation of Coulomb scattering phase shift shifts // Bull. Acad. Sci. KazSSR ser. phys.-math. 1981. № 6. P.24-26.

55. Reid R.V. Local phenomenological nucleon - nucleon potentials // Ann. Phys. 1968. V.50. P.411-448.

56. Dubovichenko S.B., Mazhitov M. Variation calculations of the ^{6,7}Li nuclei in cluster models with forbidden states // Bull. Acad. Sci. KazSSR ser. phys.-math. 1987. №4. P.55-64.

57. Neudatchin V.G., Kukulin V.I., Boyarkina A.N., Korennoy V.P. A microscopic substantiated optical potential for αt system including nucleon exchange // Lett. Nuovo Cim., 1972, V.5, P.834-838.

58. Neudatchin V.G., Kukulin V.I., Korotkikh V.L., Korennoy V.P. A microscopically substantiated local optical potential for $\alpha\alpha$ scattering // Phys. Lett., 1971, V.34B, P.581-583.

59. Kurdyumov I.V., Neudatchin V.G., Smirnov Y.F., Korennoy V.P. The high energy limit for the αd form factors in the ^{6}Li nuclei // Phys. Lett., 1972, V.40B, P.607-610.

60. Neudachin V.G., Smirnov Yu.F. Forbidden states in systems of two and three composite particles // Modern problems of optics and atomic physics. Kiev: Kiev State University. 1974. P.225-241.

61. Dubovichenko S.B., Dzhazairov-Kakhramanov A.V. Calculation of coulomb form factors of lithium nuclei in a cluster model based on potentials with forbidden states // Phys. Atom. Nucl. 1994. V.57. P.733-740.

62. Van Niftrik G., Brokman K., Van Oers W. Elastic scattering of 51 MeV alpha particles from helium // Congr. Int. Phys. Nucl. Patis. 1964, V.2, P.858-860.

63. Mukhamedzhanov A.M., Tribble R. E. Connection between asymptotic normalization coefficients, sub threshold bound states, and resonances // Phys. Rev. 1999. V.C59. P.3418-3424.

64. Angulo C. et al. A compilation of charged-particle induced thermonuclear reaction rates // Nucl. Phys. 1999. V.A656. P.3-183.

65. Plattner G.R., Viollier R.D. Coupling constants of commonly used nuclear probes // Nucl. Phys. 1981. V.A365. P.8-12.

66. Blokhintsev L.D., Borbey I., Dolinsky E.I. Nuclear vertex constants // Phys. Part. Nucl. 1977. V.8. P.1189-1245.

67. Kukulin V.I., Vorontchev V.T., Pomerantsev V.N Three body calculation of A=9 nuclei with super-symmetric $\alpha\alpha$ potential // Few Body Syst. 1995. V.1. P.191-202.

68. Voronchev V.T. et al. The study of the structure and properties of nuclei with A = 9 in the framework of multi-cluster dynamic model $2\alpha + N$ // Phys. Atom. Nucl. 1994. V.57. P.1964-1980.

69. Kukulin V.I. et al. Detailed study of the cluster structure of light nuclei in a three body model. I. Ground state of ^{6}Li // Nucl. Phys. 1984. V.A417. P.128-156.

70. Kukulin V.I. et al. Detailed study of the cluster structure of light nuclei in a three body model. II. The spectrum of low lying of nuclei with A=6 // Nucl. Phys. 1986. V.A453. P.365-388.

71. Kukulin V.I. et al. Detailed study of the cluster structure of light nuclei in a three body model. III. Electromagnetic structure of ^{6}Li // Nucl. Phys. 1990. V.A517. P.221-263.

72. Varshalovich D.A., Moskaliev A.N., Khersonsky V.K. Quantum theory of angular momentum. L.: Nauka 1973. 436p.

73. Dubovichenko S.B. Variational methods in the three-body model //

Bull. Kaz.GASA. Almaty. Kazakhstan. 2003. №9(10). P.227-232.

74. Dubovichenko S.B. A computer program for calculating the characteristics of the nucleus ^{7}Li // Bull. Kaz.NTU. Almaty. Kazakhstan. 2004. №5. P.174-182.

75. http://physics.nist.gov/cgi-bin/cuu/Value?mud|search_for =atomnuc!

76. Juster F.P. et al. Tritium electromagnetic form factors // Phys. Rev. Lett. 1985. V.55. P.2261-2264.

77. Beck D.H. et al. Tritium form factors at low q // Phys. Rev. 1984. V.C30. P.1403-1408.

78. Sick I. Precise nuclear radii from electron scattering // Phys. Lett. 1982. V.B116. P.212-214.

79. Dubovichenko S.B., Uzikov Yu.N. Astrophysical *S*-factors of reactions with light nuclei // Phys. Part. Nucl. 2011. V.42. P.251-301.

80. Dubovichenko S.B. Light nuclei and nuclear astrophysics. Second Edition, corrected and enlarged. Saarbrucken: Lambert Academy Publ. GmbH&Co. KG. 2013. 316p.

81. Afnan I.R., Tang Y.C. Investigation of nuclear three-and four-body systems with soft-core nucleon-nucleon potentials // Phys. Rev. 1968. V.175. P.1337-1345.

82. Krasnopolsky V.M., Kukulin V.I. A new many particle variational method // Czech. J. Phys. 1977. V.B27. P.290-304; Krasnopolsky V.M., Kukulin V.I. A stochastic variational method for few body systems // J. Phys. 1977. V.G3. P.795-811.

83. Dubovichenko S.B. Phase shift analysis of ^{4}He-^{4}He scattering at energies of 40–50 MeV // Rus. Phys. J. 2007. V.50. P.605-611.

84. Heydenberg N.P., Temmer G.M. Alpha-Alpha scattering at low energies // Phys. Rev. 1956. V.104. P.123-134.

85. Russel J.L. et al. Scattering of alpha particles from Helium // Phys. Rev. 1956. V.104. P.135-142.

86. Tombrello T.A., Senhouse L.S. Elastic scattering of Alpha particles from Helium // Phys. Rev. 1963. V.129. P.2252-2258.

87. Nilson R. et al. Alpha-Alpha particle scattering in the energy range 13 to 22.9 MeV // Phys. Rev. 1956. V.104. P.1673-1680.

88. Nilson R. et al. Investigation of excited states in ^{8}Be by α-particle scattering from Helium // Phys. Rev. 1958. V.109. P.850-860.

89. Steigert F.E., Samson M.B. Alpha-Alpha scattering from 12.88 to 21.62 MeV // Phys. Rev. 1953. V.92. P.660-664.

90. Chien W.S., Brown R.E. Study of the $\alpha\alpha$ system below 15 MeV // Phys. Rev. 1970. V.C10. P.1767-1784.

91. Bredin D.J. et al. The scattering of alpha particles by helium // Proc. Roy. Soc. 1959. V.A251. P.143-155.

92. Darriulat P., Igo G., Pugh H.G. Elastic scattering of alpha particles by helium between 53 and 120 MeV // Phys. Rev. 1965. V.137. P.B315-B323.

93. Conzett H.E. et al. Alpha-alpha scattering in the 36.8 to 47.3 MeV // Phys. Rev. 1960. V.117. P.1075-1079.

94. Igo G. Optical model analysis of the scattering of alpha particles from helium // Phys. Rev. 1960. V.117. P.1079-1085.

95. Burcham W.E. et al. Alpha-alpha scattering at 38/5 MeV // Nucl. Phys. 1957. V.3. P.217-220.

96. Burtebaev N. et al. Reprint № 88-01 INP. Alma-Ata. Kazakhstan. 1988. (in Russian)

97. Van Niftrik G. J.C. et al. Elastic scattering of 51 MeV alpha particles from helium // In "Compt. Congr. Int. Phys. Nucl." Paris. 1964. V.2. P.858-860.

98. Dubovichenko S.B. A computer program for the phase shift analysis of the elastic ^{4}He^{4}He // Book: Current problems and challenges of informatization in Kazakhstan. Almaty. Kazakhstan. 2004. P.327-351.

99. Dubovichenko S.B., Burtebayev N., Dzhazairov-Kakhramanov A.V., Zazulin D.M. Phase shift shift analysis and potential description of the elastic ^{4}He^{12}C scattering at low energies // Uz. J. Phys. 2009. V.11. № 2. P.87-94.

100. Jones C.M. et al. The scattering of alpha particles from ^{12}C // Nucl. Phys. 1962. V.37. P.1-9.

101. Dubovichenko S.B. Photonuclear processes in the ^{4}He^{12}C channel of the ^{16}O nucleus in potential cluster models // Phys. Atom. Nucl. 1996. V.59. P.421-427.

102. Plaga R. et al. The scattering of alpha particles from ^{12}C and the ^{12}C(α,γ)^{16}O stellar reaction rate // Nucl. Phys. 1987. V.A465. P.291-316.

103. Tilley D. R., Weller H. R., Cheves C. M. Energy levels of light nuclei A=16,17 // Nucl. Phys. 1993. V.A564. P.1-183.

104. Dubovichenko S.B. et al. Phase shift shifts analysis of elastic $^4He^{12}C$ scattering at energies 1.5-6.5 MeV // Dokl. Nat. Acad. Sci. Rep. Kazakhstan. 2008. №6. P.24-32.

105. Dubovichenko S.B. et al. Phase shift shifts analysis and potential description of elastic $^4He^{12}C$ scattering at low energies // Rus. Phys. J. 2009. V.52. P.715-724.

106. Dubovichenko S.B., Dzhazairov-Kakhramanov A.V. Astrophysical *S*-factor of the radiative $^4He^{12}C$ capture reaction at low energies // Bull. Russian Academy of Sciences: Physics. 2011. V.75. P.1517-1522; Dubovichenko S.B., Dzhazairov-Kakhramanov A.V. Astrophysical *S*-factor of the $^4He^{12}C$ radiative captures at low energies // Uz. J. Phys. 2009. V.11. №4. P.239-246; Dubovichenko S.B., Dzhazairov-Kakhramanov A.V. Astrophysical *S*-factor $^4He^{12}C$ radiative capture at low energies // Dokl. Nat. Acad. Sci. Rep. Kazakhstan. 2009. №2. P.9-15.

107. Salpeter E.E. Nuclear reactions in stars // Phys. Rev. 1957. V.107. P.516-525; Salpeter E.E. Nuclear Reactions in stars without hydrogen // Astrophys. Jour. 1952. V.115. P.326; Rolfs C. Nuclear reactions in stars far below the Coulomb barrier // Prog. Part. Nucl. Phys. 2007. V.59. P.43-50.

108. Dubovichenko S.B. Program for seek of phase shift shifts elastic scattering for particles with spin 1/2 // Bull. Kaz.NTU. Almaty. Kazakhstan. 204. №3. P.137-144.

109. Dubovichenko S.B. Phase shift shifts analysis of the differential cross cross section for elastic $p^{12}C$ scattering at astrophysical energies // Bull. Nat. Acad. Sci. Rep. Kazakhstan. ser. phys.-math. 2007. №6. P.58-67.

110. Jahns M.F., Bernstein E.M. Polarization in pα scattering // Phys. Rev. 1967. V.162. P.871-877.

111. Barnard A., Jones C., Well J. Elastic scattering of 2-11 MeV proton by ^4He // Nucl. Phys. 1964. V.50. P.604-620.

112. Brown R.I., Haeberli W., Saladin J.X. Polarization in the scattering of protons by α particles // Nucl. Phys. 1963. V.47. P.212-213.

113. Jackson H.L. et al. The $^{12}C(p,p)^{12}C$ differential cross cross section // Phys. Rev. 1953. V.89. P.365-269.

114. Jackson H.L. et al. The excited states of the ^{13}N nucleus // Phys. Rev. 1953. V.89. P.370-374.

115. Dubovichenko S.B. Phase shift anlysis of elastic $p^{12}C$ scattering for astrophysical energies // Rus. Phys. J. 2008. V.51. P.1136-1143.

116. Zazulin D.M. et al. Scattering of protons from ^{12}C // The 6th Int. Conf. "Modern Problems of Nuclear Physics" Tashkent. Uzbekistan. 2006. P.127; Baktybaev M.K. et al. Elastic scattering of protons from ^{12}C, ^{16}O and ^{27}Al // The 4th Eurasia Conf. "Nucl. Sci. and its Appl." Baku. Azerbaijan. 2006. P.56.

117. Moss S.J., Haeberli W. The polarization of protons scattered by Carbon // Nucl. Phys. 1965. V.72. P.417-435.

118. Barnard A.C.L. et al. Cross cross section as a function of angle and complex phase shift shifts for the scattering of protons from ^{12}C // Nucl. Phys. 1966. V.86. P.130-144.

119. Lane R.O. et al. The Angular Distributions of Neutrons Scattered from Various Nuclei // Ann. Phys. 1961. V.12. P.135.

120. Ajzenberg-Selove F. Energy level of light nuclei A=13,14,15 // Nucl. Phys. 1991. V.A523. P.1-196.

121. Heil M. et al. The (n,γ) cross cross section of ^{7}Li // Astrophys. Jour. 1998. V.507. P.997-1002; Guimaraes V. and Bertulani C.A. Light radioactive nuclei capture reactions with phenomenological potential models // arXiv:0912.0221v1 [nucl-th] 1 Dec 2009; Masayuki Igashira, Toshiro Ohsaki Neutron capture nucleosynthesis in the Universe // Sci. Tech. Adv. Materials 2004. V.5. P.567-573; Nagai Y. et al. Fast neutron capture reactions in nuclear astrophysics // Hyperfine Interactions 1996. V.103. P.43-48; Liu Z.H. et al. Asymptotic normalization coefficients and neutron halo of the excited states in ^{12}B and ^{13}C // Phys. Rev. 2001. V.C64. P.034312(1-5); Horvath A. et al. Cross cross section for the astrophysical $^{14}C(n,\gamma)^{15}C$ reaction via the inverse reaction // Astrophys. Jour. 2002. V.570. P.926-933.

122. Dubovichenko S.B. Thermonuclear processes of the Universe. Almaty: APHI 2010. 339p.; http://nuclphys.sinp.msu.ru/thpu/index.html. (in Russian).

123. Dubovichenko S.B. Thermonuclear Processes of the Universe. First English edition. New-York: NOVA Sci. Publ. 2012. 194p.; https://www.novapublishers.com/catalog/product_info.php?products_id=31125.

124. Adelberger E.G. et al. Solar fusion cross cross sections. II. The pp chain and CNO cycles // Rev. Mod. Phys. 2011. V.83. P.195-245.

125. Dubovichenko S.B., Dzhazairov-Kakhramanov A.V. Astrophysical *S*-factor for $p^{12}C \rightarrow {}^{13}N\gamma$ radiative capture // Rus. Phys. J. 2009. V.52.

P.833-840.

126. Henderson J.D. et al. Capture and elastic scattering of proton be ^{14}C // Phys. Rev. 1968. V.172. P.1058-1062.

127. Bartholomew G.A. et al. Capture radiative and neutrons from the bombardment of ^{14}C with protons // Can. Jour. Phys. 1955. V. 33(8). P.441-456; Bartholomew G.A. et al. Note on the T = 3/2 State in ^{15}N // Can. Jour. Phys. 1956. V. 34. P.147.

128. Dubovichenko S.B. Neutron Capture by Light Nuclei at Astrophysical Energies // Phys. Part. Nucl. 2013. V.44. P.803-847; Dubovichenko S.B., Dzhazairov-Kakhramanov A.V., Burkova N.A. Neutron radiative capture by ^{2}H, ^{6}Li, ^{7}Li, ^{12}C and ^{13}C at astrophysical energies // Int. J. Mod. Phys. 2013. V.E22. P.1350028(1-52); Dubovichenko S.B., Dzhazairov-Kakhramanov A.V., Afanasyeva N.V. Neutron radiative capture by ^{9}Be, ^{14}C, ^{14}N, ^{15}N and ^{16}O at astrophysical energies // Int. J. Mod. Phys. 2013. V.E22. P.1350075(1-53); Dubovichenko S.B., Dzhazairov-Kakhramanov A.V. Neutron radiative capture by ^{2}H, ^{6}Li, ^{7}Li, ^{12}C, ^{13}C, ^{14}C and ^{14}N at astrophysical energies // Book: The Universe Evolution. Astrophysical and Nuclear Aspects. New-York, NOVA Sci. Publ. 2013. P.49-108.

129. Dubovichenko S.B., Dzhazairov-Kakhramanov A.V. Astrophysical *S*-factors of radiative capture of protons on ^{2}H, ^{3}H, ^{6}Li and ^{12}C nuclei // Int. J. Mod. Phys. 2012. V.E21. P.1250039(1-44).

130. Itzykson C., Nauenberg M. Unitary groups: Representations and decompositions // Rev. Mod. Phys. 1966. V. 38. P. 95-101.

131. Dubovichenko S.B. Light nuclei and nuclear astrophysics. Second Edition, corrected and enlarged. Germany, Saarbrucken: Lambert Academy Publ. GmbH&Co. KG. 2013. 320p.

132. Dubovichenko S.B. Dzhazairov-Kakhramanov A.V. Astrophysical *S*-factor of the radiative $p^{2}H$ capture // Euro. Phys. J. 2009. V.A39. P.139-143; Dubovichenko S.B., Dzhazairov-Kakhramanov A.V. The $^{7}Li(n,\gamma)^{8}Li$ radiative capture at astrophysical energies // Ann. der Phys. 2012. V.524. P.850-861.

133. Dubovichenko S.B., Dzhazairov-Kakhramanov A.V. Phase shift shifts analysis of $p^{14}C$ scattering at energy $^{2}S_{1/2}$ resonance // Rus. Phys. J. 2015. V.58. №9. P.1258-1264

134. Igashira M. et al. Measurement of the $^{16}O(n,\gamma)^{17}O$ reaction cross

cross section at stellar energies and critical role of nonresonance P-wave neutron capture // Astrophys. Jour. 1995. V.441. P.L89-L92; Igashira M., Kitazawa H. and Takaura K. Valence-neutron capture in the 434 keV $P_{3/2}$-wave resonance of ^{16}O // Nucl. Phys. 1992. V.A536. P.285-296.

135. Hickey G. T. et al. R-matrix and Phase shift-Shift analyses of neutron polarization measurements from $n^{16}O$ scattering // Nucl. Phys. 1974. V.A225. P.470-480.

136. Johnson C. H., Fowler J. L. Scattering of neutrons from ^{16}O in the 2.2- to 4.2-MeV energy range // Phys. Rev. 1967. V.162. P.890-899.

137. Fowler J.L., Cohn H.O. Oxygen differential neutron scattering and phenomenological nuclear potentials // Phys. Rev. 1958. V.109. P.89-93.

138. Okazaki A. Scattering of polarized neutrons by heavy nuclei // Phys. Rev. 1955. V.99. P.55-58.

139. Schouky I. Untersuchung der niveaustruktur von ^{17}O und ^{29}Si im bereich zwischen neutronenbindungsenergie und 12 MeV anregungsenergie // KFK-2503. 7708.

140. http://www-nds.iaea.org/exfor/exfor.htm .

141. Dubovichenko S.B. Calculation method of the nuclear characteristics. Nuclear and thermonuclear processes. Second edition, revised and updated. Germany, Saarbrucken: Lambert Acad. Publ. GmbH&Co. KG. 2012. 425p.; https://www.lap-publishing.com/catalog/details //store/ru/book/978-3-659-21137-9/metody-rascheta-yadernyh-kharacteristic. (in Russian).

142. Huang J.T., Bertulani C.A., Guimaraes V. Radiative capture of protons and neutrons at astrophysical energies and potential models // Atom. Data and Nucl. Data Tabl. 2010. V.96. P.824-847.

143. http://cdfe.sinp.msu.ru/cgi-bin/muh/radchartnucl.cgi?zmin=0&zmax=14&tdata=123456 .

144. Salisbury S.R. and Richards H.T. ^{17}F Level Parameters // Phys. Rev. 1962. V.126. P.2147-2158.

145. Henry R.R., Philips G.C., Reich C.W., and Russell J.L. Elastic scattering of proton by Oxygen in the energy region of 2.5 to 5/6 MeV // Bull. Amer. Phys. Soc. 1956. V.1. P.96.

146. Salisbury S., Hardie G., Oppliger L., and Bangle R. Proton-Oxygen Differential Scattering Cross Cross sections // Phys. Rev. 1962. V.126. P.2143-2146.

147. Blue R.A. and Haeberli W. Polarization of Protons Elastically

Scattered by Oxygen // Phys. Rev. 1965. V.137. №2B. P.B284-B293.

148. Gomes V., Douglas R.A., Polga T. and Sala O. The E_p = 2.66 MeV resonance in $^{16}O(p,p)^{16}O$ // Nucl. Phys. 1965. V.A68.P.417-425.

149. Trachslin W. and Brown L. Polarization and phase shift shifts in $^{12}C(p,p)^{12}C$ and $^{16}O(p,p)^{16}O$ from 1.5 and 3 MeV // Nucl. Phys. 1967. V.A101. P.273-287.

150. Amirikas R., Jamieson D.N. and Dooley S.P. Measurement of (p,p) elastic cross cross sections for C, O and Si in the energy range 1.0-3.5 MeV // Nucl. Instr. Meth. in Phys. Res. 1993. V.B77. P.110-116.

151. Gurbich A.F. Evaluation of non-Rutherford proton elastic scattering for oxygen // Nucl. Instr. Meth. in Phys. Res. 1997. V.B129. P.311-316.

152. Braun M., Fried T. Elastic backscattering cross cross section of proton on Oxygen // Z. Phys. 1983. V.A311. P.173-175.

153. Ramos A.R. et al. Measurement of (p,p) elastic differential cross-cross sections for carbon, nitrogen, oxygen, aluminium and silicon in the 500–2500 keV range at 140_ and 178_ laboratory scattering angles // Nucl. Instr. Meth. in Phys. Res. 2002. V.B190. P.95-99.

154. Chow H.C., Griffithsa G.M., Hall T.H. The $^{16}O(p,\gamma)^{17}F$ Direct Capture Cross Cross section with an Extrapolation to Astrophysical Energies // Can. Jour. Phys. 1975. V.53. P.1672-1687.

155. Luomajarvi M., Rauhala E. and Hautala M. Oxygen detection by non - Rutherford proton backscattering below 2.5 MeV // MIN 1985. V.B9. P.255-258.

156. Morlock R. et al. Halo Properties of the First $1/2^+$ State in ^{17}F from the $^{16}O(p, \gamma)^{17}F$ Reaction // Phys. Rev.Lett. 1997. V.79. P.3837-3840.

157. Burtebayev N.T., Dubovichenko S.B., Zazulin D.M., Dzhazairov-Kakhramanov A.V., Kerimkulov Zh.K., Nassurlla M., Mukhamejanov Y.S., Omarov Ch.T., Tkackenko A.S., Shmygaleva T.A. New measuremrnts and phase shift analysis of elastic $p^{16}O$-scattering at astrophysical energies // In press.

158. Dubovichenko S.B. et al. Astrophysical *S*-factor of radiative p^6Li capture at low energies // Rus. Phys. J. 2010. V.53. P.743-749; Dubovichenko S.B. Astrophysical *S*-factor radiative p^6Li capture // Dokl. Nat. Acad. Sci. Rep. Kazakhstan. 2009. №6. P.41-45.

159. Petitjean C., Brown L., Seyler R. Polarization and phase shift shifts in $^6Li(p,p)^6Li$ from 0.5 to 5.6 MeV // Nucl. Phys. 1969. V.A129.

P.209-219.

160. Baktybaev M.K. et al. The scattering of protons from ^{6}Li and ^{7}Li nuclei // The 4th Eurasia Conf. "Nucl. Sci. and its Appl." Baku. Azerbaijan. 2006. P.62; Burtebaev N. et al. The new experimental data on the elastic scattering of protons from ^{6}Li, ^{7}Li, ^{16}O and ^{27}Al nuclei // The 5th Eurasian Conf. "Nucl. Sci. and its Appl.". Ankara. Turkey. 2008. P.40.

161. Dubovichenko S.B. et al. Astrophysical S factor for the radiative-capture reaction p^{6}Li $\rightarrow$ ^{7}Beγ // Phys. Atom. Nucl. 2011. V.74. P.984-1000.

162. Skill M. et al. Differential cross cross section and analyzing power for elastic scattering of protons on ^{6}Li below 2 MeV // Nucl. Phys. 1995. V.A581. P.93-106.

163. Dubovichenko S.B., Dzhazairov-Kakhramanov A.V. Phase shift analysis of elastic p^{6}Li scattering at astrophysical energies // Rus. Phys. J. 2010. V.53. P.458-464.

164. Tombrello T.A. Phase shift shift analysis for ^{3}He(p,p)^{3}He // Phys. Rev. 1965. V.138. P.B40-B47.

165. Clegg T. et al. The elastic scattering of protons from ^{3}He from 4.5 to 11.5 MeV // Nucl. Phys. 1964. V.50. P.621-628.

166. Tombrello T.A. et al. The scattering of protons from ^{3}He // Nucl. Phys. 1962. V.39. P.541-550.

167. Hebbard D.F., Vogl J.L. Elastic scattering and radiative capture of protons by ^{13}C // Nucl. Phys. 1960. V.21. P.652-675.

168. Galster W. et al. Target and detection techniques for the ^{13}N(p,γ)^{14}O reaction using radioactive ion beams: ^{13}C(p,γ)^{14}N reaction as a test case // Phys. Rev. 1991. V.C44. P.2776-2787.

169. Dubovichenko S.B. Phase shift shifts analysis of the elastic p^{13}C scattering // Phys. Atom. Nucl. 2012. V.75. P.285-290.

170. Dubovichenko S.B. Astrophysical *S*-factor radiative p^{13}C capture // Phys. Atom. Nucl. 2012. V.75. P.173-181.

171. Fowler W.A. Experimental and Theoretical Nuclear Astrophysics: the Quest for the Original of the Elements. Nobel Lecture. Stockholm. 8 Dec. 1983.

172. Seagrave J.D., Cranberg L., Simmons J.E. Elastic Scattering of Fast Neutrons by Tritium and ^{3}He // Phys. Rev. 1960. V.119. P.1981-1991.

173. Sayres A.R., Jones K.W., Wu C.S. Interaction of Neutrons with ^{3}He // Phys. Rev. 1961. V.122. P.1853-1863.

174. Haesner B. et al. Measurements of the ^{3}He and the ^{4}He total neutron cross cross sections up to 40 MeV // Phys. Rev. 1983. V.C28. P.995-999.

175. Tilley D.R., Weller H.R., Hale G.M. Energy levels of light nuclei A=4 // Nucl. Phys. 1992. V.A541. P.1-157.

176. Kankowsky R. et al. Elastic scattering of polarized protons on tritons between 4 and 12 MeV // Nucl. Phys. 1976. V.A263. P.29-46.

177. Dubovichenko S.B., Omarov Ch.T. Phase shift shifts analysis of n^{3}He elastic scattering // Rus. Phys. J. 2016. V.59. P.884-891.

178. Dubovichenko S.B. Astrophysical S factors of radiative ^{3}He^{4}He, ^{3}H^{4}He, and ^{2}H^{4}He capture // Phys. Atom. Nucl. 2010. V.73. P.1517-1522; Dubovichenko S.B. Astrophysical *S*-factor of the p^{7}Li $\rightarrow$ ^{8}Beγ capture at low energies // Rus. Phys. J. 2010. V.53. P.1254-1263; Dubovichenko S.B. Astrophysical *S*-factor of the p^{9}Be $\rightarrow$ ^{10}Bγ radiative capture // Rus. Phys. J. 2011. V.54. P.814-821.

AUTHOR INFORMATION

Dubovichenko Sergey Borisovich - Laureate of the al-Farabi State Prize of the Republic of Kazakhstan (RK) in the field of science and technology; doctor of physical and mathematical sciences (on specialties 01.04.16 - physics of an atomic nucleus and elementary particles and 05.13.18 - mathematical modeling, numerical methods and complexes of programs) in the RK and the Russian Federation (RF), professor RK;

vice-president and academician of the European Academy of Natural Sciences (EU), academician of the Peter's Academy of Sciences and Arts (RF), academician of the Russian Academy of Natural History (RF), academician of the International Academy of Informatization (RK), academician of the New York Academy of Sciences (US);

member of the International Astronomical Union (IAU); member of the American Physical Society (US), member of the European Physical Society (EU);

laureate of the European Gold Medal, Gauss Medal and Honorary Cross "Merit";

laureate of the State Scientific Stipend of RK, laureate of the International Soros Grant, laureate of the Komsomol Prize of Kaz.SSR 1984 (in former USSR);

chief of Kazakhstan department (www.eans.kz) of European Academy of Natural sciences (www.eanw.org) in the field of physics and astrophysics;

head of the laboratory "Nuclear astrophysics" at Fesenkov Astrophysical Institute of the National Center of Space Researches and Technologies of Aerospace Agency of Ministry Defense and Aerospace Industry of RK.

E-mail: dubovichenko@mail.ru , dubovichenko@gmail.com
Web-site: www.dubovichenko.ru

Fesenkov Astrophysical Institute - Observatory 23, Kamenskoe plato, 050020, Almaty, Republic of Kazakhstan, www.aphi.kz